



THE UNIVERSITY OF QUEENSLAND
AUSTRALIA

Site-Specific Weed Management Using Remote Sensing

Nik Norasma Che'Ya

Bachelor of Science Geoinformatic

Master of Geomatic Engineering

A thesis submitted for the degree of Doctor of Philosophy at

The University of Queensland in 2016

School of Agriculture and Food Sciences

Abstract

The objective of this research was to develop a method to map weeds in sorghum as the first step as a procedure to control them using site-specific weed management (SSWM). Site-specific weed management is a method to limit the application of herbicides only to areas with weeds. Accurate mapping of weeds is a pre-requisite for applying SSWM. Analysis of hyperspectral remote sensing imagery is recognized as a potentially cost effective technique for discriminating between weeds and crop plants. This research involved: i) collecting hyperspectral reflectance spectra from weeds and sorghum plants, ii) Stepwise Linear Discriminant Analysis (SLDA) to identify the most significant spectral bands, iii) Linear Discrimination Analysis (LDA) to test the accuracy of the SLDA bands for classifying weeds and sorghum, and iv) analysis of customized multispectral imagery to produce maps which detected weeds in the sorghum crop.

Hyperspectral signatures of weeds and sorghum were obtained using a FieldSpec® Handheld2™ spectroradiometer with a spectral range from 325 nm to 1075 nm. Spectra were recorded for different weed species and sorghum plants for three years, 2012 to 2014. Data were collected at four different stages of plant growth each year, from week one to week four after planting.

The results show that it is feasible to discriminate spectral profiles of weeds from each other weeds and from sorghum plants. Statistical Analysis Software (SAS) was used to identify the most significant spectral bands (10 nm width) from the hyperspectral reflectance data using SLDA. All weeds and sorghum were correctly classified in 2012 using LDA for week four reflectance data. In 2013, the classification accuracy increased with stage of growth (weeks one to four) from 85% to 90%. In 2014, the classification accuracy also increased with stage of growth (weeks two to four) from 90% to 100%. Combinations of spectral bands were analysed to reduce the number of potential bands identified from the SLDA results. Spectral bands centred on 930, 890, 710, 700, 560 and 500 nm were common to the 20 most significant spectral bands identified by SLDA analysis each year. Six spectral bands 850, 720, 710, 680, 560 and 440 nm were subsequently selected for use in multispectral image collection. They were selected based on maximizing the differences and similarities between the 2013 weed and crop reflectance profiles. These bands were used for the band-pass filters in the Tetracam MCA 6 camera used for collecting high spatial resolution terrestrial and aerial imagery.

The imagery was analysed using Object-Based Image Analysis (OBIA) and Vegetation Index Analysis (VIA) to classify weeds and sorghum plants. OBIA identified weeds more successfully than VIA. The accuracy of OBIA classification was tested using two methods. Confusion matrices were used to measure the Coefficient of Agreement (Khat), Overall Accuracy

and Producer's and User Accuracies. Geometry matrices were used to measure under and over segmentation. The Overall accuracy and Khat for all the weeds was more than 80% and 70% respectively for mosaic imagery. These results are considered high and moderate for effectiveness in discrimination respectively.

The results of this research are limited by the weed species that grew in the sorghum crop at Gatton, Queensland, the spectral resolution of the imagery and the image analysis methods. To ensure the wider applicability of the procedures, methods presented in this thesis need to be tested on other sorghum crops in different locations.

Key Words: Weed-crop classification, hyperspectral reflectance, weed mapping, site-specific weed management, weed detection and image processing.

Declaration by author

This thesis is composed of my original work, and contains no material previously published or written by another person except where due reference has been made in the text. I have clearly stated the contribution by others to jointly-authored works that I have included in my thesis.

I have clearly stated the contribution of others to my thesis as a whole, including statistical assistance, survey design, data analysis, significant technical procedures, professional editorial advice, and any other original research work used or reported in my thesis. The content of my thesis is the result of work I have carried out since the commencement of my research higher degree candidature and does not include a substantial part of work that has been submitted to qualify for the award of any other degree or diploma in any university or other tertiary institution. I have clearly stated which parts of my thesis, if any, have been submitted to qualify for another award.

I acknowledge that an electronic copy of my thesis must be lodged with the University Library and, subject to the policy and procedures of The University of Queensland, the thesis be made available for research and study in accordance with the Copyright Act 1968 unless a period of embargo has been approved by the Dean of the Graduate School.

I acknowledge that copyright of all material contained in my thesis resides with the copyright holder(s) of that material. Where appropriate I have obtained copyright permission from the copyright holder to reproduce material in this thesis.

Publications during candidature

CONFERENCE:

Oral presentation. ‘Hyperspectral discrimination of weeds using hyperspectral Radiometry’ at 5th Asian Conference on Precision Agriculture (ACPA), Jeju, Korea, 25-28 June 2013.

Publications included in this thesis

“No publications included”.

Contributions by others to the thesis

“No contributions by others”.

Statement of parts of the thesis submitted to qualify for the award of another degree

“None”.

Acknowledgements

All the praises and thanks be to Allah, Alhamdulillah. I started my PhD journey eager to learn new things and travel to a different country. Without the guidance of my advisors, my PhD would have seemed like an endless journey full of sweat and tears, but the discouragements I experienced taught me about life. I would like to express my great gratitude to my advisors: Dr. Madan Gupta (UQ), Dr. Doug George (UQ), Dr. Michael Widderick (DAFF) and Dr. Dipak Paudyal (ESRI), for their patient guidance and valuable and constructive suggestions over the past four years. I doubt that my PhD would be finished without those around me who were really supportive and encouraging especially Dr. Ernest Dunwoody and Mr. Allan Lisle (UQ Statistician). I extend my sincere thanks to Dr. Ernest Dunwoody for his guidance, patience in proofing my manuscripts and inspiring advice, which always kept me motivated. I would like to express my appreciation to Mr. Brett Jahnke (Field Officer), Tristine Blackall (Librarian), Dr. Badri Basnet (Lecturer in Spatial Science, USQ), Terry and Mitchell Byrne (USQ UAV flight team), Steve Heinold (Tetracam Specialist, USA), Dr. Farrah Melissa Muharam, Dr. Mehdi Saberioon and Fredi Satya Candra Rosaji. I would also thank the Ministry of Higher Education Malaysia and Universiti Putra Malaysia which gave me the opportunity to undertake my PhD. Appreciation must go to my colleagues and friends Dr. Jamaliah Laham, Dr. Ammar Abdul Aziz, Dr. Muhammad Kamal, Dr. Farah Hanani, Dr. Aliya Azlan, Solecha Ruseani, Ainatul Asyila, Siti Liyana, Mohd Hafiz, Nur Syazwani, Syahira Isahak, Nadiah Fackeer, Siti Khadijah, Khairatul Najwa, Mohd Afizul, Mohd Izzudin, Nur Ilyana, Zairihan Halim, Mohd Hafis, Sri Lestari and all who gave me support and encouragement to ensure that I kept thinking positively along my PhD journey. I thank my beloved mum, Nik Radiah Raja Ibrahim, dad, mother in law, sisters and brothers who always prayed for my success. Finally, thanks and recognition goes to my husband, Mohd Yusri Md. Yusof, who always supports me in everything I do and also, my baby girl, Nur Aisyah Ellysya. She is my strength to help complete my journey. She is a very strong girl, who has sacrificed being with me for almost a year. I really appreciate you honey. I love you so much baby. Thanks so much for understanding the situation. Alhamdulillah...

“So, Verily, with every hardship, there is ease.

Verily, with every hardship, there is ease,”

The Holly Quran 94: 5-6

Keywords

weed-crop classification, hyperspectral reflectance, weed mapping, site-specific weed management, weed detection, image processing.

Australian and New Zealand Standard Research Classifications (ANZSRC)

ANZSRC Code: 070308, Crop and Pasture Protection (Pests, Diseases and Weeds) 100%

Fields of Research (FoR) Classification

FoR code: 0703, Crop and Pasture and Production, 100%

Table of Contents

Abstract	ii
Declaration by author	iv
Acknowledgements	vi
Table of Contents	viii
List of Figures	xiv
List of Tables	xvii
List of Abbreviations	xx

CHAPTER 1

INTRODUCTION

1.1	BACKGROUND	1
1.2	PROBLEM STATEMENT	2
1.3	AIM OF RESEARCH	4
1.4	OBJECTIVES	4
1.5	SIGNIFICANCE OF STUDY	4
1.6	LIMITATIONS OF STUDY	5
1.7	CONCLUSIONS	5

CHAPTER 2

LITERATURE REVIEW

2.1	INTRODUCTION	7
2.2	WEED CONTROL SYSTEMS	12
2.2.1	Mechanical and thermal weed control	12
2.2.2	Conventional chemical weed control	12
2.2.3	Precision weed control	13
2.2.3.1	Variable rate technology	15
2.2.3.2	Detection systems	16
2.2.4	Vegetation reflectance	17
2.3	REMOTE SENSING FOR WEED MANAGEMENT	19
2.3.1	Hyperspectral reflectance for weed classification	19
2.3.2	Remote sensing	21
2.4	IMAGE COLLECTION	22
2.4.1	Unmanned Aerial Vehicle	22
2.4.2	Ground mounted systems	25
2.5	IMAGE PROCESSING	27
2.5.1	Weed detection image processing procedures	29
2.5.2	UAV weed identification applications	30

2.5.3	Multispectral imagery for weed discrimination	31
2.6	CONCLUSIONS	32

CHAPTER 3

GENERAL METHODOLOGY

3.1	INTRODUCTION	34
3.2	OVERVIEW	34
3.3	EXPERIMENTAL DESIGN	37
3.3.1	Study area	37
3.3.2	Field layout	38
3.4	DATA COLLECTION AND PRE-PROCESSING	41
3.4.1	Hyperspectral data	42
3.4.2	Moisture content	44
3.4.3	Imagery	44
3.4.3.1	Power Supply	46
3.4.3.2	Saving time and Flight Planning	47
3.4.3.3	Image Extraction	49
3.4.3.4	Downloading images	49
3.4.3.5	Creating initial multi Tifs image files	51
3.4.3.6	Band alignment	52
3.4.3.7	Revised (Corrected < 100 m) Multiband Tifs	55
3.4.4	Ground truth data	55
3.4.5	Statistical procedure	55
3.4.6	Validation	56
3.5	CONCLUSIONS	56

CHAPTER 4

IDENTIFICATION OF SPECTRAL DIFFERENCES BETWEEN WEEDS AND SORGHUM

4.1	INTRODUCTION	57
4.2	LITERATURE REVIEW	58
4.2.1	Spectral reflectance of vegetation	58
4.2.2	Effect of moisture on spectral reflectance	60
4.2.3	Weed discrimination analysis using spectral reflectance	62
4.2.4	Spectral Reflectance Analysis	62
4.3	MATERIALS AND METHODS	63
4.3.1	Spectral data	63
4.3.1.1	Data collection	63
4.3.1.2	Pre-processing procedures	66

4.3.2	Moisture content analysis	66
4.4	RESULTS	67
4.4.1	Reflectance results	67
4.4.2	First Derivative results	72
4.4.3	Effect of moisture content on reflectance	76
4.5	DISCUSSION AND ANALYSIS	79
4.5.1	Effect of moisture on species reflectance	79
4.5.2	Species reflectance values	80
4.5.3	First Derivative Values	82
4.6	CONCLUSIONS	83

CHAPTER 5

SPECTRAL BANDS FOR DISCRIMINATION OF WEEDS IN SORGHUM

5.1	INTRODUCTION	84
5.2	LITERATURE REVIEW	85
5.2.1	Identification of different spectral classification bands	86
5.2.2	Accuracy testing	88
5.3	METHODS	88
5.3.1	Spectral separability procedures	89
5.3.1.1	Classification Procedure	89
5.3.1.2	Validation Procedure	90
5.3.2	Selection of Optimum Band Combinations	90
5.4	RESULTS	92
5.4.1	Identification of Significant Bands	92
5.4.2	Classification and Validation	95
5.4.3	Optimum Band Combinations	96
5.5	DISCUSSION AND ANALYSIS	101
5.5.1	Band Identification	102
5.5.2	Classification and Validation	103
5.5.3	Optimal Bands	104
5.6	CONCLUSIONS	106

CHAPTER 6

IMAGE PROCESSING FOR DETECTING WEEDS IN SORGHUM

6.1	INTRODUCTION	107
6.2	LITERATURE REVIEW	107
6.2.1	Object Based Image Analysis	107
6.2.2	Vegetation Index Analysis (VIA)	110
6.2.3	Image Mosaicing and Geometric Rectification	112
6.2.4	Accuracy Assessment	112
6.3	METHODS	113
6.3.1	Image Collection	113
6.3.2	Image Processing Workflow	114
6.3.3	Mosaicing	114
6.3.4	Object Based Image Analysis (OBIA) Procedures	115
6.3.4.1	Image Analysis Workflow	116
6.3.4.2	Classification Hierarchy and Development of Rule Sets	117
6.3.4.3	Application of OBIA Rule Sets	119
6.3.5	Vegetation Index Analysis (VIA)	123
6.3.6	Error Assessment Procedures	124
6.3.6.1	Confusion Matrix Assessment	124
6.3.6.2	Geometric Assessment	126
6.4	RESULTS	131
6.4.1	OBIA and Analysis Results	131
6.4.1.1	OBIA Results for Highest Spatial Resolution Imagery (0.87 mm)	131
6.4.1.2	OBIA Results for Medium Spatial Resolution Imagery (10.83 mm)	133
6.4.1.3	OBIA Results for Low Spatial Resolution Imagery (20.31 mm)	135
6.4.2	Vegetation Index Analysis Results	137
6.4.2.1	Vegetation Results for Highest Spatial Resolution Imagery (0.87 mm)	137
6.4.2.2	Vegetation Index Results for Medium Spatial Resolution Imagery (10.83 mm)	138
6.4.2.3	Vegetation Index Results for Lowest Spatial Resolution (20.31 mm)	138
6.4.3	Mosaic Analysis Results	141
6.5	ACCURACY ASSESSMENT	144
6.5.1	OBIA Analysis Accuracy	144
6.5.1.1	Confusion Matrix Accuracy Analysis (Spatial Resolution: 0.87 mm)	144
6.5.1.2	Geometric Accuracy Analysis	149
6.5.1.3	Mosaic Analysis Accuracy	151
6.6	DISCUSSION	151
6.6.1	Spectral Resolution	152

6.6.2	Spatial Resolution	152
6.6.3	Stage of Growth	153
6.6.4	Image Processing	154
6.7	CONCLUSIONS	156

CHAPTER 7

CONCLUSION AND RECOMMENDATIONS

7.1	INTRODUCTION	158
7.2	MAIN FINDINGS AND OUTCOMES	158
7.2.1	Weed and crop spectral discrimination (Objective one)	159
7.2.2	Multispectral bands selected for weed and crop discrimination (Objective two)	159
7.2.3	Image processing procedure for weed and crop separation (Objective three)	160
7.2.4	Weed mapping in sorghum (Objective four)	160
7.3	LIMITATION AND FUTURE RESEARCH	161
7.4	CONTRIBUTION TO KNOWLEDGE	162
References		163
Appendix A.	R Code	180
Appendix B.	Three-band combinations of seven available band-pass filters (2013)	182
Appendix C.	Six-band combinations of eight available band-pass filters (2013)	183
Appendix D.	The combination of five bands based on six most accurate for Validation 2014 data	184
Appendix E.	The combination of four bands based on six most accurate for Validation data 2014	184
Appendix F.	The combination of three bands of the six most accurate for Validation data 2014	184
Appendix G.	Calibration and validation analysis for weeks one – four using 20 significant bands (2013)	185
Appendix H.	Calibration and validation analysis for week two – four using all 20 significant bands (2014)	185
Appendix I.	Calibration and validation analysis for weeks one – four using eight available bands (2013)	186
Appendix J.	Classification results for all 6-band combinations based on the bands in Appendix C	187
Appendix K.	Classification results for all 3-band combinations based on the bands in Appendix B	188
Appendix L.	Calibration and validation analysis for weeks two – four using 6-band combinations (2014)	189
Appendix M.	Classification accuracy of 5-band combinations (2014)	189
Appendix N.	Classification results (%) for all 4-band combinations for 2014	190

Appendix O.	Classification accuracy of 4-band combinations (2014)	191
Appendix P.	Classification results (%) for all 3-band combinations for 2014.	192
Appendix Q.	Classification accuracy of 3-band combinations (2014)	193
Appendix R.	Nutgrass quadrats at two stages of growth for 0.87 resolution	194
Appendix S.	Sorghum non pre-emergence quadrats at two stages of growth for 0.87 resolution	195
Appendix T.	Pigweed quadrats at two stages of growth for 0.87 resolution	196
Appendix U.	Bellvine quadrats at two stages of growth for 0.87 resolution	197
Appendix V.	Liverseed grass quadrats at two stages of growth for 0.87 resolution	198
Appendix W.	Sorghum pre-emergence quadrats at two stages of growth for 0.87 resolution	2189
Appendix X.	Nutgrass quadrats at week three for 10.83mm resolution	200
Appendix Y.	Sorghum non pre-emergence quadrats at week three for 10.83mm resolution	201
Appendix Z.	Pigweed quadrats at week three for 10.83 mm resolution	202
Appendix AA.	Bellvine quadrats at week three for 10.83 mm resolution	203
Appendix BB.	Liverseed grass quadrats at week three for 10.83 mm resolution	204
Appendix CC.	Sorghum pre-emergence quadrats at week three for 10.83 mm resolution	205
Appendix DD.	Pigweed quadrats at week three for 20.31 mm resolution	206
Appendix EE.	Nutgrass quadrats at week three for 20.31mm resolution	207
Appendix FF.	Sorghum non pre-emergence quadrats at week three for 20.31 mm resolution	208
Appendix GG.	Bellvine quadrats at week three for 20.31 mm resolution	209
Appendix HH.	Sorghum pre-emergence quadrats at week three for 20.31 mm resolution	210
Appendix II.	Liverseed grass quadrats at week three for 20.31 mm resolution	211
Appendix JJ.	VI Analysis for 10.83 mm	212
Appendix KK	VI Analysis for 20.31 mm	216

List of Figures

Figure 2-1	Sorghum Growth Stage Development (University of Illinois 2012)	7
Figure 2-2	Life cycle of an annual weed (Widderick, 2009)	11
Figure 2-3	The spatial resolution of weed control in a field (Christensen et al. 2009)	14
Figure 2-4	Three variations of precision farming strategies for site-specific weed control (Bill et al. 2012).	14
Figure 2-5	Hypothetical Leaf Cross-section (Purves et al 2014)	18
Figure 2-6	Vegetation spectrum in detail (Elowitz 2015)	19
Figure 2-7	Flowchart of the process of plants detection and discrimination (Schuster et al. 2007)	27
Figure 2-8	Relationship of image resolutions, level of information detail and map accuracy (Kamal et al. 2015)	29
Figure 3-1	Details of the data collection	35
Figure 3-2	Overview of the spectral data collection	35
Figure 3-3	Workflow of the methodology	36
Figure 3-4	Location of the study area	37
Figure 3-5	Case 95 tractor (a) and Nodet planter (b)	38
Figure 3-6	Position of loci and quadrats in 2013	39
Figure 3-7	Details of loci and quadrats in 2013	39
Figure 3-8	Layout of replicates in 2014	40
Figure 3-9	Data collection in the study	42
Figure 3-10	Hyperspectral data collection	42
Figure 3-11	Collecting spectral signatures using the FieldSpec® HandHeld 2™ Spectrograph with fibre optic attached.	43
Figure 3-12	Weeds in L1Q1 from week one to week four, 2013	43
Figure 3-13	<i>Mini</i> Multi Channel Array (MCA6) camera attached to the Mikrokopter JR11X (A) and MCA 6 in close up without cover (B)	45
Figure 3-14	Communications between the Mikrokopter and sensor auto-pilot and the ground controller using Mikrokopter software	46
Figure 3-15	Taking the quadrant image using a jig	48
Figure 3-16	Flowchart for pre-processing MCA 6 bands imagery	49
Figure 3-17	Steps for directly copying the MCA 6 imagery from the CF cards	50
Figure 3-18	Procedure for transferring MCA 6 imagery file to a computer using PixelWrench2 Software	50
Figure 3-19	Create initial multiband Tifs	51
Figure 3-20	Details of the MCA file settings	52
Figure 3-21	The position of the sensors in the MCA 6 camera (Tetracam 2015)	53
Figure 3-22	Create a new MCA file	53
Figure 3-23	The X and Y correction in green colour	54
Figure 3-24	Before and after setting of the MCA, X Y for correction values for band alignment	54
Figure 3-25	The steps used for band alignment correction	55
Figure 4-1	Effect of the earth's atmosphere and vegetation on reflectance,	58

	absorption, and transmission of light (University of Hawaii 2009)	
Figure 4-2	Atmospheric reflectance, transmittance, and absorption of Big Bluestem grass axial leaf surface (Jensen 2016, p. 321)	59
Figure 4-3	The electromagnetic (EM) spectrum (University of Hawaii 2009)	59
Figure 4-4	Typical reflectance spectra of vegetation at different wavelengths (Li et al. 2014)	60
Figure 4-5	Differences in reflected light between a healthy and unhealthy leaf (Ortiz and Shaw 2011)	61
Figure 4-6	Typical spectral reflectance curve of healthy vegetation depicting different absorption and reflectance regions peaks (Shilpakala 2014)	61
Figure 4-7	Hyperspectral data download and pre-processing	65
Figure 4-8	Average spectral reflectance profile for 2012	67
Figure 4-9	Average spectral reflectance profiles for 2013(Week one to four)	68
Figure 4-10	Average spectral reflectance profiles for 2014 (Week two to four)	71
Figure 4-11	First Derivative spectral graph	72
Figure 4-12	FD spectral profiles for 2013 (Week one to four)	73
Figure 4-13	FD spectra profiles for 2014 (Week two to four)	75
Figure 4-14	Moisture content for all species (2013)	77
Figure 5-1	Species classification procedure (2012)	89
Figure 5-2	Species classification procedure (2013 and 2014)	90
Figure 5-3	Accuracy evaluation of band combinations	92
Figure 6-1	Visualization of OBIA result (A) and Reference Map (B) $*\cap =$ Intersection	110
Figure 6-2	Flowchart of the image analysis process	114
Figure 6-3	Workflow for mosaicing in Agisoft Photoscan	115
Figure 6-4	Growth stages analysis at different spatial resolution	116
Figure 6-5	Flowchart of the methodology process (Kamal et al. 2015)	116
Figure 6-6	Flow chart for image processing using OBIA analysis.	117
Figure 6-7	Hierarchy for weed discrimination classification. Schematic modified from Laliberte et al (2010) and Slaughter (2014)	117
Figure 6-8	Process tree from eCognition Developer used the weed classification	118
Figure 6-9	The raw image before the segmentation process showing sorghum, nutgrass (weed), shadow and soil at 0.87 mm resolution for Quadrat 1 for nutgrass (Q1NG)	120
Figure 6-10	Segmentation with outlines (Scale parameter: 40) (a); segmentation without outlines (b)	120
Figure 6-11	Classification for shadow, soil and vegetation	121
Figure 6-12	Segmentation between soil and vegetation (Scale setting: 10)	121
Figure 6-13	Selected samples for each class	122
Figure 6-14	Sorghum and weeds was misclassified (a) and reclassify in vegetation class (b) using “Enclosed” function	122
Figure 6-15	Classification between sorghum and weeds	123
Figure 6-16	Details of dataset for VIA analysis	123
Figure 6-17	Confusion matrix at different growth stages	125

Figure 6-18	The Fishnet on the top of the OBIA classification and RGB maps	126
Figure 6-19	The original image (a) and (b) is the visual interpretation (as Reference Map) from digitization	126
Figure 6-20	Comparison between Reference and OBIA image maps	127
Figure 6-21	The new field (Class) added in the attribute table	127
Figure 6-22	Comparison between OBIA image and Reference Map	127
Figure 6-23	The merge results by using “dissolve” tool	128
Figure 6-24	Sorghum class in both maps	128
Figure 6-25	The matching area for the soil class in both maps (Intersect Result) $*\cap = \text{Intersection}$	129
Figure 6-26	Difference between Reference and OBIA Maps	130
Figure 6-27	Symmetrical Difference Map showing areas of over and under-segmentation (Symmetrical Difference Result)	130
Figure 6-28	The merge function applied to the Intersect and Symmetrical difference results for soil class	130
Figure 6-29	Mosaic image at 5.42 mm resolution	141
Figure 6-30	Mosaic image at 10.83 mm resolution	142
Figure 6-31	Mosaic image at 20.31 mm resolution	143
Figure 6-32	Confusion matrix analysis for 17 December 2014 quadrats	144
Figure 6-33	Summary of accuracies for Confusion Matrix analysis at 0.87 mm	148
Figure 6-34	Geometric analysis accuracy assessment for 0.87 mm	149

List of Tables

Table 2-1	Growth stages for grain sorghum (Mississippi State 2014)	8
Table 2-2	Description of weed species (Wood 2000)	9
Table 2-3	Summary of weed control in past 50 years (Reeves 2008)	10
Table 2-4	Comparison of mechanical, conventional chemical and automated precision chemical weed control (De Baerdemaeker 2014)	12
Table 2-5	Five herbicides and the crops in which resistant weeds occur in the world (Heap 2016 and Zimdahl 2013)	13
Table 2-6	Sensor-based intensive technology (Lee et al. 2010)	16
Table 2-7	Leaf pigment absorption	18
Table 2-8	The common spectral regions (Jensen 2016, p. 315)	19
Table 2-9	Some of the current sensors and platforms with spatial and spectral resolutions potentially useful for SSWM imagery (Lopez-Granados 2010)	21
Table 2-10	Typical types of small unmanned aerial vehicles ^a (Sankaran et al. 2015)	22
Table 2-11	Different types of sensors used in plant phenotype characterization (Sankaran et al. 2015)	23
Table 3-1	Data collection for each year	36
Table 3-2	Sorghum planting	37
Table 3-3	Details for each replicate	41
Table 3-4	Annual hyperspectral data collection at different stages of growth (Week one to week four)	42
Table 3-5	Weeds species occurring each year	43
Table 3-6	Summary specifications for UAV platforms (Bueren et al. 2015)	44
Table 3-7	Data and flight plan for image collection (2014)	47
Table 3-8	Sensor properties adapted by Bueren et al. (2015)	47
Table 3-9	Comparison of the spectral resolutions between the UQ Tetracam MCA 6 camera (Tetracam 2015) and Landsat 7 ETM+ and World View II (Jensen 2007)	48
Table 4-1	Summary of hyperspectral satellites (Thenkabail et al. 2000)	62
Table 4-2	FieldSpec® HandHeld 2 Spectroradiometer properties (ASDi 2014)	64
Table 4-3	Weeds species collected each year	64
Table 4-4	Binned data	66
Table 4-5	Seven Landsat (ETM) bands	67
Table 4-6	Correlation of MC with sorghum reflectance	77
Table 4-7	Correlation raw spectral for amaranth	78
Table 4-8	Correlation raw spectral for nutgrass	78
Table 4-9	Correlation raw spectral for liverseed grass	78
Table 4-10	Correlation raw spectral for mallow weed	79
Table 4-11	Correlation of First Derivative reflectance for all species (2013)	79
Table 4-12	Summary of effect of MC on reflectance	80
Table 5-1	Weed and crop plants discriminated using hyperspectral data	86
Table 5-2	Selected bands for plants identification reported by previous investigators	87
Table 5-3	Eight priority bands	91
Table 5-4	Top 6-band combinations for 2013	91

Table 5-5	Band combination tested for accuracy	91
Table 5-6	Significant bands from Stepwise Linear Discriminant Analysis of 2012 data	92
Table 5-7	Significant bands from Stepwise Linear Discriminant Analysis of 2013 data	93
Table 5-8	Twenty most significant bands from Stepwise Linear Discriminant Analysis of the 2014 data	94
Table 5-9	Bands common to all 3 years	94
Table 5-10	Frequency of bands by region	94
Table 5-11	Classification by literature review bands and SLDA bands (2012 data)	95
Table 5-12	Classification results for the 20 most significant bands in 2013 data.	96
Table 5-13	Classification results for the 20 most significant bands in 2014 data	96
Table 5-14	Classification results for the seven bands 2013 data (Table 4-5)	97
Table 5-15	Classification results for the five most accurate combinations of the Landsat (ETM) 3-band combinations (Validation, 2013)	97
Table 5-16	Classification results for the five most accurate combinations of the priority 6-band combinations (Validation, 2013)	98
Table 5-17	Classification results using the calibration “rule set” for the six most significant bands in 2014 data	98
Table 5-18	Classification results (%) for all 5-band combinations for 2014 Validation data	99
Table 5-19	Classification results (%) for the top five 4-band combinations for 2014 (Validation data)	100
Table 5-20	Classification results (%) for the top five 3-band combinations for 2014 Validation data	101
Table 6-1	Agriculture mapping applications using OBIA	109
Table 6-2	Details of VIA from the literature review	111
Table 6-3	Description of the accuracy (Lehmann et al. 2015)	113
Table 6-4	Geomatic assessment formula (Belgiu and Dragut 2014)	113
Table 6-5	Resolution for mosaic image	115
Table 6-6	Rule sets parameters for different spatial resolution	119
Table 6-7	Vegetation Indices used in image processing	124
Table 6-8	The band value central wavelength assignment for each spectral region	124
Table 6-9	The error matrix for nutgrass at 0.87 mm	125
Table 6-10	Area comparison for OBIA and Reference Maps	128
Table 6-11	Area Fit Index (AFI)	128
Table 6-12	Results for Geometric calculation (Example: Soil)	129
Table 6-13	Nutgrass and sorghum non pre-emergence quadrats at two stages of growth	131
Table 6-14	Pigweed and sorghum pre-emergence quadrats at two stages of growth	132
Table 6-15	Bellvine and liverseed grass quadrats at two stages of growth	133
Table 6-16	Nutgrass and sorghum non pre-emergence at 10.83 mm spatial resolution	133
Table 6-17	Pigweed and bellvine at 10.83 mm spatial resolution	134
Table 6-18	Liverseed grass and sorghum pre-emergence at 10.83 mm spatial resolution	135

Table 6-19	Pigweed and nutgrass at 20.31 mm spatial resolution	136
Table 6-20	Sorghum non pre-emergence and bellvine at 20.31 mm spatial resolution	136
Table 6-21	Sorghum pre-emergence and liverseed grass at 20.31 mm resolution	137
Table 6-22	The three different resolution at week three	137
Table 6-23	VI analysis for 0.87 mm	139
Table 6-24	Error Matrix for 0.87 mm resolution (Week three: 17th Dec. 2014)	145
Table 6-25	Error Matrix for 0.87 mm resolution (Week three: 18th Dec. 2014)	146
Table 6-26	Error Matrix for 0.87 mm resolution (Week four)	147
Table 6-27	Summary of Overall and Khat accuracies for 10.83 and 20.31 mm spatial resolution	148
Table 6-28	Area Fit Index for the species	149
Table 6-29	Geometric assessment values for 0.87 mm resolution (Weeds)	150
Table 6-30	Geometric assessment values for 0.87 mm resolution (Sorghum)	150
Table 6-31	Geometric assessment values for 0.87 mm resolution (Soil)	150
Table 6-32	Confusion matrix for mosaic image resolution	151
Table 6-33	Rule sets parameters for different spatial resolution	152

Abbreviations

AFI	Area Fit Index
ATP	Adenosine TriPhosphate
ADC	Agricultural Digital Camera
ASCI	American Standard Code for Information Interchange
ANOVA	Analysis of Variance
ASD	Analytical Spectral Device Corporation
ANN	Artificial Neural Network
B	Bellvine
CWL	Central Wavelength
CART	Classification and Regression Tree analysis
CIVE	Color index of vegetation
CIR	Colour-Infrared
CMOS	Complementary metal-oxide semiconductor
CF	Computer Flash
DAFF	Department of Agriculture, Fisheries and Forestry
DGVI	Derivative Green Vegetation Index
DSLR	Digital Single-Lens Reflex
DTM	Digital Terrain Model
DRONES	Dynamic Remotely Operated Navigation Equipment
DVI	Different Vegetation Index
EM	Electromagnetic
ExG	Excess Green
ExGR	Excess green minus excess red
FS	Field Servers
FD	First Derivative
GA	Genetic Algorithms
GIS	Geographical Information System
GB	Gigabyte
HRSI	High-resolution satellite imagery
HSI	Hue-Saturation-Intensity
iTC	integrated Terrain Compensation
κ	kappa
Khat	Coefficient of Agreement
LAI	Leaf Area Index
LS	Liverseed Grass
LAN	Local Area Network
LiDAR	Light detection and ranging
L1Q1	Locus No. 1, Quadrat No. 1
MExR	Modified Excess Red
MLC	Maximum Likelihood Classification
MMF	Maximum Matching Feature

MIR	Middle Infrared
MNF	mize Noise Fraction
MODIS	Moderate resolution Imaging Spectrometer
MOG	Mixture of Gaussian
MC	Moisture Content
MTMF	Mixture Tuned Matched Filtering
MTVI1	Modified Triangular Vegetation Index 1
NDYI	Normalized Difference Yellowness Index
NGRDI	Normalized green-red difference index
NIR	Near Infra-Red
NN	Neural Network
NNC	Neural Network Classifier
NDVI	Normalized Difference Vegetation Index
NG	Nutgrass
NRRCI	NIR, Red-edge and Red Combine Index
OBIA	Object-Based Image Analysis
OSeg	Over-segmentation
PA	Precision Agriculture
PLS-DA	Partial Least Square-Discriminate Analysis
PLS	Partial-Least-Square regression
PF	Precision Farming
PW2	Pixel Wrench 2
PCA	Principle Component Analysis
RTK	Real Time Kinematic
RTK GPS	Real Time Kinematic Global Positioning System
ROI	Regions of Interest
RMSE	Root Mean Square
RVI	Red Vegetation Index
RVSI	Red-edge Veg. Stress Index
Q1NG1	Quadrat 1 for Nutgrass
Qr	Quality rate
SOM	Self Organising Map
SAM	Spectral Mixture Analysis
SfM	Structure from Motion
SVD	Singular Values Decomposition
SNP	Sorghum non pre-emergence
SP	Sorghum Pre-emergence
SAM	Spectral Angle Mapper
SAVI	Soil-adjusted vegetation index
SSWM	Site-specific weed management
SLDA	Stepwise Linear Discriminant Analysis
SVN	Support Vector Networks
Tukey HSD	Tukey Honesty Significant Difference
TVI	Triangular Veg. Index
USeg	Under-segmentation

UQ	University of Queensland
UAVs	Unmanned aerial vehicles
UAV	Unmanned Aerial Vehicles
VEG	Vegetation
VIA	Vegetation Index Analysis
VI	Vegetation Index
VI _s	Vegetation Indexes
VIS	Visible
VRT	Variable Rate Technology
WI	Woebbecke index
Wk	Week

Chapter 1

INTRODUCTION

1.1 BACKGROUND

Australia produces 2.2 million tonnes of grain sorghum annually which is mainly harvested from Queensland and New South Wales (USDA, 2016). Sixty percent of this production occurs in Queensland (Department of Agriculture and Fisheries 2012). Sorghum is a summer crop, which is planted between September and January each year. At this time of the year weed infestation is inevitable and it reduces grain yield if not controlled (Department of Agriculture and Fisheries 2012).

Weeds cause yield loss because they compete with crop plants for moisture, nutrients and sunlight (Birch et al. 2011). Potential yield loss due to uncontrolled weed growth is estimated to be 43% globally (Oerke 2006). The Department of Agriculture, Fisheries and Forestry (DAFF) reported that weeds cause the loss of AUD\$4 billion annually in Australia and this increases each year (Goktogan et al. 2010).

Weeds are controlled by herbicides in Australia, applied either as a blanket application to the whole field or to banded areas within rows. Neither method is sensitive to the spatial variability of the weeds (Birch et al. 2011). These methods can harm the crop, use unnecessary amounts of herbicide, increase the cost of production, contribute to herbicide resistance and cause environmental side effects (De Baerdemaeker 2014). Herbicide resistance is a critical problem in Australian cropping systems (Evans and Diggle 2008). These problems can be reduced by more targeted methods of herbicide application. Site-specific weed management (SSWM) is one method that has been proposed to achieve this (Torres-Sanchez et al. 2013b). In this procedure, farmers only apply the right amount of herbicide to the specific location at the right time. This can minimise chemical usage and herbicide resistance because it decreases the opportunity for selection of herbicide tolerant strains of weeds by minimizing the chance of survival through application of suboptimal concentrations of herbicide.

The concepts of Precision Farming (PF) and Precision Agriculture (PA) were introduced globally in 1990 (Khorramnia et al. 2014). Spraying herbicide at the right dosage at the right time and in the precise location of the weed is an application of PA and provides a better approach to weed control than blanket herbicide application (Okamoto et al. 2014). It requires specific information about the location (distribution) of each weed (Kiani and Jafari 2012).

Discrimination between weeds and crop plants is the first step needed to apply SSWM (Gutjahr and Gerhards 2010). Visible wavelength remote sensing is one method of acquiring information for SSWM application (Pena et al. 2013). However, the use of satellite imagery for weed detection at the early stages of weed growth is limited by the lack of spatial and spectral resolution of the satellite sensors to detect small plants (Pena et al. 2013). Unmanned aerial vehicles (UAVs) or drones are an alternative means of collecting high spatial and temporal resolution Visible (VIS) and Near Infra-Red (NIR) imagery (Garcia-Ruiz et al. 2015). They are easily deployed, relatively low-cost and have a flexible payload capability that allows them to be fitted with lightweight sensors such as multispectral cameras (Bueren et al. 2015).

Multispectral remote sensing refers to the collection of reflected, emitted or back-scattered energy from an object of interest in multiple bands (regions) of the electromagnetic spectrum (Jensen 2016). The bands are sensitive to different features of the object so they can be used to detect weeds and crop plants on the basis of difference in spectral signatures (Garcia-Ruiz et al. 2015). Image processing techniques potentially can be used to identify the weeds separate from the sorghum plants and thereby produce an accurate weed map from the multispectral imagery (Lee et al. 2010). This research has the potential to demonstrate a procedure for identifying spectrally unique signatures from the weeds and sorghum plants and use them as the basis for multispectral imagery to map weeds in sorghum.

1.2 PROBLEM STATEMENT

The main concerns with chemical weed control are its cost, and effects on crop productivity and environment (Ortiz-Monasterio and Lobell 2007; Martin et al. 2011). One potential solution to reduce the amount of herbicide is to apply herbicides at precisely the right weed location, at the right time and in the right concentration. This requires a record of precisely where each weed is located so that the herbicide sprayer can be activated to spray only for each weed or patch of weeds (Ortiz-Monasterio and Lobell 2007; Birch et al. 2011). Identification of weeds separate from crop plants can be done by appropriate image processing methods (Lee et al. 2010).

Satellite imagery is limited in doing this because of weather conditions (cloud cover) and lack of spatial, spectral and temporal resolution (Gumz 2007; Eisenbeiss and Sauerbier 2011). Imagery obtained at later stages of weed growth, when the weeds are larger, and easier to distinguish from the crop, is not suitable for herbicide weed mapping because more herbicide is needed to kill the weeds; this costs more and may result in poorer control (Pena-Barragan et al. 2012a). It is possible that weeds already may have reduced crop yield at this later stage of crop growth and it may not be possible to use some herbicides beyond certain stages of crop growth. The

limitations of satellite imagery for weed mapping can be overcome by using imagery collected by UAVs (Gumz 2007). The temporal and spatial resolution of UAV collected imagery can be adjusted to match the size of the weeds at their different stages of growth. The spectral resolution of UAV collected visible and NIR imagery depends on the filters fitted to the selected sensor.

Hyperspectral and multispectral data can be used to detect spectral differences between weeds and crop plants (Garcia-Ruiz et al. 2015). The weed species reflect unique spectral signatures that can potentially be processed to produce a weed map. However, to achieve this, several technical issues need to be solved:

- i. The weeds need to be detected in the sorghum crop when they are at an early stage of growth and physically very small. This raises the questions of:
 - a. When is the best early stage of growth at which to detect and discriminate the reflectance of weeds and sorghum plants?
 - b. What type of data needs to be collected to identify the weeds from the sorghum plants at the early growth stage?
 - c. What is the difference in reflectance between weeds and sorghum?
 - d. What statistical methods are appropriate to detect and discriminate between the reflectance of weeds and sorghum?
- ii. The need for an image of the crop when the weeds are at an early growth stage raises the questions of:
 - a. Can UAVs be used to collect a suitable image of the weeds and sorghum?
 - b. What type of sensor can collect imagery that discriminates between weeds and sorghum?
 - c. What are suitable spectral, spatial and temporal resolutions for detecting weeds and sorghum plants for weed mapping?
- iii. The need for the weeds to be identified separately from the crop plants raises questions of:
 - a. How do we identify the weed species from the crop plants using multispectral imagery?
 - b. What are the procedures to collect static and UAV multispectral imagery for weed detection?
 - c. How should the data be processed to detect and discriminate weeds and sorghum plants?
 - d. How accurate is the detection of weed and sorghum plants?

These questions were investigated in this thesis to determine the best solution to produce a weed map for sorghum.

1.3 AIM OF RESEARCH

The overall aim of this research was to develop a weed map for site-specific weed control in sorghum. In so doing, the following specific research objectives were developed.

1.4 OBJECTIVES

- i. To discriminate between weeds and sorghum plants.
- ii. To identify multispectral image bands that could be used to discriminate between different common weed species and sorghum plants.
- iii. To evaluate image processing procedures to separate weed species and sorghum plants using the multispectral imagery.
- iv. To use image processing to develop a weed map for a field of sorghum.

1.5 SIGNIFICANCE OF STUDY

The significance of this study is its demonstration of a procedure to identify the spectral bands that can be used to discriminate between weed and sorghum plants at an early stage of growth, the use of this information to collect multispectral imagery and the processing of it to create a weed discrimination map for sorghum. This is consistent with the approach recommended by Gumz (2007). The same procedure may be used for creating weed maps for different crops.

A weed map provides information about the location and density of individual weeds and patches of weeds in the crop. The pattern of distribution of weeds within the crop and their stage of growth provide the information needed to precisely apply the optimal dose of herbicides to kill the weeds while having minimal impact on the crop and the environment. The weed map can be uploaded to a tractor fitted with automatic guidance and computer controlled spraying equipment to apply the herbicide at the precise locations.

Specific bands of visible and NIR radiation, chosen from the spectral analysis, can be used as a guideline for selecting image sensor bands. A camera, modified to include these bands, can be used to photograph the crop. The identification of “weed detection” spectral bands for a variety of crops has the potential to lead to the development of weed detection cameras and integrated processing procedures for other forms of applications such as pest and disease detection.

1.6 LIMITATIONS OF STUDY

The accuracy of the weed map is based on the precision of the image and accuracy of the analysis. One of the limitations of this study was the difficulty in getting consistent data as outlined below.

In the first year of research (2012), only hyperspectral data was collected and the results were not replicated. In the second year (2013), an improved field design was used along with a replicated data-sampling plan. This enabled the hyperspectral data to be validated, and unique spectra and spectral bands to be identified. In the third year (2014) the experimental design of the field sample sites was further refined, hyperspectral reflectance data was collected and multispectral (6 bands) image data was collected in a replicated manner at different stages of weed growth.

The results are based on weeds found in grain sorghum crops grown in the Lockyer Valley in Queensland, Australia. Grain sorghum crops grown in different areas are likely to have slightly different spectral signatures and the weed species may have different reflectance profiles. The bands that provided discrimination in this study may not be suitable for the same species of weed at different places. Also, the same weed species may not occur every year under the same field conditions.

1.7 CONCLUSIONS

This research investigates a systematic way of determining how to separate weeds from sorghum plants by first analysing the spectral reflectance differences between the species followed by determining the multispectral bands that yield maximum discrimination. These bands were used as filters in a multi-sensor (six) camera to collect static and low-level overflight imagery for analysis to separate weeds from sorghum to produce a weed map. Weed maps produced in this manner have the potential for being used to direct precise herbicide applications with the associated benefits of reduced chemical cost and environment side effects.

The thesis is comprised of seven chapters. Chapter 2 provides a review of the literature on current weed management technology, UAV image collection technology and image processing procedures related to weed detection followed by Chapter 3 which covers general methodology common to the three research chapters that follow. Chapter 4 covers the identification of spectral differences in the reflectance of weeds and sorghum plants; Chapter 5 covers the identification and selection of spectral bands for distinguishing between weeds and sorghum plants and Chapter 6

evaluates image processing options for detecting weeds and sorghum plants in multispectral imagery. Chapter 7 provides a summary of the findings and recommendations for further research.

Chapter 2

LITERATURE REVIEW

2.1 INTRODUCTION

Sorghum is one of the major dry land crops grown in Queensland. It is used in rotation with other crops and has the advantage of requiring less water than other grain crops (Department of Agriculture and Fisheries 2012).

There are nine recognised stages in the growth of sorghum (Figure 2-1). Stage zero is emergence and stage nine is physiological maturity (Vanderlip 1993). Sorghum reaches maturity 100 days after emergence. The details for each stage are described in Table 2-1.

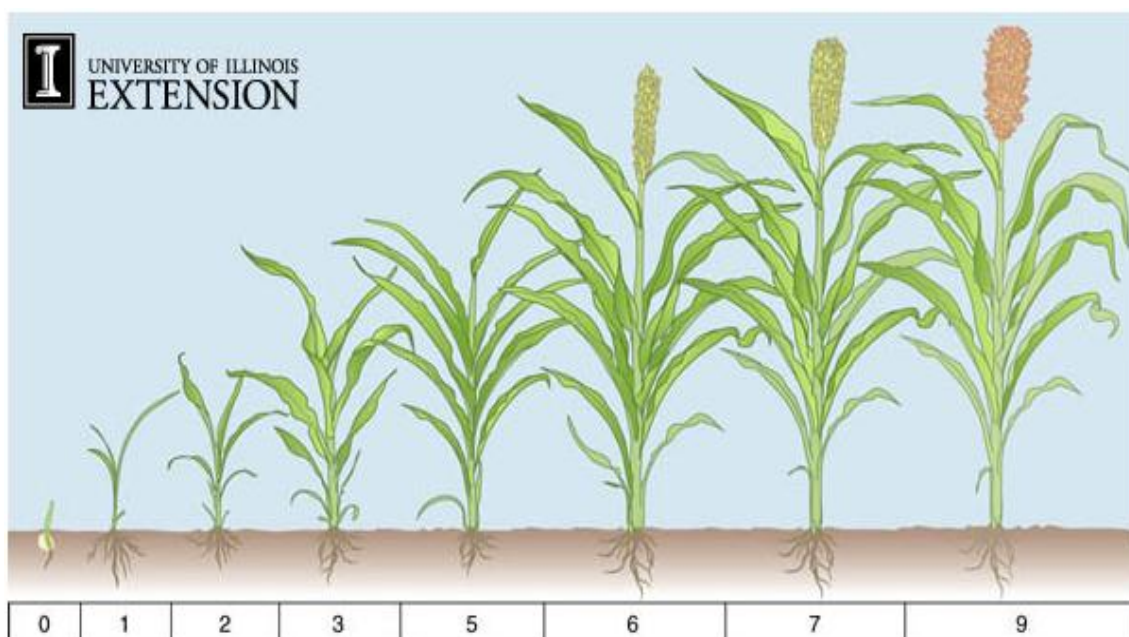


Figure 2-1 Sorghum Growth Stage Development (University of Illinois 2012)

Table 2-1 Growth stages for grain sorghum (Mississippi State 2014)

Stage	Identifying characteristics	Approximate days after emergence
0	Emergence - Seedlings emerge from the soil.	0
1	Three-leaf stage (Three leaves completely emerged, collars present).	10
2	Five-leaf stage.	20
3	Growing Point Differentiation (head development begins) - Rapid growth and nutrient uptake begins.	30
5	Boot stage (head enclosed in swollen flag leaf sheath) - Severe moisture stress will limit head exertion from the flag-leaf sheath, preventing pollination.	50
6	Half-bloom - Hot, dry weather can reduce seed set at this stage.	60
7	Soft dough - About 50% of the grain dry weight has accumulated.	70
8	Hard dough - About 75% of the grain dry weight has accumulated.	85
9	Physiological maturity - A dark spot on the opposite side of the kernel from the embryo forms (similar to black layer in corn). Dry matter accumulation is complete.	100

Sorghum plants are affected by weeds in their early stages of growth. The weeds compete for sunlight, moisture, nutrients and attract pests (Vanderlip 1993; Monaco et al. 2001). The best time to control weeds is also in their early stages of growth (Pena et al. 2013; Torres-Sanchez et al. 2013b). For example, grain production is reduced about 10% by one pigweed plant per linear metre of row if the infestation is left uncontrolled until the three-leaf stage (Smith and Scott 2010).

The common weeds in grain sorghum in Queensland are listed and illustrated in Table 2-2. They are all annual weeds except for nutgrass which is perennial (Wood 2000). Most of these weeds occur in various crops such as maize and soy bean (Hoang and Binh 2015), sorghum and cotton (Kandhro et al. 2014), carrots (Aitkenhead et al. 2003), cotton (Eure et al. 2015) and sunflowers (Lopez-Granados et al. 2015). The difference in the environment of these crops may influence the spectral signature of the weeds.

The traditional way of managing weeds in agricultural crops is either to cultivate or to spray with pre-emergence and knockdown herbicides. This has been practised for the past 50 years. The use of herbicides has resulted in the development of herbicide resistance in weeds and detrimental environmental side effects (Reeves 2008) (Table 2-3).

Table 2-2 Description of weed species (Wood 2000).






Plants	Description	Flowers and Fruiting
<p>Amaranth (C4) (<i>Amaranthus macrocarpus</i>)</p> 	<p>Small seedlings have purple veins and leaf margins. Seedlings are more prostrate than other amaranth seedlings apart from native amaranth.</p> <p>Mature plants are prostrate to semi-erect, with hairless, reddish-white stems. The leaves are notched at the tip.</p>	<p>Reddish-white, in dense clusters at the leaf forks. Fruiting capsules are 3–5 mm long, pear-shaped, soft and wrinkled and occur at the leaf forks.</p>
<p>Pigweed (C4) (<i>Portulaca oleracea</i>)</p> 	<p>Seed leaves are fleshy and elongated oval-shaped. The first true leaf is club-shaped, waxy, with purple margins and on a short stalk.</p> <p>Mature plants are fleshy and prostrate. Leaves are opposite, oval, crinkly, have purple margins and flattened or slightly notched at the tip. One leaf of each pair is smaller than the other in seedling and adults.</p>	<p>Single pink to purple flowers occur in cup-like structures in the leaf forks. Leaf stalks are variable on length and swollen and cup-like at the base.</p>
<p>Awnless Barnyard Grass (C4) (<i>Echinochloa colona</i>)</p> 	<p>The seedling tillers are flattened with purplish colouring at the base. The absence of a ligule is a key identification point.</p> <p>Purplish-red bands across the leaves can occur; these are a variant known as zebra. Mature plants are prostrate to semi-erect, 0.2–0.6 m tall, tufted with slender hairless stems and often purplish at the base.</p>	<p>The spikelets forming the seedhead become smaller towards the tip, and the spikelets are arranged in rows on one side of the spike. Awns on the seed spikelet are generally absent.</p>
<p>Nutgrass (<i>Cyperus rotundus</i>)</p> 	<p>Nutgrass is sedge rather than a grass. True seedlings of nutgrass are rarely produced. New seedling-like shoots grow from tubers. Seedlings are erect with shiny leaves tapering to a point.</p> <p>Mature plants are grass-like, up to 0.3 m tall, with an extensive system in a cluster at ground level.</p>	<p>Yellow, nutgrass and downy nutgrass are similar, but do not have tubers in chains and mature plants are taller. Seed heads are borne on triangular stems, which have several leaves near the top.</p>
<p>Bellive (<i>Ipomea plebeia</i>)</p> 	<p>Seed leaves are v-shaped with a broad flat base extending slightly beyond the sides. The true leaves have scattered hairs, with a notched base, becoming more pronounced as leaves mature. The notched leaf base formed by large basal lobes is very pronounced and regular.</p> <p>Mature plants are prostrate or climbing.</p>	<p>Flowers are white, trumpet-shaped and arise from the leaf forks.</p>

Table 2-2 (continued) Description of weed species (Wood 2000).




Plants	Description	Flowers and Fruiting
Mallow Weed (<i>Malva</i> sp) 	<p>Seed leaves are reverse heart-shaped, with long purple stalks. The first true leaf is rounded with a notched base, slight lobes and rounded teeth. Subsequently leaves are more wrinkled with shallow lobes and green or purplish-green stalks.</p> <p>Mature plants are woody-based and sprawling or upright. Leaves are alternate, wrinkled, rounded with a notched base and rounded teeth. Leaf stalks up 0.24 m long.</p>	<p>Pale pink to white with five short petals, and clustered in the leaf forks. Fruit comprises eight 12 wedge-shaped segment.</p>
Fat Hen (<i>Chenopodium album</i>) 	<p>Seed leaves are elongated and oval-shaped. The first pair of true leaves is oval and has a truncated base. Subsequent leaves are triangular with toothed margins. Young leaves are whitish-green due to a wax coating.</p> <p>Mature plants are erect and branched, with ribbed, green or re-tinged stems.</p>	<p>Greenish-white to reddish-white flowers are clustered on the tips of branches. Leaves are mealy-white, roughly diamond-shaped with wavy to toothed margins.</p>
Urochloa, Liver seed Grass (<i>Urochoa panicoides</i>) 	<p>Seedlings are yellowish-green, with hairs on the leaf sheaths and leaf margins. A key identification feature is the very broad leaves. The ligule is a low, papery rim, capped with short hairs.</p> <p>Mature plants are prostrate or ascending, up to 0.6 m tall, and tufted. Stems can sometimes take root where joints touch the ground.</p> <p>Seed occur in two rows on one side of the spike.</p>	<p>Leaves are usually hairy; especially on the margins, and margins are crinkled. The seed head has two to seven spikes arising from the main stem at well-spaced intervals.</p>

Table 2-3 Summary of weed control in past 50 years (Reeves 2008)

Year	Major impact
1970s	Herbicide decade – bipyridyls, selective pre and post-emergence herbicides developed
1980s	Minimum tillage decade – glyphosate, conservation tillage, oilseeds, pulse, crop intensification, more herbicides
1990s	Herbicide resistance decade – resistance, cross resistance, awareness, research, management strategies
2000s	Precision agriculture decade – seed band management, GPS/auto steer, water-use efficiency, 'new' species of resistant weeds; more herbicide resistance

Weed life cycles need to be understood to improve weed management (Widderick 2009).

Most of the weed species reported by Wood (2000) are annual plants that complete their cycle from

seed to seed in less than one year (Figure 2-2). In general, these plants germinate in spring continue to grow until summer when they flower and then die in the autumn.

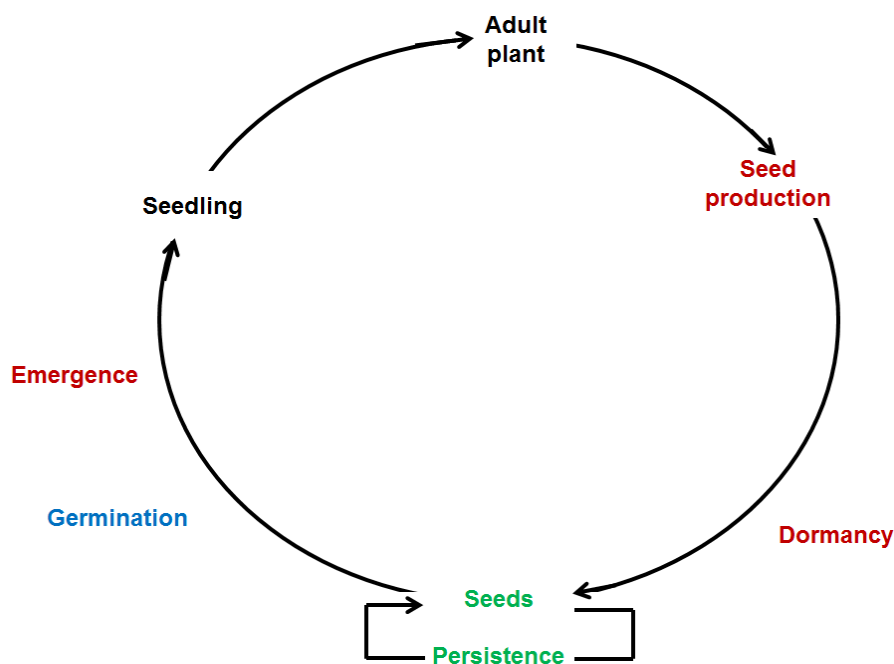


Figure 2-2 Life cycle of an annual weed (Widderick, 2009)

Sorghum is a C4 photosynthetic plant. C4 plants grow best under high temperature and optimum light conditions for photosynthesis. This achieves high growth rates and high dry matter production per unit of water used. The main concern from an agricultural perspective is competition with other plants (crop and weeds) for nutrients (nitrogen, phosphorus, and potassium) (Zimdahl 2013).

The similarities and differences between conventional chemical, automated precision chemical and mechanical weed control methods are summarised in Table 2-4. All weed control methods have limitations (De Baerdemaeker 2014). New approaches to weed control are needed to overcome the shortcomings of the present control methods. Novel approaches would ideally have less impact on the environment and the target crop and cost less. Technologies such as remote sensing and site-specific weed management (SSWM) could potentially meet this need (De Baerdemaeker 2014).

Site-specific weed management targets weed patches based on either the density of the weeds and or the species composition. This approach involves locating and mapping the position of the weeds. A map is used to direct precise application of the herbicides (Birch et al. 2011). This reduces the amount of chemical needed to control the weeds (Kunisch 2002; Lopez-Granados 2010). To achieve this, the patches of weeds need to be detected early enough to be controlled before they have an adverse effect on the crop (Andujar et al. 2012; Pena et al. 2013).

Table 2-4 Comparison of mechanical, conventional chemical and automated precision chemical weed control (De Baerdemaeker 2014)

Weed Control	Similarities	Differences
<ul style="list-style-type: none"> • Mechanical • Conventional chemical • Automated precision chemical 	<ul style="list-style-type: none"> • General crop and weed growth knowledge. • Optimal timing for control. • Extensive testing required. • Specialized and local knowledge. • Machine safety requirements. 	<ul style="list-style-type: none"> • Smaller working width for mechanical control. • Higher cost for mechanical control. • Few equipment manufactures for conventional weed control. • Chemical companies contribute to herbicide resistant (HR) weeds. • Automation requires less government approval. • Spacing and guidance critical for automation control system. • No synthetic chemicals can be used in organic production. • Closed canopy limits mechanical control. • Weed and pest control allows multiuse for chemical equipment.

2.2 WEED CONTROL SYSTEMS

2.2.1 Mechanical and thermal weed control

This approach uses mechanical or thermal control of weeds either because of the absence of chemical control equipment and or suitable chemicals or a desire to meet organic production requirements (Deng et al. 2010). Weeds can be mechanically uprooted by cultivation or thermally treated to kill them. Heat treatment is cost effective and causes minimal harm to the environment. However, it requires precise knowledge of where the weeds are in the field (Parsons et al. 2009) and an accurate tractor guidance system (Okamoto et al. 2014).

Haff et al. (2011) designed an automatic tomato weeding system that adopted a new technique called x-ray detection. The x-ray based system automatically identified the stem of the tomato plant and guided knives to cut the weeds without cutting the tomato plant stem (Haff et al. 2011). The knives were controlled by a signal from the x-ray detection equipment. The accuracy of identifying the tomato plants when the equipment was travelling at 1.6 kilometres per hour (km/h) was 90.7%. Integration of this technology with Real Time Kinematic Global Positioning System (RTK GPS) equipment may advance weed management.

2.2.2 Conventional chemical weed control

Herbicides are effective and popular for weed control and are necessary to maintain crop yield and quality (Harker et al. 2013; Pena et al. 2013). It is done by post emergence spot spraying

herbicides such as Atrazine plus, Fluroxypyr (Starane®, Rifle®, Tomigan®), Tordon 75D® + 2,4-D amine, Tordon 75D®, 2,4-D amine, Sempra® and Dicamba (Bullen 2002). The dosage of the herbicide depends on the type and size of crop and weed (Bullen 2002).

Chemical weed control can cause herbicide resistance, species shifts and changes in species dominance. It may cause damage to the crop and yield loss, herbicide resistance and increases in the cost of production (Peltzer et al. 2009). The main causes of herbicide resistance are application at the wrong stage of growth and spraying the whole area when there are only a few weeds at isolated spots (Lopez-Granados et al. 2015). Herbicide resistant weeds are very difficult to control. Table 2.5 shows the main herbicides to which resistance has developed and the crops in which the resistance occurs (Zimdahl 2013).

Table 2-5 Five herbicides and the crops in which resistant weeds occur in the world (Heap 2016 and Zimdahl 2013)

Herbicides	County	Resistant Crops
Bromoxynil	United State (US), Canada	Cotton, potato and tobacco
Glyphosate	Australia, US, Malaysia, South Africa, Chile, Brazil, Spain, Argentina, China, France, Colombia, Czech Republic, Paraguay, Italy, Mexico, Poland	Canola, corn, cotton, potato, soybean, tobacco and tomato
Glufosinate	US and Malaysia	Alfalfa, barley, canola, corn, creeping bentgrass, peanut, rice, sugar beet, sugarcane, soy bean and tomato
Sethoxydim	Australia, Canada, South Africa, United Kingdom, Mexico, Brazil, Italy, Iran, China	Corn
2,4-D Amine	Canada, Indonesia, Malaysia, New Zealand, Philippines, Spain, Hungary, Thailand	Cotton and potato

Consumers and farmers in Japan demand non-chemical or low-chemical agricultural production because they understand the environmental effects of using chemicals and want to preserve the world for future generations (Okamoto et al. 2014). Okamoto et al. (2014) recommended implementing a robotic weed control system that limits chemical usage in agriculture. However, this technology is expensive and still in the testing phase.

Precision weed control may be a solution to fill the gap between conventional chemical and automated mechanical weed control. Herbicide use can be reduced by specifically targeting the weed patches. To do this, the weed patches need to be accurately detected.

2.2.3 Precision weed control

The aim of precision application of chemicals for weed control is to reduce the amount of chemical used to control the weeds (Okamoto et al. 2014) by applying them to exactly where the weeds are located. Site-specific weed management has the potential to reduce herbicide use by 40 -

60%, decrease fuel consumption and increase farmer income (Jensen et al. 2012). Site-specific weed management is the integration of machinery or equipment embedded with technologies that detect weeds growing in a crop so as to maximize the chance of successfully controlling the weed (Christensen et al. 2009). There are four levels of spatial resolution for the control of weeds on a farm (Figure 2-3):

- Treatment of individual plants with highly accurate spraying nozzles, controllable mechanical implements or laser beams.
- Treatment of a grid adapted to the resolution, e.g. adjusting the spraying with a nozzle or a hoe unit.
- Treatment of weed patches or subfields with clusters of weed plants.
- Uniform treatment of the whole field.

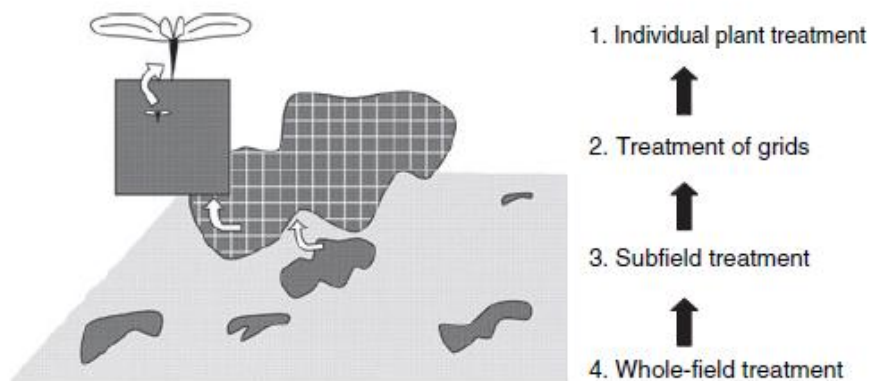


Figure 2-3 The spatial resolution of weed control in a field (Christensen et al. 2009)

There are three different ways of undertaking site-specific weed control (Figure 2-4).

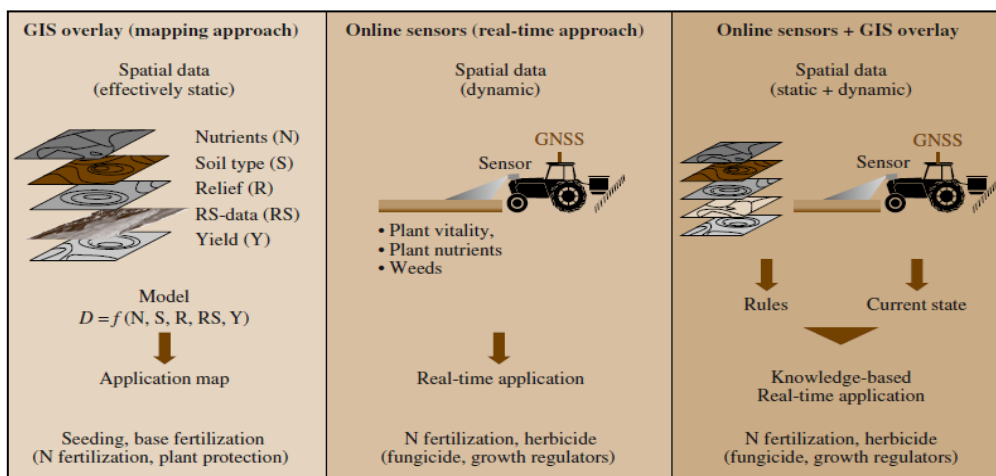


Figure 2-4 Three variations of precision farming strategies for site-specific weed control (Bill et al. 2012).

These methods can also be used to precisely control the input of fertilizers and pesticides as well as herbicides. The first method, GIS overlay, involves mapping the area ahead of time and using appropriate map overlays to generate a vector map to guide the application of crop inputs. The second method, online sensor, detects plant characteristics (crop or weed) and activates the application of nutrients or herbicides in real time. The third method, a combination of online sensor and GIS overlay methods, also produces application maps that can direct where to apply fertilizers, pesticides, growth regulators and herbicides (Bill et al. 2012). Numerous investigators recommended that methods to detect weeds accurately in crops be developed (Armstrong et al. 2007; Christensen et al. 2011; Everitt et al. 2011; Berge et al. 2012). Gumz (2007) recommended SSWM be developed to reduce the cost of weed control.

An alternative to SSWM is control of weeds through patch weed management. Patch weed management is the spraying of patches of weeds. It saves chemicals, reduces cost and has less effect on the environment (Agrawal et al. 2012) but is less specific than SSWM. In Norway, Berge et al. (2012) developed a novel machine vision algorithm, Weedcer to detect weed patches. This estimated the proportions of young weed leaves and cereal crop leaves in high resolution RGB images and used real-time site-specific spraying to control annual broadleaf weeds. Weedcer computes a set of significant features for each component, based on colour and a set of shape parameters (Berge et al. 2012).

2.2.3.1 Variable rate technology

Variable Rate Technology (VRT) uses field spatial information management variables to optimize agronomic inputs. VRT allows the use of the precise amount of herbicide required to control weeds. The components of a VRT system are a computer controller, GPS receiver, and Geographical Information System (GIS) database (map). The computer controller uses the map or database to adjust the application rate of the crop input. The location coordinates are used by the computer to monitor the system location of the applicator on the map. The computer controls the rate of input based on instructions from the GIS database map and these are applied as the applicator reaches the location of each weed recorded on the map. The exact quantity of herbicide applied at each location is determined by the weed map.

This reduces the amount of herbicide applied (Fernandes et al. 2014). For instance, in a potato field both mono and dicotyledonous weeds were detected by GPSMap 278 (Cepl and Kasal 2010) to produce a weed map. The weed map allowed herbicides to be sprayed only where the weeds were located thereby reducing herbicides uses, expenses and environmental exposure (Cepl and Kasal 2010). Cepl and Kasal (2010) found that 44% of conventional herbicide use could be saved based on the application map.

2.2.3.2 Detection systems

Advanced sensor-intensive technology and automation in crop production are expected to improve productivity and quality with minimal environmental impact (Lee et al. 2010). Plant nutrient, moisture level, soil condition and plant health can be monitored using remote or local sensor networks. However, to accomplish this, the information has to be collected with high spatial accuracy and at a high resolution. The three main steps in weed mapping are image acquisition, automatic image stitching of colour and binary images and photomosaicing (Liu et al. 2013). There are five groups of sensor-intensive technologies used in agricultural applications (Table 2-6).

Table 2-6 Sensor-based intensive technology (Lee et al. 2010)

Sensor-intensive technologies	Description
Novel control technologies.	Controlling chemical and nutrient use to reduce cost and environmental impact and improve worker safety.
Robotic and mechatronic operators.	Increase productivity and decrease labour cost. Example fruit thinning, pruning and harvesting.
Autonomous navigation systems.	Harvesting, spraying and utility vehicle. The sensors are sensitive to the local crop conditions.
Precision Agriculture.	Yield mapping, prediction, soil sensing, nutrient and pesticide application and irrigation control. Extensive use of sensors for targeting the local crop with accurate doses of chemicals.
Pest and disease monitoring.	Spaced-based or airborne remote sensing and ground based systems using proximal non-contact sensing.

It is becoming more common to use sensors for field data collection. These sensors are the latest technology for real-time weed identification and detection (Christensen et al. 2009). Common sensors used in crop detection include field electronic sensors, spectroradiometers, machine vision, airborne multispectral and hyperspectral imagery sensors, satellite imagery and thermal imaging sensors (Lee et al. 2010). Spectral reflectance, multispectral images and Normalized Differential Vegetation Index (NDVI) can be integrated to acquire reliable and accurate information about the condition of the field crop (Lan et al. 2009). UV-induced fluorescence sensors for weed detection allow real-time automatic spot spraying within a corn crop (Longchamps et al. 2010). Ultrasonic sensors that can be mounted on a tractor for weed discrimination (Andujar et al. 2011) work by measuring the density of grasses and broad leaved weeds. This method allows for real-time, spatially selective weed control techniques, either as the sole weed detection system or in combination with other detection tools.

GreenseekerTM is a commercial sensor, which has been used in crop management to collect red and near-infra red (NIR) in real time (Lan et al. 2009). The sensor is adjustable in 15 degree increments and is mounted on an adjustable-length pole to set the sensor parallel to the target canopy. The NDVI data was derived from the ratio of red to near infrared (Red/NIR) using the GreenseekerTM sensor. This indicated that GreenseekerTM could be used as an alternative to collect

the red and NIR spectral reflectance of plants to calculate NDVI and to correlate with other data such as visual weed control, weed dry matter and digital photography in the inter-row area of soybean and corn (Merotto Jr et al. 2012). The research showed that the NDVI positively correlated with the digital photography in weed leaf coverage (Merotto Jr et al. 2012).

Similar research has been done using Weedseeker® PhD600 (NTech Industries Inc. Ukiah, CA) to detect weeds in cotton (Sui et al. 2008). This method involves mounting the unit on a GPS guidance tractor. The spray nozzles are activated when the electronic signal detects weeds. They reported that it saved 80% of the annual herbicide cost (Hummel and Stoller 2002).

Detectspray is an optoelectronic sensor that uses 646 nm and 850 nm reflectance to distinguish weeds from soil (Biller 1998). Detectspray automatically sprays the weeds based on detection by the sensor. It reduced the usage of herbicides by 70%. Field Servers (FS) are a combination of the agriculture sensors (collecting field data) and wireless transmission that transmit the data to a central point.

These were implemented in Thailand and Japan for monitoring crop conditions (Lee et al. 2010, p. 9). Field servers are useful for monitoring crops using a Local Area Network (LAN) configuration. These are very expensive if they only serve a small number of the sensors (Lee et al. 2010). They reduced the amount of labour to monitor rice paddies especially for counting insects (Fukatsu et al. 2012). This was done using FS and high resolution digital cameras pointed at insect pheromone traps. The images and temperature records were sent wireless every 5 minutes to a central point where the insect count and images were analysed. Results show that monitoring based on the FS technique minimised human error and standardised data processing. This concept might be able to be applied to weed management by modification of the functions in the FS unit (Fukatsu et al. 2012).

2.2.4 Vegetation reflectance

Photosynthesis is the process that produces sugar for plants using the energy from sunlight. The green pigment chlorophyll absorbs the energy in sunlight, transforming it into functional chemical energy. The light energy is stored in simple sugar molecules (glucose) that are produced when carbon dioxide and water are combined to form sugar in the plant chloroplasts. “*Oxygen is released as a by-product*” (Jensen 2007, p. 356). Cellular respiration then uses these sugars to release energy which is stored as adenosine triphosphate (ATP) (Farabee 2007).

Remote sensing can measure the reflectance from the leaf of the incident electromagnetic energy and obtain information about the vegetation from the reflectance. Plants reflect NIR

radiation and absorb the visible wavelengths. Sensors can be used to measure the NIR spectrum.

Figure 2-5 shows the structure of a green plant leaf (Purves et al 2014).

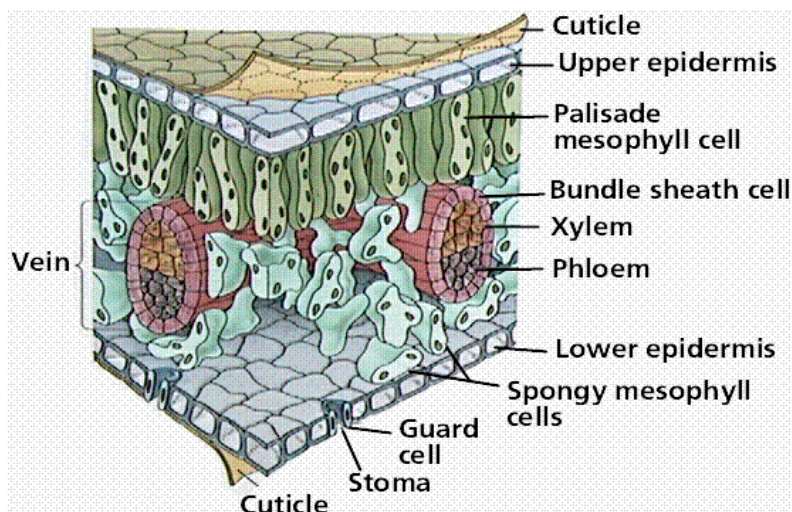


Figure 2-5 Hypothetical Leaf Cross-section (Purves et al 2014)

The stomata act as guard cells in controlling gaseous exchange in the leaves (Jensen 2007). Plants reflect visible and NIR radiation differently depending on the pigments in the leaf and the structure of the leaf (Purves et al 2014). The upper layer of cells, the epidermis, absorbs sunlight, which is then absorbed or reflected by other layers of cells depending on their structure and chemical composition. The palisade mesophyll, consisting of elongated cells arranged vertically, contains most of the chlorophyll. Chlorophyll is a protein responsible for capturing photons and powering photosynthesis (Jensen 2007). The spongy parenchyma is the lower level of cells in the leaf that primarily allows the circulation of gases.

The major biophysical and biochemical characteristics of vegetation that affect spectral reflectance are leaf area index (LAI), concentration of chlorophyll A and B, canopy structure and height, chemical composition of the biomass, water content, leaf nutrient concentration and evapotranspiration rate (Im and Jensen 2008; Arafat et al. 2013a). Chlorophyll absorbs light from the entire visible spectrum, except green wavelengths (Schliep et al. 2013). The most significant light absorption pigments and their absorption wavelengths are shown in Table 2-7 (Zwiggelaar 1998).

Table 2-7 Leaf pigment absorption

Pigments	Wavelength (nm)
Chlorophyll A	435, 670 - 680 and 740
Chlorophyll B	480 and 650
α -carotenoid	420, 440 and 470
β -carotenoid	425, 450 and 480
Anthocyanin	400 - 550
Lutein	425, 445 and 475
Violaxanthin	425, 450 and 475

Near Infra-Red, red-edge and Green regions are the optimal regions for discrimination between different species (Wilson et al. 2014). The position and magnitude of the red-edge zone depends on the amount and type of chlorophyll pigmentation in the leaf (Blackburn 2007). Reflectance from the NIR and red-edge regions produces the most accurate discrimination of aquatic weeds in the United States (Everitt et al. 2011).

Leaf structure and the processes that occur in it affect the spectral reflectance from it. Figure 2-6 shows the spectral profile of a typical green leaf.

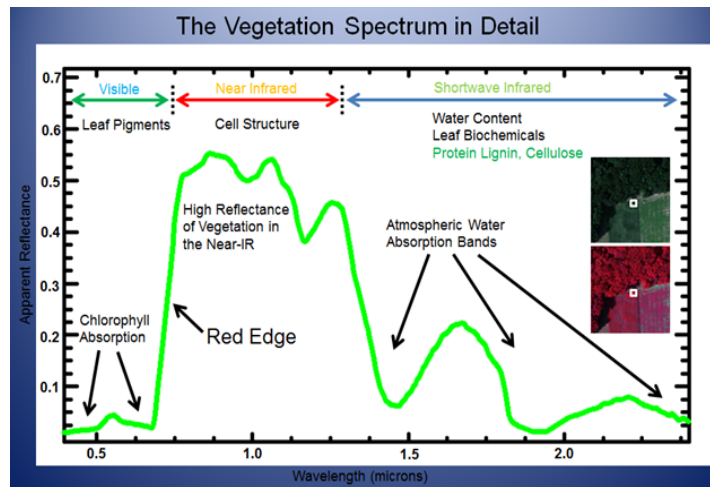


Figure 2-6 Vegetation spectrum in detail (Elowitz 2015)

This profile illustrates the high reflectivity in the NIR region and absorption in the Red region. The change in red-edge reflectance spectra is due to the change in anthocyanin pigment in the leaves. Table 2-8 shows the common spectral regions for typical plants (Jensen 2016, p. 315).

Table 2-8 The common spectral regions (Jensen 2016, p. 315)

Spectral Region	Wavelengths
NIR	0.73 – 1.30 μm
Red-edge	0.69 – 0.72 μm
Red	0.6 – 0.68 μm
Green	0.5 – 0.59 μm
Blue	0.4 – 0.49 μm

2.3 REMOTE SENSING FOR WEED MANAGEMENT

2.3.1 Hyperspectral reflectance for weed classification

Weed mapping is challenging because of the similarity in reflectance between the weeds and the crop. Hyperspectral sensing may provide a way to identify differences between weed and crop

plants. This approach has been shown to improve conventional methods of weed detection to cost effectively map invasive species (Glenn et al. 2005).

Reflectance spectroscopy and imaging techniques can be used to detect different types of plants. The differentiation is based on the differences in the plant's reflectance. The pigments inside the leaf and the leaf structure absorb and reflect light differently (Carter 1993).

Hyperspectral remote sensing is widely used for different agricultural applications such as soil analysis mapping (Gholizadeh et al. 2013), LAI analysis of agro-systems (Delegido et al. 2013), grassland species classification (Dale et al. 2013), disease detection (Calderon et al. 2013), plant stress (Carter 1993) and separation of crop species (Wilson et al. 2014). Multispectral imagery was used to estimate nitrogen content and predict grain yield at different stages of rice growth (Saberioon et al. 2013).

The higher spectral resolution of the imagery from hyperspectral sensors provides increased potential to discriminate weeds from crop plants (Psomas et al. 2005). Hyperspectral imagery was used to predict concentrations of macronutrients in pastures in the Kruger National Park, South Africa (Mutanga and Skidmore 2004) and different types of dry grassland in Switzerland (Psomas et al. 2005).

The difference in plant leaf structure and pigment influences the spectral reflectance of the plants (Lillesand et al. 2004, p. 20). The ability to discriminate between weeds and crop plants depends on their spectral separability (Batte and Ehsani 2006). Temporal variation, physical structure of the surface and leaf cell structure also affect spectral separation (Zwiggelaar 1998). Spectral and spatial data were successfully used to distinguish weeds and crop plants under laboratory conditions (Lamb and Brown 2001).

Many processing methods have been used to distinguish the reflectance of weeds from crop plants. These include Artificial Neural Network (ANN), Principal Component Analysis (PCA), Stepwise Linear Discriminant Analysis (SLDA) and Linear Discriminant Analysis (LDA) (de Castro et al. 2012; Eddy et al. 2013). A combination of two methods, ANN and PCA, produced the most accurate classification in discriminating between weeds and crop plants (Li and He 2008; Liu et al. 2010). Artificial Neural Network and Maximum Likelihood Classification (MLC) were tested to distinguish between redroot pigweed and wild oats in Southern Alberta, Canada. The results showed that ANN was more accurate for redroot pigweed and wild oats species (Eddy et al. 2008).

Principal Component Analysis and SLDA have been used to select wavelengths to separate different plant species (Yang and Everitt 2010b). These methods increased classification accuracy by 10%. Stepwise Linear Discriminant Analysis was used to select the significant bands to distinguish weeds from crop plants (de Castro et al. 2012). The comparison of spectral reflectance between two crops and five weed species was tested and produced 90% accuracy using SLDA and

LDA (Smith and Blackshaw 2003). The combination of Partial-Least-Square regression (PLS) and LDA to identify weeds in wheat showed good discrimination (Rabatel et al. 2011).

2.3.2 Remote sensing

Remote sensing is both the science and the art of obtaining information about features on the earth using equipment or devices without direct contact with the earth (Jensen 2005). Radiometric spatial information about the earth's surface can be acquired from either aircraft, UAVs or satellite platforms in digital form (Richards 2013). Visible and NIR imagery is available from many different sensors at many different resolutions. High-resolution satellite imagery (HRSI) was introduced in 1999 with the launch of the IKONOS satellite with a spatial resolution of 1 m for pan images. Since then other high-resolution satellites have been launched, such as EROS-A, QuickBird, Orbview-3, EROS-B, Worldview-1, GeoEye-1 and Worldview-2 (Crespi et al. 2011) and WorldView-3.

Table 2-9 shows the advanced sensors and platforms potentially available for collecting imagery for Site-Specific Weed Management.

Table 2-9 Some of the current sensors and platforms with spatial and spectral resolutions potentially useful for SSWM imagery (Lopez-Granados 2010)

Sensor and platforms	Spatial resolution (m)	Waveband interval (nm)	Altitude (km)	Revisit time (Days)
Multispectral satellite				
IKONOS	4*	450-900 [†]	681	1.5
QuickBird	2.44*	450-900 [†]	450	1-3.5
WorldView II	0.46*, 1.85	396-808	681	3
WorldView III	0.31*, 1.24	400-1040	617	<1.0
GeoEye-1 (former OrbView5)	1.64*	450-920 [†]	681	2.1-2.8
Aircraft				
Daedalus 1268	3.44 [§]	420-13000 [¶]	1.37	
Conventional turboprop	0.30	400-900**	1.52	
Drone				
Unmanned aerial vehicle (UAV)	0.15 [§]	490;530;570;670;700;750;800 ^{††}	0.15	
Hyperspectral airborne				
AVNIR [#]	1	430-1012 (10 nm)	1.5	
CASI	1-3 [§]	400-1000 (1.9 nm)	0.84-3.5	
AHS	2-3.44 [§]	430-12500 (13-300 nm)	1-1.37	
HyMap	2	450-2500 (20-10 nm)	2	
AVIRIS	4	400-2500 (10 nm)	3.8	

*1, 0.61, and 0.5 m spatial resolution in Panchromatic for IKONOS, QuickBird and GeoEye respectively.

[†]Bands: Blue, 450–520; Green, 520–600; Red, 630–690; Near-infrared, 760–900.

[‡]Bands: Blue, 450–510; Green, 510–580; Red, 650–690; Near-infrared, 780–920.

[§]Spatial resolution depends on flight altitude and camera field of view (FOV). Some examples as follows: angular FOV of 85.92° and 1.376 km flight altitude yield 3.44 m pixel for Daedalus and AHS; angular FOV of 42.8° x 34.7° and 0.150 km flight altitude generate 0.15 m pixel size for UAV; angular FOV of 60° and 2 km flight altitude yield 2 m pixel for Hymap. For Hyperspectral imagery, pixel size can also depends on the program to capture the image

[¶]Fixed channels of Daedalus 1268: 420–450; 450–520; 520–600; 600–620; 630–690; 690–750; 760–900; 910–1050; 1550–1750; 2080–2350; 8500–13000.

**Bands: Blue, 400–500; Green, 500–600; Red, 600–700; Near-Infrared, 700–900.

^{††}These channel centres are just an example

[#]AVNIR, Airborne Visible and Near-Infrared; CASI, Compact Airborne Spectrographic Imager; AHS, Airborne Hyperspectral Scanner; AVIRIS, Airborne Visible/Infrared Imaging Spectrometer.

Multispectral broadband sensors acquire images in 3 - 7 bands of around 100 nm width, while hyperspectral sensors identify narrower and contiguous wavelength bands that are usually < 10 nm in width. Small variations in reflectivity can be detected in hyperspectral images because the bandwidths are very narrow. Multispectral bands are broader and each band is less sensitive to specific plants and objects (Lopez-Granados 2010). The suitable pixel size is based on the smallest discernible object. This determines the spatial resolution for the image.



Reflectance spectra respond uniquely to plant species at the canopy or single-leaf scale and can be used in calculations to classify the species (Lopez-Granados 2010). Vegetation indices such as NDVI, Excess green (ExG), Color index of vegetation (CIVE) and generic algorithms (GA) can be calculated from the imagery. Generic Algorithm analysis has been successfully used in Hue-Saturation-Intensity (HIS) analysis for weed detection in soybeans (Tang et al. 2000).

2.4 IMAGE COLLECTION

2.4.1 Unmanned Aerial Vehicles

Unmanned Aerial Vehicles (UAV) are small planes or helicopters, sometimes called DRONES (Dynamic Remotely Operated Navigation Equipment) operated by remote control that can be used to capture imagery. Table 2-10 shows the different types of UAVs and the benefits and limitations of each type (Sankaran et al. 2015).

Table 2-10 Typical types of small unmanned aerial vehicles.^a (Sankaran et al. 2015)

Type	Payload ^b (kg)	Flight time ^b (min)	Benefits	Limitations	Examples ^a
Parachute	1.5	10-30	<ul style="list-style-type: none"> • Simple operation 	<ul style="list-style-type: none"> • Not operable in windy conditions • Have limited payload 	HawkEye
Blimps	>3.0	~600	<ul style="list-style-type: none"> • Simple operation 	<ul style="list-style-type: none"> • Not operable in windy conditions • Have limited payload 	AB1100, Cameron Fabric Engineering
 Rotocopter	0.8–8.0	8–120	<ul style="list-style-type: none"> • Applicable with waypoint navigation • Hovering capabilities • Can hold range of sensors from thermal, multispectral to hyperspectral cameras 	<ul style="list-style-type: none"> • Payload may limit battery usage and flight time 	DJI Inspire, Mikrocopter ARK OktoXL 6S12, Yamaha RMAX
 Fixed wing	1.0–10	30–240	<ul style="list-style-type: none"> • Better flight time • Multiple sensors can be mounted • Limited hovering capacity 	<ul style="list-style-type: none"> • Lower speeds are required for image stitching 	Landcaster Precision Hawk, senseFly eBee

^a This provides an overview of different UAV platform types and there may be many commercial companies developing similar types.
^b Approximate values taken from manufacturer specification.

The spectral and spatial resolution of the images depends on the sensors carried by the UAV. It is not necessary to use expensive sensors to map an area because it can be done using a typical digital camera such as a Canon 550D 15 Megapixel, DSLR (Digital Single-Lens Reflex), with a Canon EF-S 18-55 mm F/3.5 – 5.6 IS lens (Turner et al. 2012). However, to detect the occurrence of specific diseases, pests and weeds, it is necessary to use a multispectral or thermal sensor camera (Berni et al. 2009a; Rey et al. 2013). The type of sensor should be matched to the type of information to be collected. The sensors can collect higher spatial resolution imagery than satellite sensors and at a lower cost (Torres-Sanchez and Lopez-Granados et al. 2013). There are many different sensors used in agricultural applications (Table 2-11).

Table 2-11 Different types of sensors used in plant phenotype characterization (Sankaran et al. 2015) (continued)

Sensor type	Details	Applications	Limitations	References ^a
Fluorescence sensor	Passive sensing-visible and near infrared regions	Photosynthesis, chlorophyll, water stress	<ul style="list-style-type: none"> • Not developed for UAV research yet • Can be subject to background noise 	(Chappelle et al. 1984; Gamon et al. 1990; Flexas et al. 2000; Evain et al. 2004; Xing et al. 2006; Chaerle et al. 2007)
Digital camera (RGB)	Gray scale or RGB colour images (texture analysis)	Visible properties, outer defects, greenness, growth	<ul style="list-style-type: none"> • Limited to visual spectral bands and properties 	(Lu et al. 2011; Kipp et al. 2014; Klodt et al. 2015)
Multispectral camera /colour-infrared camera	Few spectral bands for each pixel in visible-infrared region	Multiple plant responses to nutrient deficiency, water stress, diseases	<ul style="list-style-type: none"> • Limited to few spectral bands 	(Moshou et al. 2005; Blasco et al. 2007; Lenk et al. 2007; Svensgaard et al. 2014; Zaman-Allah et al. 2015)
Spectrometer	Visible-near infrared spectra averaged over a given field-of-view	Detecting disease, stress and crop responses	<ul style="list-style-type: none"> • Background such as soil may affect the data quality • Possibilities of spectral mixing • More applicable for ground-based systems 	(Carter 1993; Delwiche and Graybosch 2002; Belasque Jr et al. 2008; Naidu et al. 2009)
3D camera	Infrared laser based detection using time-of-flight information	Physical attributes such as plant height and canopy density	<ul style="list-style-type: none"> • Lower accuracies • Field applications can be limiting 	(Jin and Tang 2009; Chene et al. 2012)
LiDAR (Light Detection and Ranging) sensor	Physical measures resulting from laser (600–1000 nm) time-of-flight	Accurate estimates of plant/tree height and volume	<ul style="list-style-type: none"> • Sensitive to small variations in path length 	(Donoghue et al. 2007; Koenig et al. 2015; Müller-Linow et al. 2015)

Table 2-11 (continued) Different types of sensors used in plant phenotype characterization (Sankaran et al. 2015)

Sensor type	Sensor type	Sensor type	Sensor type	Sensor type
SONAR (Sound Navigation and Ranging) sensor	Sound propagation is used to detect objects based on time-of-flight	Mapping and quantification of the canopy volumes, digital control of application rates in sprayers or fertilizer spreader	<ul style="list-style-type: none"> • Sensitivity limited by acoustic absorption, background noise, etc. • Lower sampling rate than laser-based sensing 	(Tumbo et al. 2002)
Hyperspectral camera	Continuous or discrete spectra for each pixel in visible-infrared region	Plant stress, produce quality, and safety control	<ul style="list-style-type: none"> • Image processing is challenging • Sensors can be expensive 	(Moshou et al. 2005; Delalieux et al. 2007; Gowen et al. 2007; Qin et al. 2009; Seiffert et al. 2010)
Thermal sensor or camera	Temperature of each pixel (for sensor with radiometric calibration) related to thermal infrared emissions	Stomatal conductance, plant responses to water stress and diseases	<ul style="list-style-type: none"> • Environmental conditions affect the performance • Very small temperature differences are not detectable • High resolution cameras are heavier 	(Chaerle and Van Der Straeten 2000; Leinonen and Jones 2004; Jones et al. 2009b; Costa et al. 2013)

UAVs are used in many applications such as forestry (Wallace et al. 2012), rangeland ecology research (Chang et al. 2004; Mancini et al. 2013) and agriculture (Nebiker et al. 2008; Berni et al. 2009b; Gay et al. 2009; Laliberte et al. 2011; Delegido et al. 2013; Leon and Woodroffe 2013). Additional features include temporal flexibility, data streaming, real-time processing, on-demand imagery and reduced costs compared to the alternatives (Knipling 1970; Swain et al. 2007; Berni et al. 2009b; Eisenbeiss and Sauerbier 2011; Wallace et al. 2012).

Applications of remote sensing using UAVs have increased recently (Laliberte et al. 2011). Goktogan et al. (2010) cited the work of Herwitz et al. (2002) who showed the potential of precision agriculture to use a solar-powered Pathfinder-Plus UAV developed by NASA and AeroVironment. This is a high altitude machine fitted with both multispectral and hyperspectral imaging systems used in Kauai Coffee Plantations.

Another example is X-Copter, a UAV for rice monitoring and management. It can carry up to a 30 kg payload and fly for more than an hour (Shim et al. 2009). It is very convenient for agricultural purposes because it is fitted with a pump system. The flight computer controls the pump to apply fertilizer in an accurate way. This provides an opportunity for farmers to save labour cost (Shim et al. 2009).

UAVs are capable of capturing imagery in high risk situations. They can also be flown below clouds and in light rain. (Berni et al. 2009). A further big advantage is that they are not limited by physiological conditions that would affect human pilots of light planes. FieldCopter is a UAV that can carry multispectral sensors for soil and crop analysis (Van der Wal et al. 2013). It is capable of flying and capturing imagery in more than 70% of weather conditions compared to satellite imagery.

The weight and size of sensors is the main limitation on the use of low cost UAVs. The small or medium format UAVs are normally less stable under windy condition than the larger UAVs and their navigation control systems are not as accurate (Sankaran et al. 2015). Other considerations for lower cost UAVs include flight-path planning systems, control under high speed conditions, low altitude of flight and data downloading during the flight (Yan et al. 2009). For instance, the low-altitude platform utilising a 1.8 m diameter medium balloon was used to position a multispectral sensor in a wheat crop. Although the data collection was low-cost and simple, the results show a high correlation between the aerial imagery and the grain yield and strong correlation between imagery and grain protein (Jensen et al. 2007).

Good imagery depends on the UAV, sensor types and flight plan (Sankaran et al. 2015). All aspects need to be considered before flying any UAV applications. In addition geometric correction and geocoding are also important into producing an accurate weed map (Xiang and Tian 2011). Xiang and Tian (2011) developed automatic georeferenced images and found the position error to be less than 90 cm. This is considered high enough accuracy for site-specific application. The accuracy of the geo-referencing of the images depends on the altitude of the UAV. At altitudes of 30 to 100 m, a moderate number of control points results in a high accuracy georeferenced image but if the flying height is above 100 m, the GCPs need to be arranged systematically for ortho-mosaicing (Gomez-Candon et al. 2014).

Image pre-processing such as image alignment and orthorectification is important before in-depth processing of image analysis. Image analysis for weed detection in crop plants is challenging if pre-processing is done poorly. An accurate weed map will be produced by a proper and specific configuration of UAV planning. High spectral resolution of the sensors also influences the usefulness of the imagery for weed detection.

2.4.2 Ground mounted systems

Weed mapping by analysing ground-based images was initially started in Germany (Schuster et al. 2007). A camera was mounted on a tractor to collect imagery for a 76 ha sugar beet crop. The imagery was processed using both semi and automatic weed mapping procedures to

compare it with manual weed mapping. This method employed six major steps to automatically detect and discriminate plants. It began with loading the RGB image and transforming it to another colour space, followed by frame detection before a binarisation process (choice of a threshold). Next, there is detection of the region of interest (plants), a feature extraction process and finally, plant allocation (Figure 2-7). The result showed that automatic weed mapping could be expanded to an online system for site-specific herbicide application.

Another technique to produce a weed map is by using machine vision to provide image based precision guidance. It is a low cost sensor attached to a tractor that detects three basic colours such as red (~ 600 nm), green (~ 550 nm) and blue (~ 450 nm) and can be used for site-specific weed management (Lee et al. 2010).

Another successful example was tested in the greenhouse to detect rows of sugar beets (Bakker et al. 2008). It used a Basler 301fc (0.3 Megapixel) colour camera. The images were processed using the Hough transform (Bakker et al. 2008) to recognize the straight rows. This method may be useful to detect weeds after definition of the crop row because the weeds can be easily identified in the inter-row part of the image.

The advantage of ground mounted, real time application systems are that applications can be modified based on user intervention. Variable illumination due to time of day and weather conditions limit (Bakker et al. 2008) applications or requires the use of an artificial source of illumination (Martin et al. 2011).

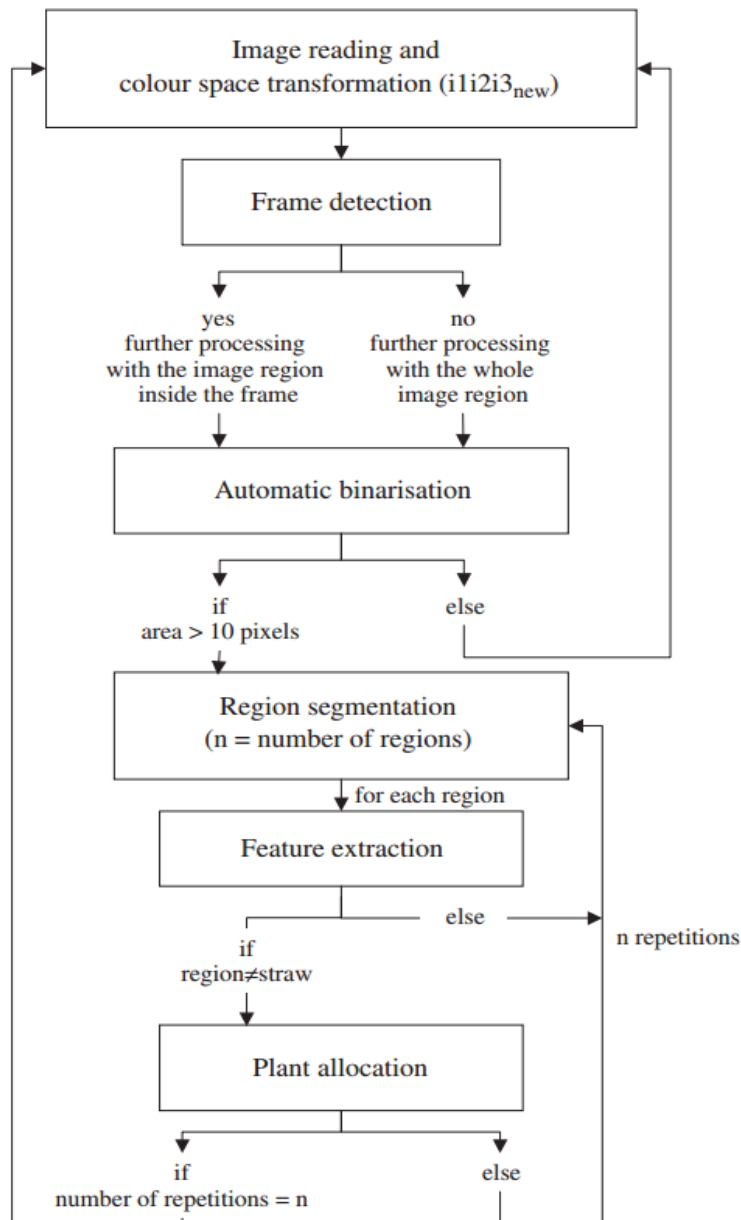


Figure 2-7 Flowchart of the process of plants detection and discrimination (Schuster et al. 2007)

2.5 IMAGE PROCESSING

Image processing procedures offer various ways to produce maps from imagery such as rangeland maps (Laliberte et al. 2011), yield maps (Smit et al. 2010), irrigation maps (Sankaran et al. 2015), vegetation monitoring maps (Berni et al. 2009; Johansen et al. 2010; Aziz 2014; Aasen et al. 2015; Kamal et al. 2015), and weed maps (Andujar et al. 2011; Birch et al. 2011; Pérez-Ortiz et al. 2015). Spectral Mixture Analysis (SMA) was used to map invasive aquatic vegetation using hyperspectral imaging (Underwood et al. 2006). This method discriminated between native and

invasive species in the Sacramento-San Joaquin Delta. They achieved high accuracy for identification of Brazilian waterweed and water hyacinth species at 93% and 73% respectively.

Another procedure for weed detection is Mixture Tuned Matched Filtering (MTMF). MTMF uses hyperspectral imagery to discriminate weeds from crop plants (Glenn et al. 2005). Moshou et al. (2013) also used hyperspectral imagery and achieved 98 % and 94 % accuracy in weed discrimination using a Mixture of Gaussian (MOG) and Self Organising Map (SOM) classifiers respectively. Torres-Sospedra and Nebot (2014) detected weeds in orange groves using Neural Network (NN) analysis. This approach was used to determine the main features in the grove and to separate the weeds from the soil. Linear discriminant analysis (LDA), multilayered NN, and Principal Components Analysis (PCA) procedures successfully discriminated weeds and crop plants in Asian crops (Okamoto et al. 2014). Sub-pixel component analysis was used to map patches of weeds in coarse resolution imagery (Quickbird and IKONOS) (Gillieson et al. 2006). Smit et al. (2010) combined thresholding and graph based techniques to classify and enhance images of rows of vines obtained with artificial light.

Steward and Tian (1999) used applied segmentation for detecting rows in soy bean crops. First, they normalised the hue, saturation and intensity (HSI) components of the image (0-255) to transform the RGB image data into HSI image space. After normalisation, they used a genetic algorithm (GA) to segment the image into plant and background regions. This produced an equivalent performance to cluster analysis and suggests that such an approach could overcome the effects of variable outdoor lighting condition.

The high resolution in large scale imagery is an essential feature for detecting weeds (Mesas-Carrascosa et al. 2015). Unmanned Aerial System (UAS) were used to collect the imagery to detect weeds in crops (Pena-Barragan et al. 2012a). Low altitude remote sensing (LARS) systems are currently attractive tools for site specific farm data collection (Saberioon et al. 2014). LARS systems are also capable of collecting high temporal as well as spatial resolution imagery (Laliberte et al. 2011; Saberioon et al. 2014). Different spatial resolutions using VIA also show that higher spatial resolution produces more accurate classification. This is consistent with Kamal et al. (2015), who found that low-resolution images had limited ability to depict mangrove features compared with high-resolution images. Figure 2-8 illustrates the relationship between accuracy of the classification and spatial and spectral resolution. This demonstrates the relationship between spatial and spectral resolution, number of classes and classification accuracy. A higher spatial resolution produces a high accuracy.

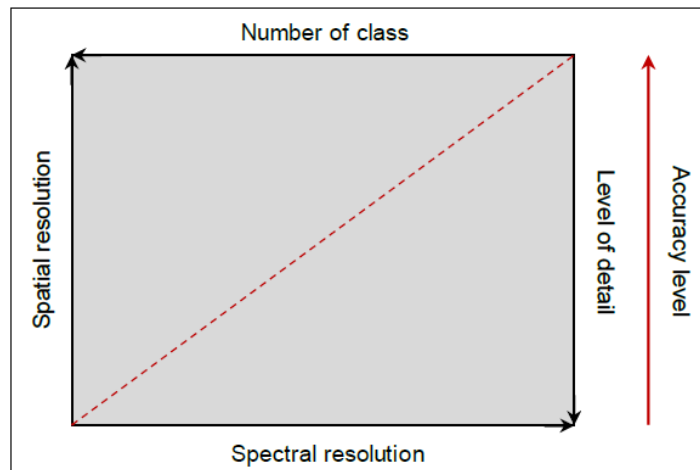


Figure 2-8 Relationship of image resolutions, level of information detail and map accuracy (Kamal et al. 2015)

2.5.1 Weed detection image processing procedures

Image processing procedures for weed detection are challenging due to occlusion, poor contrast between leaves of the crop and weeds, and random plant and leaf orientations (Lamb and Brown 2001). Both hyperspectral and multispectral remote sensing technologies have the potential for detecting weed infestations and nitrogen stresses in crops (Goel et al. 2003). The differences in spectral signatures between different species and plants under different physiological conditions provide a basis for their detection (Zwiggelaar 1998). The similarity in morphological and spectral characteristic of plants requires high resolution imagery to resolve.

There are a number of processing techniques used for detecting weeds from imagery (Penuelas et al. 1993). These include Maximum Likelihood Classifier (MLC) (Noonan and Chafer 2007), Maximum Matching Feature (MMF), Support Vector Networks (SVN), Spectral Angle Mapper (SAM) segmentation (Nicolai et al. 2007), Self-Organizing Maps (SOM) (Manevski et al. 2011), Object-Based Image Analysis (OBIA) (Torres-Sánchez et al. 2015), Neural Network Classifier (NNC) and Principle Component Analysis (PCA) (Almeida and Filho 2004; Golzarian and Frick 2011).

Classification of images of wheat, ryegrass and brome grass species at early stages using PCA has been successful (Golzarian and Frick 2011). The combination of colour, texture and shape has been used to discriminate ryegrass and brome grass using PCA. Results showed that PCA could discriminate weeds up to 85% accurately.

SPOT5 XI (10 m) satellite imagery was used for four classification regimes for mapping willows at the catchment scale by the different classification methods (Noonan and Chafer 2007). The first step was ML classification to distinguish between autumn and winter images. Secondly, ML classifies the bi-seasonal composition image. Thirdly was a SAM classification of a minimized

noise fraction (MNF) transformation of the multi-season composite image. Final, SAM classification was of a 5 x 5 median filtered MNF transformation of the multi-season composition image. MNF transformation is a modified version of the PCA that aims at segregating noise in the image data. The classification accuracy had a kappa = 0.58 and 0.34 for SAM-MNF and ML respectively. However, the classification accuracy for the SAM-MNF increased to 75% after using a 5 x 5 median filter. The spectral separability of willow from SPOT5 imagery was limited. This could be tested using higher resolution satellite imagery such as QuickBird (DigitalGlobe) or WorldView II to test the ML classification method (Noonan and Chafer 2007).

QuickBird imagery was used successfully in mapping giant reeds (*Arundo donax*) in Mexico using 4 spectral bands, blue, green, red, and NIR with a spatial resolution at 2.4 m (Yang et al. 2011). Three classification methods, minimum distance, Mahalanobis distance and MLC were used to classify water, giant reeds and mixed cover using ERDAS IMAGINE software (Yang et al. 2011). All classification methods produced a highly accurate classification (> 90%).

Another similar method was used to map broom snakeweed (*Gutierrezia sarothrae*) in western North America (Yang and Everitt 2010a). A comparison between three types of images, airborne hyperspectral imagery, aerial colour-infrared (CIR) imagery and multispectral digital imagery using MNF distance, Mahalanobis distance, ML, and SAM classification showed that ML produced the most accurate classification, mapping more than 90% of snakeweed accurately

Hough transform and Gabor filtering were used to detect weeds from virtual digital camera images (Jones et al. 2009a). Both methods were compared for row-crop weed discrimination in wheat. The Hough transform was more accurate than Gabor filtering producing a 90% accurate classification.

Object-based image analysis was also used to detect weeds in maize (Pena-Barragan et al. 2012a; Pena et al. 2013). A MCA 6 camera was used to collect the imagery (Pena et al. 2012a). The OBIA technique began by calculating row orientation, followed by discriminating between vegetation and bare soil, defining seed-objects, identification and classification of the first crop row and identification and classification of the remaining crop rows. It achieved an accuracy of 90% classification for satellite imagery.

2.5.2 UAV weed identification applications

A rotary UAV was used for surveillance and management of aquatic weeds in the east coast of Australia as a cost-effective technique (Goktogan et al. 2010). Image processing was done using a SVM approach and transferred into vector data format. The spatial resolution at the flying height

of 30 m was 2 cm. A similar resolution was used to successfully map weeds in a maize crop. (Pena et al. 2013 and Perez-Ortiz et al. 2015).

In Italy, the first research using UAVs for mapping was successful in vineyard plant vigour based on NDVI (Primicerio et al. 2012). The UAV was a six-rotor machine that flew autonomously. A multi-spectral camera and a spectroradiometer were used to capture imagery and record the hyperspectral reflectance data respectively. Higher NDVI values indicated higher plant vigour (Fernandes et al. 2014).

Weeds were detected with 99% accuracy from multispectral imagery collected at 30 m height using a micro-drone (md4-1000) in maize (Pena-Barragan et al. 2012a). A similar approach using the same UAV for site-specific (Torres-Sanchez et al. 2013a) weed mapping in an early stage of maize (Pena et al. 2013; Pena et al. 2015). This showed that the spectral and spatial resolution of the imagery is important to map weeds in the crop plants. Additionally, the early growing season was found to be very suitable for collecting data because the weeds were small and the UAV could fly at a low altitude to capture high spatial resolution imagery (Torres-Sanchez et al. 2013a). This showed that five – six true leaves allowed for higher accuracy weed detection. This allows the weeds to be identified early. The configuration and specification of the UAV are important to facilitate collection and detection of weeds in the crop at an early stage (Torres-Sanchez et al. 2013a).

2.5.3 Multispectral imagery for weed discrimination

Multispectral imagery is not as common as RGB imagery in the literature reports (Laliberte et al. 2011). Multispectral imagery has more bands than RGB imagery but less than hyperspectral which has hundreds of bands to choose from (Lee et al. 2010, p. 4). The Tetracam camera offers the opportunity to change the combination of band filters to match particular applications. They are available in 12, 6 and 4 sensor models (MCA) (Torres-Sanchez et al. 2013a; Lopez-Granados et al. 2015) and the Agricultural Digital Camera (ADC) model (Saberioon et al. 2013) which has three bands.

The MCA 6 (6 band model) camera was used successfully to map weeds in sunflowers with 100% accuracy at a 15% weed threshold using a UAV flown at 30 m altitude (Lopez-Granados et al. 2015). The 10 nm spectral bands (mid-point) were blue (B: 450 nm), green (G: 530 nm), red (R: 670 and 700 nm), red-edge (red-edge: 740 nm) and NIR (NIR: 780 nm). Different spectral bands were used to collect imagery in maize. These were 530, 550, 570 nm for green, 670 nm for red, 700, 800 nm for NIR (Pena-Barragan et al. 2013). They produced an accuracy of 86% at 30 m altitude (Pena-Barragan et al. 2013).

These studies established that multispectral imagery can be used to identify and detect weeds in crops. Most of the applications used the MCA 6 camera from Tetracam (Pena-Barragan et al. 2013; Torres-Sanchez et al. 2013a; Torres-Sanchez et al. 2014; Bueren et al. 2015; Lopez-Granados et al. 2015; Perez-Ortiz et al. 2015; Torres-Sánchez et al. 2015).

Weed mapping in sugar beets (Garcia-Ruiz et al. 2015) used 10 nm wide band-pass filters of 488, 550, 610 and 675 nm for the visible region and 70 and 940 nm for the NIR region in a MCA 6 camera. The spectroradiometer data measured defined the relationship of the significant spectra in the images. It used segmentation analysis to classify vegetation and non-vegetation classes by using NDVI. A Partial Least Square-Discriminate Analysis (PLS-DA) model was used to construct the best images by targeting highly significant bands for discrimination. The Regions of Interest (ROI) was selected from the images to build the calibration library. It showed that weed and crop plants can be classified using UAV multispectral imagery. It was more than 95% accurate.

In Japan, weed mapping was done successfully using an airborne digital sensor system (ADS40; Pasco Company, Tokyo, Japan) in a citrus orchard (Ye et al. 2007). It used 430 – 490 nm for blue, 535 – 585 nm for green and 610 – 660 nm for red regions with a spatial resolution of 0.2 m. An object-oriented approach was used to classify the image using eCognition Elements 4.0 (Definiens Imaging, Munchen, Germany) with 99% accuracy.

2.6 CONCLUSIONS

As a conclusion, weed management is a major issue in agriculture. The cost of managing weeds in agriculture is very high due to farmer's practices where they typically apply the registered rate of chemical herbicide to the entire field. In the long term, this method negatively affects the crop, the environment and also increases weed resistance to herbicides. Thus, more cost effective and efficient methods with a lower environmental effect need to be developed for more sustainable farming.

Hyperspectral reflectance data has the potential to identify weeds from crop plants. By using a portable spectroradiometer, the hyperspectral reflectance of weeds can be collected. Each weed species gives different spectral signatures that help to discriminate between weed and crop plants. Based on the spectral profile, different curves can be seen for different species. A review of literature also found that Stepwise Linear Discriminate Analysis (SLDA) was one of the techniques to discriminate spectral signature for weed species. It provides a way to identify specific and unique bands for each species. These bands can then be used to select suitable band-pass filters for use in a multispectral camera for imagery collection.

Unmanned Aerial Vehicles (UAVs) can be used to collect multispectral imagery of the crop with a high spatial resolution at early growth stages. The specific bands that were uniquely associated with the weed species were used in image processing to maximize weed classification. For example, 740 nm bands might improve spectral based discrimination of sugar beet and thistles (Garcia-Ruiz et al. 2015). The imagery can be processed to produce a weed map which provides the location of the weeds using Object based image analysis (OBIA). This is a new technique for weed detection and only a few investigators have used this technique for weed detection. OBIA is potential a very suitable technique for weed detection because of its capability in detecting shape and spectral reflectance at the same time. Farmers can potentially use this information to apply herbicide to the weeds more precisely and this can reduce the amount of herbicide used thereby reducing production costs and minimising environmental impact.

The next chapter will discuss the general methodology for this research. The details of the methods will be explained in depth in the three research chapters (Chapter 4, 5 and 6).

Chapter 3

GENERAL METHODOLOGY

3.1 INTRODUCTION

This chapter describes the research methods used to develop a weed map for sorghum from imagery. The research investigated the spectral profile of weeds and sorghum from 2012 to 2014. This information was used to determine the spectral differences between the weeds and sorghum plants. These differences were used to select filters for taking the multispectral imagery of the sorghum.

Multispectral imagery was collected at different stages of crop and weed growth and at different spatial resolutions. At the same time, the moisture content of the weeds and crop was sampled to test for the effect of moisture on reflectance. The multispectral imagery was pre-processed, followed by analysis to discriminate weeds from sorghum plants. This analysis formed the basis for mapping the weeds in the sorghum crop.

The following sections outline the general methods and procedures common to all phases of the research. Detailed procedures specific to each technical chapter (Chapters 4, 5 and 6) are provided at the beginning of each of those Chapters.

3.2 OVERVIEW

This chapter outlines the procedures and techniques used to collect and process the preliminary data. It summarizes three years (2012 to 2014) of research on detecting weeds in sorghum at the University of Queensland (UQ) farm at Gatton, Queensland. The details of the study area, field layout and data collection are shown in Figure 3-1. An overview of the spectral data collection is shown in Figure 3-2.

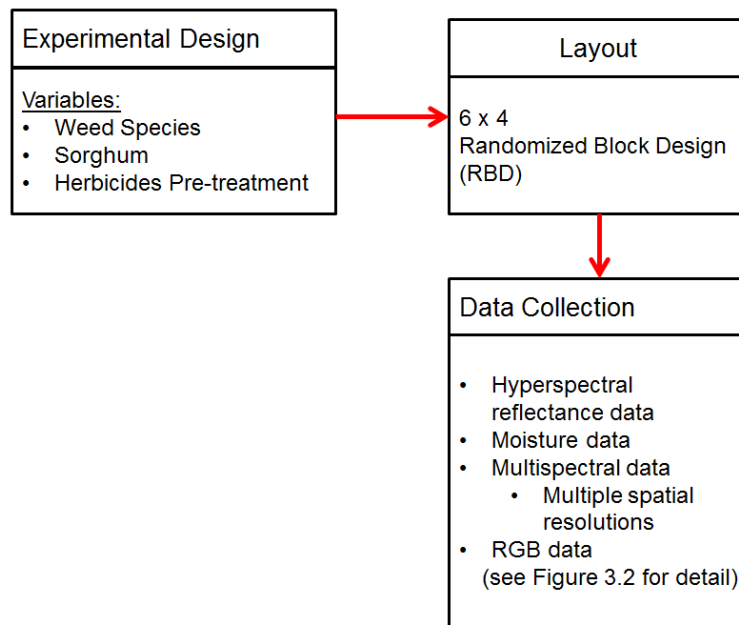


Figure 3-1 Details of the data collection

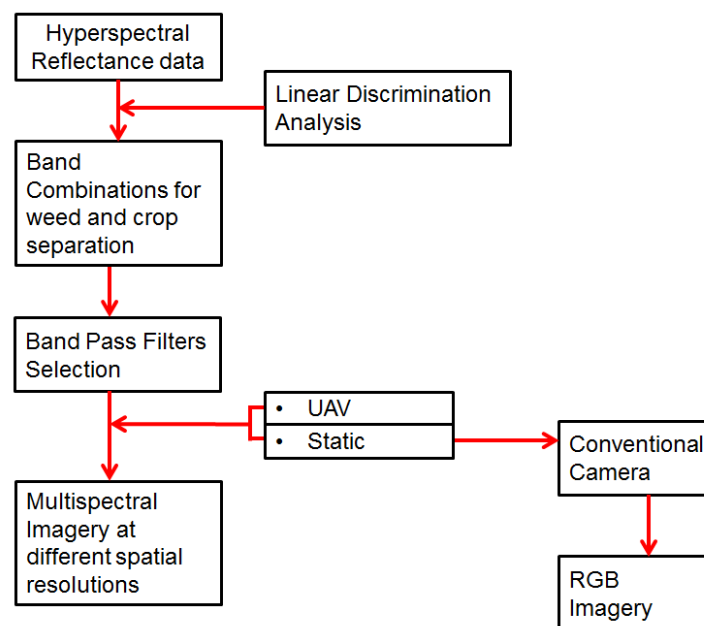


Figure 3-2 Overview of the spectral data collection

The leaf moisture content and spectral data were processed to develop the weed mapping procedures as shown in Figure 3-3. The details of the pre-processing, statistical analysis and image processing are discussed in Chapters 4, 5 and 6 respectively.

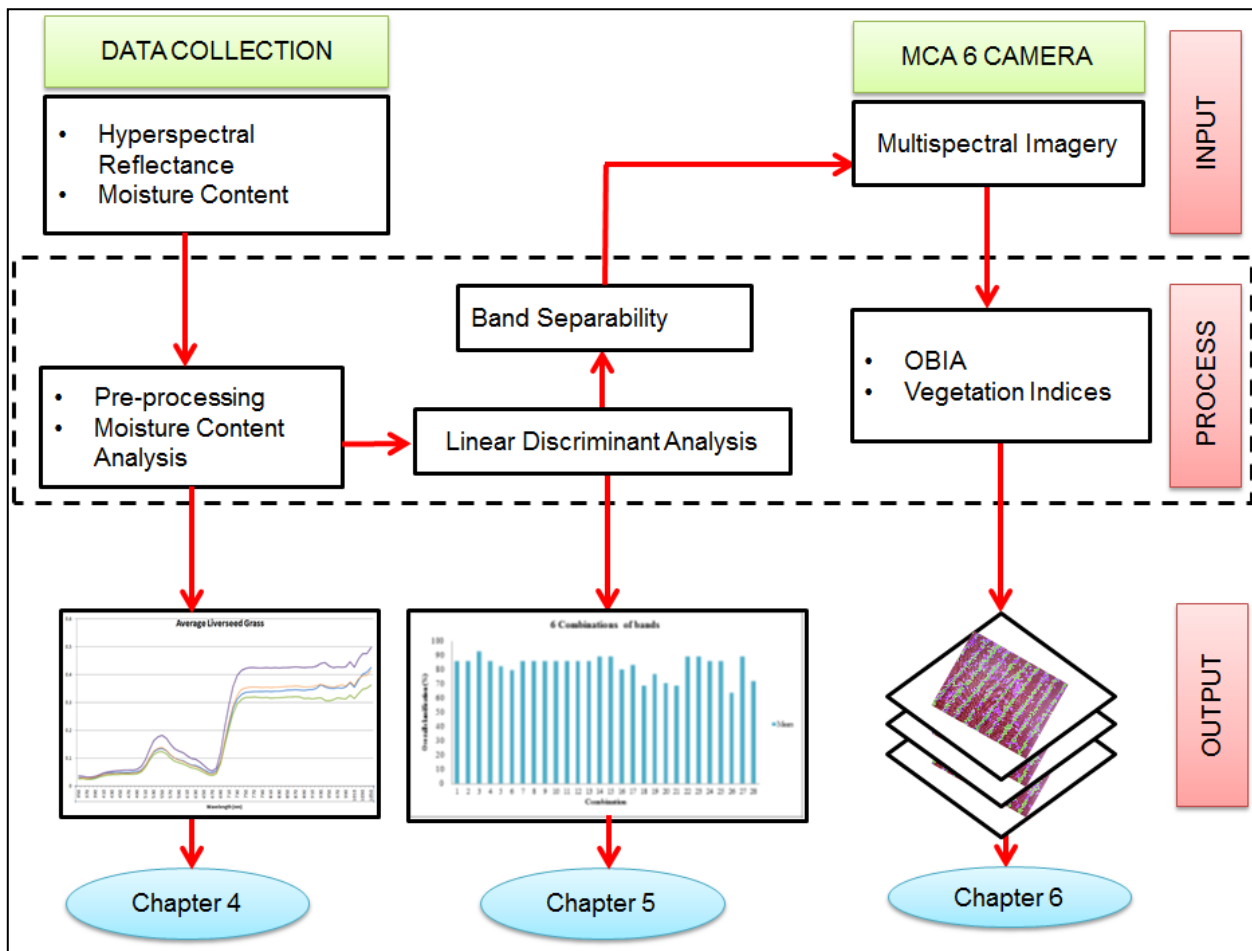


Figure 3-3 Workflow of the methodology

The field layout and data collection varied each year because of the lessons learnt from the previous year’s research. Details of the data collection for 2012 to 2014 are summarised in Table 3-1. Hyperspectral data were collected each year. Moisture content data were collected in 2013 and imagery was collected in 2014. Moisture content was measured to evaluate the relationship between moisture and reflectance of the weeds and the sorghum. Multispectral imagery was collected each year but lack of familiarity with the camera equipment and lack of appropriate bands pass filters for the camera resulted in the 2012 and 2013 imagery not being suitable for analysis.

The multispectral imagery was obtained at various altitudes to evaluate the effect of spatial resolution on weed detection. Static multispectral imagery and RGB images were also collected at 1.6 m elevation in 2014 using the MCA 6 and Canon (Power Auto-Shot SX260 HS) cameras respectively.

Table 3-1 Data collection for each year

Years	Spectral Data	Moisture Content	Multi-Spectral imagery		RGB imagery
			UAV	Static	
2012	✓	✗	✗	✗	✗
2013	✓	✓	✗	✗	✓
2014	✓	✗	✓	✓	✓

3.3 EXPERIMENTAL DESIGN

3.3.1 Study area

The study site was located at the University of Queensland, Gatton Campus (Coordinate 27°32'32.90" S, 152°19'58.88" E, WGS 84 Datum) (Figure 3-4). Summer rainfall predominantly occurs between September and March each year.

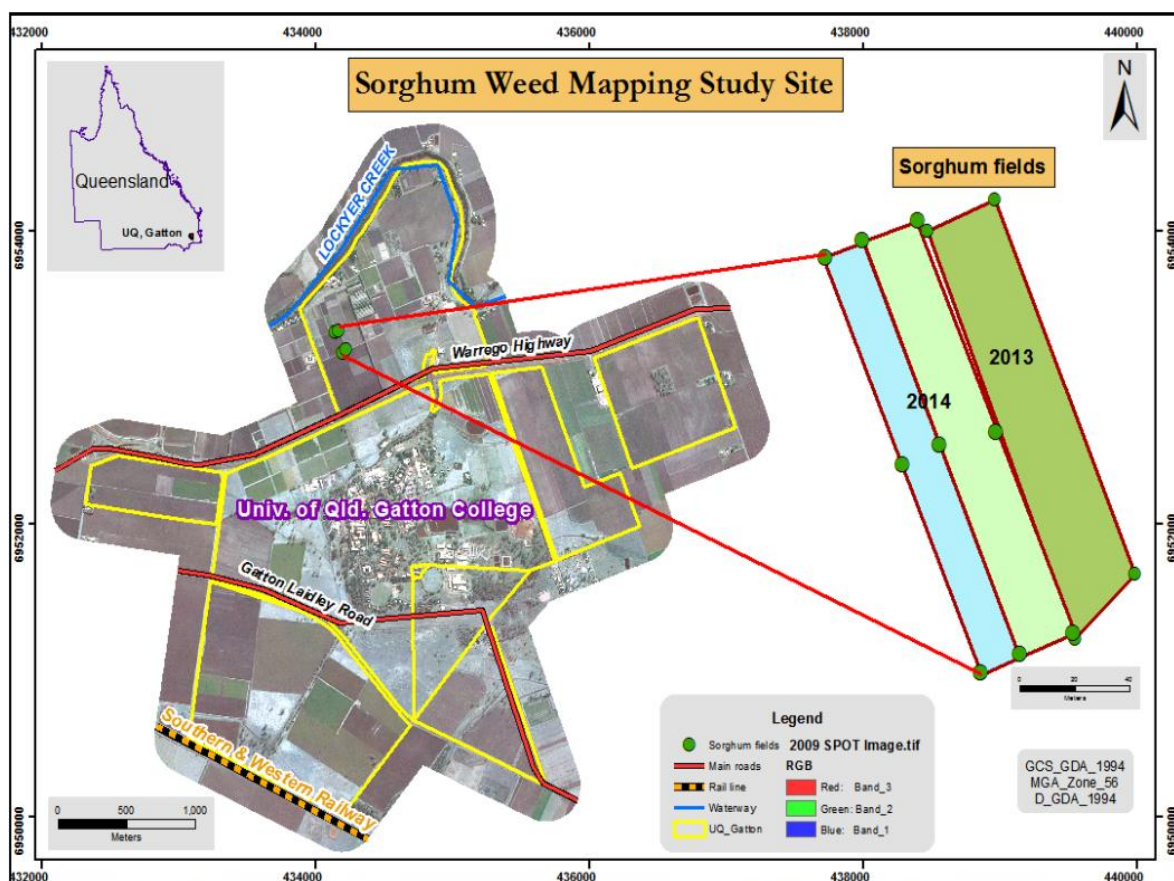


Figure 3-4 Location of the study area

Sorghum (*Sorghum bicolor* (L.) Moench ssp. Bicolor, variety: 84G22) was planted approximately 30 mm deep using a tractor fitted with precision guidance equipment on the dates shown in Table 3-2.

Table 3-2 Sorghum planting

Year	Date of planting
2012	09.10.2012
2013	25.10.2013
2014	26.11.2014

The seed was treated with Concep II (active consistent Oxabetrinil, 700 g/kg, applied at 36 g/20 kg sorghum seed) to protect it from the effect of the Dual Gold pre-emergence herbicide. A Case IH 95 tractor fitted with a four unit Nodet planter was used to plant the sorghum at 100 mm plant spacing in 75 cm width rows. A StarFire, integrated Terrain Compensation (iTC) GPS system

provided the precision guidance using the farm's Real Time Kinematic (RTK) correction signal (Figure 3-5).

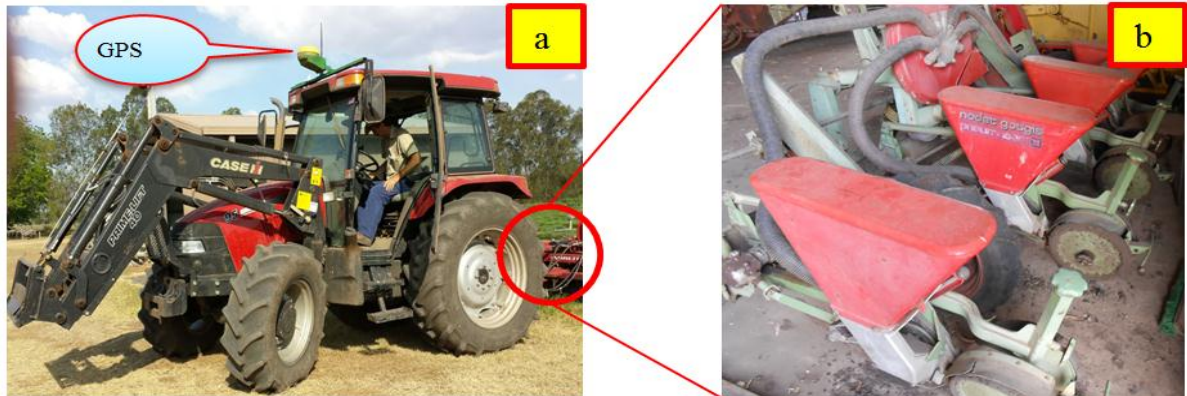


Figure 3-5 Case 95 tractor (a) and Nodet planter (b)

The experimental area was irrigated for three hours applying a total of 38 mm of water two days after each planting. During emergence, 28, 15.5 and 11 mm of rain fell on the crop in 2012, 2013 and 2014 respectively.

3.3.2 Field layout

In 2012, hyperspectral reflectance samples were taken for each weed species and for sorghum. The samples were selected at random, across the field. In 2013, sampling was reorganized. Hyperspectral reflectance samples (five) were collected from each species at four pre-set loci in the sorghum paddock (Figure 3-6).

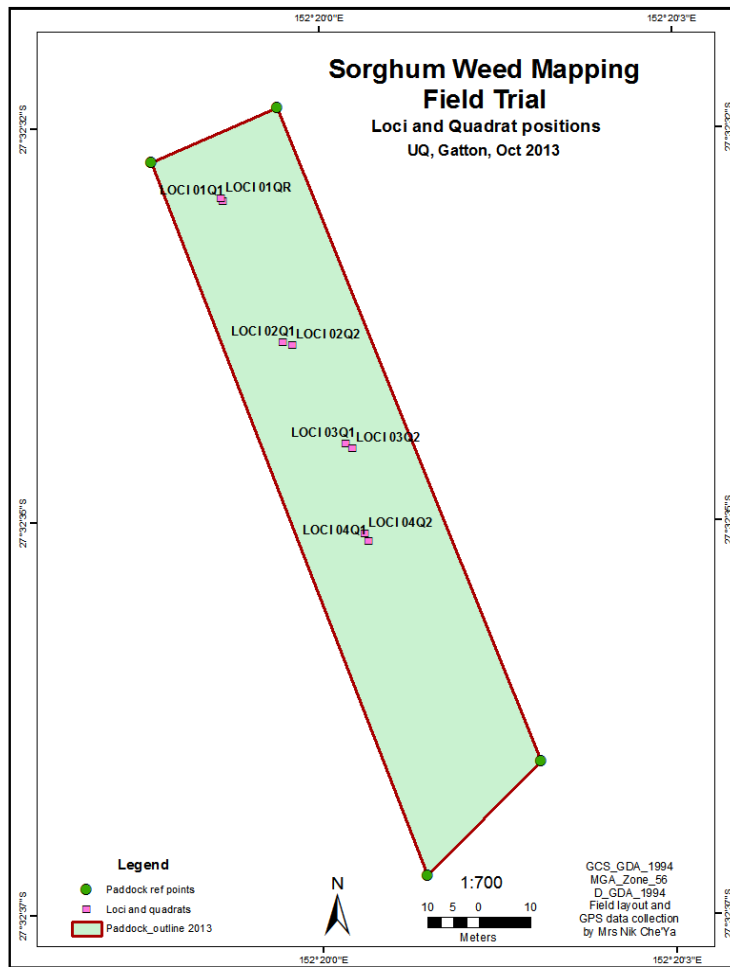


Figure 3-6 Position of loci and quadrats in 2013

Two quadrats (1m²) were positioned randomly in each locus for static image collection (Figure 3-7).

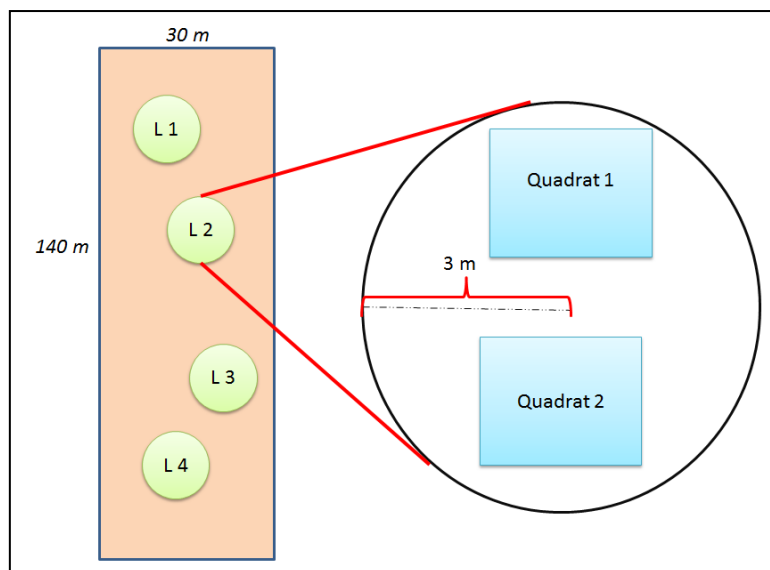


Figure 3-7 Details of loci and quadrats in 2013

In 2014, the loci were dispensed with and a full 6 x 4 randomized blocks design was implemented (Figure 3-8). The field was divided in two; one part was treated with pre-emergence herbicide and the second part was left untreated (control). Two pre-emergence herbicides were used, Gesaprim® 600 SC at a rate of 2 L/ha (active constituent 600g/l Atrazine) and DualGold® at a rate of 2 L/ha (active constituent 960 gram (g)/l S-Metolachlor). These are registered for the control of pigweed and amaranth in sorghum. Gesaprim is also registered for suppression of annual grasses (Syngenta 2015a; Syngenta 2015b). This technique was consistent with Pena et al. (2013) and Torres-Sanchez et al. (2013b).

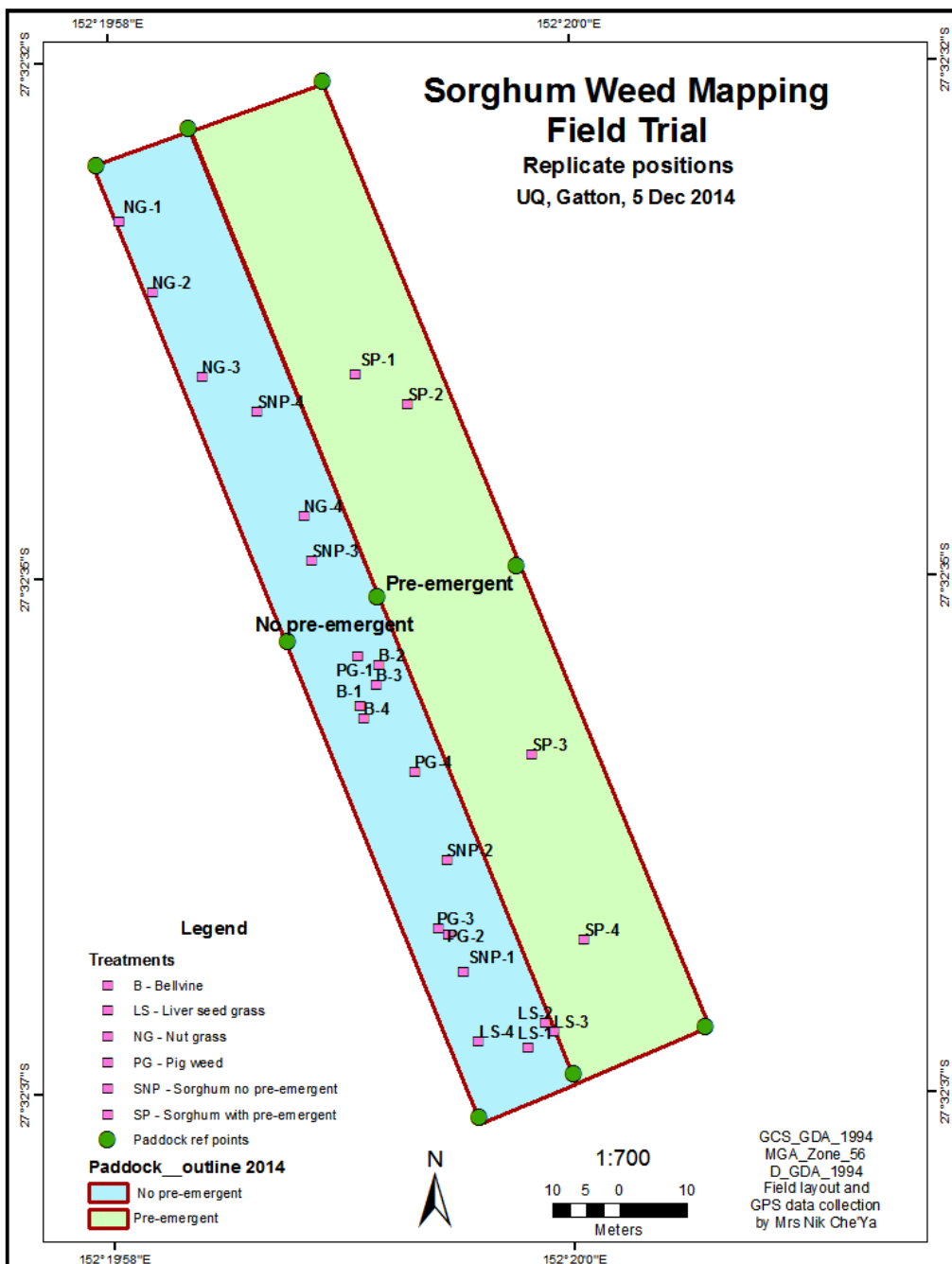


Figure 3-8 Layout of replicates in 2014

Each treatment consisted of sorghum and only one weed species: other species were removed by hand (Calha et al. 2014). The four replicates were positioned as randomly as possible. Allowance was made for some species of weeds not growing randomly in the field. The details of each replicate are given in Table 3-3.

Table 3-3 Details for each replicate

Quadrat No.	Replicate Label	Treatment
Q1	NG 1	Nutgrass
Q2	NG 2	Nutgrass
Q3	NG 3	Nutgrass
Q4	SNP 4	Sorghum Non Pre-emergence
Q5	NG 4	Nutgrass
Q6	SNP 3	Sorghum Non Pre-emergence
Q7	PG 1	Pigweed
Q8	B 1	Bellvine
Q9	B 4	Bellvine
Q10	B 3	Bellvine
Q11	B 2	Bellvine
Q12	PG 4	Pigweed
Q13	SNP 2	Sorghum Non Pre-emergence
Q14	PG 3	Pigweed
Q15	PG 2	Pigweed
Q16	SNP 1	Sorghum Non Pre-emergence
Q17	LS 2	Liverseed grass
Q18	LS 4	Liverseed grass
Q19	LS 1	Liverseed grass
Q20	LS 3	Liverseed grass
Q21	SP 4	Sorghum Pre-emergence
Q22	SP 3	Sorghum Pre-emergence
Q23	SP 2	Sorghum Pre-emergence
Q24	SP 1	Sorghum Pre-emergence

3.4 DATA COLLECTION AND PRE-PROCESSING

This section explains the procedures for data collection and pre-processing.

Figure 3-9 shows the different type of field data that were collected.

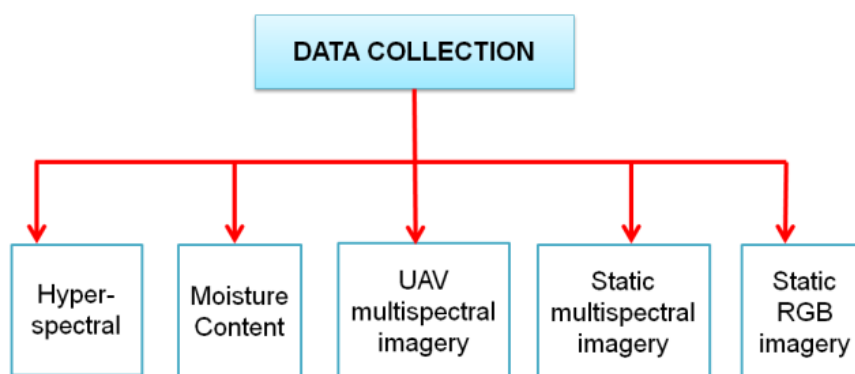


Figure 3-9 Data collection in the study

3.4.1 Hyperspectral data

Hyperspectral data consists of reflectance values for closely spaced spectral bands (Sahoo et al. 2015). They were collected each year (Table 3-4) using a Handheld FieldSpec® Spectroradiometer (Analytical Spectral Device Corporation (ASD), Inc., Boulder, CO, USA) (Figure 3-10).

In 2012, the data was collected once and this was during the fourth week of growth. In 2013, hyperspectral data were collected during weeks 1, 2, 3 and 4 of growth. In 2014, the weed species were too small to be identified one week after planting and hyperspectral data were collected at weeks 2, 3 and 4 of growth.

Table 3-4 Annual hyperspectral data collection at different stages of growth (Week one to week four)

Year	Week 1	Week 2	Week 3	Week 4
2012	x	x	x	✓
2013	✓	✓	✓	✓
2014	x	✓	✓	✓

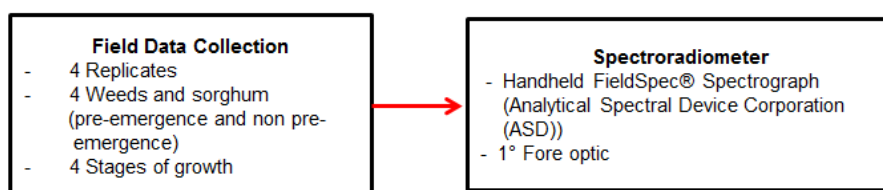


Figure 3-10 Hyperspectral data collection

Hyperspectral data were collected according to the procedures of Eddy et al. (2013). Prior to data collection, the Spectroradiometer ASD was calibrated using the manufacturer's white Spectralon® reference disc. The device has a spectral range from 325 nm to 1075 nm, a spectral resolution of < 3 nm and it was fitted with a fibre optic cable connected to a 1 degree solid radius fore optic. The fore optic sampling lens was positioned less than 5 cm from the leaf surfaces in open sunlight (Figure 3-11). The spectral signature was only collected from the middle top of the leaf

surface. The foreoptic was used at distance of less than 5 cm from the leaf surface under field conditions to avoid collecting misleading data. To ensure the correct data was collected. The same procedure was used for collecting the spectra for all samples. The spectral reflectance data for each sample and species was averaged to get the most accurate value. Use of a fibre optic cable was a practical way to collect the reflectance from the target because the leaves were very small especially during the early stages of growth.



Figure 3-11 Collecting spectral signatures using the FieldSpec® HandHeld 2™ Spectroradiometer with fibre optic attached.

Weeds that occurred in the sorghum crop in 2012 to 2014 are listed in Table 3-5.

Table 3-5 Weeds species occurring each year

Weeds species	2012	2013	2014
Amaranth (<i>Amaranthus macrocarpus</i>)	✓	✓	✗
Pigweed (<i>Portulaca oleracea</i>)	✓	✗	✓
Awnless Barnyard Grass (<i>Echinochloa colona</i>)	✓	✗	✗
Mallow Weed (<i>Malva sp</i>)	✓	✓	✗
Nutgrass (<i>Cyperus rotundus</i>)	✓	✓	✓
Fat Hen (<i>Chenopodium album</i>)	✓	✗	✗
Liver seed Grass (<i>Urochoa panicoides</i>)	✗	✓	✓
Bellivne (<i>Ipomea plebeia</i>)	✗	✗	✓

The plants were labelled to ensure that reflectance samples were taken from the same plants on subsequent samplings. Figure 3-12 shows plant growth quadrat L1Q1 (Locus No. 1, Quadrat No. 1) for weeks 1 to 4 after planting in 2013.

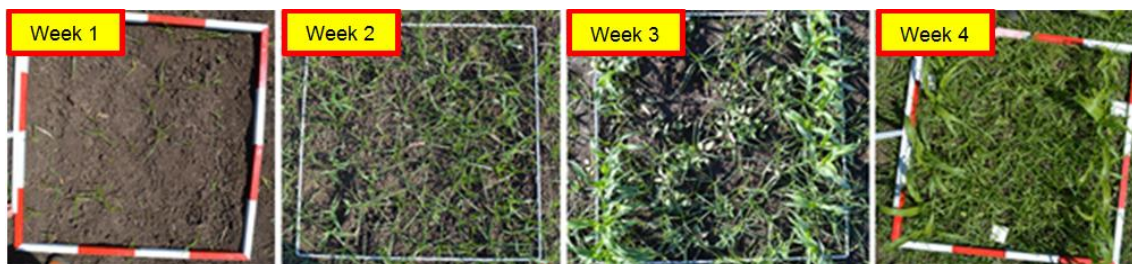


Figure 3-12 Weeds in L1Q1 from week one to week four, 2013

3.4.2 Moisture content

Leaf samples for moisture content (MC) analysis were collected each week in 2013. They were taken randomly for each species within three metres of each locus and put in small plastic vials for laboratory analysis. In the laboratory, the fresh weight of each sample was recorded. They were then transferred to the drying oven (set at 65 °C) for three days, after which they were weighed to record the dry weight. The MC was calculated as a percentage of the fresh weight of the samples.

3.4.3 Imagery

Multispectral imagery was taken using a Mikrokopter JR11X UAV (Figure 3-13A). The JR11X UAV provides an aerial platform suitable for mounting a conventional and multispectral camera (Bueren et al. 2015). It has eight rotary blades, can carry up to five kg and is capable of stationary hovering. This latter feature is required for acquiring long exposure images. Control is by an autopilot using a GPS controller (Table 3-6). The flight controllers consist of three Gyroscopes (for maintaining orientation) and three accelerometers (for measuring acceleration). It has three navigational controllers, an electronic compass, an air pressure sensor and an autopilot.

Table 3-6 Summary specifications for UAV platforms (Bueren et al. 2015)

Name	Specifications
Manufacturer	Mikrokopter
Weight (g)	1900
Max. Payload (g)	1000
Power source	Lipo, 4200 mAh, 14.8 V
Endurance (Max)	One hour
GPS Navigation	Ublox LEA 6s GPS chip
Features	Open Source Gyro-stabilized camera mount
Sensor	MCA 6

The sensor was a multispectral camera (MCA 6 made by Tetracam Chatsworth, CA, USA (Figure 3-13B) with 6 Complementary metal-oxide semiconductor (CMOS) sensors capable of being fitted with different wavelength filters. Similar equipment was used by other investigators (Laliberte et al. 2011; Castillejo-Gonzalez et al. 2014; Borra-Serrano et al. 2015; Perez-Ortiz et al. 2015; Torres-Sánchez et al. 2015), although mounted on different types of UAVs such as the BAT 3 UAS (MLB Co., Mountain View, CA, USA) and the Maxi Jocker 3 (Garcia-Ruiz et al. 2015).



Figure 3-13 *Mini Multi Channel Array (MCA6) camera attached to the Mikrokopter JR11X (A) and MCA 6 in close up without cover (B)*

The communications between the radio control pilot, the ground station and control points with the Mikrokopter UAV are shown in Figure 3-14. An operator manually controls the UAV during take-off and landing using the radio control pilot. During flight, the UAV automatically follows the preloaded flight path (series of waypoints) and hovers over each for a pre-set time interval. The operator can monitor the information delivered by the telemetry system between the UAV and the computer, such as UAV position, altitude, speed, battery storage level, radio control signal quality and wind speed using the mission planning software (Mission Planner) (Mission Planner 2013; Torres-Sanchez et al. 2013b).

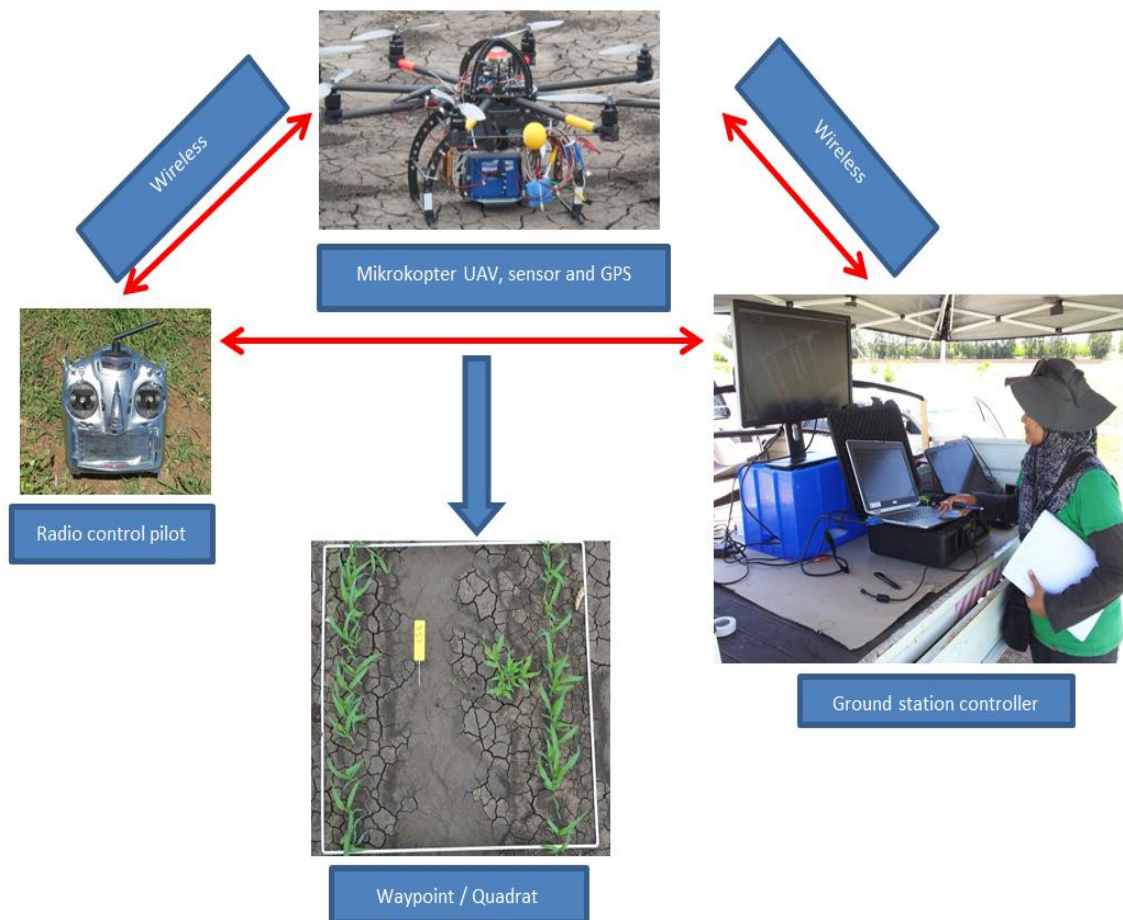


Figure 3-14 Communications between the Mikrokopter and sensor auto-pilot and the ground controller using Mikrokopter software

3.4.3.1 Power Supply

High-density lithium batteries (Lipo brand) were used to power the UAV and the MCA 6 camera. The length of flight depended on the battery storage capacity, its operating temperature, crosswind speed and height above the ground. The batteries were cooled and recharged between flights and the power supply was monitored during data collection flights. The battery operating temperature became critical during the hot summer weather. The flight plan involved flying the UAV at different altitudes (Table 3-7). The higher altitude flights use more power to cover the study area and this increased the battery temperature to unsafe levels. This was overcome by cooling the battery while recharging between flights. This extended the flight time and avoided damage to the UAV due to running out of power leading to an uncontrolled landing.

Table 3-7 Data and flight plan for image collection (2014)

Date	Altitudes above ground	Resolution (mm)	Camera
Week 3			
15.12.2014	1.6 m (Static Image)	0.87	MCA 6
17.12.2014	20 m (UAV)	10.83	
18.12.2014	37.5 m (UAV)	20.31	
Week 4			
22.12.2014	1.6 m (Static Image)	0.87	MCA 6
23.12.2014	10 m (Mosaic Imagery)	5.42	
	20 m (Mosaic Imagery)	10.83	
	37.5 m (Mosaic Imagery)	20.31	

MCA 6 camera static images were collected using a custom-made jig which positioned the camera 1.6 m above the ground (Figure 3-15). The jig also held a small 12 V battery used to power the MCA 6 camera and a DVD controller for the MCA 6 camera. The DVD controller allowed preview of the image before capture. Use of a jig enabled quick, repetitive and consistent imaging of the experimental quadrats. The spatial resolution of the image at 1.6 m was 0.87 mm.

3.4.3.2 Saving time and Flight Planning

Two cameras were flown on the UAV, the MCA 6 (Tetracam) and a Canon Power Auto-Shot SX260 HS (Table 3-8). The MCA 6 camera is equipped with six, 2 Gigabyte (GB) Computer Flash (CF) storage discs, one for each sensor. The Canon Power Auto-Shot has one high capacity SC card for data storage.

Table 3-8 Sensor properties adapted by Bueren et al. (2015)

Description	MCA 6 camera	Canon Power Auto-Shot SX260 HS
Company	Tetracam	Canon
Type	Six bands multispectral	Visible RGB with GPS
Field of View	38.3° x 31.0°	0.07 x 0.03 x 0.1 m
Spectral sensors	Six	One
Spectral range	Much larger nm, user selectable	N/A
Image size	1280 x 1024	1024 X 786
Image format	RAW	JPEG
Dynamic Range	10 or 8 bit	8 bit
Weight (g)	790	231
Handling	Interval mode	Auto / Manual

The MCA 6 camera can be configured to capture both 8-bit RAW and 10-bit RAW format images. The type of imagery selected depends on the user's applications. The data format influences the amount of time needed to save each image (due to file size) and this needs to be considered in scheduling the time between successive image capture points to avoid mis-capture of images. Careful flight organisation is required to plan the time between image capture waypoints, UAV travel time between the waypoints, total in-the-air time, battery temperature and available battery power.

10-bit RAW files required 11 seconds to save and 8-bit RAW files required three seconds to save. Flight planning needed to allow sufficient time between image capture points for the storing the data from the previous image before the exposure for the next image was triggered. If insufficient time was allowed, subsequent image capture was delayed until the previous image capture had completed. This resulted in the subsequent image not capturing its predefined waypoint location correctly. The time required to save images also affects the amount of overlap in mosaic images.



Figure 3-15 Taking the quadrant image using a jig

The MCA 6 imagery had a similar spectral resolution to that of World View II imagery. A comparison of their spectral resolutions is shown in Table 3-9.

Table 3-9 Comparison of the spectral resolutions between the UQ Tetracam MCA 6 camera (Tetracam 2015) and Landsat 7 ETM+ and World View II (Jensen 2007)

MCA 6 camera				Landsat 7 ETM					World View II				
Channel #	λ (nm)			B	Name	λ (nm)			B	Name	λ (nm)		
	F	Mid-Point	To			From	Mid-Point	To			From	Mid-Point	To
Slave 1	437	440	443	1	Blue	450	483	515	1	Coastal	400	425	450
Slave 2	557	560	463	2	Green	525	565	605	2	Blue	450	480	510
Slave 3	677	680	683	3	Red	630	660	690	3	Green	510	545	580
Slave 4	707	710	713	4	NIR	750	825	900	4	Yellow	585	605	625
Slave 5	847	850	853	5	MIR	1550	1650	1750	5	Red	630	660	690
Master	717	720	723	6	TIR	10400	11450	12500	6	Red-edge	705	725	745
				7	FIR	2080	2215	2350	7	Near IR1	770	835	895
C: Central band, B: Band, NIR: Near Infrared, MIR: Middle Infrared, TIR: Thermal Infrared and FIR: Far Infrared, F: From									8	Near IR2	950	950	1040

3.4.3.3 Image Extraction

The pre-processing steps for the multispectral imagery are shown in Figure 3-16. Images were downloaded as six separate files (one for each sensor) from the CF cards to a computer where they were converted from their RAW format to a six-page TIF file format using Pixel Wrench 2 (PW2) software (Tetracam 2015). Each image had to be correctly aligned prior to restacking them into aligned six-page Tifs files. The aligned six-page Tifs files were then exported to six- band Tifs files for use in conventional image processing software.

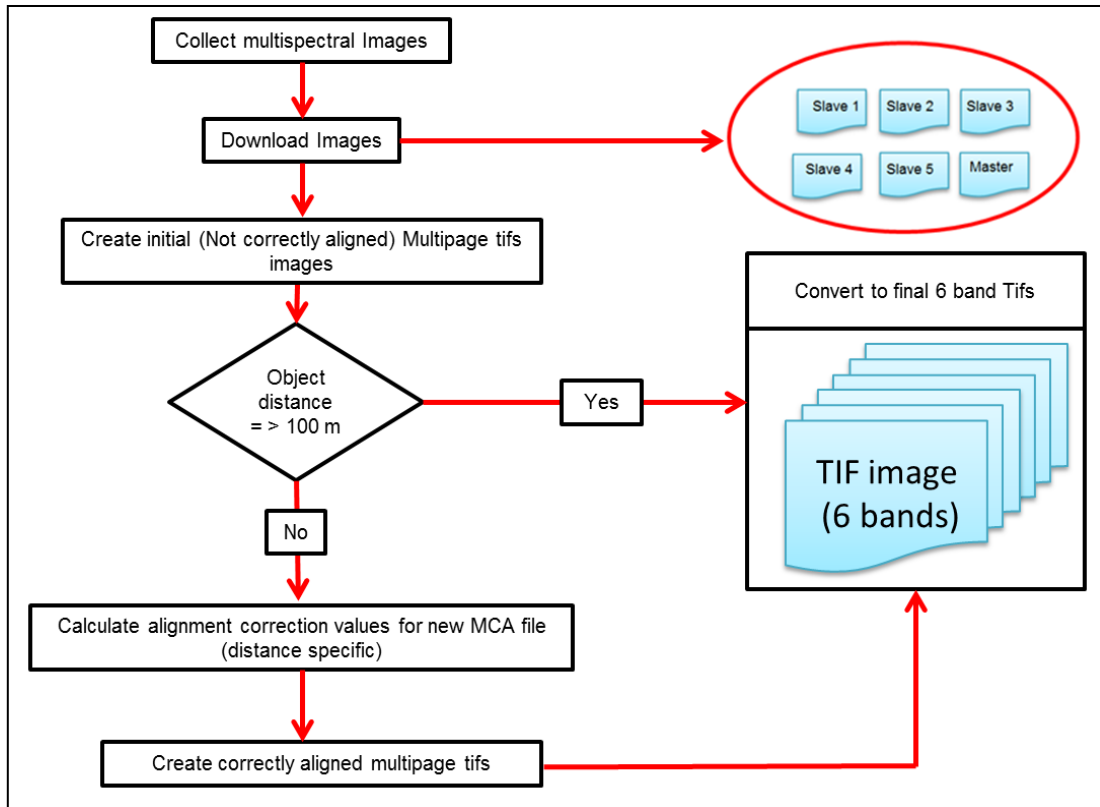


Figure 3-16 Flowchart for pre-processing MCA 6 bands imagery

3.4.3.4 Downloading images

There are two options for downloading imagery from the MCA 6. One is to use the CF card directly by inserting it into a card reader (Laliberte et al., 2011) as shown in Figure 3-17.

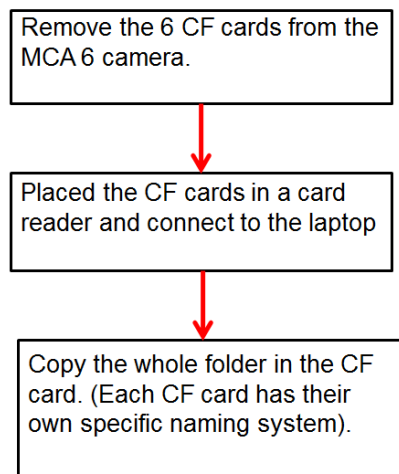


Figure 3-17 Steps for directly copying the MCA 6 imagery from the CF cards

The second way of downloading imagery files is by connecting the MCA 6 to a computer using a USB cable and downloading the imagery to the hard disk on the computer (faster than the previous method) (Figure 3-18). The MCA 6 camera has to be powered up to allow the transfer process to occur. In this method the files are transferred using the GPS Log Distiller function in the PW2 software. All the raw files were downloaded as a group in one large folder organised in sequential order from Master to Slave 5.

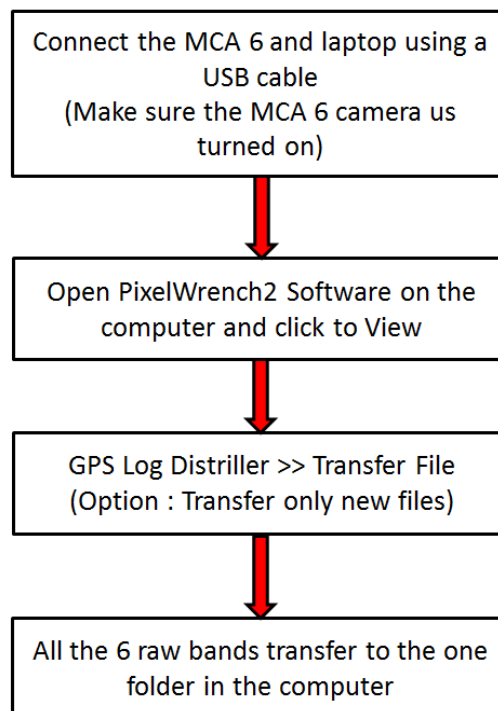


Figure 3-18 Procedure for transferring MCA 6 imagery file to a computer using PixelWrench2 Software

3.4.3.5 Creating initial multi Tifs image files

The multiband tifs for each exposure were created using the MCA alignment file. The MCA alignment file aligns all the bands in a single exposure for an object distance above 100 m. For object distances < 100 m, a corrected MCA file has to be used following the steps shown in Figure 3-19.

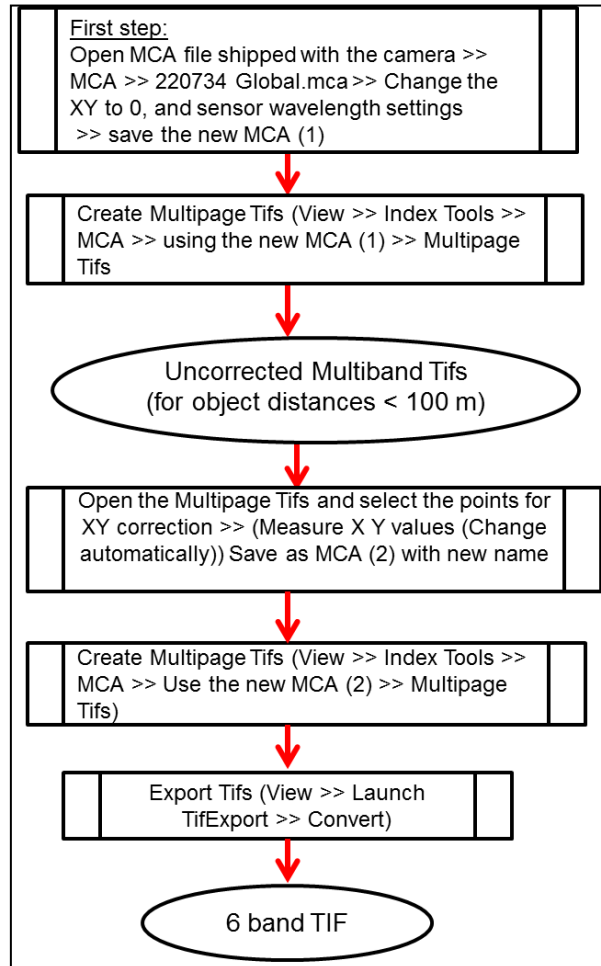
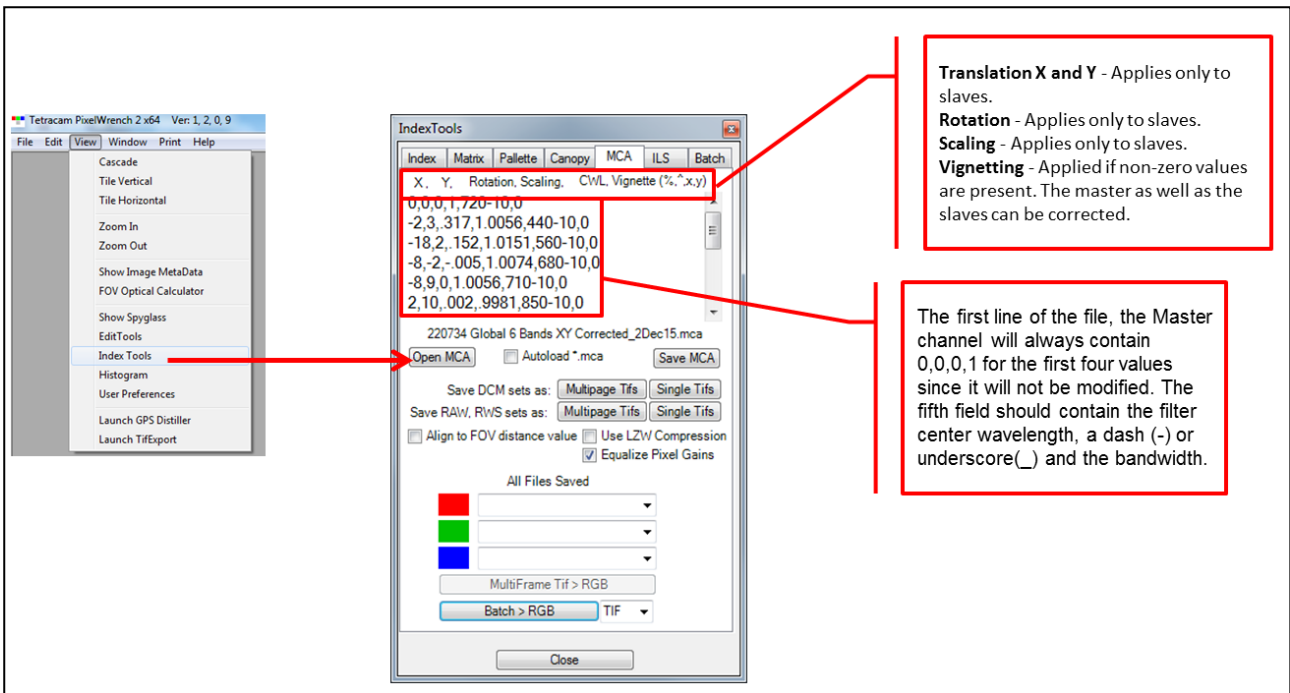


Figure 3-19 Create initial multiband Tifs

The first step in creating the initial multipage Tifs is to upload the Global.mca file provided by Tetracam (Figure 3-20). Note that the X, Y, Rotation, Scaling, Central Wavelength (CWL) and Vignette information are separated by commas (,).



Translation X and Y - Applies only to slaves.
Rotation - Applies only to slaves.
Scaling - Applies only to slaves.
Vignetting - Applied if non-zero values are present. The master as well as the slaves can be corrected.

The first line of the file, the Master channel will always contain 0,0,0,1 for the first four values since it will not be modified. The fifth field should contain the filter center wavelength, a dash (-) or underscore(_) and the bandwidth.

Figure 3-20 Details of the MCA file settings

3.4.3.6 Band alignment

The bands have to be aligned in each image based on the distance of the sensor to the object. This involves creating a different MCA file for each altitude below 100 m. The distance between the sensor and the object needs to be known precisely.

The sensors are positioned side by side in the camera (Figure 3-21). Band alignment is necessary to align all the channel images with each other. The sensors in the MCA 6 camera are optically aligned by default for images at an infinite distance (> 100 m) (Tetracam 2015). However, when images are acquired at closer distances, such as from a low flying UAV or from a ground mounted position, the separate channel images are not properly aligned because of the spatial separation of the sensors (Tetracam 2015). To correctly align them the distance of the sensor from the object has to be known accurately.

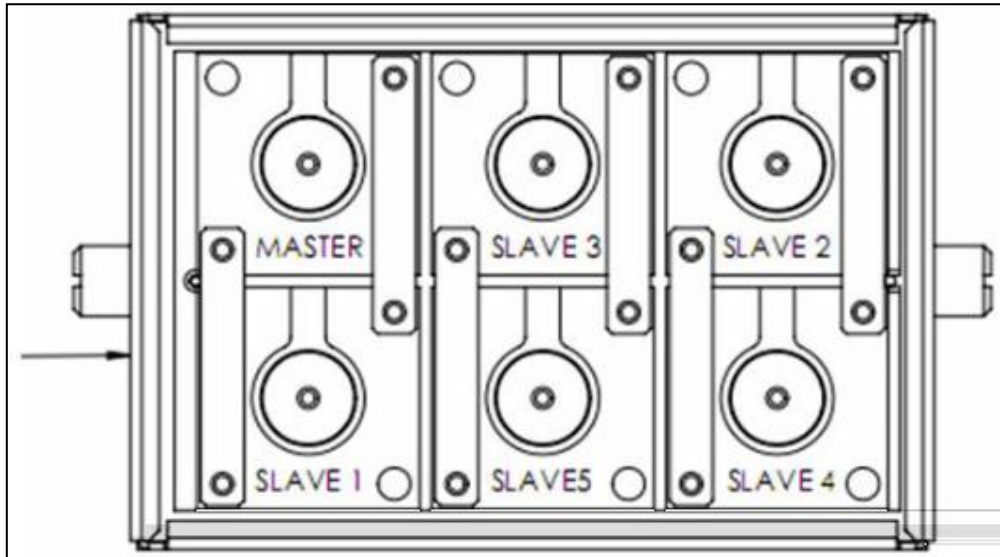


Figure 3-21 The position of the sensors in the MCA 6 camera (Tetracam 2015)

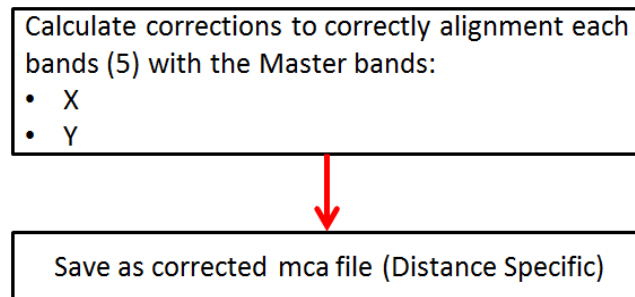


Figure 3-22 Create a new MCA file

Uncorrected multipage Tifs were created from the RAW files using the Global MCA file with X and Y set to 0. Then the correctly aligned MCA file was created as follows (Tetracam 2015):

- i. Open the multipage Tifs file
- ii. Beginning with the Master band image (reference for the slaves.), zoom in on the image using the Spyglass tool.
- iii. Identify a small distant object near the center of the Master band image.
- iv. Put the cross hairs on the defined object in the Master image and click on it and press and hold “T” on the keyboard.
- v. The X and Y label in the MCA file window turns green in colour indicating that the XY point has been recorded (Figure 3-23).
- vi. Then, click the green label to set the new point.
- vii. Use Page Up to go to the Page 2 image and repeat the procedure,
- viii. Put the crosshair on the same point in image no. 2 (Slave 1), click and hold “T”,
- ix. X and Y label in the MCA file window becomes green again,

- x. Click on the green label (X and Y) to set the new point. This procedure inserts the corrected X and Y values in the MCA file for each slave image.

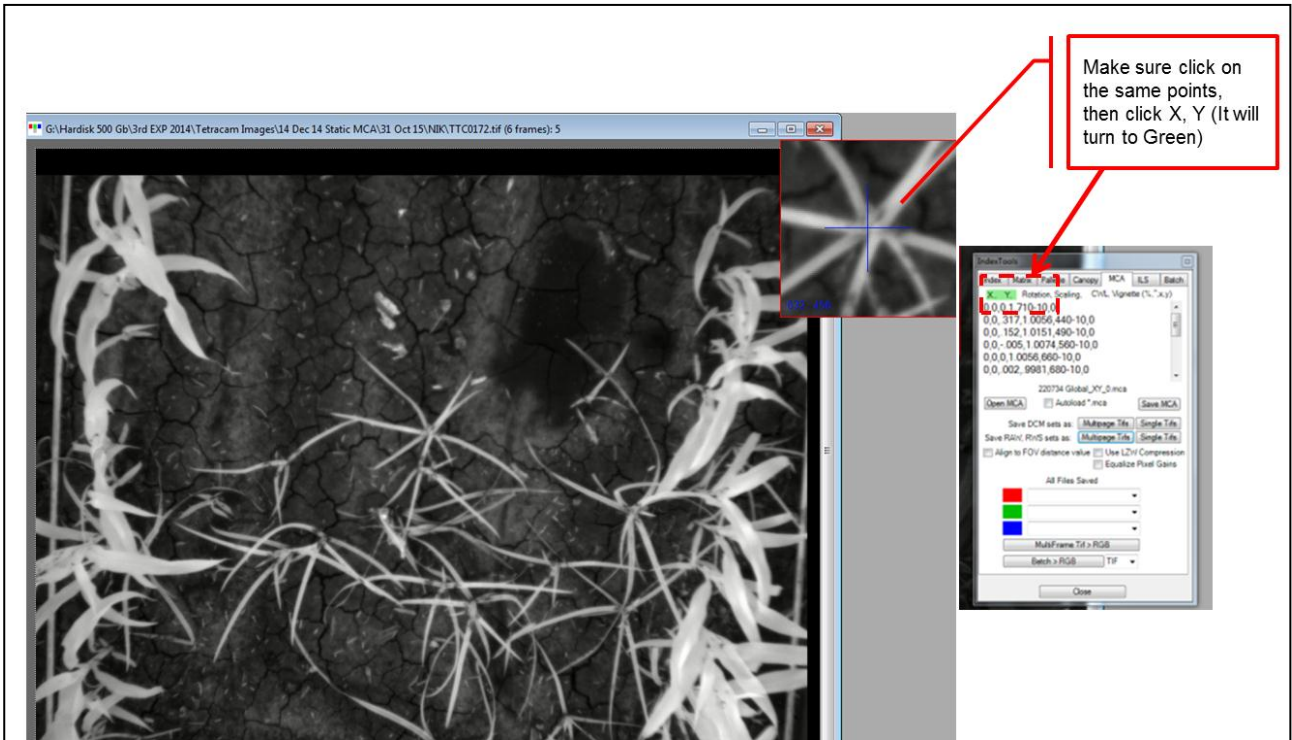


Figure 3-23 The X and Y correction in green colour

After doing this for the entire slave channels, save the MCA file using a different name (indicating object distance) and rebuild the RAW to TIF image using the new MCA as shown in Figure 3-24.

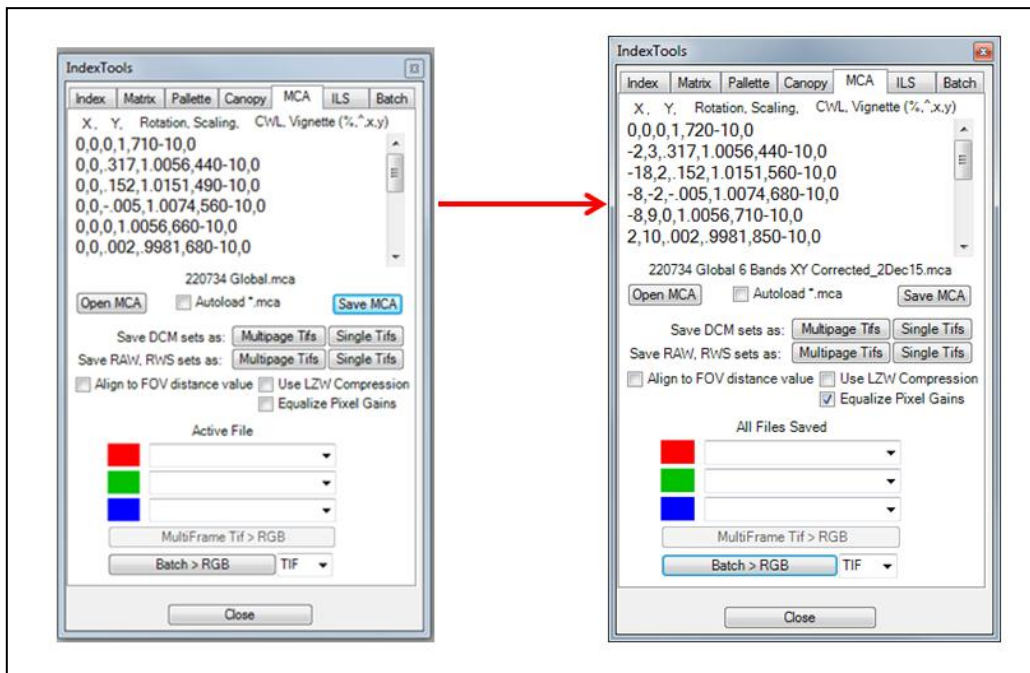


Figure 3-24 Before and after setting of the MCA, X Y for correction values for band alignment

3.4.3.7 Revised (Corrected < 100 m) Multiband Tifs

The correctly aligned 6-band Multipage Tifs were now ready for conversion to 6 band TIF format. These six bands were aligned correctly using TifExport Tool in PW2. Subsequently the Multipage Tifs were converted to TIF format (Figure 3-25).

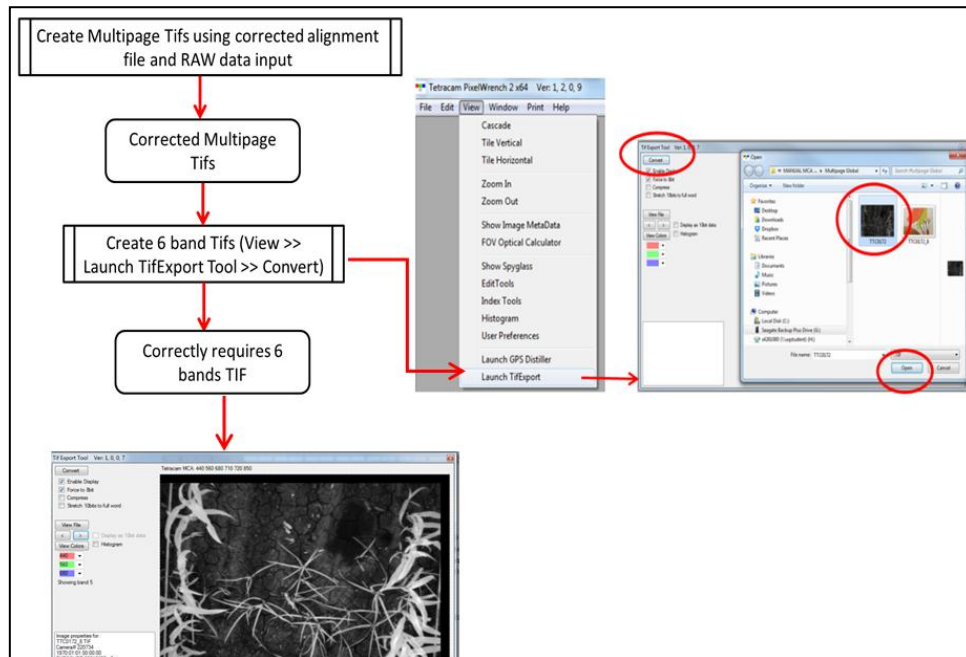


Figure 3-25 The steps used for band alignment correction

3.4.4 Ground truth data

An RGB image was captured for each quadrat every week using a digital camera (Canon Power Auto-Shot SX260 HS). This provided a conventional record of the stage of plant growth. Each quadrat's location was captured using a Trimble Juno GPS. This information was used to map the experimental sites.

3.4.5 Statistical procedure

Hyperspectral data were analysed to find the wavelengths at which the reflectance between the species was greatest. Reflectance values were grouped into 10 nm bins to facilitate processing. The effect of moisture on reflectance was tested for the 6 bands that ended up being used in the hyperspectral camera as detailed in Chapter 5 (Table 5-5). The combinations of spectral bands which yielded the highest degree of discrimination between all species were determined by LDA as described in Chapter 5.

3.4.6 Validation

A subset of the hyperspectral data was set aside as independent data for use for accuracy testing. The results of the LDA were tested for accuracy by using the Kappa method and the independent data set. This is a common and well established procedure for testing the accuracy (Cohen 1960; Congalton 1991).

3.5 CONCLUSIONS

This chapter described the sorghum cropping procedures and the field layout for the reflectance and image data collection sites each year. This was followed by a description of the reflectance and image collection procedures, download methods and preliminary processing of the data. The hyperspectral reflectance data was needed to find the significant bands for classifying each plant species. This was done using statistical procedures as outlined in Chapter 4. The significant bands were then used to guide selection of the band pass filters for the multispectral camera.

Multispectral imagery was captured using a MCA 6 camera attached to a UAV. The initial data was in RAW format and the steps needed to process and align the imagery to create 6 band TIF images were described. The step of the alignment proses was explained in details under 3.4.3 section. However, the minor geometric distortion cannot be corrected and it was an expected result since the imagery was taken below 100 m from the ground. It was advised by Tetracam¹ expertise about the distortions correction.

The following Chapters discuss the techniques for processing the hyperspectral data, analysing it to identify the priority wavelengths for classification of the species and processing of the imagery to produce weed maps.

¹ Mr Steve Heinold (Tetracam Expert, USA) Email: steve@tetracam.com.

Chapter 4

IDENTIFICATION OF SPECTRAL DIFFERENCES BETWEEN WEEDS AND SORGHUM

4.1 INTRODUCTION

Conventional weed control is very expensive (Zhang et al. 1998). It is based on the assumption that weeds are distributed across an entire field. Consequently, farmers use more energy and herbicides than are actually necessary to control the weeds and at the same time this creates potentially negative environmental effects (Kumar et al. 2015).

Site-specific weed management is a method of limiting the application of herbicide to only weedy areas (de Castro et al. 2012). Accurate mapping of weeds is a pre-requisite for its successful implementation (Whiteside et al. 2012). The spectral similarity of the weeds and crop plants makes them difficult to separate to produce a weed map (Andujar et al. 2012).

Remote sensing imagery can be used to detect the presence of weeds in a crop (Everitt et al. 2011). Hyperspectral remote sensing is recognized as the most cost effective and up-to-date technique (Gholizadeh et al. 2013) for detecting weeds in crops (Surface Optics Corporation 2015). Specifically they state that:

“Some of the benefits of hyperspectral and multispectral imaging are that these technologies are: low cost (when compared with traditional scouting methods), give consistent results, simple to use, allow for rapid assessments, are non-destructive, highly accurate, and have a broad range of applications”.

This chapter reviews the spectral reflectance of vegetation and weed species, and the effect of Moisture Content (MC) on hyperspectral reflectance. The identification of spectral reflectance differences between weeds and sorghum is essential for successful weed mapping. This chapter will focus on pre-processing of the hyperspectral reflectance data and correlation between MC and hyperspectral reflectance of weeds and sorghum.

4.2 LITERATURE REVIEW

In their early stages of growth, weed and crop plants look very much alike. However, it is very important to detect them apart at the early stages of growth, because weeds can have a larger effect on the growth of the crop at the early stage than at later stages (Calderón et al. 2015; Lopez-Granados et al. 2015). Hyperspectral data can be used to detect differences between weed and crop plants at the early growth stage (Siddiqi et al. 2014). Zwiggelaar (1998) and Torres-Sanchez et al. (2013b) used hyperspectral data to distinguish between weed and crop plants in their early growth stages. Weed maps based on the spectral difference between the species offer an appropriate method to apply herbicides to only weedy areas at the early stages of crop growth (Pena-Barragan et al. 2012a).

4.2.1 Spectral reflectance of vegetation

Plants respond to solar radiation from the sun. The radiation is either reflected, absorbed or transmitted (Figure 4-1). Figure 4-2 shows an example of the reflected, absorbed and transmitted radiation by Big Bluestem Grass as detected by a laboratory spectroradiometer. Variables such as chlorophyll, water content and cell-to-air space ratio affect the amount of absorption (Smith and Blackshaw 2003).

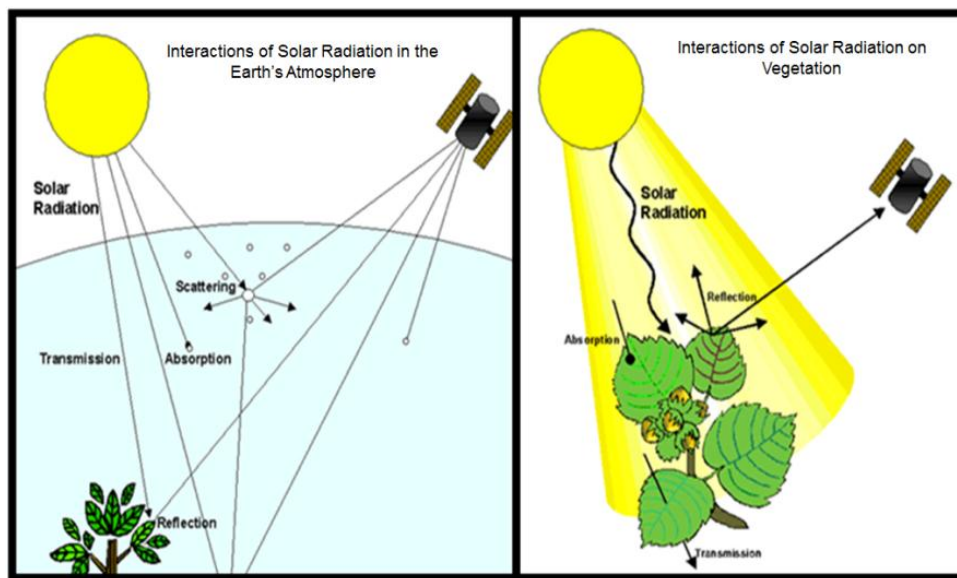


Figure 4-1 Effect of the earth's atmosphere and vegetation on reflectance, absorption, and transmission of light (University of Hawaii 2009)

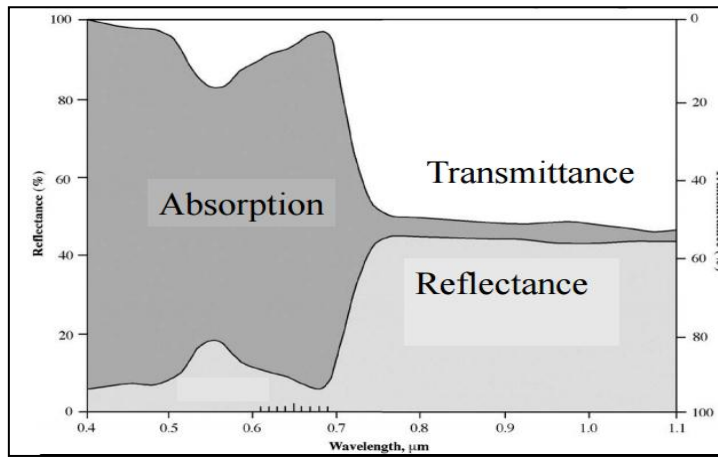


Figure 4-2 Atmospheric reflectance, transmittance, and absorption of Big Bluestem grass axial leaf surface (Jensen 2016, p. 321)

Electromagnetic (EM) radiation is a series of wavelengths ranging from gamma rays to radio waves (Figure 4-3) however, only the visible spectrum (400 – 700 nm) can be seen by the human eye (Lee et al. 2010). Reflection of light from plants involves interaction between EM radiation and the pigments, water and intercellular air spaces in the plant leaf (Jensen 2007, p. 356). Plant pigments play a significant role in the biosphere because they affect the EM radiation in the living plant (Blackburn 2007).

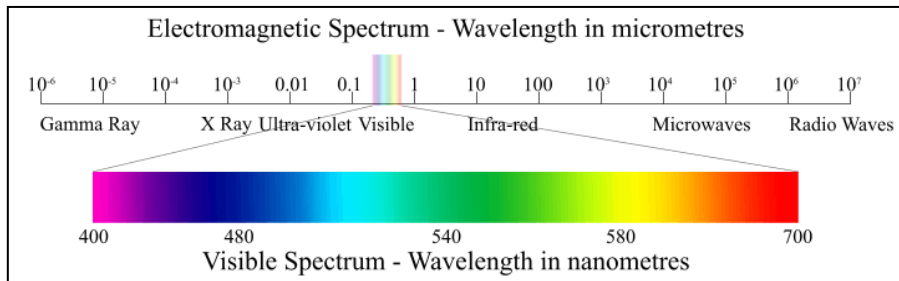


Figure 4-3 The electromagnetic (EM) spectrum (University of Hawaii 2009)

Different plants reflect EM radiation differently and this reflectance can be measured using a spectroradiometer. This allows the different spectral reflectance profile of each plant to be identified (Figure 4-4).

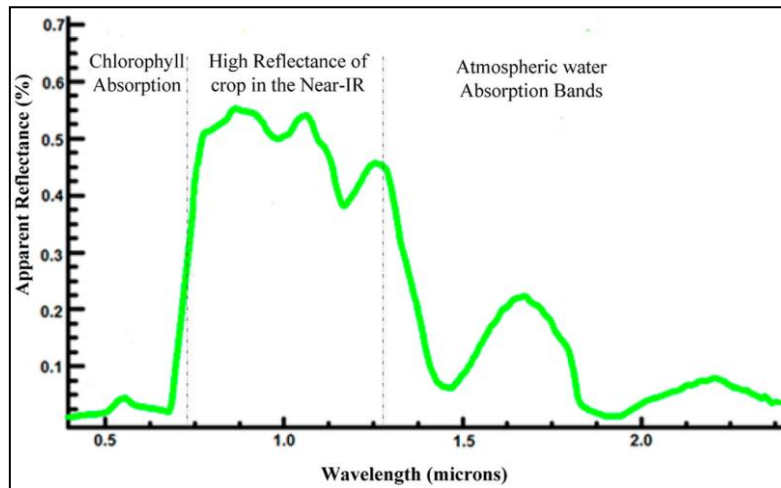


Figure 4-4 Typical reflectance spectra of vegetation at different wavelengths (Li et al. 2014)

The range between 700 nm to 730 nm (NIR) is very significant for species discrimination (Smith and Blackshaw 2003) because of the high reflectance of light by the leaf mesophyll (Castro-Esau 2006). “*The photosynthetic process begins when sunlight strikes chloroplasts, which are small bodies in the leaf that contain a green substance called chlorophyll*”, (Jensen 2016, p. 316). The chlorophyll concentration provides an accurate, although indirect estimate of a plant’s nutrient status and can be a predictor of crop stress (Blackburn 2007). The carotenoids are composed of carotenes and xanthophyll which also absorb incident radiation and change the reflection spectra during the photosynthesis process (Blackburn 2007).

4.2.2 Effect of moisture on spectral reflectance

Spectral reflectance is influenced by water, proteins and carbon constituents of plants (Li et al. 2014). A plant’s condition can be predicted from its reflectance because the reflectance is changed by the condition of the plant. Moreover, MC, surface and internal structure and pigment concentration all affect the spectral reflectance of leaves (Blackburn 2007). NIR radiation is highly reflected by healthy plants compared to blue and red radiation (Figure 4-5). Healthy plants have a low reflectance in the Middle Infrared (MIR) and the VIS spectra (Ortiz and Shaw 2011).

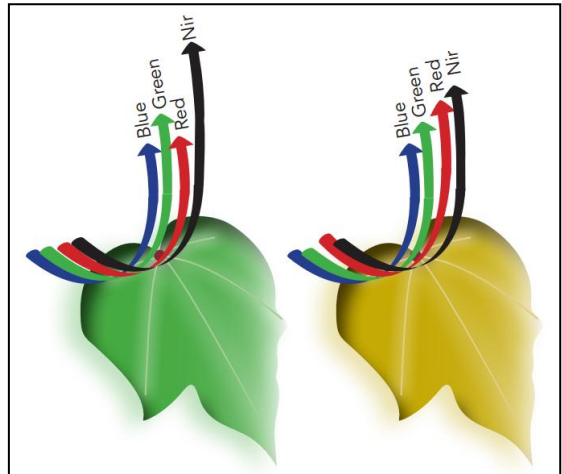


Figure 4-5 Differences in reflected light between a healthy and unhealthy leaf (Ortiz and Shaw 2011)

The hypothesis is that the reflectance in the MIR region increases as the moisture content of the leaves decreases and that this is an indicator of moisture status (Jensen 2016, p. 324). The intercellular air space decreases when plant water decreases. Transpiration is important to cool down the leaf, keep water flowing in the plant and ensure a stable supply of dissolved minerals from the soil (Jensen 2016, p. 324). It causes the plant to lose water through the stomata.

Plants reflect strongly in the NIR and their reflection declines steadily in the MIR depending on the ambient temperature (Figure 4-6). The amount of water in plants can affect emission in the MIR (Shilpakala 2014). Water absorbs strongly in the 2600, 1900 and 1400 nm MIR regions. In the visible region, changes in reflectance are not affected as much by water as they are in the MIR. There needs to be a 50% loss of water in a plant before it changes the visible reflectance spectra (Jensen 2016, p. 324).

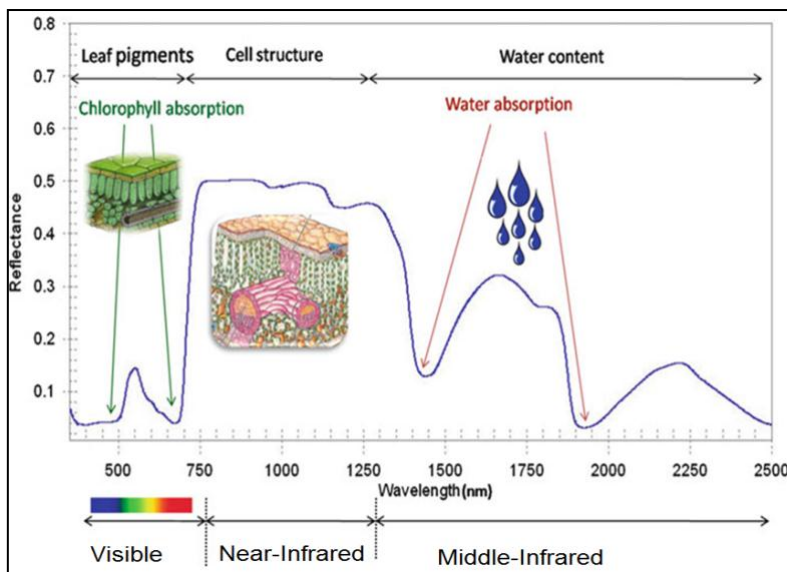


Figure 4-6 Typical spectral reflectance curve of healthy vegetation depicting different absorption and reflectance regions peaks (Shilpakala 2014)

4.2.3 Weed discrimination analysis using spectral reflectance

Remote sensing in the hyperspectral region is done by a range of sensors such as Hyperion, the Hyperspectral Imaging Spectrometer Sensor, Warfighter-1 and MODIS (Moderate resolution Imaging Spectrometer). Each of these has been developed for a particular application (Table 4-1).

Table 4-1 Summary of hyperspectral satellites (Thenkabail et al. 2000)

Hyperspectral Satellite	Description
Hyperion	220 spectral bands 10 nm width bands 30 m spatial resolution Carried on the National Atmospheric and Space Administration (NASA) New Millennium Program's Earth Observer-1 (EO-1) satellite
Hyperspectral Imaging Spectrometer Sensor	105 spectral bands 30 m spatial resolution Carried on the Australia Resource Information Environment Satellite
Warfighter-1	200 spectral bands Carried on board the ORBVIEW-4 satellite
MODIS	36 spectral bands (with 10 in visible, 6 in shortwave/middle infrared, 5 in thermal infrared regions) 250 to 1000 m spatial resolution

Hyperspectral information can be used to discriminate weeds from crop plants based on the wavelengths which show the most difference between the weeds and crop plants. Such remote sensing provides information for protection and monitoring of crop biophysical characteristics based on the narrow spectral bands of significance to agricultural crops (Thenkabail et al. 2000; Arafat et al. 2013b; Calderón et al. 2015). The advantage of hyperspectral data is that it can be used in machine learning programs which increase the accuracy of supervised classification (Thenkabail et al. 2000). However, it is expensive and there is a delay in capturing it. Ground based hyperspectral imagery is less expensive (Saberioon et al. 2014) compared to satellite hyperspectral imagery and it can be captured quicker.

4.2.4 Spectral Reflectance Analysis

Reflectance can be displayed graphically as spectral profile with multiple collections averaged to produce a composite spectral profile. Additionally, reflectance in ranges of wavelength can be averaged to create “binned” reflectance wavelength the bin ranges selected to coincide with the same bands filters wavelength ranges. This produces a more stable spectral profile. Inspection of these spectral profiles can be used to identify differences in reflectance between species (Lucieer et al. 2014).

The rate of change in reflectance with change in wavelength can be measured by calculating the First Derivative (FD). Conversion of the direct reflectance data into first derivative form

measures the rate of change in reflectance with change in wavelength. This removes baseline shifts so that peaks in the spectral profile are more clearly visible (Nicolai et al. 2007). This helps identify the most important reflectance wavelengths.

The First Derivative of each reflectance spectra was calculated as shown in Equation 1 (Shafri et al. 2011).

$$FD = \frac{R}{R} = \frac{Ry_2 - Ry_1}{\lambda x_2 - \lambda x_1} \quad (1)$$

Where:

FD = First Derivative

Ry_1, Ry_2 = Reflectance of the first and second reflectance pairs n_1 and n_2

$\lambda x_1, \lambda x_2$ = Wavelength of first and second reflectance pairs n_1 and n_2

n = Position of reflectance.

The FD is a measure of the amount and direction of the change in reflectance between each pair of wavelength bins (Holden and LeDrew 1998). The typical leaf will peak at 710 nm for the FD reflectance because of the relationship between red-edge and the chlorophyll concentration (Blackburn 2006).

4.3 MATERIALS AND METHODS

4.3.1 Spectral data

4.3.1.1 Data collection

Hyperspectral reflectance data was collected using a FieldSpec® HandHeld 2 Spectroradiometer (Analytical Spectral Device Corporation (ASD), Inc., Boulder, CO, USA). The advantages of the FieldSpec® HandHeld 2 spectroradiometer are that it is cost effective, user friendly, versatile and durable (ASDi 2014). It has a highly sensitive detector array with a low stray light grating, a built-in shutter, DriftLock dark current compensation and second-order filtering that produces a high signal-to-noise spectrum in under a second (ASDi 2014) (Table 4-2).

Table 4-2 FieldSpec® HandHeld 2 Spectroradiometer properties (ASDi 2014)

Specification	Information
Design	An ergonomic dual position “D” handle.
Weight	1.17 kg including batteries.
Wavelength range	325 nm – 1075 nm
Accuracy	±1 nm
Optional GPS	Yes

Weed species for which reflectance was collected from 2012 to 2014 are listed in Table 4-3. Data collection was done under field conditions and so was expected to include natural variation in the reflectance of the weeds. Nutgrass was the only weed that persisted from year to year because it is very difficult to kill and survives in the soil.

Table 4-3 Weeds species collected each year.

Weeds species	Abbreviation	2012	2013	2014
Amaranth (<i>Amaranthus macrocarpus</i>)	AM	✓	✓	✗
Pigweed (<i>Portulaca oleracea</i>)	PG	✓	✗	✓
Awnless Barnyard Grass (<i>Echinochloa colona</i>)	BG	✓	✗	✗
Mallow Weed (<i>Malva sp</i>)	MW	✓	✓	✗
Nutgrass (<i>Cyperus rotundus</i>)	NG	✓	✓	✓
Fat Hen (<i>Chenopodium album</i>)	FH	✓	✗	✗
Liverseed Grass (<i>Urochoa panicoides</i>)	LS	✗	✓	✓
Bellvine (<i>Ipomea plebeia</i>)	B	✗	✗	✓

(a) Data download

The raw data (*.asd format) was downloaded to a computer using HH2 Sync software from the ASD company (Step one, Figure 4-7). An IDFile for each capture was created using MS Excel (unique ID for each plant species and number) (Step two, Figure 4-7). The raw data was transformed into ASCII (American Standard Code for Information Interchange) format (*.txt) using ViewSpec Pro Software (ASD, Inc.) (Step three, Figure 4-7). Each reflectance was captured in a single file (spectral file) but there was no IDFile automatically generated for each reflectance capture. A transformation process was used to combine (Step four, Figure 4-7) each spectral file and IDFile into a single large MS Excel MasterFile (Step five, Figure 4-7). This was done using an R software code (Calderón et al. 2015) which merged the spectral file Id and the unique IDFile (Appendix A). The data collected for all weeks was combined into the MasterFile.

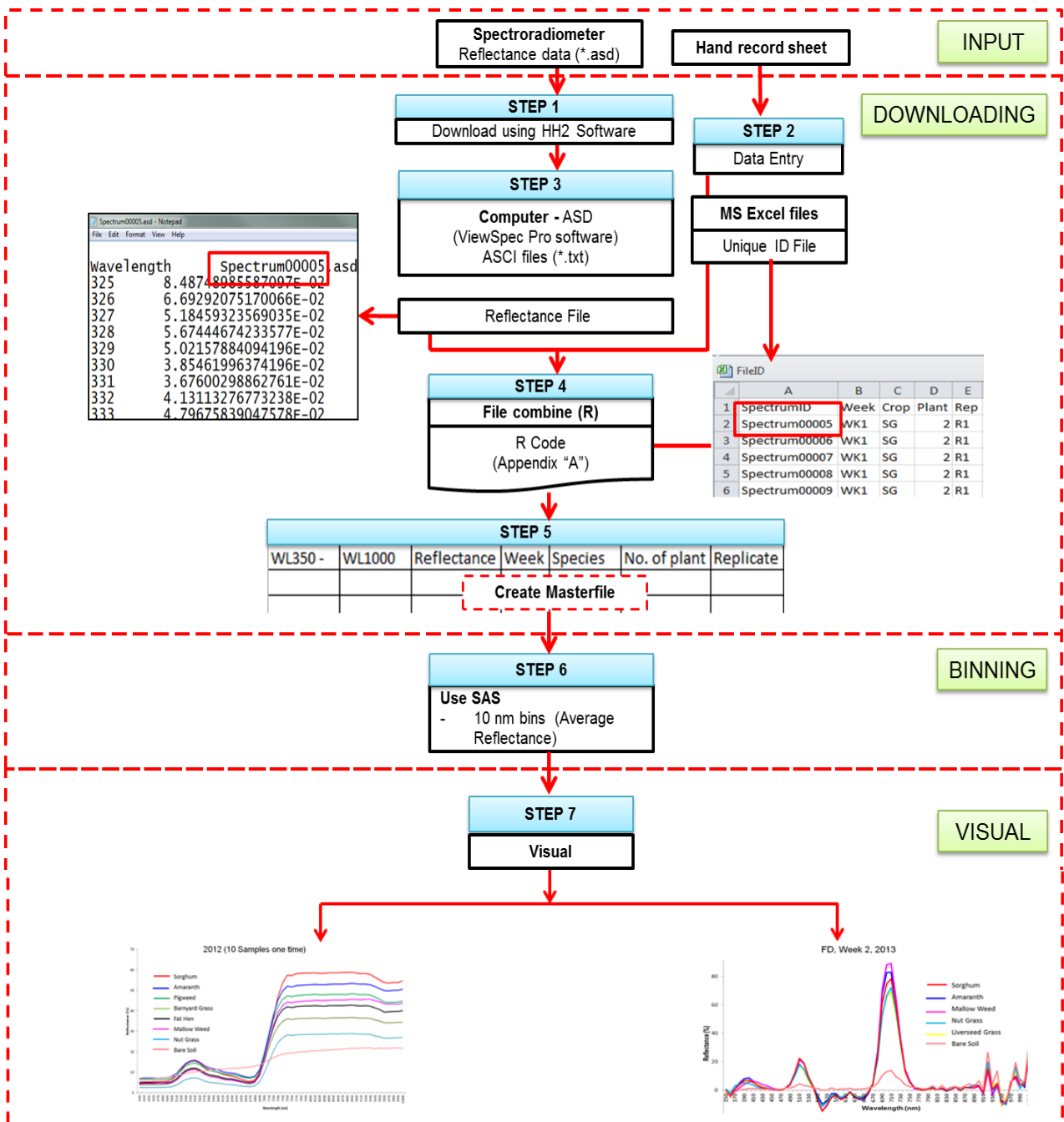


Figure 4-7 Hyperspectral data download and pre-processing

4.3.1.2 Pre-processing procedures

(a) Binning

Pre-processing is used to smooth the reflectance values to increase the reliability of the subsequent analysis (Nicolai et al. 2007). Hyperspectral reflectance data was collected from four replicated plots at each stages of growth as discussed in Chapter 3. The sixth step (Figure 4-7) was binning the reflectance data into 10 nm bins (Table 4-4) using SAS software. The bins used in 2014 were 10 nm because the band pass filters for the camera were 10 nm wide.

Table 4-4 Binned data

Year	Bin Size
2012	5 nm
2013	5 nm
2014	10 nm

(b) Spectral Display

The profiles for all species were visualized graphically (Step Seven, Figure 4-7).

(c) First Derivative analysis

The FD were calculated in MS Excel and displayed as shown in Step seven, Figure 4-7.

4.3.2 Moisture content analysis

In 2013 leaf samples from each weed species and sorghum were collected weekly for moisture analysis. The samples were selected randomly for each species within three metres of each locus (Figure 3.7, Chapter 3) and put into small plastic vials for laboratory analysis.

In the laboratory, the fresh weight of each sample was recorded. All samples were dried for 3 days at 65 °C. The samples were then weighed and the plant moisture content was calculated as follows (Equation 2):

$$MC (\%) = ((FW - DW) / FW) * 100 \quad (2)$$

Where:

MC = Moisture Content

FW = Wet weight, g

DW = Dry weight, g

The potential effect of moisture on reflectance was tested by correlating MC with leaf reflectance. The correlation was done for reflectance from the seven bands listed in Table 4-5. The seven bands were chosen based on Landsat ETM.

Table 4-5 Seven Landsat (ETM) bands

Spectral Region	Bands (midpoint)
1	660 nm
2	680 nm
3	710 nm
4	720 nm
5	730 nm
6	750 nm
7	830 nm

4.4 RESULTS

4.4.1 Reflectance results

Spectral reflectance profile for 2012 is shown graphically for each type of weed and for sorghum and for soil in Figure 4-8. Basically the spectral profile showed a low reflectance in the visible region with small peak in the green region, an increase beginning at 690 nm reaching a plateau in the NIR region. These are typical of green plant reflectance spectra. A comparison of the profiles shows that there is a larger difference in reflectance between species at some wavelengths compared to other wavelengths.

Species differences show up at specific wavelengths. In the visible spectrum (450 nm – 680 nm), all plant spectral signatures were very similar and many overlapped each other, while in the infrared region (680 nm – 990 nm) the spectra of different species separated from each other.

Sorghum had the highest NIR reflectance compared to the weed species in 2012 (Figure 4-8). The second highest reflectance was amaranth and followed by pigweed. Nutgrass had the lowest reflectance followed by barnyard grass. Pigweed, mallow weed and fat hen had reflectance spectra that were close to each other compared to the other weeds.

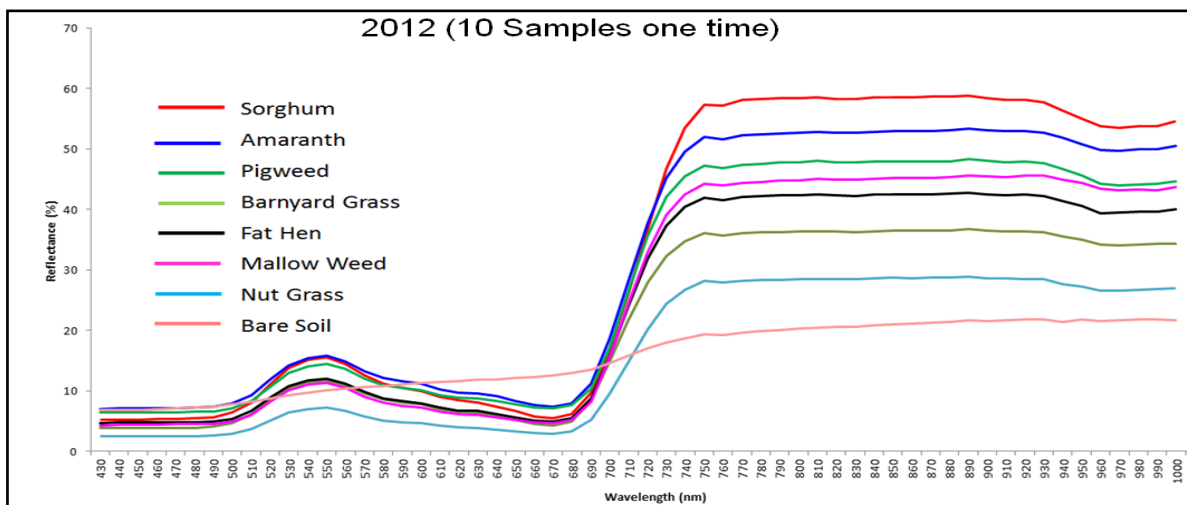


Figure 4-8 Average spectral reflectance profile for 2012

Spectral reflectance profiles for 2013 are shown graphically for each type of weed and for sorghum and for soil in Figure 4-9. Some of the spectral signatures in the range between 690 nm - 740 nm are very close to each other while others are further apart (Figure 4-9). The differences between the species are greater at the longer wavelengths, towards 740 nm (NIR).

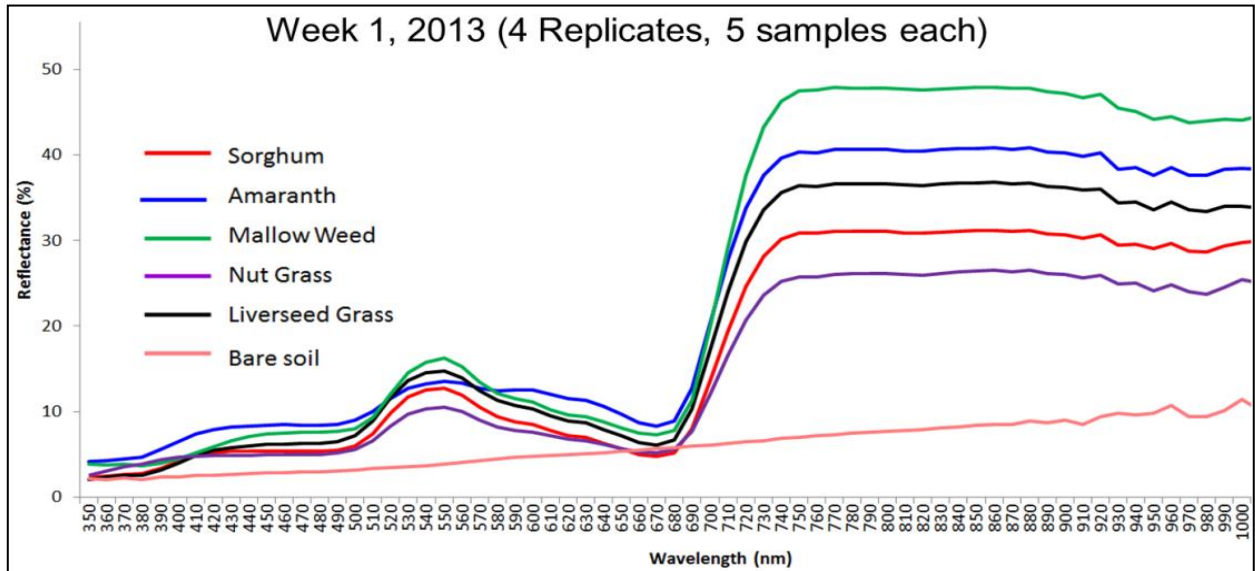


Figure 4-9 Average spectral reflectance profiles for 2013 (Week one) (continued)

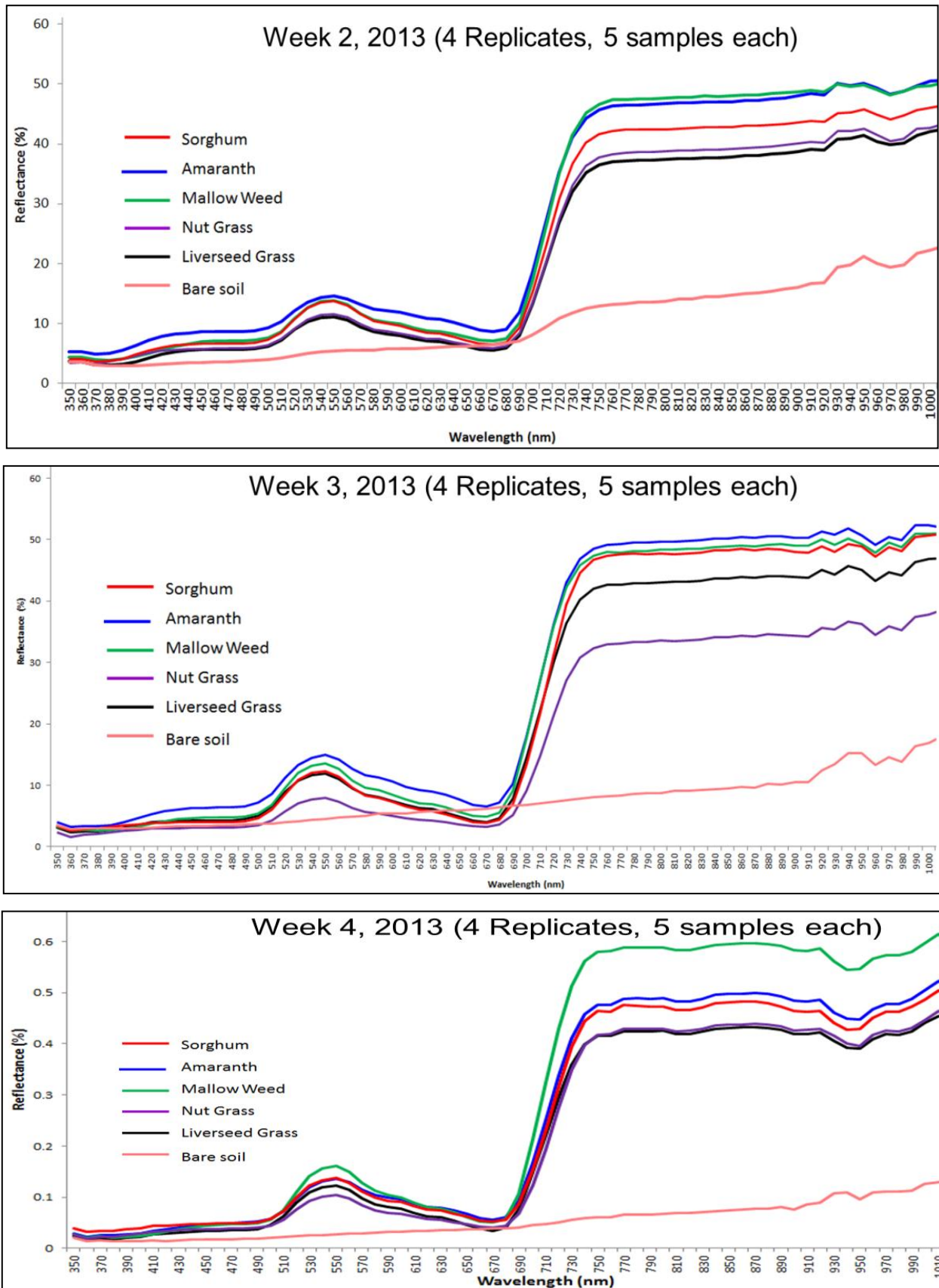


Figure 4-9 (continued) Average spectral reflectance profiles for 2013 (Week two to four)

The relative position of the species profiles in 2013 was different from 2012. Unlike in 2012, sorghum's spectral profile in 2013 was intermediate in reflectance between the weed species. In the NIR region, mallow weed and nutgrass had the highest and lowest reflectance respectively in week one (2013). In week two mallow weed and amaranth had similar reflectance values and liverseed grass and nutgrass were lower compared to reflectance of other species. In week three, nutgrass had the lowest reflectance compared to the others. In week four, amaranth and sorghum were almost similar to amaranth. Nutgrass and liverseed grass still had the lowest reflectance and almost overlapped each other. Mallow weed shows the highest reflectance compared to the others and separated distinctly from the other species almost every week.

Spectral reflectance profiles for 2014 are shown in Figure 4-10. In 2014, pigweed had the highest reflectance in week two (first week of record in 2014) followed by bellvine (Figure 4-10). Both sorghums (non pre-emergence and pre-emergence) had similar reflectance at this stage and almost overlapped from 550 nm to 710 nm. The weed species with the closest spectral profile to sorghum is liverseed grass. Its spectral profile is very close to sorghum at all wavelengths below 720 nm, however it diverges above 720 nm.

By week three of 2014, liverseed grass had the highest reflectance and nutgrass had the lowest reflectance. Pigweed at this stage had a lower reflectance and overlapped with the pre-emergence sorghum reflectance. In the green region (550 nm) all the species overlapped except bellvine and liverseed grass.

The spectral reflectance profiles of most species were closer together in week four than they were in week three, except for pre-emergence sorghum and nutgrass. Sorghum treated with pre-emergence herbicide had the highest reflectance and nutgrass had the lowest reflectance in the NIR region in week four. However, in the green region (540 nm) all species overlapped except bellvine and sorghum non pre-emergence.

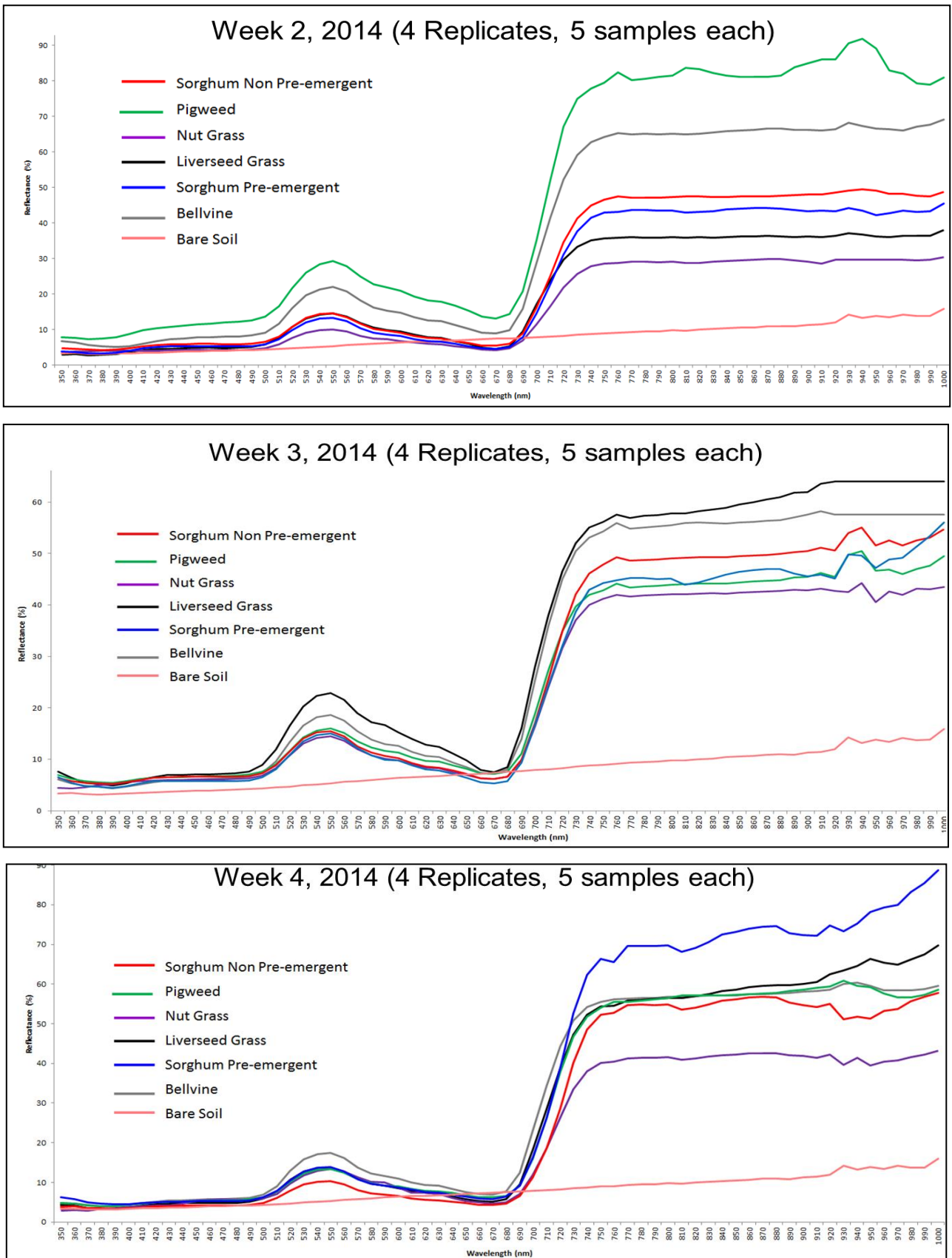


Figure 4-10 Average spectral reflectance profiles for 2014 (Week two to four)

4.4.2 First Derivative results

The graphs of the First Derivative of the reflectance profiles (rate of change in profile) are shown in Figure 4-11, Figure 4-12 and Figure 4-13. Overall they show that the sorghum and weeds have a small reflectance peak around 510 nm and a large FD reflectance peak in the red-edge region (680 nm – 730 nm). However, each species responds uniquely in these regions.

In 2012, week four sorghum (Figure 4-11) had the largest rate of change (FD) and nutgrass had the lowest rate of change. Other species had intermediate rates of changes. It shows that between 700 nm to 710 nm, rates of changes for all species separate widely except amaranth and pigweed which were very close to each other.

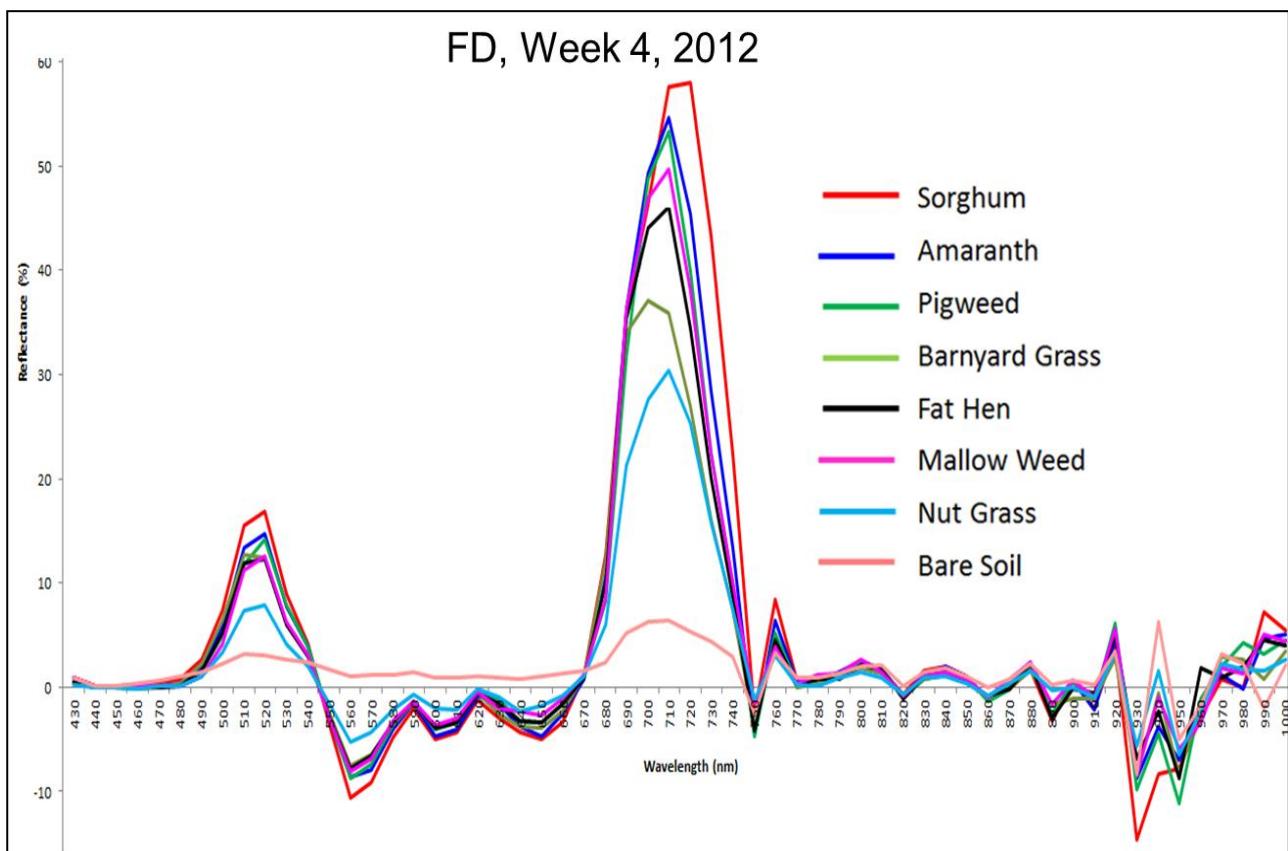


Figure 4-11 First Derivative spectral graph

In 2013 (Figure 4-12), mallow weed had the highest rate of change in the red edge region in weeks one, two and four and was equivalent to sorghum in week three.

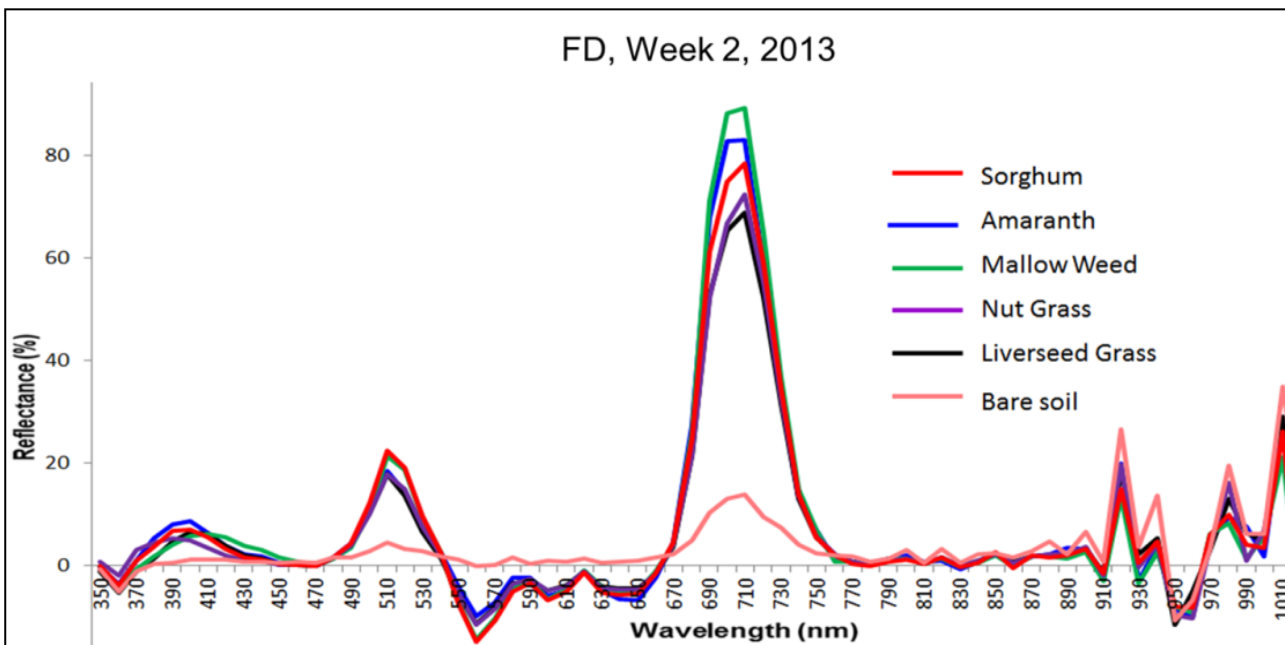
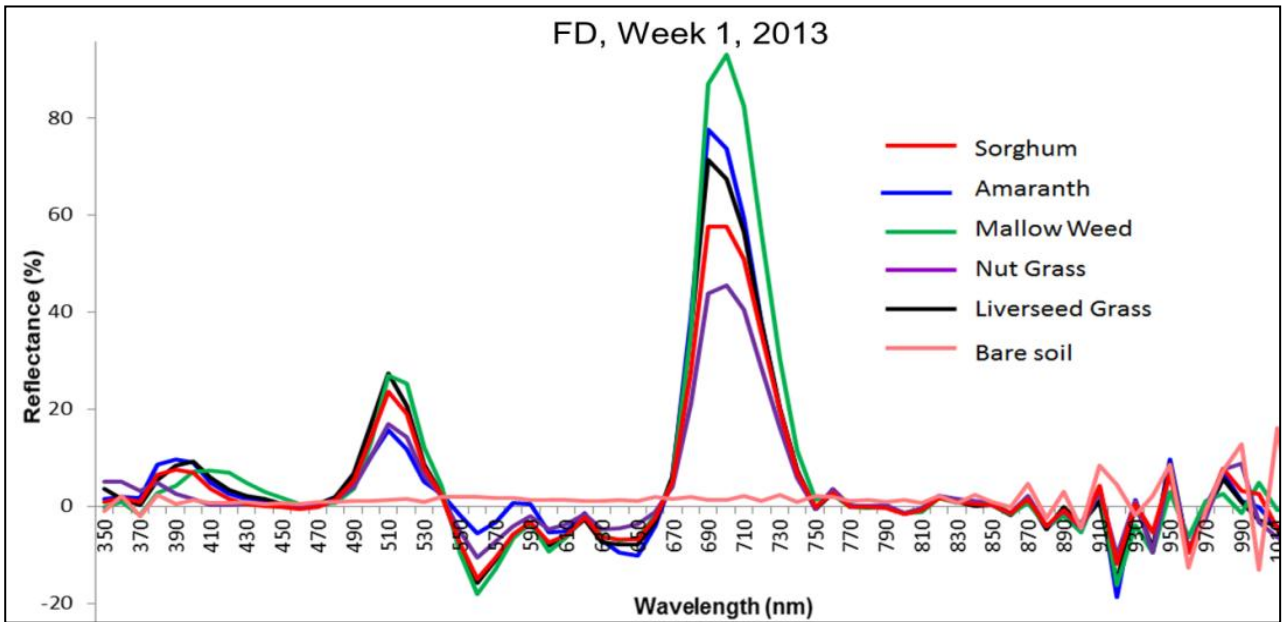


Figure 4-12 FD spectral profiles for 2013 (Week one and two) (continued)

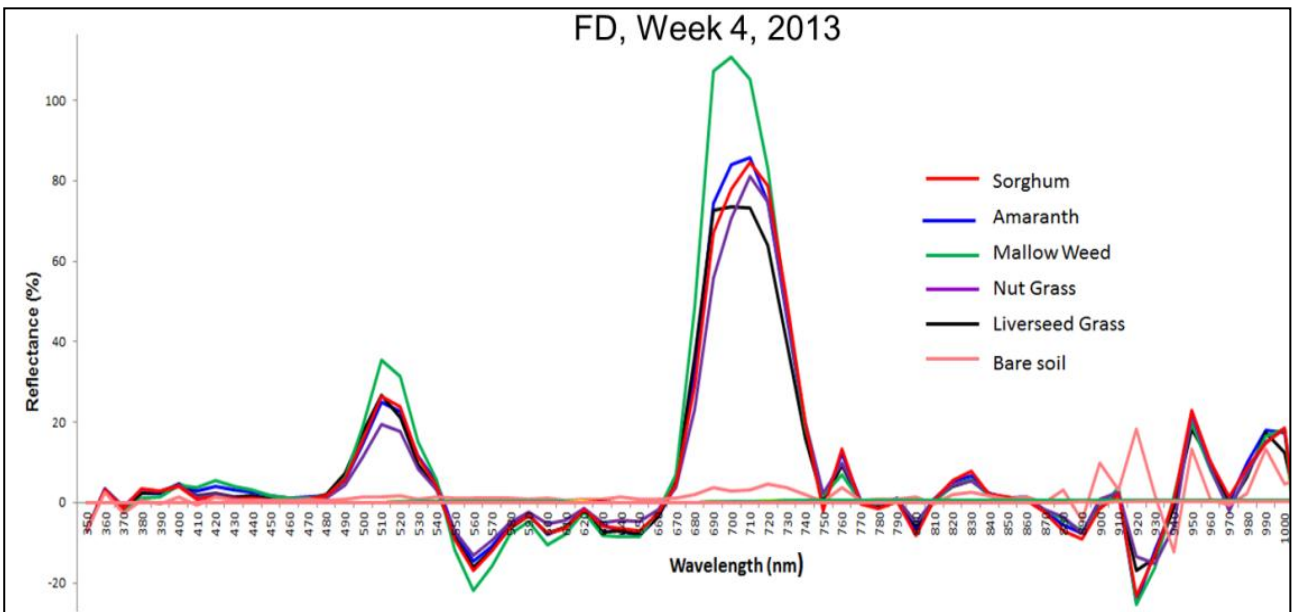
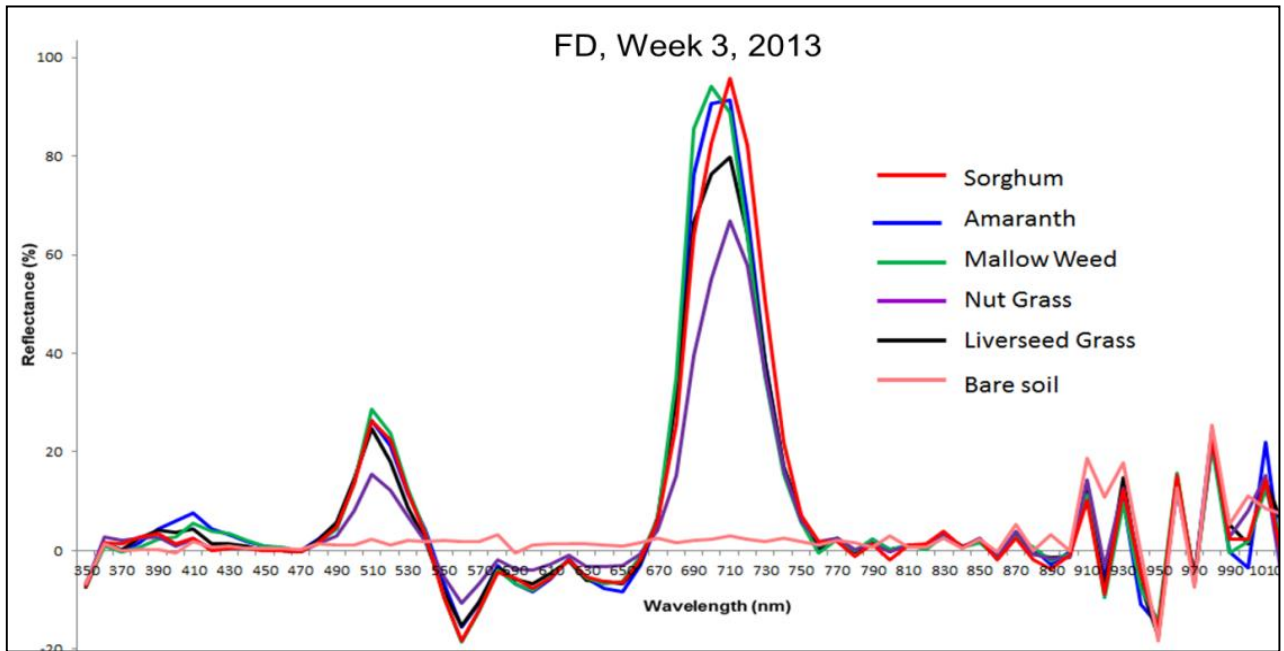


Figure 4-12 (continued) FD spectral profiles for 2013 (Week 3 and 4)

In weeks one and two, all the species separated widely. However, the FD reflectance between species overlapped more from week three to week four. In week three, nutgrass and liverseed grass were widely separated compared to other weeds. Each week, nutgrass showed the lowest rate of change except in week four. In week four, mallow weed had a 20% higher FD reflectance compared to the next highest FD reflectance which was for amaranth. Liverseed grass had the lowest FD reflectance in week four.

In 2014, weeds and sorghum again had varying rates of change in different weeks (Figure 4-13). In week two, pigweed had the highest rate of change in the red edge region followed by

bellvine. In weeks three and four, liverseed grass and pre-emergence sorghum had the highest rate of change respectively. Nutgrass had the lowest rate of change for all weeks. Pre-emergence and non pre-emergence sorghum had slightly different FD reflectance from each other even though they are the same species. In week two, sorghum non pre-emergence had a higher rate of change in reflectance than sorghum pre-emergence. Both rates of change were intermediate. In week three, they separated more widely until in week four, sorghum pre-emergence had the highest FD reflectance of all species. It was much higher than sorghum non pre-emergence. Nutgrass showed the lowest FD reflectance each week. The FD reflectance for bellvine peaked at 690 nm rather than at 710 – 720 nm for the other species. It had the same magnitude as pigweed, liverseed grass and non pre-emergence sorghum. According to Lamb et al. 2010, this is due to the environmental effects experienced by the plant at the time because some leaves may exhibit a latent bimodal FD spectral characteristic. For example at 705 and 725 nm it has the distinct shapes of the chlorophyll red-edge for ryegrass (Lamb et al. 2010). Lamb et al. 2010 added that the Leaf Area Index (LAI) was sensitive to the first peak of the chlorotic leaves. However, in this research, the spectral reflectance only was collected to discriminate the weed species. It is useful if it can be related to the chlorophyll content as Lamb et al. (2010) demonstrated for the estimation of nitrogen concentration in ryegrass. The concept can be used to improve the analysis and prediction.

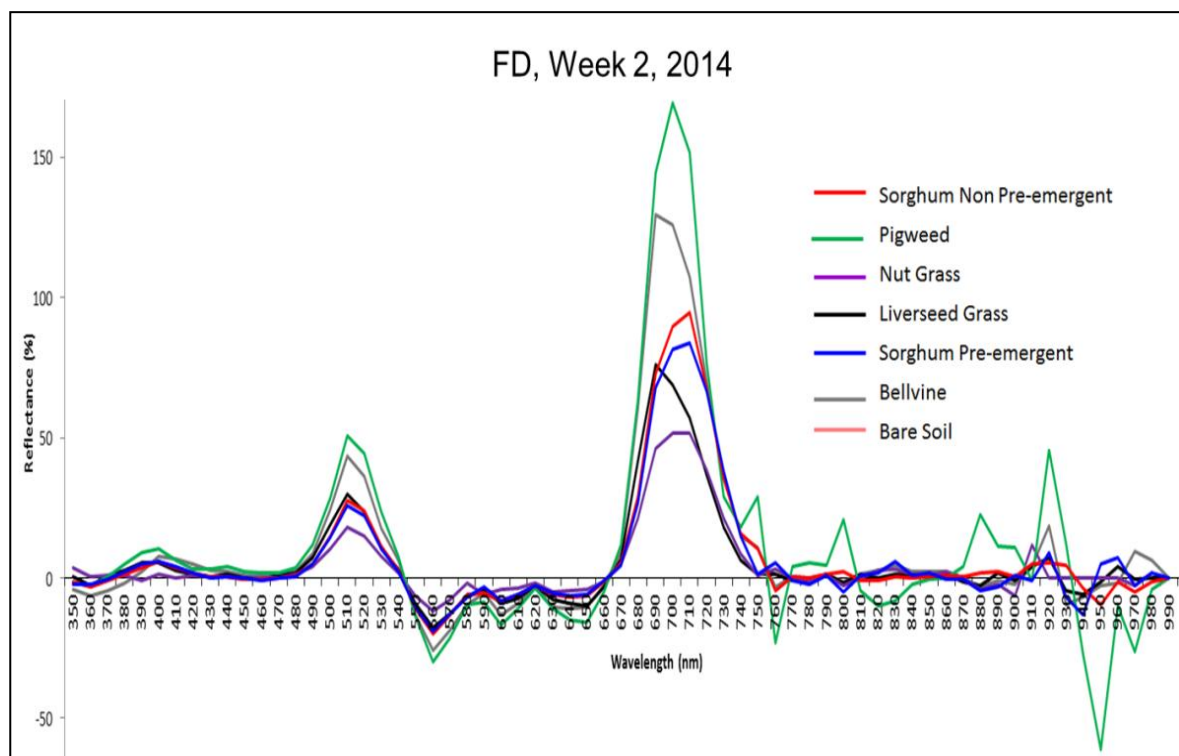


Figure 4-13 FD spectra profiles for 2014 (Week two) (continued)

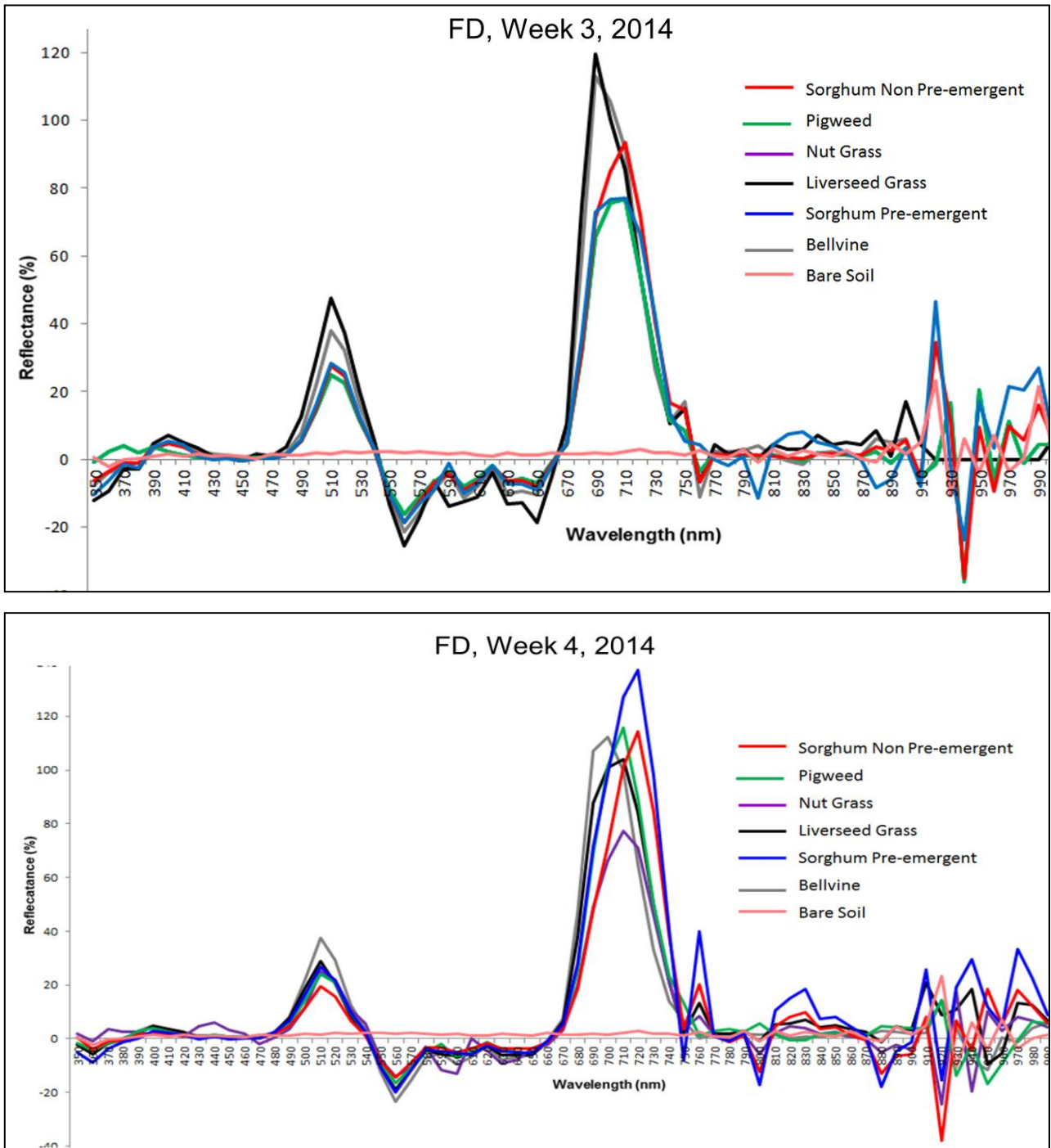


Figure 4-13 (continued) FD spectra profiles for 2014 (Week three and four)

4.4.3 Effect of moisture content on reflectance

The average moisture content for four species at weeks two through four after planting in 2013 is shown in Figure 4-14. At week two most of the species had 80% or more MC. There is more variation in moisture content in week three. The MC peaked at week three for all species. Sorghum and nutgrass showed a strong decrease in week four.

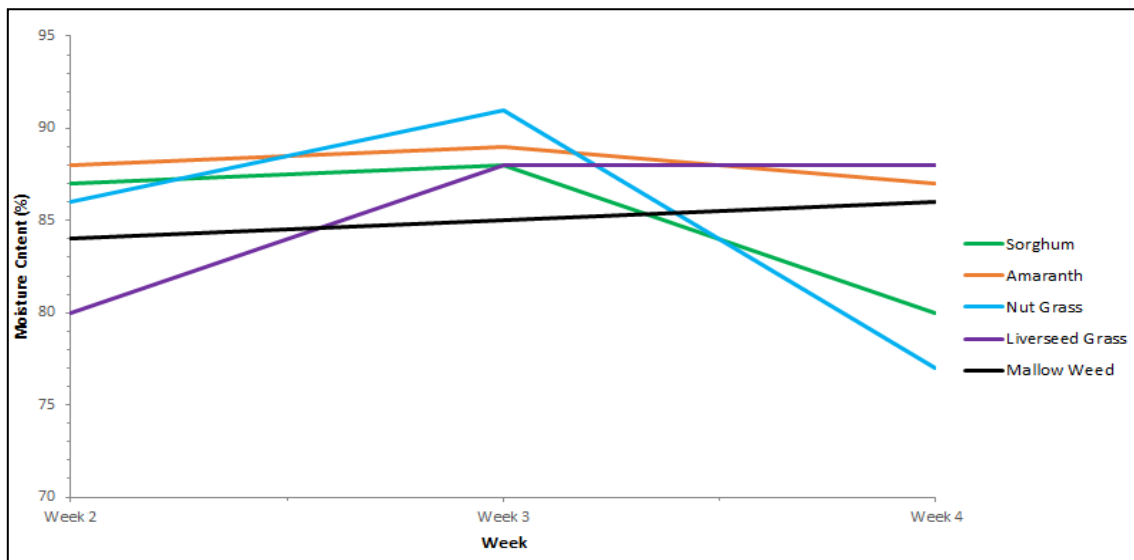


Figure 4-14 Moisture content for all species (2013)

The correlation analysis results for each species for the bands listed in Table 4-5 are shown in Table 4-6, Table 4-7, Table 4-8, Table 4-9 and Table 4-10. The results for sorghum show that the values for 750, 720 and 710 nm were strongly correlated with moisture content ($R > 0.8$) (Table 4-6). These results indicate a potential moisture influence on reflectance at these wavelengths for sorghum. Reflectance from the other bands does not show a consistent pattern of response to moisture content for sorghum.

Table 4-6 Correlation of MC with sorghum reflectance

Moisture Content	Week 2	Week 3	Week 4	Correlation Values	
	87%	88%	80%	R	R ²
Band mid wavelength (nm)	Reflectance (Table 4-5)				
830	0.43	0.48	0.47	-0.22	0.05
750	0.42	0.48	0.08	*1.00	*1.00
730	0.37	0.39	0.39	-0.40	0.16
720	0.31	0.31	0.07	*0.99	*0.99
710	0.23	0.22	0.06	*0.99	*0.97
680	0.07	0.04	0.06	-0.30	0.09
660	0.07	0.04	0.03	0.61	0.37

= High correlation ($R > 0.80$)

The correlation between amaranth reflectance and moisture content for weeks two to four (Table 4-7) shows that the reflectance at 750, 730, 720 and 710 nm was strongly correlated with moisture content ($R > 0.8$). All R-values show a positive correlation.

Table 4-7 Correlation raw spectral for amaranth

Moisture Content	Week 2	Week 3	Week 4	Correlation values	
	88%	89%	87%	R	R ²
Band mid wavelength (nm)	Reflectance (Table 4-5)				
830	0.47	0.50	0.49	0.33	0.11
750	0.46	0.49	0.09	*0.90	*0.81
730	0.41	0.43	0.41	*0.87	0.75
720	0.35	0.31	0.06	*0.80	0.63
710	0.27	0.27	0.05	*0.87	0.75
680	0.09	0.07	0.06	0.33	0.11
660	0.09	0.07	0.02	0.69	0.48

 = High correlation (R > 0.80)

The correlation for nutgrass reflectance and moisture content for weeks two to four (Table 4-8) shows that the reflectance at 750 nm was strongly positively correlated, however reflectance at 830 nm and 730 nm was strongly negatively correlated (R > 0.8).

Table 4-8 Correlation raw spectral for nutgrass

Moisture Content	Week 2	Week 3	Week 4	Correlations values	
	86%	91%	77%	R	R ²
Band mid wavelength (nm)	Reflectance (Table 4-5)				
830	0.39	0.34	0.43	*-0.97	*0.95
750	0.38	0.32	0.06	*0.86	0.74
730	0.33	0.27	0.35	*-0.90	*0.82
720	0.28	0.21	0.05	0.79	0.62
710	0.20	0.15	0.04	0.78	0.61
680	0.06	0.04	0.04	0.16	0.03
660	0.06	0.03	0.01	0.54	0.29

 = High correlation (R > 0.80)

Table 4-9 shows that the correlation of reflectance for liverseed grass with moisture content for weeks two to four at 830 nm and 730 nm was strongly positively. At 680 nm and 660 nm reflectance, it was strongly negatively correlated with moisture content. Reflectance from the other bands does not show a consistent pattern of response to moisture content.

Table 4-9 Correlation raw spectral for liverseed grass

Moisture Content	Week 2	Week 3	Week 4	Correlations values	
	80%	88%	88%	R	R ²
Band mid wavelength (nm)	Reflectance (Table 4-5)				
830	0.38	0.43	0.42	*0.98	*0.96
750	0.36	0.42	0.11	-0.33	0.11
730	0.32	0.36	0.36	*1.00	*1.00
720	0.27	0.30	0.09	-0.38	0.15
710	0.20	0.22	0.07	-0.39	0.15
680	0.06	0.05	0.04	*-0.87	0.75
660	0.06	0.04	0.02	*-0.87	0.75

 = High correlation (R > 0.80)

The correlation of reflectance of mallow weed with moisture content for weeks two to four (Table 4-10) at 680 nm and 660 nm was strongly negatively correlated ($R > 0.8$). Reflectance from the other bands does not show a consistent pattern of response to moisture content.

Table 4-10 Correlation raw spectral for mallow weed

Moisture Content	Week 2	Week 3	Week 4	Correlation values	
	84%	85%	86%	R	R ²
Band mid wavelength (nm)	Reflectance (Table 4-5)				
830	0.48	0.49	0.59	0.68	0.46
750	0.47	0.47	0.07	-0.64	0.40
730	0.41	0.42	0.51	0.70	0.50
720	0.35	0.36	0.06	-0.63	0.39
710	0.26	0.27	0.05	-0.62	0.38
680	0.07	0.05	0.01	*-0.88	0.77
660	0.08	0.06	0.06	*-0.96	*0.92

= High correlation ($R > 0.80$)

The correlation of moisture content with FD reflectance was tested for all species from weeks two through four in 2013 (Table 4-11). The results show an overall low correlation ($R < 0.8$) between the FD reflectance and MC for all bands.

Table 4-11 Correlation of First Derivative reflectance for all species (2013)

Species	Sorghum		Mallow Weed		Amaranth		Nutgrass		Liverseed Grass	
	R	R ²	R	R ²	R	R ²	R	R ²	R	R ²
FD830	-0.67	0.45	-0.11	0.01	-0.62	0.38	-0.57	0.32	-0.07	0.00
FD750	-0.14	0.02	-0.07	0.00	-0.62	0.38	-0.18	0.03	0.37	0.14
FD730	-0.14	0.02	-0.09	0.01	-0.71	0.50	-0.36	0.13	0.42	0.18
FD720	0.07	0.00	-0.12	0.01	-0.58	0.34	-0.26	0.07	0.38	0.14
FD710	-0.01	0.00	-0.22	0.05	-0.56	0.31	-0.37	0.14	0.48	0.23
FD680	0.13	0.02	-0.09	0.01	-0.37	0.14	-0.03	0.00	0.46	0.21
FD660	0.40	0.16	0.43	0.18	0.50	0.25	0.56	0.31	-0.06	0.00

4.5 DISCUSSION AND ANALYSIS

4.5.1 Effect of moisture on species reflectance

Differences in the spectral reflectance of plants occur during the growing season due to change in cell size, chemical composition and water concentration (Zwiggelaar 1998; Calderón et al. 2015). Reflectance is high in the NIR region except in the water absorption bands at 1450 and 970 nm (Zwiggelaar 1998). Moisture content measurement in this research was based on the water content of leaves.

The moisture correlation analysis focused on seven bands ranging from 830 nm to 660 nm (Table 4-5) because these were the bands for which band-pass filters were available for the MCA 6 camera in 2013. An et al. (2015) showed that the spectral bands that are sensitive to moisture content are 1450, 970, 750 and 690 nm. Carter and Knapp (2001) found that the 700 nm and 550 nm bands were the bands of maximum difference in reflectance and can be used to identify plant stress. The results from this study (Table 4-12) show that reflectance was correlated both positively and negatively with moisture content at specific wavelengths for specific species. For example, at 750 nm there was a strong positive correlation between reflectance and MC in sorghum, amaranth and nutgrass but not in liverseed grass and mallow weed. Also, at 730 nm there was a positive correlation between reflectance and MC in amaranth and liverseed grass but strong negative correlation with reflectance from nutgrass.

Reflectance of nutgrass showed a negative correlation with MC at 830 nm and liverseed grass showed a positive correlation with MC at 830 nm. Other weeds showed no correlation with MC at 830 nm. The pattern of correlation between MC and reflectance varied for each species. For instance at 720 nm, only sorghum and amaranth were positively correlated but not for nutgrass, mallow weed and liverseed grass. Others species were intermediate. There was a negative correlation with MC at 680 nm for mallow weed and liverseed grass.

Table 4-12 Summary of effect of MC on reflectance

Band	Nutgrass	Mallow weed	Sorghum	Amaranth	Liverseed grass
830	-	<i>i</i>	<i>i</i>	<i>i</i>	+
750	+	<i>i</i>	+	+	<i>i</i>
730	-	<i>i</i>	<i>i</i>	+	+
720	<i>i</i>	<i>i</i>	+	+	<i>i</i>
710	<i>i</i>	<i>i</i>	+	+	<i>i</i>
680	<i>i</i>	-	<i>i</i>	<i>i</i>	-
660	<i>i</i>	-	<i>i</i>	<i>i</i>	-
+ = positive correction - = negative correlation <i>i</i> = indeterminate effect					

In summary, moisture content of these species does not appear to have a consistent effect on reflectance for the bands being measured in this analysis. Accordingly, the moisture content of the leaves was not considered any further in this research.

4.5.2 Species reflectance values

Hyperspectral reflectance of weed and crop plants depends on the characteristics of the species. Understanding of spectral reflectance is important to predict the condition of the species. Every species contains different chemical components which are influenced by its physical environment. Use of a combination of visible, NIR and thermal IR spectra has been found to give

very good results in species classification (Price 1987; Kefyalew et al. 2005; Voss et al. 2010). The hyperspectral profiles for each weed species and for crop plants were shown to be useful in species classification (Siddiqi et al. 2014). Reflectance in the NIR (940 – 900 nm), red (700 – 650 nm) and green (550 – 500 nm) was influenced by the chemical composition in the leaf and had a very strong relationship to the crop characteristics (Prasad et al. 2011).

The early growing season (1-4 weeks after planting) is the best time to see the differences in spectral reflectance of a species (Zwiggelaar 1998). One of the difficulties during data collection under the field condition at this stage is small size and similar visual characteristics of the leaves leading to potential mistaken identification. When the size of the leaf is too small, the spectrometer probe may accept reflectance from surrounding areas including the soil and other plants. Mature plants are more difficult to control with herbicides so it is unlikely that weed maps based on detection at later stages of growth would be useful.

The spectral profiles in 2012 show that sorghum and nutgrass had the highest and lowest reflectance respectively. In 2012, reflectance data was collected once during week four after planting. All species from which reflectance values were collected were advanced in growth. Sorghum had the largest reflectance compared with other species. This can be seen from the spectral profile in Figure 4-8.

The spectral profiles for 2013 were collected for four weeds plus sorghum at four stages of growth (Figure 4-9). Differences between the species were evident in the green, red-edge and NIR regions. However, because the differences were most evident in the NIR region this discussion focuses on this region. The reflectance pattern in this region changed from week to week. The largest separation between species occurred at week one, when the plants were smallest and the least separation occurred at week three. At week two, mallow weed and amaranth had a higher reflectance than sorghum, and nutgrass and liverseed grass had a lower reflectance. At week four, this same pattern persisted except that the reflectance of amaranth had moved closer to that of sorghum.

The 2013 results suggested the use of reflectance between 800 nm (NIR) to 690 nm (red-edge) for discriminating between these species (Figure 4-9). This is consistent with the findings of Smith and Blackshaw (2003) who obtained 90 and 98% accuracy in classification when using visible and red-edge wavelengths.

A similar pattern was found in the NIR region in the 2014 data collection. Reflectance values for the earliest week in this year (second week after planting) show that each species separated widely in the NIR region. The spectral profiles became closer together as the plants aged (week two to week four). The pre-emergence sorghum reflectance increased steadily from week two to week four by which time it was higher than the reflectance for other species. The reflectance of

liverseed grass also increased steadily relative to other species. The reflectance of pigweed, bellvine and non pre-emergence sorghum grouped together as the plants aged. Nutgrass exhibited the lowest spectral profiles at all growth stages. This was similar to 2013.

It is important to understand how crop plants are affected by weeds in their surroundings. Weeds compete with crop plants for essential resources for growth (Sankaran et al. 2015). The effect of this is visible at week four where the pre-emergence sorghum has a much higher reflectance than the non pre-emergence sorghum indicating better growth in the absence of weeds. In the non pre-emergence area, the weeds compete with the sorghum and each species has a similar amount of reflectance in the NIR. A similar pattern of reduced hyperspectral reflectance due to species competition was found by Kodagoda and Zhang (2010). Most of the species had similar reflectance by week four. At this stage of growth, maximum separation between the spectral profiles occurred at 720 nm. This confirms why 720 nm is significant for discriminating weeds from sorghum.

4.5.3 First Derivative Values

The First Derivative of the spectral profile shows the rate of change of reflectance. The NIR spectral window of 730 – 720 nm appears to generate the highest FD reflectance for all species. In 2012, the FD graphs show that sorghum had a higher rate of change than the other species (Figure 4-11). The area of overlap in Figure 4-8 shows as separate peaks in Figure 4-11.

In 2013, the pattern of the spectral profiles appears consistent for each week (Figure 4-9). The differences between bands become apparent in the 2013 FD graph (Figure 4-12). It shows that in week one, the FD profiles separated widely in the NIR region. This indicates that during the early stage of weed growth, the FD reflectance profiles could be used to classify the species accurately. In weeks two, three and four, the reflectance profiles were close together and this is confirmed by the FD analysis (Figure 4-12). Because the spectral reflectances are closer together, the species may be more difficult to separate at these stages.

In 2014, the FD graphs were consistent with the spectral profile graphs where the pattern was different for each week (Figure 4-13). In week one, pigweed showed the highest rate of change while in week two, pigweed had the lowest rate of change and in week four, it had the second highest rate of change. In week four, pre-emergence sorghum had the highest peak in the NIR region and this was expected since the weeds were controlled by the pre-emergence herbicides. This is consistent with weeds influencing the growth of the crop if not controlled (Sankaran et al. 2015).

4.6 CONCLUSIONS

This chapter explored the use of hyperspectral reflectance data to identify the differences between weed species and sorghum. The potential influence of moisture content on reflectance was investigated. Moisture content was found not to affect reflectance from weeds and sorghum in the wavelengths of interest in this research.

Hyperspectral raw reflectance data were binned and plotted for each species for each year. The profiles are generally consistent with previous vegetation profiles; however, differences between species were readily apparent. The relative differences in reflectance between species change with stage of growth are greatest in the green, red-edge and NIR regions.

The binned raw reflectance values were converted to First Derivative reflectance values and graphed. The FD graphs show the differences in the spectral profiles clearer than can be seen in the raw reflectance profiles. This allows the identification of the bands that are most likely to be significant for species classification. It is essential to collect the correct multispectral imagery for weed detection in the sorghum crop. The details of the statistical analysis of the reflectance data to identify suitable bands for classification of the species and for use in a multispectral camera are presented in the next chapter.

Chapter 5

SPECTRAL BANDS FOR DISCRIMINATION OF WEEDS IN SORGHUM

5.1 INTRODUCTION

The previous chapters discussed the differences and similarity of the spectral reflectance for the weeds and sorghum and the relationship between the MC of each weeds. This information on spectral reflectance is essential for selecting the imagery to create weed maps to discriminate weeds from sorghum. The imagery needs to be based on spectral bands which contain the differences in reflectance between the weeds and sorghum. Knowledge of the spectral differences between species can be used to improve classification of plant species from satellite or aerial imagery. Satellite remote sensing imagery provides wide coverage of an area but in this application, it was not suitable for weed detection due to the size of the target weeds, spatial and spectral resolution of the imagery, real time information requirement, cost and cloud cover (Eddy et al. 2013).

Arafat et al. (2013b) used Linear Discriminant Analysis (LDA) on 2500 to 400 nm hyperspectral data to discriminate between winter (wheat and clover) and summer crops (maize and rice). For example, clover was uniquely identified by wavelengths in the 1299 to 727 nm zone, while wheat was uniquely identified by the wavelengths in three zones, 712 to 350 nm, 1562 to 451 nm and 2349 to 1951 nm. Maize was uniquely identified by the spectral zone of 1299 to 730 nm and rice by three zones, 713 to 350 nm, 1532 to 1451 nm and 2349 to 1951 nm. This research established that different species have unique spectral reflectance patterns.

The following section provides more detail about how other investigators identified spectral differences between weeds and crops and how they used this information for weed mapping. The statistical procedures for identifying the bands of wavelengths which give the best separation and classification of the weeds are discussed. Finally, the results and accuracy of classification are presented and discussed. The results of this analysis were used to select band-pass filters for image classification as discussed in Chapter 6.

5.2 LITERATURE REVIEW

This section discusses the procedures for discriminating between weeds and crops using hyperspectral remote sensing. Every plant interacts with sunlight with the sunlight being absorbed, transmitted and reflected. The reflectance of light depends on leaf pigments and structure. The pattern of reflectance is unique to each plant. It indicates whether the plant is healthy or under stress. Plant species can be identified based on their unique spectral reflectance (Amelinckx 2010). Schmidt and Skidmore (2004) (cited in Amelinckx (2010)) found that the difference in spectral reflectance between the examined objects is greater than that difference in the spectral separability within examined objects. Weed and crop plants each have their own spectral signatures and discrimination between them can be measured using the differences in their spectral signatures (Vrindts et al. 2002).

Carvalho et al. (2013) found species could be discriminated by using reflectance from flowers and leaves. Flower spectra were more prominent and brighter in colour and variety than leaf spectra. However, while they could accurately determine the species from flower reflectance data, they found that leaf reflectance was needed to accurately determine nitrogen levels in the plants.

Spectral differences can also be used to study exposure to ecological processes (competition, disease, invasiveness and biological control of plant abundance such as insects) (Carvalho et al. 2013). The leaf area index, chlorophyll content, pigment content and vegetation indices are also useful features for improving weed discrimination (Kodagoda and Zhang 2010). The chlorophyll absorbs more in the red and less in the NIR and this ratio often is used for biomass or vegetation indices in remote sensing applications (Kodagoda and Zhang 2010). It is very beneficial to monitor spectral reflectance to identify the plant species efficiently and to save time (Castro-Esau 2006). However, using airborne hyperspectral or satellite hyperspectral is very expensive (Castro-Esau 2006) compared to UAV sourced imagery.

There are many techniques that can be used to uniquely identify and classify species based on their spectral profiles. Some of the currently reported results are summarized in Table 5-1.

Table 5-1 Weed and crop plants discriminated using hyperspectral data

Discrimination of Vegetation	Processing Method	Sources
Soybean, canola, wheat, oat and barley	Stepwise Linear Discriminant Analysis (SLDA)	(Wilson et al. 2014)
Weed and crop plant discrimination	SLDA, LDA and Support Vector Machines (SVMs)	(Siddiqi et al. 2014)
Wheat, clover maize and rice	One way Analysis of Variance (ANOVA) and Tukey's HSD post Hoc Analysis and LDA	(Arafat et al. 2013b)
Corn (Zea mays), Ranunculus repens, Cirsium arvense, Sinapis arvensis, Stellaria media, Taraxacum officinale, Poa annua, Polygonum persicaria, Urtica dioica, Oxalis europaea and Medicago lupulina	Learning method, Mixture of Gaussians (MOG) and Self Organising Map (SOM)	(Moshou et al. 2013)
Cruciferous weeds, broad bean and winter wheat	SLDA, neural networks (multilayer perception (MLP) and radial basis function (RBF)).	(de Castro et al. 2012)
Pines trees	Discrete Wavelet Transform (DWT), SLDA and LDA	(Banskota et al. 2011)
Aquatic weed	SLDA	(Everitt et al. 2011)
Papyrus vegetation	ANOVA, Classification and Regression Tree Analysis (CART) and Jeffries-Matusita (JM)	(Adam and Mutanga 2009)
Cotton, potato, soybean, corn and sunflower	PCA, lambda-lambda models, SLDA, derivative greenness vegetation indices, Normalized Different Vegetation Index (NDVI), regression equation, optimal multiple narrow band (OMNBR) and soil adjusted Vegetation Index	(Thenkabail et al. (2000); Thenkabail et al. (2004))
Riparian forests, burn grassland, resurgence zones, crops and several types of savannah and pastures	Band ratios and Principal Component Analysis (PCA)	(Almeida and Filho 2004)
Weed crop discrimination	SLDA	(Smith and Blackshaw 2003)
Weed and crop plants	SLDA	(Borregaard et al. 2000)
Weed and crop plant discrimination	Continuous Models (Kulbelka-Munk Theory, Plate Model, Goudriaan model) and Description Models (Markov Chain, Geometrical Optics and Monte Carlo approach)	(Zwiggelaar 1998)
Cabbage and calabrese, barley, chickweed, charlock, wild radish, canola, shepherds purse, fat hen and wild oat	Bayesian classifier	(Favier et al. 1999)
Crops agriculture and soil	Gram-Schmidt (A postol 1957), and PCA	(Price 1992)

5.2.1 Identification of different spectral classification bands

Developed by Fisher (1936), Linear Discriminant Analysis is a classical statistical approach which is widely used for the classification of hyperspectral data (Zhang et al. 1998; Sankaran et al. 2015). Stepwise Linear Discriminant analysis can be used to choose a viable subset of data from a very large initial set of data for subsequent LDA (Noble and Brown 2009; Prasad et al. 2011).

Linear Discriminate Analysis constructs a classification rule from data in known groups (the ‘training data’) which can then be applied to new samples from unknown groups (Noble and Brown 2009). LDA was used to discriminate weeds in winter wheat in Spain with almost 100% accuracy (de Castro et al. 2012). The results of the Spanish research, in which *Sinapis* spp and *Diplotaxis* spp were discriminated with a high level of accuracy, illustrated that LDA could be used for identifying weeds in winter and summer crops.

Linear Discriminant Analysis can be used to optimise selection of wavelengths in spectral zones for different types of crops (Noble and Brown 2009). Noble and Brown (2009) discriminated between weeds in wheat, tomatoes and soybean crops using hyperspectral reflectance data between 400 to 1000 nm with a 52% accuracy. The most significant bands were 959, 948, 719, 667 and 594 nm. Siddiqi et al. (2014) achieved 98% classification accuracy in separating weeds from crop plants using this method. Prasad et al. (2011) recommended that sensors should be designed for specific applications for vegetation studies by excluding redundant bands. Previous investigators found many bands useful for discriminating between species and these are summarised in Table 5-2.

Table 5-2 Selected bands for plants identification reported by previous investigators

Spectrum Colour	Reflectance Band Centre (nm)	References
Near Infrared (NIR)	815, 810	(Vrindts et al. 2002; Kefyalew et al. 2005; Wilson et al. 2014)
	800, 780, 755	(Daughtry and Walthall 1998; Kleynen et al. 2005; Wilson et al. 2014)
Red-edge	750, 720, 710	(Elvidge and Chen 1995; Daughtry and Walthall 1998; Shaw et al. 1998; Clevers 1999; Thenkabail et al. 2004; Kefyalew et al. 2005; Vaiphasa et al. 2005)
Red	675	(Vrindts et al. 2002; Fyfe 2003; Wilson et al. 2014)
	670,660,655, 600	(Daughtry and Walthall 1998; Kefyalew et al. 2005; Hutto et al. 2006)
Green	565	(Hochberg et al. 2003)
	555	(Vrindts et al. 2002; Thenkabail et al. 2004)
	550, 540, 535	(Schepers et al. 1996; Daughtry and Walthall 1998; Thenkabail et al. 2002; Fyfe 2003; Kefyalew et al. 2005; Wilson et al. 2014)
	520	(Elvidge and Chen 1995; Thenkabail et al. 2002)
Blue	500, 495	(Fyfe 2003; Thenkabail et al. 2004; Kefyalew et al. 2005; Wilson et al. 2014)

ANOVA (Analysis of Variance), Tukey HSD (Tukey Honesty Significant Difference) post hoc analysis and LDA have all been used to identify spectrally significant bands between weed and crop plants in summer and winter crops (Arafat et al. 2013b). Adam and Mutanga (2009) used ANOVA to identify an initial list of wavelengths to discriminate between papyrus (*Cyrus papyrus* L.) and the other wetland species. They used Classification and Regression Tree analysis (CART)

for the second step to reduce the number of significant wavelengths to eight which they considered to be suitable for use in image collection.

Principal Component Analysis (PCA) is a multivariate technique which decomposes the correlation matrix between samples by estimating Eigen values. This is typically done using Singular Values Decomposition (SVD). Principal Component Analysis constructs a series of uncorrelated linear combinations of the original variables to describe the relationships between data points. The method maximizes separation between data points rather than separation between groups (Almeida and Filho 2004).

Linear discriminant analysis classifies data more accurately than PCA because LDA delivers more class separability and draws a decision region between given classes while PCA modifies the shape and location of the original data in transforming it to a different data space (Calderón et al. 2015).

5.2.2 Accuracy testing

It is important to evaluate the accuracy of the classification procedures to confirm the spectrally different bands. If the methods were not validated, the wrong bands could be selected for image analysis. Accuracy can be tested by using an independent set of data or by using a different classification procedure.

Multivariate analyses (LDA and SVM) were used to test the accuracy of species identified from hyperspectral reflectance data (Calderón et al. 2015). The classification accuracy for both methods was evaluated by the overall accuracy value and the kappa (κ) coefficient. It included commission and omission errors for all classes (Calderón et al. 2015).

Neural Network (NN) analysis (NN1 = one hidden neuron and NN2 = two hidden neurons) and LDA have been used to discriminate between sugar beets and volunteer potatoes using hyperspectral reflectance (Nieuwenhuizen et al. 2010). Both methods were used to select the potential bands to discriminate between the species. NN2 was the best classification method compared to LDA and NN1. However, LDA was reported as a faster processing method compared to NN analysis (Nieuwenhuizen et al. 2010).

5.3 METHODS

This study uses Stepwise Linear Discriminate Analysis and LDA to identify the best bands to classify the weeds and sorghum. It was involved with spectral separability process and analysed the optimal bands combination for weed classification.

5.3.1 Spectral separability procedures

The hyperspectral data was downloaded and organised in a Master File, binned and subjected to First Derivative analysis as discussed in Chapter 4. The resulting cleaned data were used for discriminant analysis between weeds and crop plants as outlined in this chapter. The methodology uses three different years of data (Chapter 3). The details for each year are a little different and are explained in the following sections.

5.3.1.1 Classification Procedure

Species were classified from the 2012 FD reflectance data as shown in Figure 5-1. The most significant bands were selected by two methods, *i.* SLDA and *ii.* Literature Review. Both sets of bands were used in LDA to classify the weeds and sorghum.

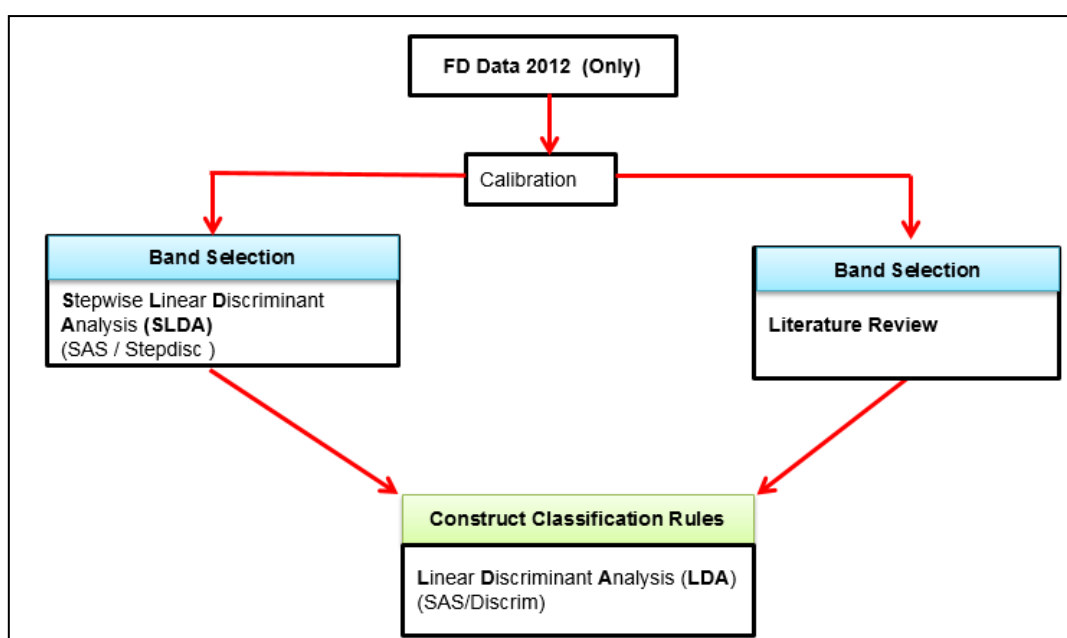


Figure 5-1 Species classification procedure (2012)

The 2013 and 2014 FD reflectance data were processed differently (Figure 5-2). They were first divided randomly into two groups, Calibration data and Validation data. The Calibration group had 70% of the data and the Validation group had 30% of the data.

The 20 most significant bands were identified from the Calibration data each year by using SLDA. This was implemented by the STEPDISC procedure within the SAS software (Noble and Brown 2009). SLDA identifies the most significant bands by eliminating variables (reflectance bands) within the statistical model that do not offer extra statistic to help separate the species (Calderón et al. 2015).

LDA was used to construct the “rule set” from the 20 significant bands. This “rule set” was used in the validation process.

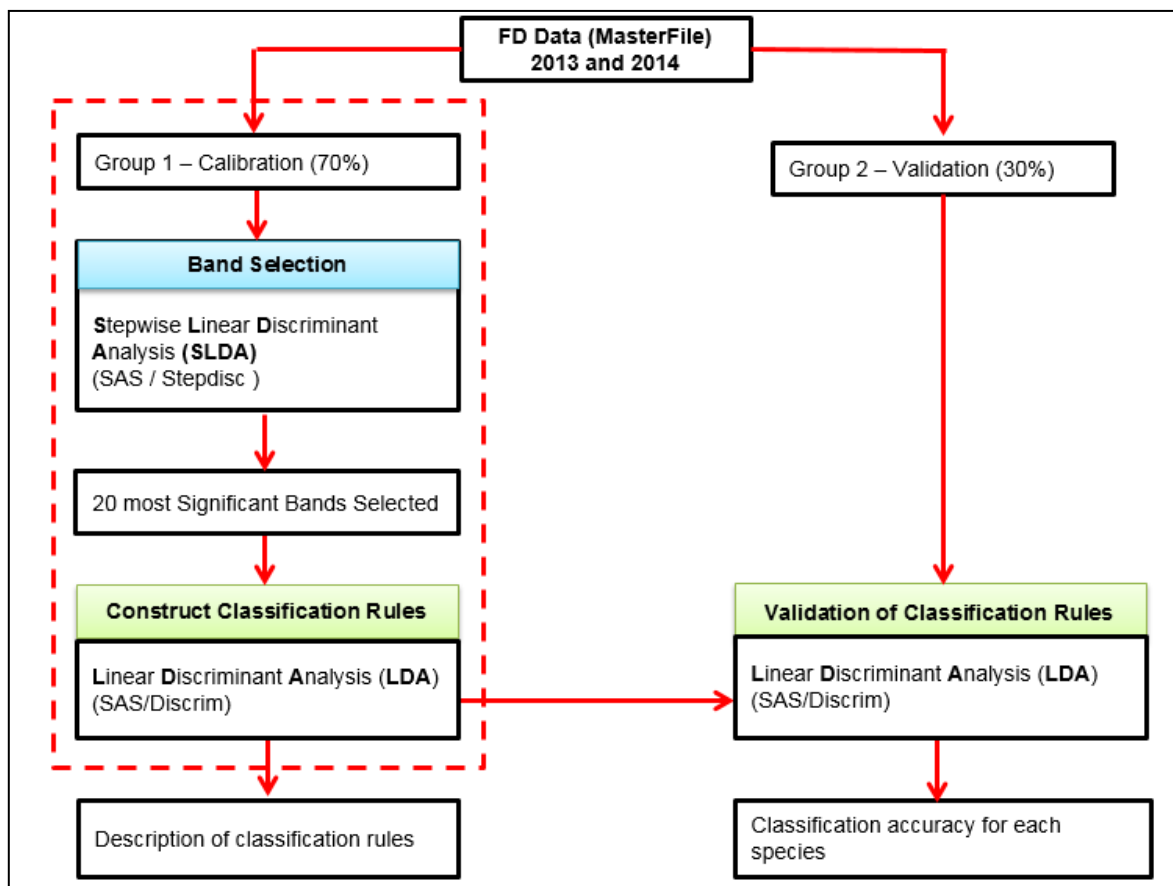


Figure 5-2 Species classification procedure (2013 and 2014)

5.3.1.2 Validation Procedure

The 2012 FD data was not validated because 2013 data was available by the time the validation procedure was agreed upon. The 2013 and 2014 FD data was used to test the “rule set” developed from the LDA analysis (Figure 5-2). LDA was used on the Validation data and the accuracy for each species was calculated each week.

5.3.2 Selection of Optimum Band Combinations

This section outlines how the number of original bands was narrowed down by selecting combinations of six, five, four and three bands at a time and testing the combinations for classification accuracy. This was done in a series of steps.

Firstly, the seven Landsat (ETM) bands, used for moisture content correlation with reflectance (Table 4-5), were tested for classification accuracy on the 2013 Calibration and

Validation data sets. Subsequently, all 3-band combinations of these seven bands (Appendix B) were tested for classification accuracy on the 2013 Validation data set.

Secondly, the eight best performing bands (Priority Bands) (Table 5-3) were identified from the 16 available band-pass filter wavelengths and the 20 most significant bands identified by SLDA. All 6-band combinations of the eight priority bands were tested for classification accuracy on the 2013 Validation data sets (Appendix C).

Table 5-3 Eight priority bands

Spectral Region	Eight Band filters (mid-point)
NIR	850 nm
Red-edge	750, 730, 720 and 710 nm
Red	680 nm
Green	560 nm
Blue	440 nm

Thirdly, the best performing 6-band combinations from the previous evaluation (Table 5-4) was tested on the 2014 Calibration and Validation data. This was followed by testing of all 5-band, 4-band and 3-band combinations of these 6 bands on the 2014 Validation data (Appendix D, E and F).

Table 5-4 Top 6-band combinations for 2013

Spectral Region	Bands
NIR	850 nm
Red-edge	720 and 710 nm
Red	680 nm
Green	560 nm
Blue	440 nm

A summary of all the band combinations for the accuracy testing is shown in Table 5-5.

Table 5-5 Band combination tested for accuracy

Year	Combinations	Source	Data Type	
			Calibration	Validation
2013	7-bands combination	Table 4-5	✓	✓
	6-bands combination	Table 5-3	✗	✓
	3-bands combination	Table 4-5	✗	✓
2014	6-bands combination	Table 5-4	✓	✓
	5-bands combination	Table 5-4	✗	✓
	4-bands combination	Table 5-4	✗	✓
	3-bands combination	Table 5-4	✗	✓

Figure 5-3 shows the accuracy evaluation procedure for the band combinations. The 2013 data set used the combinations selected from the eight band-pass filters that were available in 2013 (Table 4-5). The 2014 data set used combinations selected from the six best bands that were derived from analysis in 2013 (Table 5-4).

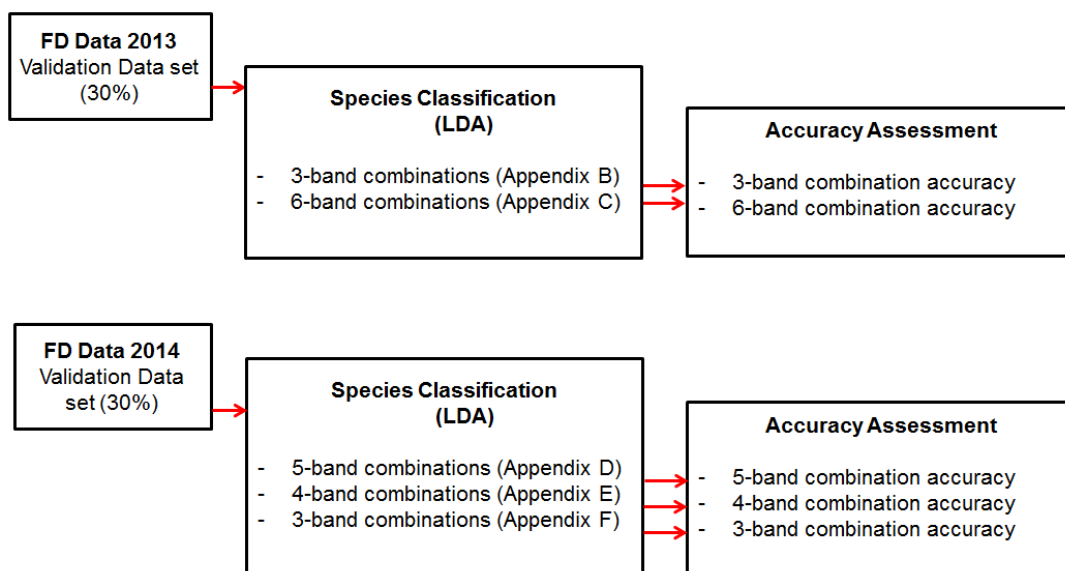


Figure 5-3 Accuracy evaluation of band combinations

5.4 RESULTS

5.4.1 Identification of Significant Bands

The significant bands for weed and sorghum classification identified by Stepwise Linear Discriminant Analysis (SLDA) from the 2012 data are shown in Table 5-6. Asterisk (*) numbers indicate the spectral bands that were found to be significant by previous investigators (Table 5-2).

Table 5-6 Significant bands from Stepwise Linear Discriminant Analysis of 2012 data

Spectrum Colour	Reflectance Band Centres (nm)
Near Infrared (NIR)	980, 955, 950, 945, 940, 930, 900, 895, 890, 885, 880, 875, 850, 840, 835, 815*, 810*, 805, 785, 770, 765, 755*
Red-edge	750*, 720*, 710*, 700, 695
Red	645
Green	580, 575, 565, 560, 535*, 505, 500
Blue	495*, 480, 475, 460, 455

In 2013, the FD reflectance data were divided into Calibration and Validation groups. The results of the SLDA analysis on the Calibration group of FD data are shown in Table 5-7. In 2014 the FD reflectance data were again divided into Calibration and Validation groups and the significant bands identified by SLDA from the Calibration group are shown in Table 5-8.

Table 5-7 Significant bands from Stepwise Linear Discriminant Analysis of 2013 data

Spectral Group	Reflectance Band Centres (nm)			
	Week 1	Week 2	Week 3	Week 4
NIR	1030	1000	1055	965
	945	895	945	935
	835	810*	890	930
		790		895
		765		
Red-edge	710*	720*	715	725
	705	710*	700	710*
	690	690	695	700
			690	695
Red	670*	665*	670*	675*
	660*	635	665*	665*
			660*	660*
			655*	640
			645	635
Green	585	590	570	595
	560	575	555*	560
	555*	540*	550*	555*
	505*	535*	525	530
		515	505	500*
Blue	490	475	460	445
	445	465	445	435
	440	445	435	
	420	385		
	410	355		
	385			
	380			
	370			

* indicate the spectral bands that were found to be significant by previous investigators (Table 5-2).

Table 5-8 Twenty most significant bands from Stepwise Linear Discriminant Analysis of the 2014 data

Spectral Group	Reflectance Band Centres (nm)		
	Week 2	Week 3	Week 4
NIR	910	930	990
	820	850	940
	770	840	930
	760	810	890
		760	840
			830
Red-edge	750*	740	740
	710*	730	710*
	690	710*	700
	680	700	690
		690	
Red	650	660*	660*
	630	650	630
	600*	640	620
		630	600*
		600*	
Green	560	560	550*
	550*	550*	540*
	540*	520*	
	530		
	500*		
Blue	470	380	450
	400	370	440
	380		420
	360		380

* indicate the spectral bands that were found to be significant by previous investigators (Table 5-2).

The significant bands common to each year are listed in Table 5-9. It shows that three bands from the NIR region (930, 890 and 810 nm), two bands from the red-edge region (710 and 700 nm) and 560 nm and 500 nm from the green and blue regions respectively were significant each year. The frequencies of the number of bands in each spectral region are shown in Table 5-10. NIR had the most number of bands each year. The green region had 20% of the bands. Red-edge and blue show the same percentages (18%) in Table 5-10 and Red has the lowest number of bands.

Table 5-9 Bands common to all 3 years

Spectral Group	Reflectance Band Centres (nm)
NIR	930, 890 and 810 nm
Red-edge	710 and 700 nm
Red	-
Green	560 nm
Blue	500 nm

Table 5-10 Frequency of bands by region

Spectral Region	2012	2013	2014	Mean	Percent (%)
Near Infrared (NIR)	22	15	15	17	28
Red-edge	5	14	13	11	18
Red	1	14	12	9	15
Green	6	19	10	12	20
Blue	6	18	10	11	18

5.4.2 Classification and Validation

LDA was used to test the significant bands for classification of weeds and sorghum. The significant bands identified from the literature (Figure 5-2) and from SLDA analysis (Table 5-6) of the 2012 data were tested and found to produce identical results (Table 5-11).

Table 5-11 Classification by literature review bands and SLDA bands (2012 data)


Species	Literature (Table 5-2)	SLDA (Table 5-6)
Amaranth (AM)	100%	100%
Sorghum (SG)	100%	100%
Barnyard (BY)	100%	100%
Fat Hen (FH)	100%	100%
Mallow Weed (MW)	100%	100%
Nutgrass (NG)	100%	100%
Pigweed (PG)	100%	100%

The significant 2013 bands (Table 5-7) were tested for classification accuracy. In week one, the bands classified the calibration data 100% accurately (Table 5-12). However, in week two the accuracy decreased to 88% for MW and 92% for SG. The accuracy was still high since both results were more than 80% accurate. In week three, SG was 92% accurately classified and in week four all the weeds and SG were 100% accurately classified. This shows that the capacity of the significant bands to classify the weeds and SG is high but varies by stage of growth.

The validation process evaluates the accuracy of the calibration “rule set” by testing the classification on independent data (Table 5-12). It shows a high accuracy for AM, LS, MW and SG in week one. Sorghum was poorly classified in weeks two, three and four of 2013 with an accuracy of 67%, 75% and 71% respectively. This is the lowest accuracy of all species. In week two, MW and SG were poorly discriminated with 75% and 67% accuracy respectively. The other species were discriminated with 100% accuracy. In week three, AM, LS and MW were classified with high accuracy, while NG and SG were only classified with 67% and 75% accuracy respectively. In week four, NG accuracy increased from 67% to 100% while AM decreased from 83% to 80% and SG decreased from 75% to 71%. Overall, the classified accuracy improved with stage of growth (Weeks one to four, 2013). In summary, the accuracy improved consistently from week three to week four. The results are displayed graphically in Appendix G.

Table 5-12 Classification results for the 20 most significant bands in 2013 data


Species	Calibration Data				Validation Data			
	Wk 1	Wk 2	Wk 3	Wk 4	Wk 1	Wk 2	Wk 3	Wk 4
Amaranth (AM)	100%	100%	100%	100%	100%	100%	83%	80%
Liverseed Grass (LS)	100%	100%	100%	100%	83%	100%	100%	100%
Mallow Weed (MW)	100%	88%	100%	100%	100%	75%	100%	100%
Nutgrass (NG)	100%	100%	100%	100%	60%	100%	67%	100%
Sorghum (SG)	100%	92%	92%	100%	83%	67%	75%	71%
Average	100%	96%	98%	100%	85%	88%	85%	90%

 = High accuracy (> 80), Wk = Week

The 20 most significant 2014 bands (Table 5-8) classified the Calibration data 100% accurately (Table 5-13). All the bands (20) classified the Validation data set 100% accurately (Table 5-13) for all weeds except LS (89%) and SNP (43%) in week two. The results are displayed graphically in Appendix H.

Table 5-13 Classification results for the 20 most significant bands in 2014 data

Species	Calibration Data			Validation Data		
	Week 2	Week 3	Week 4	Week 2	Week 3	Week 4
Bellvine (B)	100%	100%	100%	100%	100%	100%
Liverseed Grass (LS)	100%	100%	100%	89%	100%	100%
Nutgrass (NG)	100%	100%	100%	100%	100%	100%
Pigweed (PG)	100%	100%	100%	100%	100%	100%
Sorghum non pre-emergence (SNP)	100%	100%	100%	43%	100%	100%
Sorghum Pre-emergence (SP)	100%	100%	100%	100%	100%	100%
Average	100%	100%	100%	90%	100%	100%

 = High accuracy (> 80)

5.4.3 Optimum Band Combinations

The previous section presented the results of selecting the 20 most significant bands to classify the weeds and sorghum. This section presents the results of refining the number of bands to 6 for use with the MCA6 camera. Combinations of the seven Landsat (ETM) bands (Table 4-5) were tested for classification using 2013 FD Calibration and Validation data (Table 5-14).

In week 1, the bands classified AM and MW with 85% and 100% accuracy. The accuracy of MW varied from 88% to 100% from week two to week four. Between week two and three, the accuracy of AM and NG increased from 75% to 100% and 54% to 89% respectively. Overall the accuracy of classification varied with stage of growth.

Table 5-14 Classification results for the seven bands 2013 data (Table 4-5)

Species	Calibration Data				Validation Data			
	Wk 1	Wk 2	Wk 3	Wk 4	Wk 1	Wk 2	Wk 3	Wk 4
Amaranth (AM)	85%	75%	100%	82%	100%	25%	100%	60%
Liverseed Grass (LS)	14%	50%	75%	67%	17%	0%	100%	50%
Mallow Weed (MW)	100%	88%	89%	100%	50%	100%	100%	100%
Nutgrass (NG)	20%	54%	89%	91%	60%	100%	67%	100%
Sorghum (SG)	10%	54%	58%	89%	17%	33%	75%	71%
Average	46%	64%	82%	86%	49%	52%	88%	76%

= The high accuracy (> 80), Wk = Week

When the combinations were tested on the Validation data they showed a low accuracy in week one for all the species except for AM. However, the accuracy increased approximately 50% for MW and NG in week 2. The accuracy increased in week three when AM, LS and MW had 100% accuracy. In week four, MW and NG were 100% accurately classified. The results are displayed graphically in Appendix I.

The results show that the combination of 660, 680 and 710 nm bands produced the most accurate average classification (Table 5-15). The classification accuracy for all the 3-band combinations is shown in Appendix K. Liverseed grass detection accuracy varied from week one to week four (Table 5-15). During week two, it was not detected accurately (0%). This is suspected to be due to human error during data collection. Because liverseed grass was very small at week two, some spectral reflectance error was expected. However, at week three liverseed grass plants were bigger and spectral reflectances were collected accurately. Detection accuracy in week three was 100%.

Table 5-15 Classification results for the five most accurate combinations of the Landsat (ETM) 3-band combinations (Validation, 2013)

3-band combinations	AM	LS	MW	NG	Mean
660, 680, 710 nm	80%	50%	100%	100%	83%
660, 680, 720 nm	80%	50%	75%	100%	76%
680, 710, 720 nm	60%	50%	100%	100%	78%
680, 710, 730 nm	60%	50%	100%	100%	78%
680, 730, 750 nm	60%	67%	100%	50%	69%

= The high accuracy (> 80), AM = Amaranth, LS = Liverseed Grass, MW = Mallow Weed and NG = Nutgrass .

Table 5-16 shows the five most accurate 6-band combinations from the eight priority bands (Table 5-3). The best five combinations classified all species except AM, 100% accurately. The classification accuracy for all the 6-band combinations is shown in Appendix J.

Table 5-16 Classification results for the five most accurate combinations of the priority 6-band combinations (Validation, 2013)

6-band combinations	AM	LS	MW	NG	Mean
440, 560, 680, 710, 720, 850 nm	71%	100%	100%	100%	93%
440, 560, 710, 730, 750, 850 nm	57%	100%	100%	100%	89%
440, 560, 720, 730, 750, 850 nm	57%	100%	100%	100%	89%
560, 680, 710, 720, 730, 750 nm	57%	100%	100%	100%	89%
560, 680, 710, 720, 730, 850 nm	57%	100%	100%	100%	89%

■ = The high accuracy (> 80), AM = Amaranth, LS = Liverseed Grass, MW = Mallow Weed and NG = Nutgrass .

The results show a substantial improvement in classification accuracy by using more bands. Bands 710 and 680 nm occurred in the 6 and 3-band combinations that produced the highest classification accuracy.

The best six bands from 2013 were tested on 2014 FD Calibration and Validation data (Table 5-17). In week two, all species classified accurately (> 80%) except SNP. In week three, the results varied in their accuracy. In week four, the average accuracy (93%) was higher than in week two (83%).

Table 5-17 Classification results using the calibration “rule set” for the six most significant bands in 2014 data


Species	Calibration Data			Validation Data		
	Week 2	Week 3	Week 4	Week 2	Week 3	Week 4
Bellvine (B)	92%	57%	78%	71%	100%	80%
Liverseed Grass (LS)	82%	94%	100%	56%	100%	50%
Nutgrass (NG)	100%	86%	100%	100%	50%	90%
Pigweed (PG)	83%	82%	85%	63%	67%	86%
Sorghum Non pre-emergence (SNP)	38%	71%	100%	43%	67%	57%
Sorghum Pre-emergence (SP)	100%	92%	93%	100%	57%	100%
Average	83%	80%	93%	72%	74%	77%

■ = High accuracy (> 80)

Nutgrass and SP were 100% accurate in week two (Table 5-17). Bellvine and LS were 100% accurately classified in week three. Nutgrass accuracy increased from 50% to 90% from week three to week four and SNP changed from 67% to 57% accuracy from week three to week four. There was a gradual increase in average accuracy from week two to week four (72% to 77%) when tested on the 2014 Validation data. The results are displayed graphically in Appendix L. The 5-band combinations were tested using 2014 Validation data (Table 5-18).

Table 5-18 Classification results (%) for all 5-band combinations for 2014 Validation data

Combination No.	Bands (nm)	B	LS	NG	PG	SNP	SP	Mean
WEEK 2								
1	720, 440, 560, 680, 710	92	82	100	83	38	82	80
2	720, 440, 560, 680, 850	57	56	100	50	43	100	68
3	720, 440, 680, 710, 850	71	67	100	50	43	100	72
4	720, 560, 680, 710, 850	86	67	100	50	43	100	74
5	440, 560, 680, 710, 850	57	67	100	50	43	100	70
Average								73
WEEK 3								
1	720, 440, 560, 680, 710	83	75	50	100	33	57	66
2	720, 440, 560, 680, 850	83	75	67	33	33	57	58
3	720, 440, 680, 710, 850	100	100	50	56	67	57	71
4	720, 560, 680, 710, 850	83	100	50	67	67	57	71
5	440, 560, 680, 710, 850	83	100	67	56	100	57	77
Average								69
WEEK 4								
1	720, 440, 560, 680, 710	70	17	80	71	57	67	60
2	720, 440, 560, 680, 850	80	33	60	71	14	83	57
3	720, 440, 680, 710, 850	90	67	90	86	57	100	82
4	720, 560, 680, 710, 850	70	50	80	71	57	83	69
5	440, 560, 680, 710, 850	50	33	30	86	57	83	57
Average								65

 = High accuracy (> 80), B = Bellvine, LS = Liverseed Grass, NG = Nutgrass , PG = Pigweed, SNP = Sorghum non pre-emergence and SP = Sorghum Pre-emergence.

Combination one classified all the species more accurately than the other combinations in week two except for SNP (38%). Nutgrass and SP were accurately classified by all 5-band combinations in week two. In week three, B was accurately classified (> 80%) by all 5-band combinations. Liverseed grass was 100% accurately classified for all the combinations except one and two. PG was 100% accurately classified in combination one. SNP was 100% accurately classified in combination five. Nutgrass and SP were very poorly classified by all 5-band combinations in week three.

In week four, combination three had the highest accuracy for all species, except for LS and SNP. Combinations two and three classify B the most accurately. Combination one, three and four classified NG the most accurately. Pig weed was classified the most accurately by combinations three and five. Overall, SP was classified accurately by all combinations except combination one. The results are displayed graphically in Appendix M.

The 4-band combinations were tested using the 2014 FD Validation data. The five most accurate results for each week are shown in Table 5-19. In week 2, SP, B and NG were 100% accurately classified by the five most accurate combinations except in week two for B and NG. In week 3, B was accurately identified by the five most accurate combinations except combination 13. PG and SNP were 100% accurately classified by combinations 11 and 13 respectively. In week four, SP was accurately identified by the five most accurate combinations and NG was 80% accurately identified by four of the combinations. In combination 10, LS was 83% accurately

classified. B was accurately identified in combination four, six and 10. The results for all 4-band combinations are given in Appendix N and are displayed graphically in Appendix O.

Table 5-19 Classification results (%) for the top five 4-band combinations for 2014 (Validation data)

Combinations Number	Bands (nm)	B	LS	NG	PG	SNP	SP	Mean
WEEK 2								
2	720, 440, 560, 710	71	78	71	63	43	100	75
7	720, 560, 680, 710	86	56	100	50	57	100	78
9	720, 560, 710, 850	86	78	86	38	43	100	76
10	720, 680, 710, 850	86	56	86	50	57	100	76
13	560, 680, 710, 850	86	67	100	38	43	100	76
Average								76
WEEK 3								
2	720, 440, 560, 710	100	75	50	78	33	57	66
4	720, 440, 680, 710	83	75	50	67	33	71	63
9	720, 560, 710, 850	83	75	50	44	67	57	63
11	440, 560, 680, 710	83	75	50	100	33	57	66
13	560, 680, 710, 850	50	75	67	56	100	57	68
Average								65
WEEK 4								
4	720, 440, 680, 710	100	33	60	71	43	83	65
6	720, 440, 710, 850	80	67	80	86	43	83	73
8	720, 560, 680, 850	60	33	80	71	14	83	57
9	720, 560, 710, 850	70	50	80	71	43	83	66
10	720, 680, 710, 850	80	83	80	71	57	100	79
Average								68

■ = High accuracy (> 80), B = Bellvine, LS = Liverseed Grass, NG = Nutgrass ,
PG = Pigweed, SNP = Sorghum non pre-emergence and SP = Sorghum Pre-emergence.

The 3-band combinations were also tested using the 2014 FD Validation data. The five most accurate results for each week are shown in Table 5-20.

Table 5-20 Classification results (%) for the top five 3-band combinations for 2014 Validation data

Combination Number	Bands (nm)	B (%)	LS (%)	NG (%)	PG (%)	SNP (%)	SP (%)	Mean (%)
WEEK 2								
5	720, 560, 680	57	56	100	50	43	100	72
6	720, 560, 710	86	67	100	38	57	100	78
8	720, 680, 710	71	67	86	50	57	100	76
9	720, 680, 850	86	67	100	38	29	100	74
16	680, 710, 850	86	56	100	38	29	100	73
Average								75
WEEK 3								
2	720, 440, 680	83	75	33	44	33	71	57
4	720, 440, 850	100	75	67	22	33	57	59
12	440, 560, 710	83	75	17	78	33	57	57
13	440, 560, 850	83	75	50	11	67	57	57
14	560, 680, 710	50	75	50	67	67	42	59
Average								58
WEEK 4								
7	720, 560, 850	70	17	80	71	14	83	62
8	720, 680, 710	100	33	70	57	14	83	65
9	720, 680, 850	50	50	80	86	14	83	66
10	720, 710, 850	70	67	80	71	14	67	67
16	680, 710, 850	50	50	70	86	29	83	67
Average								65

■ = High accuracy (> 80), B = Bellvine, LS = Liverseed Grass, NG = Nutgrass ,
PG = Pigweed, SNP = Sorghum non pre-emergence and SP = Sorghum Pre-emergence.

Sorghum pre-emergence and nutgrass were 100% accurately identified in all five combinations in week two except in combination eight. Bellvine was 86% accurately classified by combinations six, nine and 16. In week three, bellvine was classified accurately (> 80%) by all combinations except combination 14. The other species were identified poorly. In week four, SP was identified accurately (> 80%) in four of the combinations. Nutgrass was 80% accurately classified in three combinations. Bellvine was 100% accurately classified only in combination eight and SNP and LS were poorly classified by all combinations in all weeks. The results for all 3-band combinations are given in Appendix P and are displayed graphically in Appendix Q.

5.5 DISCUSSION AND ANALYSIS

Spectral reflectance of weeds and sorghum was expected to vary because field environmental conditions constantly change. Significant bands for identification of weeds and sorghum might vary at different times and locations because of the influence of abiotic and biotic factors in the environment and variation in field conditions (Carvalho et al. 2013). The sunlight could also cause variation in reflectance at different times due to different atmospheric conditions and azimuths affecting measurement of the reflectance (Kodagoda and Zhang 2010). The size and shape of the leaves of the species also influences spectral reflectance. As shown in Chapter 4, the

spectral profiles of individual leaves of a species were very similar. This indicates that the measurement technique avoided variations in reflectance due to external factors.

5.5.1 Band Identification

Table 5-6 shows the most significant bands for the identification of weeds and sorghum in 2012. Table 5-7 and Table 5-8 show the 20 most significant bands for the identification of weeds and sorghum in 2013 and 2014 respectively. There were naturally occurring variations in the weed species each year (Table 4-3). This variation contributed to different bands being found to identify the weed species each year as illustrated by the different central band wavelengths listed for each year in Table 5-6, Table 5-7 and Table 5-8. Table 5-9 lists the bands that were found significant in all three years. The bands that were found significant by other investigators are shown in Asterisk (*) in Table 5-6, Table 5-7, Table 5-8 and Table 5-9. It can be seen by inspection that:

- (i) Some bands reoccurred as significant bands each year (eg. 930, 890, 810, 710, 700, 560 and 500 nm).
- (ii) Some bands that are significant each year were also found to be significant by other investigators (eg. 810, 720, 710, 675, 670, 660, 665, 555, 550, 540 and 535 nm).
- (iii) The number of significant bands that are common in each region in all years are in the following regions:
 - NIR, 17
 - Red-edge, 11
 - Green, 12

The significance of these bands depends on their use in combination with other bands to identify the weeds and sorghum. While they do not uniquely identify weeds and sorghum by themselves, their reoccurrence each year suggests their usefulness as part of a more limited number of bands (less than 20) to identify weeds and sorghum. The fact that other investigators (Fyfe 2003; Prasad et al. 2011; Wilson et al. 2014) found some of these bands to be significant, further suggests that these bands be carefully considered.

Discrimination between Bermuda grass (Tifway 419) and weeds was found to depend on specific wavelengths to enable consistently accurate classification (Hutto et al. 2006). The specific wavelengths were 353, 357, 360, 362, 366, 372, 385, 389, 391, 396, 405, 441, 442, 472, 726, 727, 732, and 733 nm and DA produced 98% accuracy for Bermuda grass (Tifway 419). Classification of seagrass species in south-eastern Australian estuaries required narrow bands (5 - 15 nm) centred on 675, 640, 620, 590, 575, 560, 550, 530, 500 and 440 nm (Fyfe 2003). A more limited number of bands was found to discriminate weeds in sugar beets and maize with 90% accuracy (Vrindts et al.

2002).

Borregaard et al. (2000), Vrindts et al. (2002) and Kefyalew et al. (2005) found that a combination of NIR and visible (VIS) bands increased the accuracy of classification of plants species using DA. Borregaard et al. (2000) found that 970, 897, 856, 726, 694 and 686 nm could be used to discriminate between sugar beets and weeds and 978, 970, 897, 856, 726 and 686 nm could discriminate between potatoes and weeds using LDA. NIR and red-edge region bands provided the spectral difference for classifying the healthy and infected canopy in detection of citrus greening (Li et al. 2012). The finding from this research that a combination of 850, 720, 710, 680, 560 and 440 nm bands could accurately classify weeds and sorghum, is consistent with these previously published findings.

Manevski et al. (2011), working with Mediterranean plants, concluded that high spectral resolution middle infra-red (MIR) radiation enables accurate species discrimination. Future research may need to consider spectral reflectance values from 1055 up to 2000 nm for detecting weeds in sorghum. MIR reflectance is also significantly affected by the MC of plants (Manevski et al. 2011).

5.5.2 Classification and Validation

Bands identified from the literature and bands identified by SLDA from the 2012 FD reflectance data yielded the same classification accuracy (Table 5-11). In 2013, LDA produced generally accurate results when applied to independent data (Table 5-12, Validation Section), however it was not as accurate in classifying the species as using the SLDA approach (Table 5-12, Calibration Section). In 2013, the LDA produced more accurate classification of species than in 2014 (2 species different) as shown in Table 5-13 (Validation Sections). SLDA classification in 2014 was more accurate than SLDA classifications in 2013 (compare Calibration Sections, Table 5-12 and Table 5-13).

The difference in classification accuracy between 2013 and 2014 is small and may not be statistically significant. The data did not permit measurement of the significant difference. Because many of the classifications had 100% accuracy, limited statistical testing was possible. The average classification accuracy for different growth stages did not show any obvious trend between weeks two and four.

There are similarities between the study by Gray et al. (2009) and this present study in classifying weed species. They used PCA and best spectral band combinations analysis (BSBC) together with LDA to classify hemp sesbania, palmleaf morning glory, pitted morning glory, prickly sida, sicklepod, and smallflower morning glory species in soybeans. LDA produced a higher accuracy compared to PCA analysis (Gray et al. 2009). Zhang et al. (1998) combined LDA with

partial least squares (PLS) analysis and successfully classified weeds and wheat with 100% accuracy. Although their methods were very similar to the methods used in this research, their reflectance data was different because it was from 1445 nm up to 2135 nm (short-wave infrared, SWIR).

5.5.3 Optimal Bands

The results (Section 5.4.3) provide a procedure for evaluating which band-pass filters are likely to produce images most suitable for accurately discriminating between different species of weeds and sorghum plants. It is necessary to identify the smallest number of hyperspectral bands that can accurately classify weeds from crop plants (Prasad et al. 2011). This can be done by an exhaustive review to identify redundant bands to establish the best separation of weeds from crop plants (Prasad et al. 2011). LDA was used to reduce the number of bands to 20. These were narrowed to six or less, the maximum number of sensors in the MCA 6 camera, by selecting the eight priority bands and evaluating these combinations in groups of six or less. The eight priority bands were selected from the 16 bands-pass filters that were available following inspection of the species reflectance profiles and the list of 20 significant bands.

The classification results from the seven Landsat (ETM) bands (Table 5-14) show an increasing accuracy of classification from week one to week four based on 2013 Calibration data. These bands were tested in groups of 3-band combinations. The eight priority bands were tested in groups of 6-band combinations (Table 5-3). The results show higher classification accuracy for combinations of 6-bands compared to 3-band combinations (Table 5-15). The 6-band combination with the highest accuracy (850, 720, 710, 680, 560, 440 nm) on 2013 data was tested on 2014 data (Table 5-17). At week four it gave the same classification accuracy (93%) (Table 5-17) as its mean value with the 6-band combination on 2013 data (Table 5-16). It classified the 2014 Classification data more accurately than the Validation data. Validation data was classified more than 70% accurately (Table 5-17).

These six bands were then tested in combinations of 5, 4 and 3 bands for classification of the 2014 Validation data (Table 5-18, Table 5-19 and Table 5-20). Overall, the classification accuracy between weeds and sorghum varied each week in all combinations. Inspection of the highlighted values (> 80% classification accuracy) reveals that bellvine, nutgrass and pre-emergence treated sorghum classify more accurately than other species most of the time. The classification accuracy was higher in week two for all combinations (Table 5-18, Table 5-19 and Table 5-20). In 5-band combinations, the classification accuracy decreased from 73% to 65% from week two to week four (Table 5-18). Meanwhile, for 4 and 3-band combinations, classification accuracy decreased in week

three and increased in week four (Table 5-19 and Table 5-20). There is no clear trend that more bands produce higher classification accuracy than using fewer bands in the 2014 data as was observed with the 2013 data.

These results show that combinations of six bands produced a more accurate classification compared to 3-band combinations in 2013 data (Table 5-15). The 6-band combinations showed that liver seed grass, mallow weed and nutgrass were 100% accurately identified (Table 5-16). The most accurate classification for a combination of 3-bands (83%) was produced by 660, 680, 710 nm bands. The 3-band combinations did not classify liverseed grass, mallow weed and nutgrass 100% accurately as they did in the 6-band combinations. Amaranth has a high classification accuracy in 2, 3-band combinations. Most of the 3-band combinations were suitable for classifying nutgrass and mallow weed. The 720 nm band occurred in the high classification combinations for amaranth, liverseed grass, mallow weed and nutgrass. This band has been used to classify cruciferous weeds in winter wheat and broad beans (de Castro et al. 2012).

Testing of the most accurate 6-band combinations on 2014 data (Table 5-17) found that classification accuracy increased with stage of growth (week two to week four). These results suggest that the optimal time to discriminate weeds from sorghum plants is during week four after planting. This is similar to the findings by Amelinckx (2010) who concluded that the phenological stage in the early growing season was the best stage for discriminating boreal grasslands. Phenological stage was also found to influence plant identification accuracy (Hestir et al. 2008) in Delta ecosystems. Wilson et al. (2014) used 25 spectral bands to discriminate between soybean, canola, wheat, oats and barley. They found that the optimal time to discriminate weeds in canola was approximately 55 - 60 days after planting. This is equivalent to week 4 to 5 after planting for sorghum. After week four the weeds are much larger and it is expected they would be harder to control with herbicides despite being potentially easier to identify. These results show that the growth stage affects the accuracy of classification.

Clark et al. (2005) achieved 100% classification accuracy with leaf-scale classification using LDA (40 bands). This was greater than the accuracy obtained from using maximum likelihood classification (88%) and spectral angle mapper (unspecified low classification). They showed that the scale of mapping affects the importance of the bands for classification accuracy. Optimal bands can be used to select suitable sensor band filters for imaging spectrometers such as the CASI (Compact Airborne Spectrographic Imager) and MCA 6 camera (Fyfe 2003).

Overall, the analysis showed that the optimal bands for weed identification were located in the NIR, red-edge and Green regions of the spectrum. Stepwise Linear Discriminant Analysis identified the most significant bands for classification of each species. The region with most significant bands over 3 years research was the NIR region with 28% of the bands. The Green

region had 20% of the bands and the NIR and blue regions had 18% of the most significant bands. Red has a lower percentage (15%). Each year NIR had the most bands except in 2013 when the green region had 19 bands. In 2014, NIR had the most significant numbers (15) followed by red-edge (13) (Table 5-10). Similar results were found by Kodagoda and Zhang (2010) who found that NIR and VIS had the most bands for discriminating *Bidens pilosa* L (cobbler's peg) from wheat plants. The NIR and VIS regions also had the larger number bands for discriminating plant species such as *Ceratonia siliqua*, *Olea europea*, *Pistacia lentiscus*, *Calicotome villosa* and *Genista acanthoclada* (Manevski et al. 2011). Nicolai et al. (2007) found that NIR bands were widely useful in measuring the quality of vegetation attributes. They reported that the NIR region (725, 925, 975 and 1125 nm) had more ability to discriminate pitted morning glory (*Ipomoea lacunosa*) from soybeans (Koger et al. 2004). This information indicates that the NIR region is the most sensitive region for classifying weeds in crops.

5.6 CONCLUSIONS

Selected hyperspectral reflectance bands were successfully used to identify weeds in sorghum. Linear Discriminant Analysis is an efficient way to classify weeds and sorghum plants using hyperspectral reflectance data. The most significant bands were identified by Stepwise Linear Discriminant Analysis.

In 2012, the spectral profiles classified weeds and sorghum 100% accurately. In 2013 the analysis was tested using 6-band and 3-band combinations. The results achieved good separation between amaranth, liverseed grass, mallow weed, nutgrass and sorghum using 850, 720, 710, 680, 560 and 440 nm bands. These bands were narrowed down to 5, 4 and 3-band combinations and tested on 2014 data. The significant bands for each year were 930, 890, 710, 700, 560 and 500 nm. This indicates that these bands can be used to classify weeds and sorghum in the future.

Classification accuracy increased progressively from week one to week four. The results indicate that week four is the best time to collect hyperspectral reflectance for classifying weeds and sorghum. These results may vary depending on the weed profile in the sorghum crop.

The following chapter discusses the multispectral imagery processing to classify weeds and sorghum plants. The imagery consists of 6 bands that were selected from the most significant 6-band combination from Chapter 5. The results form the basis for the weed discrimination mapping in sorghum.

Chapter 6

IMAGE PROCESSING FOR DETECTING WEEDS IN SORGHUM

6.1 INTRODUCTION

Accurate weed identification is essential for Site-Specific Weed Management (SSWM). SSWM is becoming an increasingly important part of Precision Agriculture (PA). This research investigates weed detection using image processing techniques in the most important grain crop in Queensland; sorghum.

An Unmanned Aerial Vehicle (UAV) fitted with a multispectral camera was used to identify weeds in a sorghum field. It was shown by Santi et al. (2014) that combination of Global Positioning System (GPS), Geographical Information Systems (GIS) and UAVs could improve the spatial distribution analysis in mapping the location of weeds in crops. For example, a Microdrone MD 4-1000 UAV fitted with a TetraCam MCA 6 camera (TeraCam Inc., Chatsworth, CA, USA) was used to collect imagery to identify weeds using Object-Based Image Analysis (OBIA) (Pena-Barragan et al. 2012a; Mesas-Carrascosa et al. 2015). The MCA 6 camera can collect imagery with six different spectral bands and can be flown in an UAV at any desired altitude. At 30 m altitude it produces an approximately ~ 2 cm spatial resolution images (Tetracam 2015). Gillieson et al. (2006) also found that high spectral and spatial resolution imagery could be used to identify weeds in crops. In this research OBIA and Vegetation Index Analysis (VIA) methods were used to identify weeds in sorghum at various growth stages using MCA 6 imagery collected at different spatial resolutions.

6.2 LITERATURE REVIEW

6.2.1 Object Based Image Analysis

Recent studies that applied remote sensing to detect plant types used a new type of image processing analysis known as Geographic Object-Based Image Analysis (GEOBIA) (Aziz 2014). GEOBIA is defined as:

“Geographic Object-Based Image Analysis (GEOBIA) is a sub-discipline of Geographic Information Science (GIScience) devoted to developing automated methods to partition remote

sensing imagery into meaningful image-objects, and assessing their characteristics through spatial, spectral and temporal scales, so as to generate new geographic information in GIS-ready format,"(Hay and Castilla 2008, p. 77).

Object Based Image Analysis (OBIA) is a method of segmenting a feature based on the image object. Objects can be generated based on particular attributes, such as size, texture, shape, spatial and spectra distribution. These factors can be combined with contextual and hierarchy procedures to give an accurate classification (Pena et al. 2013; Fernandes et al. 2014). This approach creates a more realistic presentation of the objects than individual pixels create (Lizarazo 2013). Moreover, the combination of contextual knowledge can produce high accuracy segregation between the classes. The final output can be converted into most other GIS formats (Arroyo et al. 2010). The OBIA method allows modifying the rule sets which govern the creation of classes which makes it suitable for use with different data sets (Lisita et al. 2013).

eCognition software (Trimble Geospatial, Munich, Germany) (Pena-Barragan et al. 2012a) applies OBIA by developing hierarchical rule sets to classify image objects. Kamal et al. (2015) and Aziz (2014) found that the rule sets need to be modified for different applications in agricultural mapping because of site, sensor and time dependence. It can produce a good classification resulting in higher accuracy mapping because the classification is derived from combinations of several attributes (Phinn et al. 2012). OBIA is time effective specifically for very high spatial resolution imagery (Johansen et al. 2011).

Different rule sets are suitable for the different data sources (Kamal et al. 2015). For instance random area of forest, mangroves, gullies and palm oil plantations were mapped using pan-sharpened Quickbird, WorldView II, Light detection and ranging (LiDAR), Landsat TM and ALOS AVNIR-2-satellite imagery over large areas (Aziz 2014; Belgiu and Dragut 2014; Kamal et al. 2015). However, weed mapping requires higher spatial resolution imagery for effective weed identification. The size of weed is small in field crops and requires high resolution for detection. UAV can fly at lower altitudes to obtain very high spatial resolution imagery (Pena-Barragan et al. 2012a). A summary of OBIA applications in agriculture monitoring are shown in Table 6-1.

Table 6-1 Agriculture mapping applications using OBIA

Mapping Applications	Sensor Platforms	Sources
Weed mapping in maize, wheat and sunflower	MCA 6 camera	(Pena-Barragan et al. 2012a; Pena et al. 2013; Torres-Sanchez et al. 2014; Lopez-Granados et al. 2015)
Giant reed mapping	Ultracam D, DMC-Intergraph, WorldView-2	Fernandes et al. (2014)
Weed mapping	Olympus RGB and MCA 6	Borra-Serrano et al. (2015)
Chalk stream macrophytes mapping	Infrared sensitive, digital single-lens reflex camera (DSLR)	Visser and Wallis (2010)
Land cover mapping	Very High Spatial Resolution multispectral	(Arroyo et al. 2010; Tormos et al. 2012)
Monitoring plant invasion	Panchromatic and colour photography, multispectral satellite Rapid Eye	Müllerová et al. (2013)
Forest Canopy Modelling	Airborne LiDAR and Quickbird Imagery	Chen and Hay (2011)
Mangrove Composition Mapping	Landsat TM, ALOS AVNIR-2, WorldView-2, and LiDAR	Kamal et al. (2015)
Mapping Geomorphic and Ecological Zones and Coral Reefs	Quickbird-II	Phinn et al. (2012)
Wetland Type and Area Different Scale	SPOT 5 imagery	Powers et al. (2012)
Mangrove Production Management in Malaysia	Landsat ETM+	Aziz (2014)

The use of OBIA in various applications has increased tremendously since 1999. It is expected to continue in the future (Blaschke 2010). However, there are some limitations in using OBIA, particularly the error associated with under-segmentation and over-segmentation. This occurs when the image objects have more than one class within them and the objects are unnecessarily broken apart in the segmentation process (Slaughter 2014; Lehmann et al. 2015).

Figure 6-1 shows the details of how under and over-segmentation are identified. The Reference Map column shows an area of soil that is not identified in the OBIA Map. Also, it identifies areas of weeds and sorghum that are misclassified in the OBIA Map.

The research investigated using a single leaf because of the accuracy of the imagery. The size of the weeds was too small in the imagery. Thus, if the spectral reflectance was collected under the canopy, the spectral variable would be widely affected by the whole weed area (the area has different weed species). In this research, I used the high resolution imagery (0.87 mm) at different growth stages. The resolution was an effective way to collect the spectra of the single leaves. The OBIA also detected single plants at the high resolution. This technique was also used by Louis et al. 2010 using a single leaf for spectral reflectance collection. They used a single leaf because the size of the leaves was too small at the early stages.

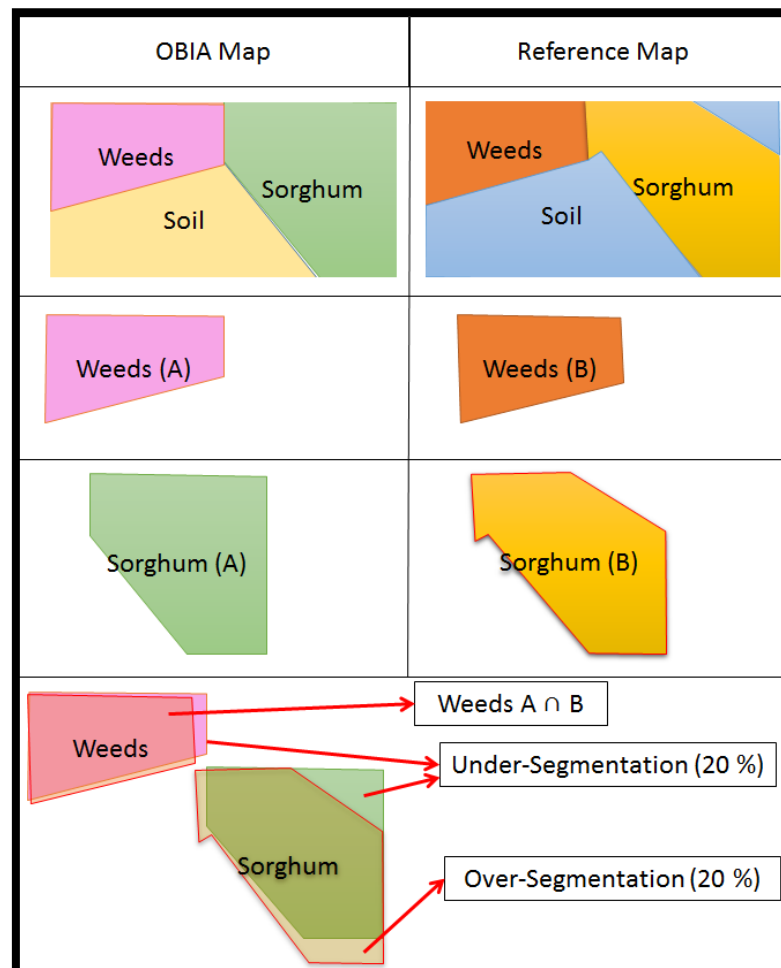


Figure 6-1 Visualization of OBIA result (A) and Reference Map (B) * \cap = Intersection

6.2.2 Vegetation Index Analysis (VIA)

Computation of Vegetation Indices (VIs) is another technique for species discrimination in image processing. The Normalized Difference Vegetation Index (NDVI) can be used to distinguish plants from the background soil and discriminate weeds from crop plants (Fernandes et al. 2014). It has been used for many applications and is widely used in disease detection (Calderon et al. 2013) such as, detecting Brownheart in ‘Braeburn’ apples (Clark et al. 2003), discrimination of grassland species (Dale et al. 2013), exploring physical and physiological attributes of vegetation (Knipling 1970) and crop row orientation analysis (Marais Sicre et al. 2014).

The NDVI and the Normalized Difference Yellowness Index (NDYI) were used to discriminate weeds in sunflower crops (Pena-Barragan et al. 2010). According to Torres-Sanchez et al. (2013) the Excess Green Index (ExG) and Normalised Green-Red Difference Index were useful in discriminating weeds, crops, and soil (Torres-Sanchez et al. 2013). According to Torres-Sanchez

et al. (2014) at least four pixels were needed to detect small objects for the 15 cm width crop rows in such images using VIs.

There are many other VIA, such as the Derivative Green Vegetation Index (DGVI), Ratio Vegetation Index (RVI), Difference Vegetation Index (DVI), and Soil-adjusted vegetation index (SAVI) that can be used to detect species of plants.

Some of the VIs used the combination of red-edge regions such as NIR, Red-edge and Red Combine Index (NRRCI) (De Castro et al. 2015) and Red-edge Vegetation Stress Index (RSVI) (Merton and Huntington 1999). The red-edge is defined as “.....*The point of maximum slope on a vegetation reflectance spectrum between the red and near-IR wavelengths,*” (Jensen 2016, p. 339). Reflectance in this region can be expected to be substantially different for different species. Table 6-2 shows the common VI used in weed and plant discrimination.

Table 6-2 Details of VIA from the literature review

Name	Formula	Sources
Normalized Red (r)	$R^*/(R+G+B)$ R* = Normalized R value (0-1), defined as $R^*=Rm$ ($Rm=255$)	(Saberioon 2014)
Normalized Green (g)	$G^*/(R+G+B)$ G* = Normalized G value (0-1), defined as $G^*=Gm$ ($Gm=255$)	
Normalized Blue (b)	$B^*/(R+G+B)$ B* = Normalized B value (0-1), defined as $B^*=Bm$ ($Bm=255$)	
Excess green (ExG)	$g - r - b$	(Torres-Sospedra and Nebot 2014)
Color index of vegetation (CIVE)	$0.441r - 0.881g + 0.385b + 18.78745$	
Vegetation (VEG)	$g/(r^a b^{(1-a)})$ with $a = 0.667$	
Excess green minus excess red (ExGR)	$ExG - 1.4r - g$	
Normalized green-red difference index (NGRDI)	$(g-r)/(g+r)$	
Woebbecke index (WI)	$(g-b)/(r-g)$	
Normalized Difference Yellowness Index (NDYI)	$(r-g)/(r+g)$	Pena-Barragan et al. (2010)
Different Vegetation Index	NIR-R	(Jordan 1969)
Excess Red (ExR)	$1.4 * R - G$	(Meyer et al. 1999)
Modified Excess Red (MExR)	$1.4 * NIR - G$	(De Castro et al. 2015)
Modified Triangular Vegetation Index 1 (MTVI1)	$1.2 * [1.2 * (NIR - G) - 2.5 * (R - G)]$	(Haboudane et al. 2004)
NIR, Red-edge and Red Combine Index (NRRCI)	$(NIR - Red-edge) / (Red-edge)$	(De Castro et al. 2015)
Triangular Veg. Index (TVI)	$0.5 * [120 * (NIR - R) - 200 * (R - G)]$	(Broge and Leblanc 2001)
Red-edge Veg. Stress Index (RVSI)	$R + Red-edge720/2 - (Red-edge720)$	(Merton and Huntington 1999)
Red Vegetation Index (RVI)	NIR/R	(Pena-Barragan et al. 2007)

6.2.3 Image Mosaicing and Geometric Rectification

To reliably georeference imagery, a GPS survey of the area needs to be conducted (Smit et al. 2010). Smit et al. (2010) collected 20 photo control panels in their vineyard to demarcate the test plots and to serve as photo control points for georeferencing. Mathews (2014) used Agisoft Photoscan software to mosaic imagery and align it with georeferenced points using Structure from Motion (SfM) algorithms. For each set of images, Agisoft PhotoScan software automatically aligns the images and builds point cloud models of the surface (Mathews 2014). Agisoft allows generating and visualising a dense point cloud model based on the estimated camera positions to combine into a single dense point cloud (Agisoft 2013).

6.2.4 Accuracy Assessment

Accuracy assessment is important for validating the classification accuracy of image processing. Confusion Matrices have been used to assess accuracy and are widely adopted (Congalton 1991; Phinn et al. 2012; Aziz 2014; Kamal et al. 2015). Commission and Omission errors can be calculated from a Confusion Matrices (Congalton 1991). Kappa analysis was used to evaluate the Confusion matrix in this research. It is a discrete multivariate technique for accuracy assessment (Jensen 2016, p. 570) and was used to compare different matrices (Congalton 1991).

A Coefficient of Agreement (Khat) statistic can be produced from the Kappa analysis. It assumes a multinomial sampling model where the variance is derived using the Delta method (Congalton 1991, p. 6). The Khat statistic was computed based on the procedure used by Thenkabail (2015) as (Equation 3):

$$\frac{N \sum_{i=1}^r x_{ii} - \sum_{i=1}^r (x_{i+} * x_{+i})}{N \sum_{i=1}^r (x_{i+} * x_{+i})} \quad (3)$$

where,

- r is the number of rows in the matrix
- x_{ii} is the number of observations in rows i and column i
- x_{i+} and x_{+i} are the marginal total of row i and column i , respectively
- N is the total number of observations

Each type of accuracy is defined in Table 6-3.

Table 6-3 Description of the accuracy (Lehmann et al. 2015)

Confusion matrix	Definition
Producer's accuracy	The Proportion of correctly classified objects to the reference samples of class.
User accuracy	The proportion of correctly classified objects within the total number of each samples classified.
Overall accuracy	The proportion of all correctly classified objects and the total samples

Another method that is commonly used in error assessment is geometric assessment. As demonstrated by Kamal et al. (2015) and Belgiu and Dragut (2014), geometric assessment evaluates the accuracy of the segmentation of the classification. The details of the geometric assessment are explained in the methodology section (6.3.6.2). Statistical analyses based on the geometric assessment method are shown in Table 6-4.

Table 6-4 Geometric assessment formula (Belgiu and Dragut 2014)

Metrics	Formula	Explanations	Authors
Over-segmentation (OSeg)	$= 1 - \left(\frac{\text{area}(xi \cap yi)}{\text{area}(xi)} \right)$ xi – reference object yj – evaluated objects	Range [0, 1] = 0 is perfect segmentation	(Clinton et al. 2010)
Under-segmentation (USeg)	$= 1 - \left(\frac{\text{area}(xi \cap yi)}{\text{area}(xi)} \right)$	Range [0, 1] = 0 is perfect segmentation	(Clinton et al. 2010)
Root Mean Square (RMSE)	$= \sqrt{\frac{oseg_{ij}^2 + useg_{ij}^2}{2}}$	Range [0, 1] = 0 is perfect segmentation	(Levine and Nazif 1985; Weidner 2008)
Area fit index (AFI)	$= \frac{\text{area}(xi) - \text{area}(yi)}{\text{area}(xi)}$	= 0.0 is perfect overlap	(Lucieer and Stein 2002)
Quality rate (Qr)	$= \frac{\text{area}(xi \cap yi)}{\text{area}(xi \cup yi)}$	Range [0, 1] = 1 is perfect segmentation	(Winter 2000)

6.3 METHODS

6.3.1 Image Collection

The MCA 6 imagery was processed using several steps. The RAW imagery collected by the MCA 6 camera, and then was converted to multiband image by using Pixel Wrench 2 (PW2) software (Tetracam 2015). The details of the data collection were explained in Chapter 3. The exposure setting for each sensor in the MCA 6 camera was set manually by prior trial and error. A handheld GPS (Trimble Juno-SB) was used to record the position of each quadrat. The 24 quadrats were randomly distributed over the field (Figure 3-8). Each mosaic image was georeferenced using ArcGIS software and the GPS references points.

6.3.2 Image Processing Workflow

The details of the image pre-processing data conversion were explained in Chapter 3 (Section 3.4.3.3 to 3.4.3.7). After pre-processing, the imagery was corrected, and ready to be classified. The imagery was mosaiced using Agisoft Photoscan software following Mathews (2014) procedures. The mosaic and single images were analysed using OBIA and VI analysis (Figure 6-2). Error assessment was done to validate the accuracy of classification.

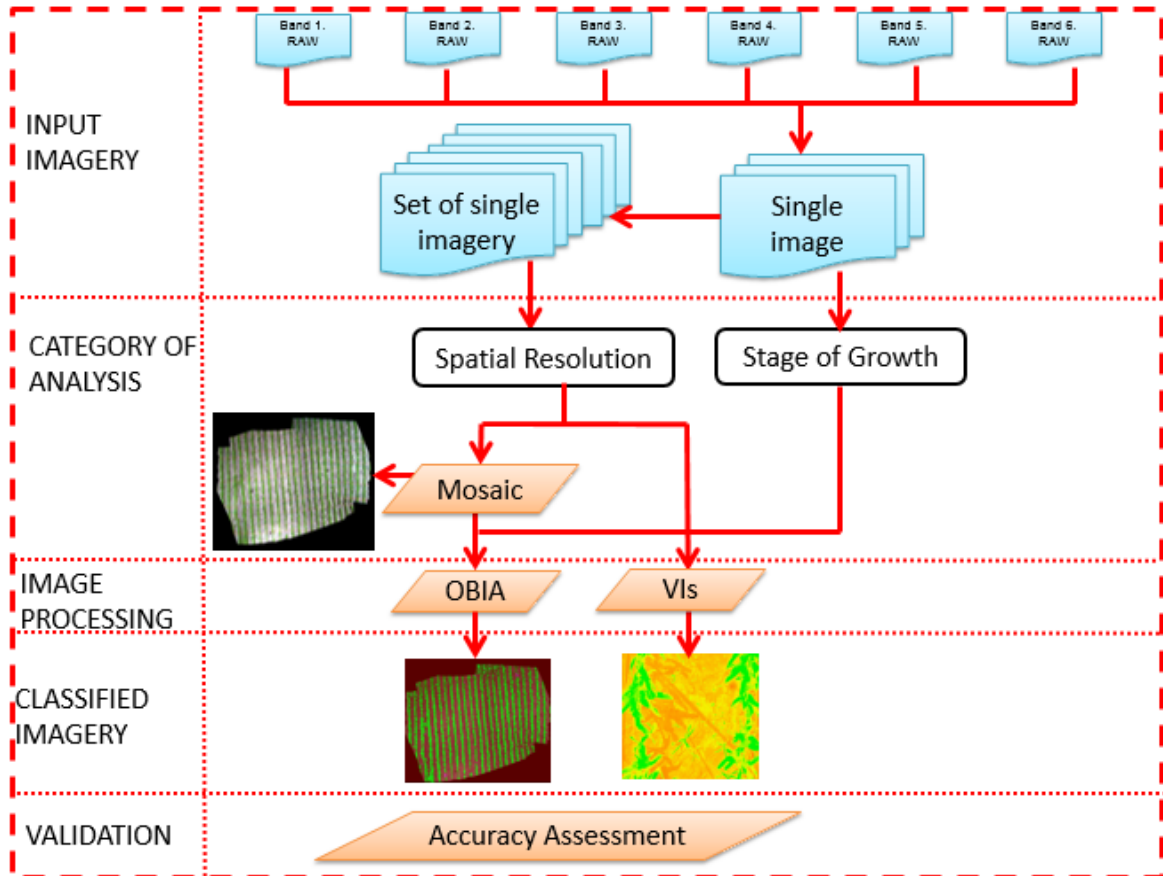


Figure 6-2 Flowchart of the image analysis process

6.3.3 Mosaicing

Agisoft PhotoScan software provides a user friendly process for mosaicing the imagery. The imagery was added and aligned using the Align Photo function (Figure 6-3). Then, the imagery generated and visualised a dense point cloud model based on the estimated camera position using Build Dense Cloud function. It calculates the depth information for each camera to be combined into a single dense point cloud (PhotoScan 2013). The geometrics of the map are reconstructed due to the poor texture of some elements of the scene and noisy or poorly focused images (Known as outliers among the points) by using the Build Mesh function (PhotoScan 2013). The images were used to build the texture exported as a mosaiced orthophoto image. Export Orthophoto function is

flexible allowing users to choose different image file types. A report of the outputs is also produced in PDF format. The details of the process were as described by Mathews (2014).

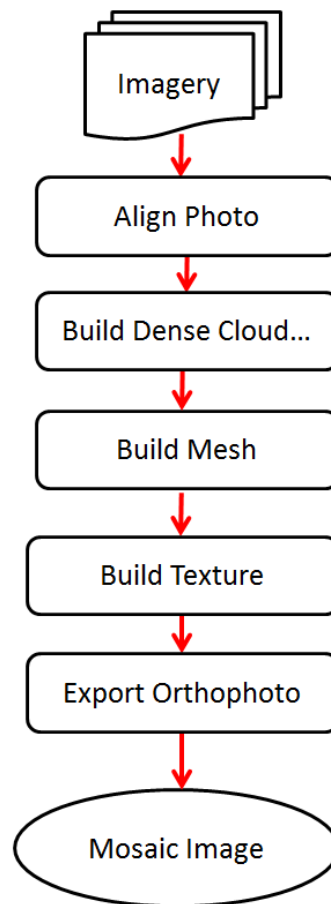


Figure 6-3 Workflow for mosaicing in Agisoft Photoscan

The MCA 6 camera was used to collect imagery at three different resolutions for mosaicing into “whole of field” images (Table 6-5). The three different heights were chosen based on the high resolution (5.42 mm, 10.83 and 20.31 mm) to investigate the suitable resolution to detect weeds in the sorghum crop.

Table 6-5 Resolution for mosaic image

Altitude (m)	Resolution (mm)
10	5.42
20	10.83
37.5	20.31

6.3.4 Object Based Image Analysis (OBIA) Procedures

The OBIA method was used to process multispectral imagery collected in week 3 and week 4 after planting. Each different spatial resolution image was processed as shown in Figure 6-4. It

shows the overall scheme by which three spatial resolutions at the stages of growth were analysed by OBIA.

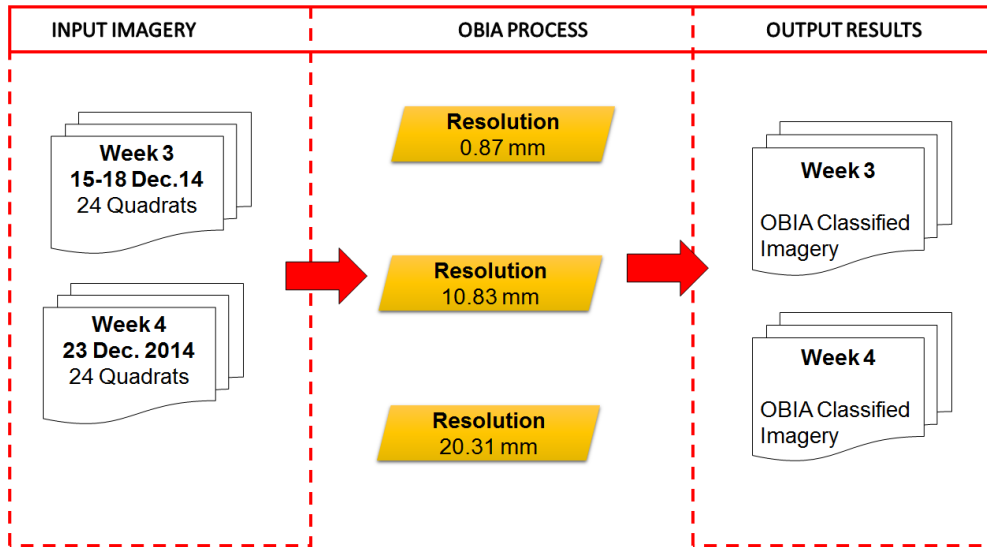


Figure 6-4 Growth stage analysis at different spatial resolutions

6.3.4.1 Image Analysis Workflow

The methodology involved developing a conceptual plan for weed detection analysis based on a review of the literature associated with weed mapping, rule set development, followed by field work and local expert knowledge as shown in Figure 6-5.

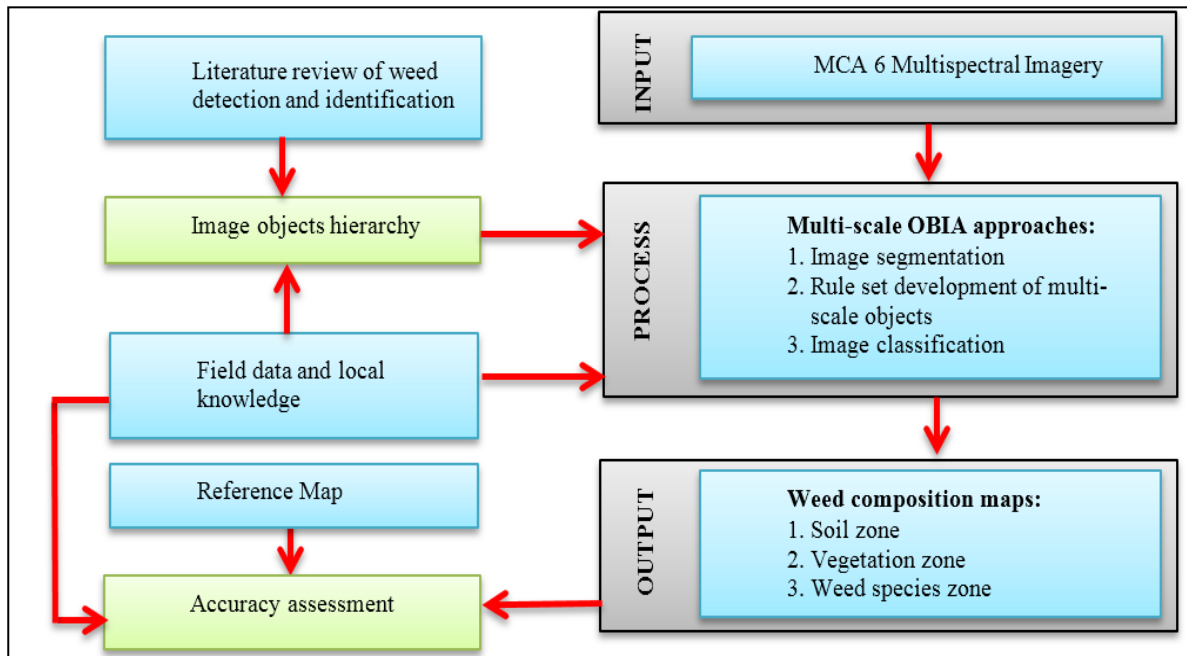


Figure 6-5 Flowchart of the methodology process (Kamal et al. 2015)

OBIA was hierarchy of steps to classify images. It can be done both manually and automatically (Johansen et al. 2011). At each level the image is segmented into objects based on their spatial, structural and spectral characteristics (Pena et al. 2015). This has also been called a

“landscape scaling ladder” concept because bigger objects are progressively segmented into smaller objects by the use of a scaling value (Kamal et al. 2015). The OBIA workflow involves two main processes. In the first process the image is segmented based on a scale defined by the user. It is also known as the super-level or parent level.

In the second process, classification is performed to identify each class of target feature (weed species) (Figure 6-6). This level is known as a sub-level or child process (Definiens Imaging 2004). The advantages of OBIA are that it provides a logical, sequential mapping process, has a clear multi-scale context for the targeted objects and their relationship and controls over the process within a certain level and object container (Kamal et al. 2015).

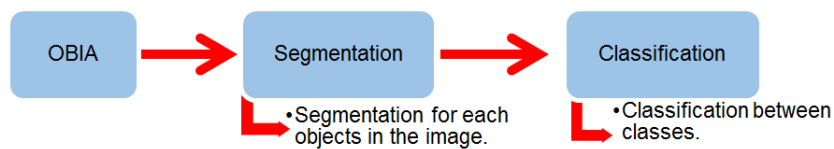


Figure 6-6 Flow chart for image processing using OBIA analysis

6.3.4.2 Classification Hierarchy and Development of Rule Sets

The images were segmented into homogeneous multi-pixel objects by using the “Multiresolution Segmentation” algorithm in eCognition software. It was also used by Phinn et al. (2012), Belgiu and Dragut (2014), Laliberte et al. (2011), Aziz (2014) and Kamal et al. (2015) to segment images for a wide range of applications. Figure 6-7 shows the hierarchy of the workflow in OBIA for weed discrimination classification.

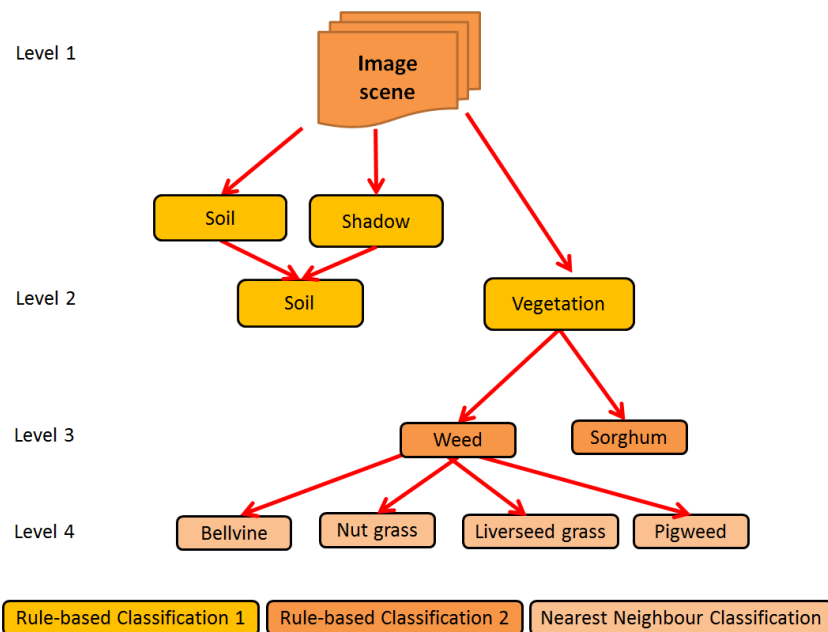


Figure 6-7 Hierarchy for weed discrimination classification. Schematic modified from Laliberte et al (2010) and Slaughter (2014)

In the first step (Level 1 to Level 2) rules were developed to segment the entire image into soil, shadow and vegetation objects. The soil and shadow objects were classified into a consolidated “soil” class. In the second step (Level 2 to Level 3) rules were developed to segment and classify the vegetation into weeds and sorghum objects. Because the experimental quadrats were monocultures of weeds, this had the effect of identifying each type of weed species as a separate object. The third step (Level 3 to Level 4) was the elimination of small misclassified objects by merging them with the adjoining larger object (“merge” function). The process was finalised by grouping the like objects together (“Enclosed” function) as shown in Figure 6-8.

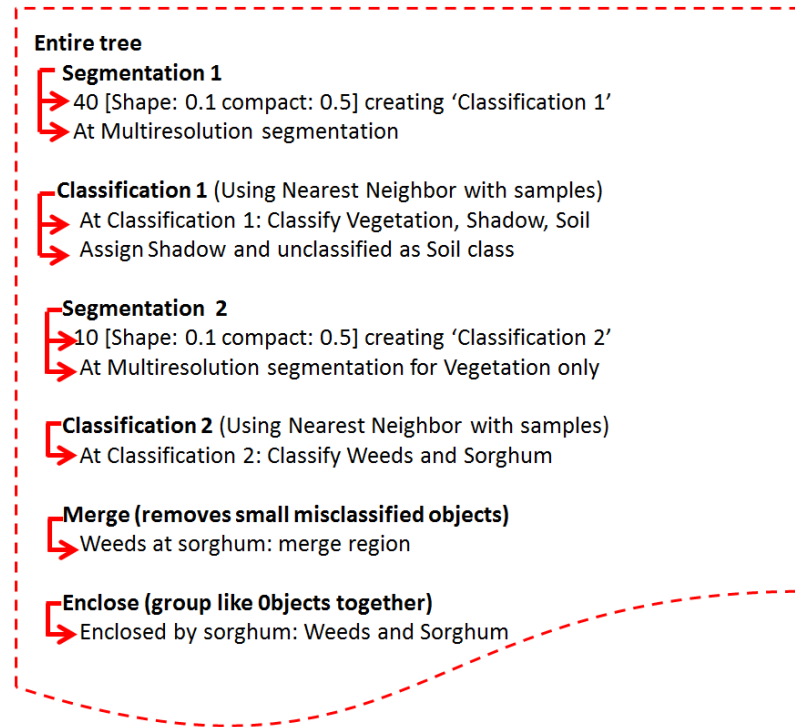


Figure 6-8 Process tree from eCognition Developer used for weed classification

The first segmentation was a “Multiresolution Segmentation” algorithm at a scale setting of 40 as shown in Figure 6-8 for 0.87 mm resolution imagery. The scale setting is very important because it affects the size of the segments. The scale parameter should be a reasonable parameter to avoid missing any information (Corbane et al. 2008). Image segmentation classifies the object class at individual pixel values and their neighbours to compute a colour criterion (h_{colour}) and shape or spatial criterion (h_{shape}) (Baatz et al. 2001). These two criteria were then used to create image objects of relatively homogeneous pixels using the general segmentation function (S_j) (Baatz et al. 2001) (Equation 4):

$$S_j = w_{colour} * h_{colour} + (1-w_{colour})*h_{shape} \quad (4)$$

where,

the weight for spectral colour (w_{colour}) versus shape is $0 \leq w_{colour} \leq 1$.

In this research, the Shape value was manually adjusted until it visualised the weed and sorghum shapes. A value of 0.1 achieved this. The colour value (wcolour) was also selected by manual adjustment to visualise the weeds and sorghum. A value of 0.5 was found to be most suitable. This setting is also consistent with what was used by Pena-Barragan et al. (2012a) in weed mapping. Six wavebands were selected in this analysis. However, different wavelength bands can be used in future research to obtain better analysis.

The Nearest Neighbour algorithm classification was applied to the three main classes by using training samples as outlined by Visser and Wallis (2010). Then, shadow and unidentified objects (the objects except shadow, soil and vegetation such as the white quadrat frame and label tag) were aggregated into the soil class by the Assigning function. This left two main classes, vegetation (sorghum and weeds) and soil (including shadow and unidentified objects).

The second segmentation focussed on the vegetation class. The size of weeds helped to identify them in the class. It was re-segmented with a scale parameter of 10 to narrow down the structure of the vegetation class as shown in Figure 6-8. This was done because the weeds are small compared to the sorghum. The re-classify process (Classification 2) was run to identify the weeds from the sorghum. The results showed that some of the sorghum class was mixed with the weed class. The “Enclosed by class” function was used to merge sorghum objects and weed objects with their adjoining objects class. This same rule set was used for successive images with some modification based on their spatial resolution. The summary of the rule sets is shown in Table 6-6.

Table 6-6 Rule sets parameters for different spatial resolution

OBIA Processing	Spatial Resolution			
	0.87 mm	5.42 mm	10.83 mm	20.31 mm
Segmentation 1				
Scale Parameters	40	50	10	50
Shape	0.1	0.1	0.1	0.1
Compact	0.5	0.5	0.5	0.5
Segmentation 2				
Scale Parameters	10	5	10	45
Shape	0.1	0.1	0.1	0.1
Compact	0.5	0.5	0.5	0.5

6.3.4.3 Application of OBIA Rule Sets

Segmentation of the whole area was used to separate the feature objects at the parent level in the hierarchy process. The segmentation used a “Multiresolution Segmentation” algorithm to break down the features using different scale settings (Figure 6-8). Figure 6-9 shows the image before the segmentation process. It shows sorghum, nutgrass (weed), shadow and soil clearly at 0.87 mm resolution for Quadrat 1 for nutgrass (Q1NG).

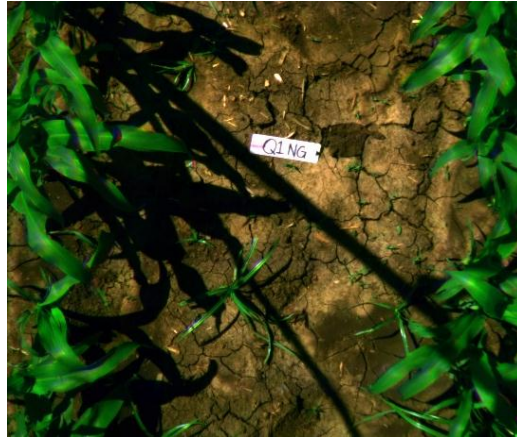


Figure 6-9 The raw image before the segmentation process showing sorghum, nutgrass (weed), shadow and soil at 0.87 mm resolution for Quadrat 1 for nutgrass (Q1NG)

Figure 6-10 shows the segmentation process at a scale setting of 40. This segmented approximately half the maximum number of objects in the image. This appeared as a practical visual setting at which to discriminate the main objects (soil and vegetation). It shows the segmentation with outlines (a) and without outlines (b). The shadow class was automatically segmented in a separation class into a soil class.

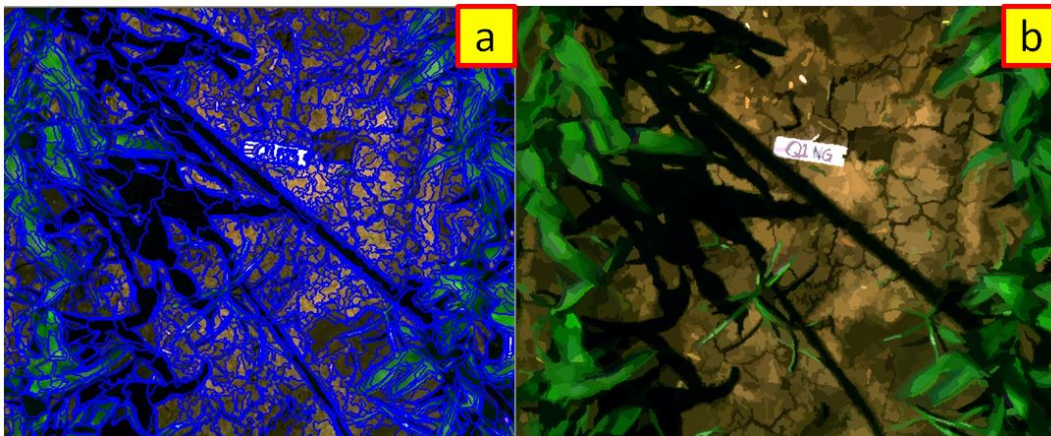


Figure 6-10 Segmentation with outlines (Scale parameter: 40) (a); segmentation without outlines (b)

The three main classes (soil, shadow and vegetation) were classified (a) using Nearest Neighbour classification (Figure 6-11). The process was done by adding a new “child” under the “parent” segmentation level and running the classification in the “child” level.

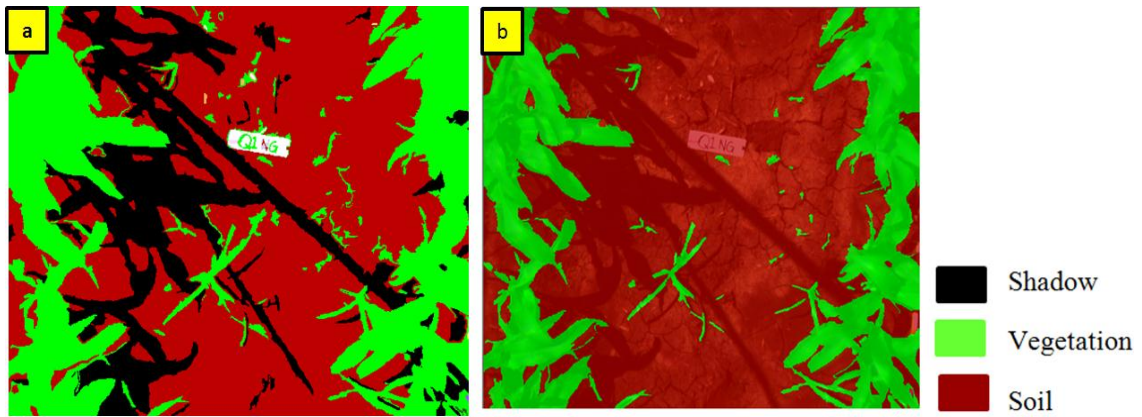


Figure 6-11 Classification for shadow, soil and vegetation

The classification processes combined the shadow and unidentified class into the soil class by adding another child level under the first classification process (Figure 6-11 b). The assumption was that the unclassified class and shadow would be added to the soil class at this stage.

The second segmentation was narrowed down for specific classes in the vegetation class by using a scale setting of 10 and the same settings for shape and compactness as the first segmentation. This segmented the vegetation class into more details (Figure 6-13).

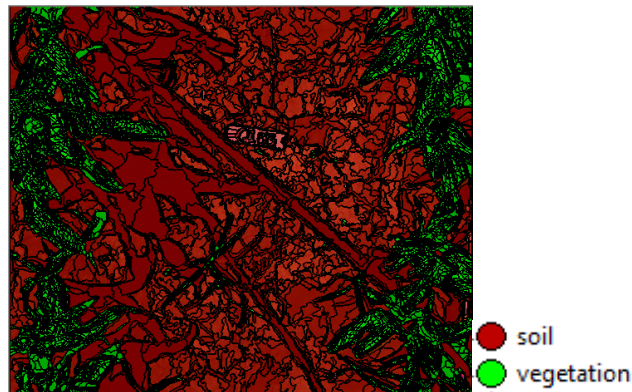


Figure 6-12 Segmentation between soil and vegetation (Scale setting: 10)

Weeds and sorghum were selected in the vegetation class in order to re-assign the sorghum and weed objects. Regions of Interest (ROI) were selected based on the objects (sorghum and weeds) by using the “Sample” function as shown in Figure 6-13. Yellow indicates the sorghum class while green indicates weeds as shown in Figure 6-13. (The green ROI do not show up in a black and white hard copy image).

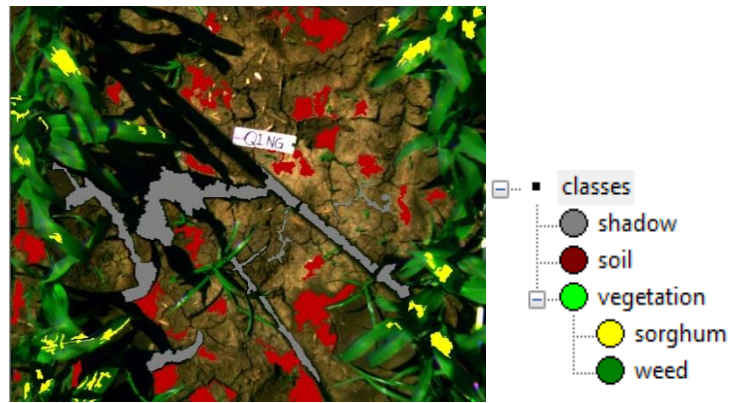


Figure 6-13 Selected samples for each class

The ROI samples for sorghum and weeds were assigned using the “Assign Class” function. Figure 6-14 (a) shows the results when the classification process was applied to the whole image. It appears that some areas of weeds and sorghum were misclassified because of their similarity in spectral resolution. However, sorghum shows up predominantly as yellow with only small areas of the sorghum classed as “weed”.

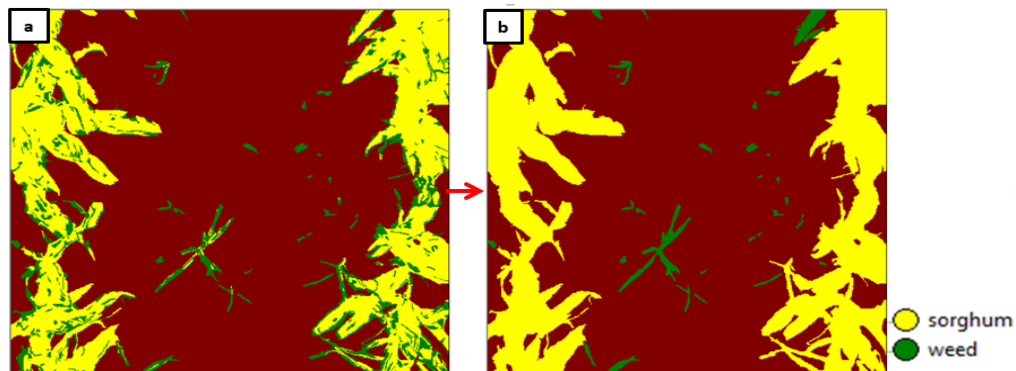


Figure 6-14 Sorghum and weeds was misclassified (a) and reclassify in vegetation class (b) using “Enclosed” function

The “Merge” function was used to merge the misclassified areas of sorghum in the sorghum class and the misclassified areas of weeds into the weed class. The final process used the “Enclose” function to join the merged objects into their respective classes (sorghum and weed) (Figure 6-14) (b). Figure 6-15 shows the final results of classifying sorghum, weeds and soil using a transparency value of 70. It shows that all the objects were classified correctly. The classification was validated by error assessment as shown in section 6.3.6.

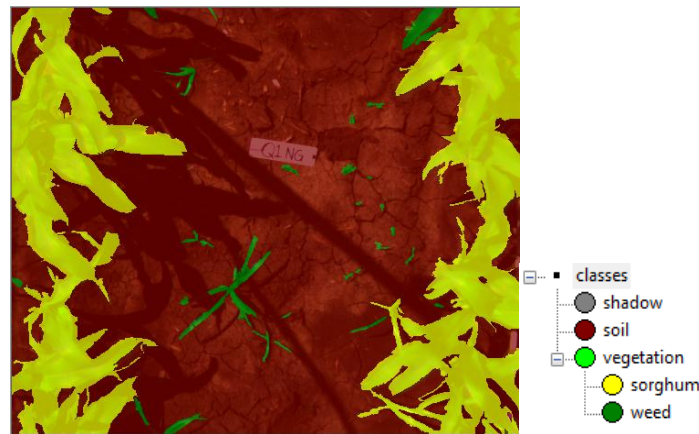


Figure 6-15 Classification between sorghum and weeds

Similar rule sets (with some modification) were used for the quadrats containing different species of weeds and at different stages of growth.

6.3.5 Vegetation Index Analysis (VIA)

The second method investigated for weed mapping was VI. It used band ratio formula to classify the images into soil, sorghum and weeds (Figure 6-16). This technique is based on enhancing the contrast between the features by manipulating pixel reflectance in one band by pixel reflectance in other bands (ESRI 2015).

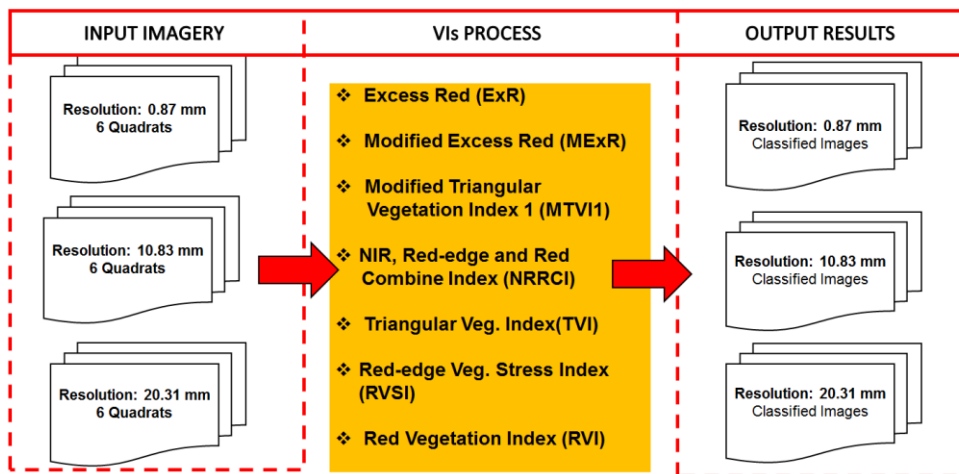


Figure 6-16 Details of dataset for VIA analysis

The equations were adapted from the existing literature and all were tested at 3 different spatial resolutions (Table 6-7). The result from the analysis was compared with the OBIA classification results. In applying the equation, the following hyperspectral bands were used as shown in Table 6-8. All the VIA analyses were calculated using the “Raster Calculator” function in ArcGIS.

Table 6-7 Vegetation Indices used in image processing

Vegetation Index	Formula	Sources
Different Vegetation Index	NIR-R	(Jordan 1969)
Excess Red (ExR)	$1.4 * R - G$	(Meyer et al. 1999)
Modified Excess Red (MExR)	$1.4 * NIR - G$	(De Castro et al. 2015)
Modified Triangular Vegetation Index 1 (MTVI1)	$1.2 * [1.2 * (NIR - G) - 2.5 * (R - G)]$	(Haboudane et al. 2004)
NIR, Red-edge and Red Combine Index (NRRCI)	$(NIR - Red-edge) / (Red-edge)$	(De Castro et al. 2015)
Triangular Veg. Index (TVI)	$0.5 * [120 * (NIR - R) - 200 * (R - G)]$	(Broge and Leblanc 2001)
Red-edge Veg. Stress Index (RVSI)	$R + Red-edge - 720 / 2 - (Red-edge - 720)$	(Merton and Huntington 1999)
Red Vegetation Index (RVI)	NIR / R	(Pena-Barragan et al. 2007)

Table 6-8 The band value (central wavelength) assignment for each spectral region

Region	Band
NIR	850 nm
Red-edge	720 nm
Red	680 nm
Green	560 nm

6.3.6 Error Assessment Procedures

Error assessment is necessary to measure the accuracy of the classification (Kamal et al. 2015). The classified images were compared with the Reference Map. The Reference Map was digitized from the original image to produce a vector file. OBIA classified images were exported to vector format. Error assessment for VIs was not done since qualitative assessment indicated it was not necessary. A similar technique was used by Aziz (2014), who found that visual examination of the classified images was sufficient.

Maps from both the digitized (Reference Map) and classified images (OBIA Map) were compared by using statistics to evaluate the accuracy of segmentation and classification of the object classes based on Belgiu and Dragut (2014) review. They used two types of error assessment:

- a) Confusion Matrix
- b) Geometric Matrix

6.3.6.1 Confusion Matrix Assessment

Confusion Matrices have been widely used for validating image classification (Phinn et al. 2012; Aziz 2014). To ensure that validations of the classification methods are comparable, a stratified systematic unaligned sampling method was used (University of Texas 2015). The Confusion Matrix was used to test the positive classification of each weed species at each stage of growth and at each spatial resolution (Figure 6-17).

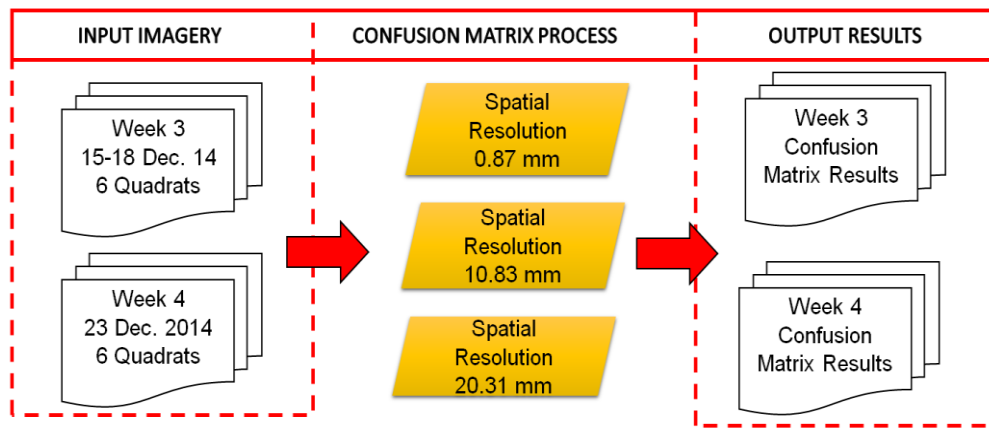


Figure 6-17 Confusion matrix at different growth stages

The classified imagery was compared with the observed imagery by grid sampling (Wollenhaupt, 1994). The classified OBIA results were exported into ArcMap software. The “Fishnet” function was used to create the systematic grid for the sampling (Figure 6-18). Samples for the soil, weeds and sorghum were chosen from the grid using “Fishnet”. The points highlighted in Figure 6-18 were weeds based on the classification image. The total sample number was recorded in the error matrix table (Table 6-9). The error matrix was calculated based on the Coefficient of Agreement (Khat). The same method was used for each different weed species.

Table 6-9 The error matrix for nutgrass at 0.87 mm

Classification	Classes	Imagery Nutgrass				User Accuracy	Commission Error
		Weed	Soil	Crop	Total		
	Weed	36	0	0	36	100%	0%
	Soil	1	73	1	75	97%	2.67%
	Crop	1	0	47	48	97%	2.08%
	Total	38	73	48	159		
	Producer's Accuracy	95%	100%	98%			
	Omission Error	5.26%	0%	2.08%			
	Overall Accuracy : 98%						
	Computation of Khat Coefficient of Agreement : 97%						

The sample points were overlaid on the Reference Map (Figure 6-18) (RGB image) and checked for classification. The results were recorded in the error matrix table (Table 6-9). All the classes were counted the same way.

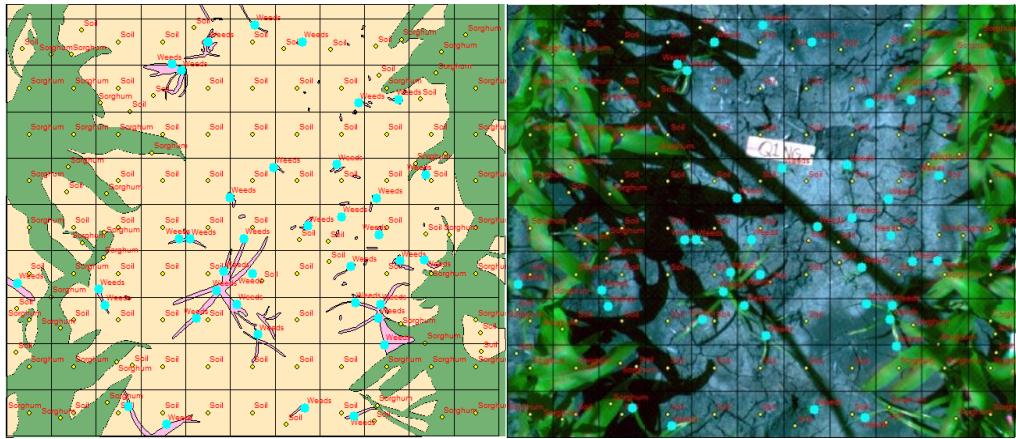


Figure 6-18 The Fishnet on the top of the OBIA classification and RGB maps

6.3.6.2 Geometric Assessment

The Geometric Assessment method adapted from Belgiu and Dragut (2014) was used to evaluate the segmentation class. Classified images need to be validated using a Reference Map or a high accuracy map that allows for an assessment of the shape, symmetry and position of the objects (Kamal et al. 2015).

Figure 6-19 shows the original image (a) and the digitised vectors (b) (by small red lines). The digitised image was classified into the three main classes (sorghum, weeds and soil).

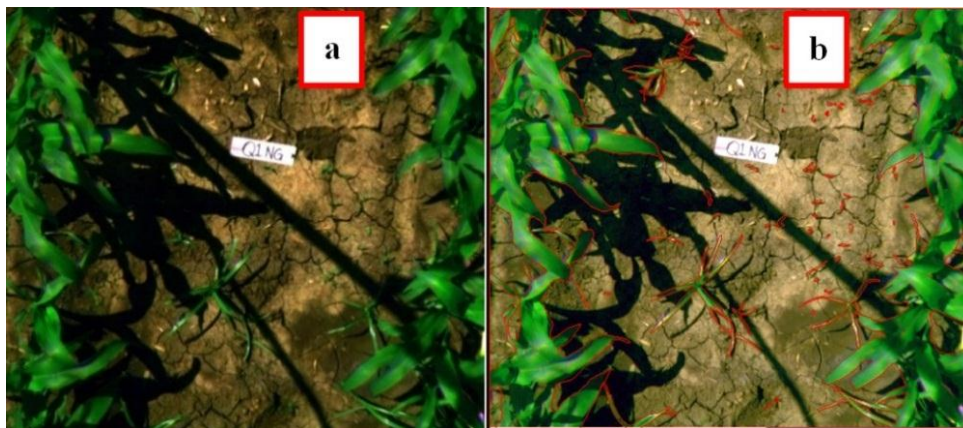


Figure 6-19 The original image (a) and (b) is the visual interpretation (as Reference Map) from digitization.

Figure 6-20 shows the three main classes (raster) derived from the digitised image. The Reference Map illustrates the detailed features compared to the OBIA Map. For example, the Reference Map classified every single plant compared to the OBIA Map that just detected the groups of plants.

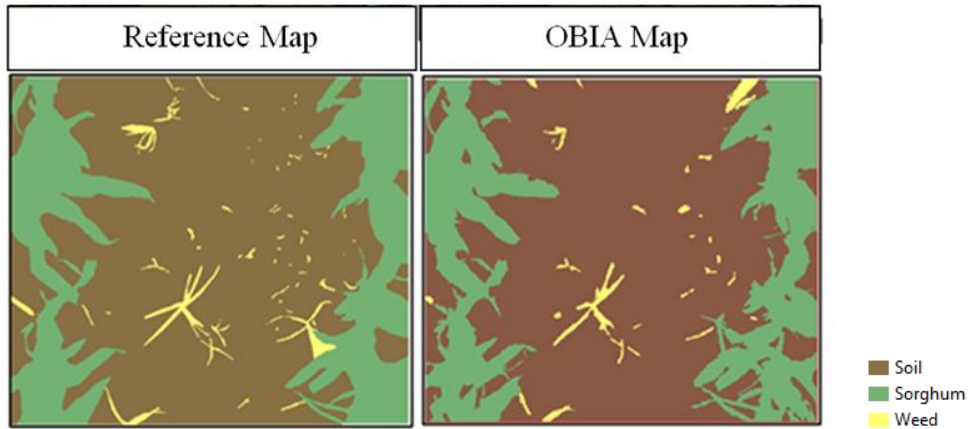


Figure 6-20 Comparison between Reference and OBIA image maps

The OBIA classified image was exported from eCognition (*.tif format) to ArcMap where it was polygonised and exported in shapefile format (Figure 6-20) by using the “Raster to Polygon” tool in AcrToolbox. It can be seen that the OBIA classified image is not as detailed as the Reference Map.

The attribute table of both images were compared by adding a new field to assign the correct name to each polygon (Figure 6-21).

FID	Shape*	ID	GRIDCODE		FID	Shape*	ID	GRIDCODE	Class
0	Polygon	1	4		0	Polygon	1	4	Sorghum
1	Polygon	2	5	→	1	Polygon	2	5	Weed
2	Polygon	3	5		2	Polygon	3	5	Weed
3	Polygon	4	2		3	Polygon	4	2	Soil

Figure 6-21 The new field (Class) added in the attribute table.

Figure 6-22 shows a comparison between the Reference Map and OBIA Map. Each map has its own attribute table with unique ID. The Reference Map and OBIA Map were overlaid. Geometric error assessment was applied to validate the classification process.

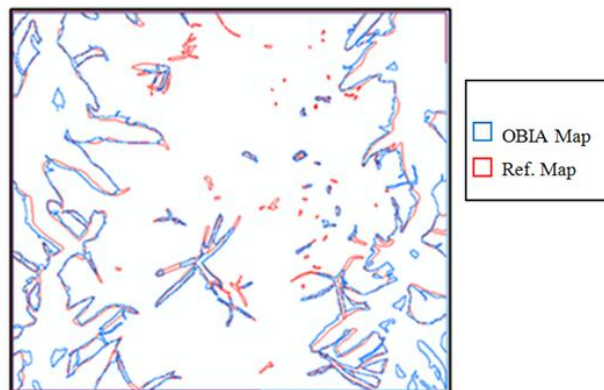


Figure 6-22 Comparison between OBIA image and Reference Map

The polygons in the OBIA Map were combined based on their classes using the “Dissolve tool” to merge the same class of each shapefile into three polygon classes shown in Figure 6-23.

obiavector					
FID	Shape *	ID	GRIDCODE	Class	
0	Polygon	1	4	Sorghum	
1	Polygon	2	5	Weed	
2	Polygon	3	5	Weed	
3	Polygon	4	2	Soil	
4	Polygon	5	2	Soil	
5	Polygon	6	5	Weed	
6	Polygon	7	5	Weed	

obia_vector			
FID	Shape	Class	
0	Polygon	Soil	
1	Polygon	Sorghum	
2	Polygon	Weed	

Figure 6-23 The merge results by using “dissolve” tool

The polygon classes in the Reference and OBIA Maps were merged to identify the areas that were common in both map classifications. The area of each merged class was calculated in the attribute table of the merged polygon shapefile. Table 6-10 shows the area by polygon class for the merged OBIA and Reference Maps. Area fit index (AFI), was calculated by using the formula based on Table 6-11.

Table 6-10 Area comparison for OBIA and Reference Maps

FID	Shape	Class	OBIA Map	Reference Map
0	Polygon	Soil	722946	72634
1	Polygon	Sorghum	295760	290505
2	Polygon	Weed	18244	23308

Table 6-11 Area Fit Index (AFI)

Class	Calculation	AFI
Soil	$(726233 - 722946)/726233$	0.0045
Sorghum	$(290504 - 295760)/290504$	-0.0181
Weed	$(23307 - 18244)/23307$	0.2172

(i) Calculation of Over and Under-Segmentation and Mean Square Root Error.

Over-segmentation, under-segmentation and RMS error were calculated for each class. Figure 6-24 illustrates the case for sorghum in both maps (Example: Soil class).

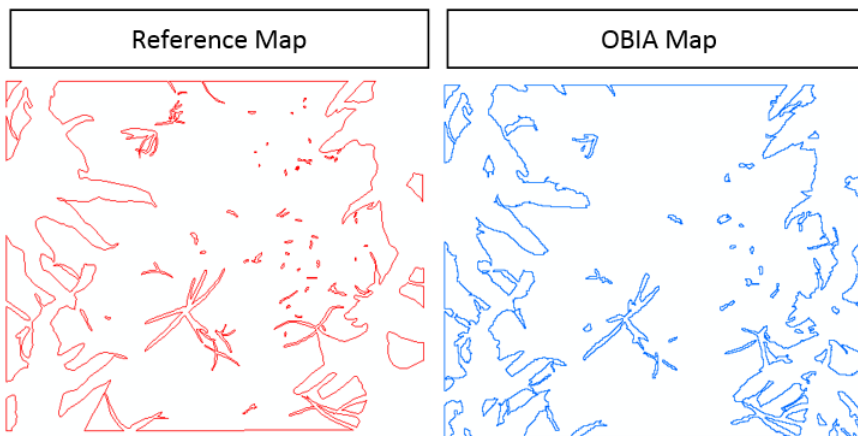


Figure 6-24: Sorghum class in both maps

The ArcGIS Intersection tool was used to match each class in both maps (Figure 6-25).



Figure 6-25: The matching area for the soil class in both maps (Intersect Result)

*∩ = Intersection

The Geometric calculation for over-segmentation and under-segmentation was used to calculate the error assessment for each class (Table 6-12).

Table 6-12 Results for Geometric calculation (Example: Soil)

Geometric calculation	Formula calculation	Results
Over-Segmentation	$= 1 - (\text{match area of soil/reference area of soil})$ $= 1 - (691951/726233)1 - (\frac{26686}{290504})$	0.05
Under-Segmentation	$= 1 - (\text{match area of soil/OBIA area of soil})$ $= 1 - (\frac{\text{match area of sorghum}}{\text{GEOBIA area of sorghum}})1 - (691951/722946)$	0.04
Root Mean Square Error for sorghum	$= \sqrt{\frac{U\text{Seg}^2 + O\text{Seg}^2}{2}}$ $= \sqrt{\frac{0.04^2 + 0.05^2}{2}} \sqrt{\frac{0.10^2 + 0.9^2}{2}}$	0.045

(ii) Calculation of Quality Rate (Qr)

Error assessment was also calculated for the Qr for each class as follows:

Quality Rate of Soil (Qr) = $\text{area } (A \cap B) / \text{area } (A \cup B)$

While, A = Reference Map

B = OBIA Classified Map

The “Symmetrical difference” tool in ArcGIS was used to calculate the Union (U) between Reference Map and the OBIA Map (Figure 6-26 and Figure 6-27).

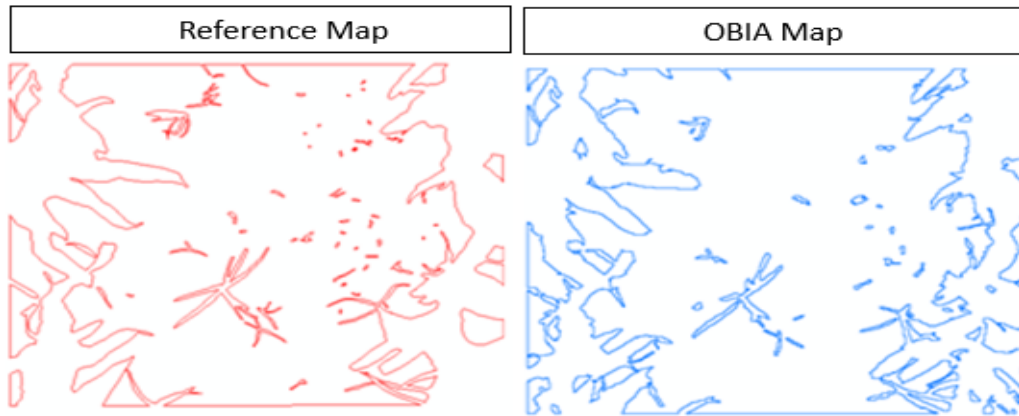


Figure 6-26 Difference between Reference and OBIA Maps



Figure 6-27: Symmetrical Difference Map showing areas of over and under-segmentation (Symmetrical Difference Result)

The “merge” function was used to merge the Intersect Results (Figure 6-25) and the Symmetrical Difference Results (Figure 6-27) in ArcGIS for the soil class (Figure 6-28).

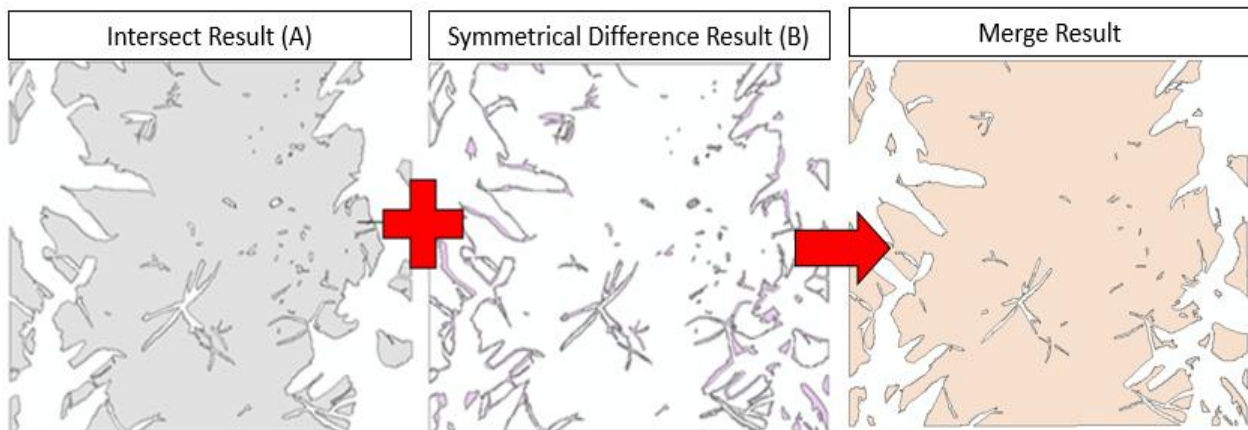


Figure 6-28 The merge function applied to the Intersect and Symmetrical difference results for soil class

The results for soil were Quality Rate of soil (Qr):

$$= 691951 / 757228$$

$$= 0.914$$

* \cap = intersection, U = Union

Results show the quality rate for soil classification was 0.914 which is considered to be a high accuracy because it is close to 1 (Winter 2000). The same steps were calculated for each weed species.

6.4 RESULTS


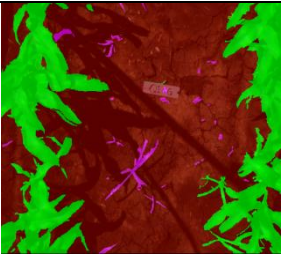
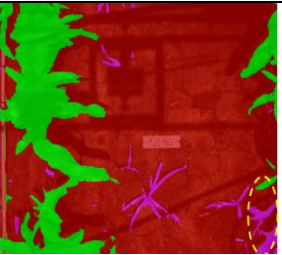
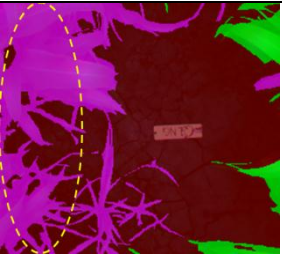

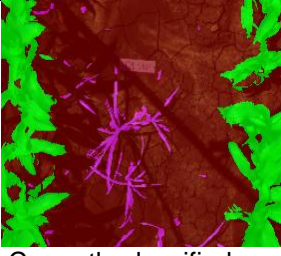

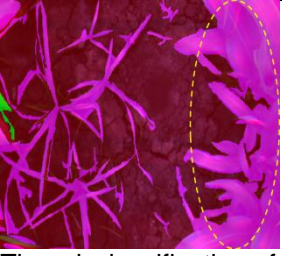
6.4.1 OBIA and Analysis Results

6.4.1.1 OBIA Results for Highest Spatial Resolution Imagery (0.87 mm)

This section presents the results for the 0.87 mm spatial resolution imagery using OBIA. Table 6-13 shows the OBIA results for all the nutgrass replicate quadrats at different stages of growth. Nutgrass in Q1NG was successfully classified in week three. Result at week four show misclassification between weeds and sorghum. It shows that sorghum was mostly classified as a weed class. Other quadrats (Q2, Q3) for nutgrass (NG) show that most of them were also misclassified (Appendix R).

Sorghum non pre-emergence quadrats illustrated similar results with NG classification. Replicate Q1SNP shows that the 17th Dec. 2014 image yielded good classification but for the rest of data were misclassified (Table 6-13). Replicate Q2SNP indicates the results were promising at week three as shown in Appendix S. The two other replicates also show misclassified nutgrass for week three and week four.

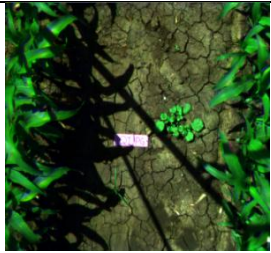
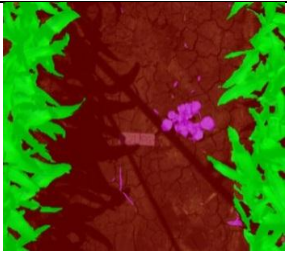
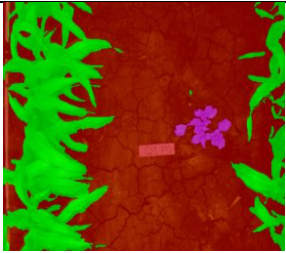
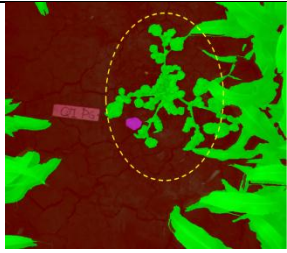
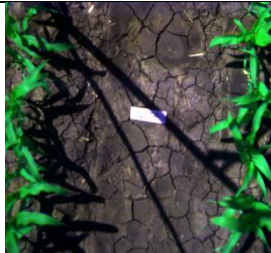
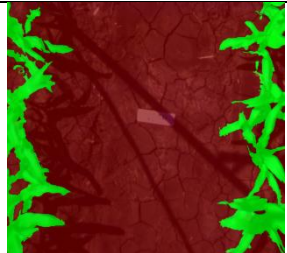
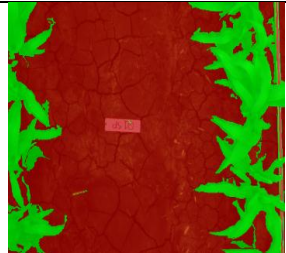
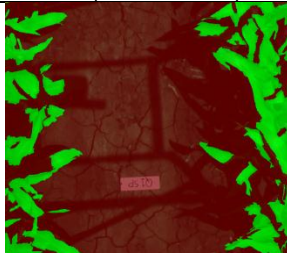
Table 6-13 Nutgrass and sorghum non pre-emergence quadrats at two stages of growth

Image height: 1.6 m	Week 3		Week 4
	17 December 2014	18 December 2014	23 December 2014
 Q1NG (Nutgrass)	 Correctly classified	 The misclassification of sorghum (In the circle)	 The misclassification of sorghum (In the circle)
 Q1SNP (Sorghum non pre-emergence)	 Correctly classified	 The misclassification of weeds (In the circle)	 The misclassification of sorghum (In the circle)

It shows clearly that Pigweed (PG) on week three was successfully identified based on the rule set (Table 6-14). However, during week four it was not successfully identified using this rule set when pigweed was identified as sorghum. Even though the shape of the pigweed and sorghum were totally different, at this stage, the same rule set did not identify the correct shape of the pigweed. This is because of the size of the weed patches, at week four pigweed was intermingled with the sorghum. In this research failures in identification occurred when the weeds were intermingled with sorghum. This occurred more frequently during the later stages of growth. Therefore, the early stage of the growth stage will help to detect the weed precisely. Overall, pigweed showed good classification at 0.87 mm at all stages of growth (Appendix T).

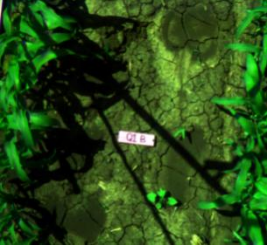
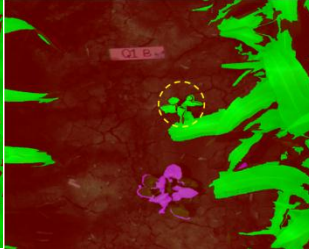

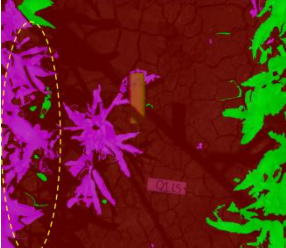


Most of the sorghum pre-emergence (SP) quadrats correctly classified sorghum and soil (Table 6-14). However, weeds were misclassified in Q3SP at week three and four (Appendix W).

Table 6-14 Pigweed and sorghum pre-emergence quadrats at two stages of growth

Image height: 1.6 m	Week 3		Week 4
	17 December 2014	18 December 2014	23 December 2014
 Q1PG (Pigweed)	 Correctly classified	 Correctly classified	 The misclassification of weeds (In the circle)
 Q1SP (Sorghum Pre-emergence)	 Correctly classified	 Correctly classified	 Correctly classified

Bellvine (B) quadrats also showed similar results to pigweed. Analysis of replicates Q1B, Q2B and Q3B show that the only image that was misclassified was on week four (Appendix U). Q4B shows the correct classification except on 17th Dec. 14 (Table 6-15). The shape of bellvine makes the classification easier and their location provides a gap between bellvine and sorghum (SG) plants. Most of them were in the middle of the quadrat which helped to identify the weeds accurately. Liverseed grass (LS) was only correctly classified in Q2LS and Q3LS on 17th Dec. 14 (Appendix V). Most of the replicates were misclassified in all weeks (Table 6-15).

Table 6-15 Bellvine and liverseed grass quadrats at two stages of growth

Image height: 1.6 m	Week 3		Week 4
	17 December 2014	18 December 2014	23 December 2014
 Q1B (Bellvine)	Correctly classified	Correctly classified	 The misclassification of weeds (In the circle)
 Q1LS (Liverseed grass)	 The misclassification of sorghum (In the circle)	 The misclassification of weeds (In the circle)	 The misclassification of weeds (In the circle)

6.4.1.2 OBIA Results for Medium Spatial Resolution Imagery (10.83 mm)

The 10.83 mm resolution imagery collected on week three after planting (Table 6-16) was analysed. Only replicate Q1NG showed correct nutgrass (NG) classification. Misclassification is particularly evident where the nutgrass is close to the SG plants (Appendix X). Sorghum non pre-emergence (SNP) quadrats were correctly classified all the time except for Q3SNP (Table 6-16). These quadrats potentially contained all types of weeds (Appendix Y) however, nutgrass was the dominant weed in these quadrats.

Table 6-16 Nutgrass and sorghum non pre-emergence at 10.83 mm spatial resolution (continued)

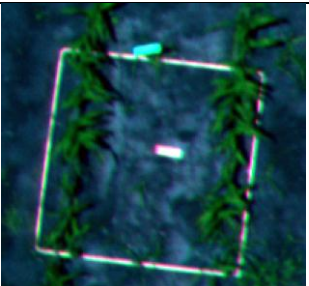
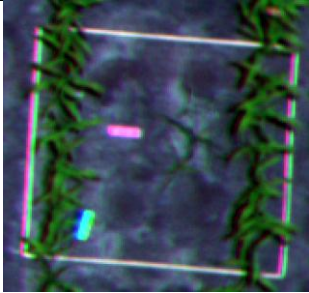
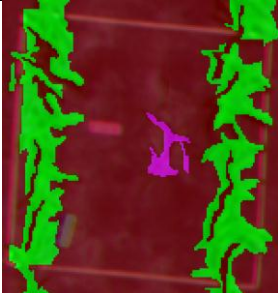
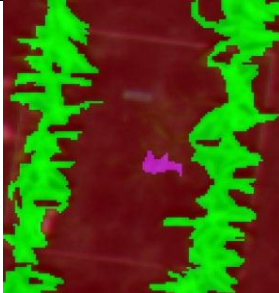
Image (20 m)	Week 3	
	15 December 2014	17 December 2014
 Q1NG (Nutgrass)	Correctly classified	Correctly classified

Table 6-16 (continued) Nutgrass and sorghum non pre-emergence at 10.83 mm spatial resolution

Image (20 m)	Week 3	
	15 December 2014	17 December 2014
 Q4SNP (Sorghum non pre-emergence)	 Correctly classified	 Correctly classified

Pigweed was correctly classified in most of the replicates (Table 6-17). Bellvine results were also similar to pigweed (Table 6-17). Almost all the replicates were successfully classified into soil, sorghum and bellvine. The size and location of the bellvine plants helped accurate identification (Appendix AA).

Table 6-17 Pigweed and bellvine at 10.83 mm spatial resolution

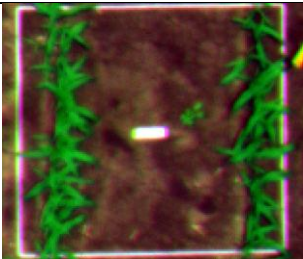
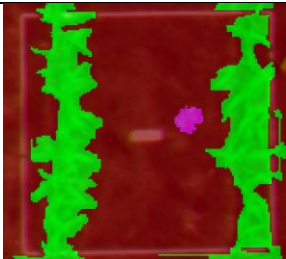
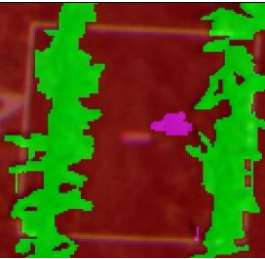
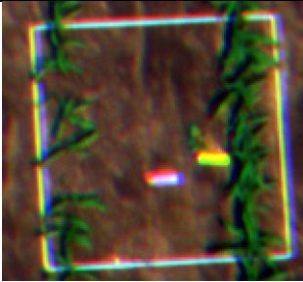
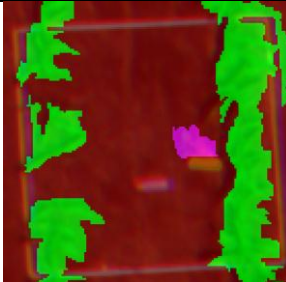
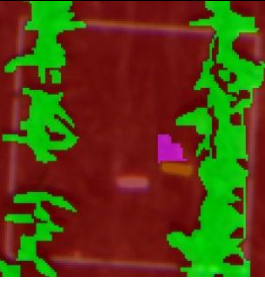
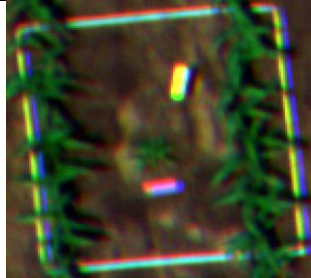
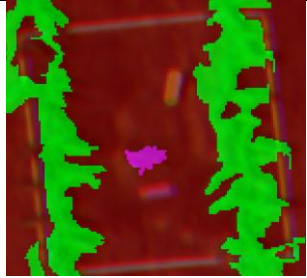
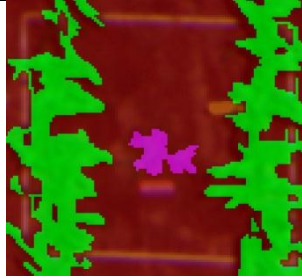
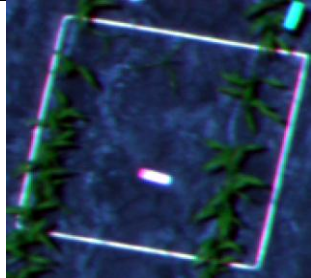
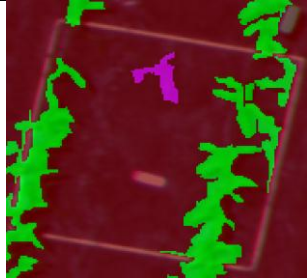
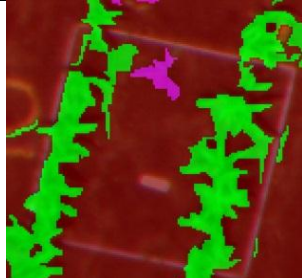
Image (20 m)	Week 3	
	15 December 2014	17 December 2014
 Q1PG	 Correctly classified	 Correctly classified
 Q2B	 Correctly classified	 Correctly classified

Table 6-18 shows the OBIA classification for liverseed grass and sorghum pre-emergence. Most of the liverseed grass was correctly classified except on the 15th December 2014 for Q4LS (Table 6-18 and Appendix BB). Table 6-18 shows the sorghum pre-emergence quadrats were accurately classified. The others quadrats for sorghum pre-emergence are shown in Appendix CC. The type of weeds was nutgrass and this is an indicator that nutgrass was a major weed in the sorghum pre-emergence area.

Table 6-18 Liverseed grass and sorghum pre-emergence at 10.83 mm spatial resolution

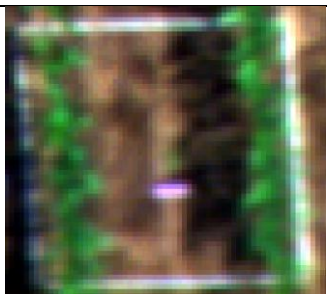
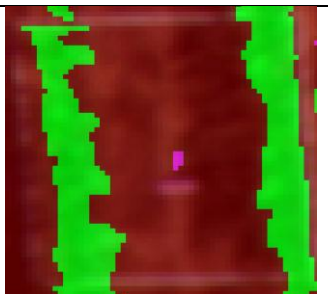
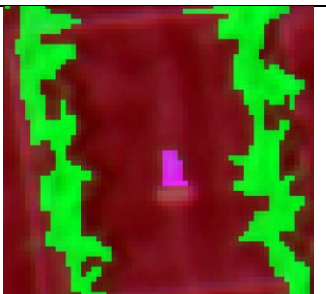


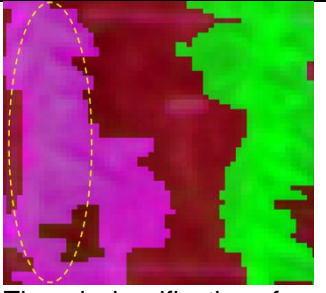
Image (20 m)	Week 3	
	15 December 2014	17 December 2014
 <p>Q2LS</p>	 <p>Correctly classified</p>	 <p>Correctly classified</p>
 <p>Q3SP</p>	 <p>Correctly classified</p>	 <p>Correctly classified</p>

6.4.1.3 OBIA Results for Low Spatial Resolution Imagery (20.31 mm)

This section presents the OBIA results for 20.31 mm resolution imagery. All 24 Quadrats were analysed for week three imagery. Table 6-19 shows the analysis for pigweed. Overall pigweed was correctly classified (Appendix DD).

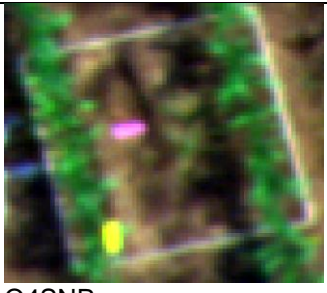
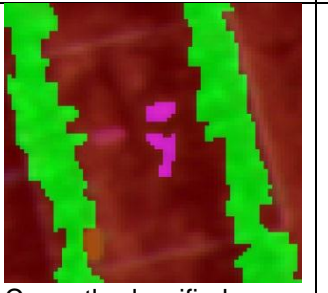
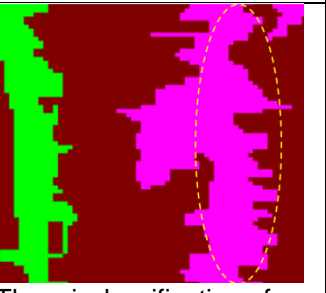
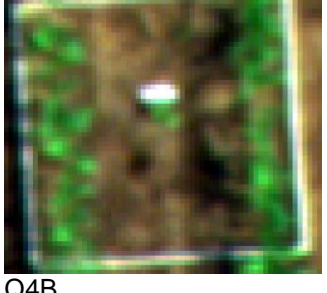
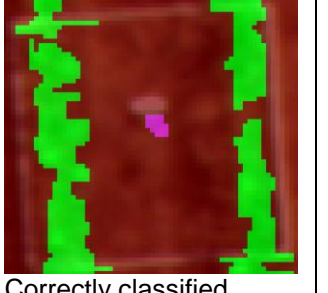
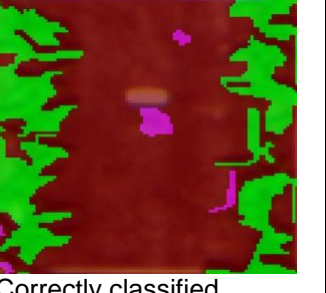
Most of the nutgrass was misclassified with only replicates Q1NG on 17th Dec. 14 showing correct classification (Appendix EE). The classification for Q4NG was misclassified on week three (Table 6-19).

Table 6-19 Pigweed and nutgrass at 20.31 mm spatial resolution

Image (37.5 m)	Week 3	
	15 December 2014	17 December 2014
 Q2PG	 Correctly classified	 Correctly classified
 Q4NG	 The misclassification of weeds (In the circle)	 The misclassification of sorghum (In the circle)

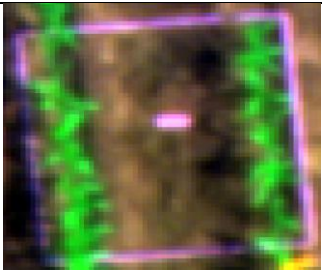
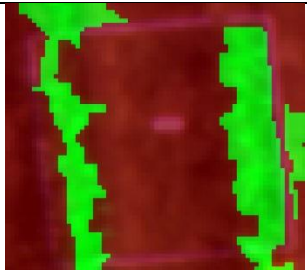
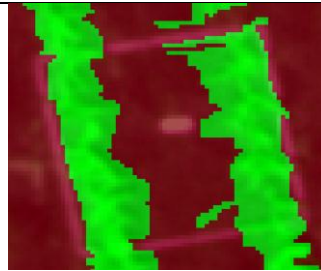
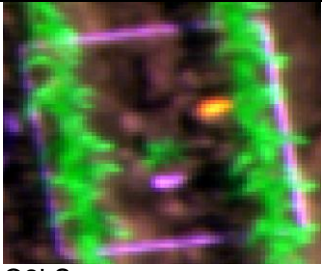
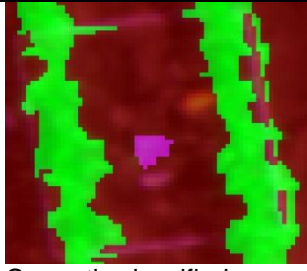
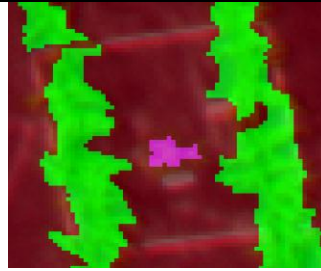
Sorghum non pre-emergence, Q1SNP, was misclassified on week three (Appendix FF). However, Q2SNP, Q3SNP (Appendix FF) and Q4SNP (Table 6-20) were correctly classified on 15th December 14. Bellvine was correctly classified on week three (Table 6-20). However bellvine was misclassified in Q2B and Q3B on 15th Dec. 14 (Appendix GG). Overall, bellvine was correctly identified at 20.31 mm spatial resolution.

Table 6-20 Sorghum non pre-emergence and bellvine at 20.31 mm spatial resolution

Image (37.5 m)	Week 3	
	15 December 2014	17 December 2014
 Q4SNP	 Correctly classified	 The misclassification of sorghum (In the circle)
 Q4B	 Correctly classified	 Correctly classified

Sorghum pre-emergence was successfully classified in Q1SP and Q2SP at week three (Table 6-21 and Appendix HH). However, sorghum was misclassified in Q3SP and Q4SP (Appendix HH). Liverseed grass was correctly classified in Q2LS on week three (Table 6-21). It was misclassified in the other quadrats (Appendix II).

Table 6-21 Sorghum pre-emergence and liverseed grass at 20.31 mm resolution

Image (37.5 m)	Week 3	
	15 December 2014	17 December 2014
 Q1SP	 Correctly classified	 Correctly classified
 Q2LS	 Correctly classified	 Correctly classified

6.4.2 Vegetation Index Analysis Results

Vegetation Index Analysis was performed at different spatial resolutions to investigate the effect of spatial resolution on classification (Table 6-22).

Table 6-22 The three different resolution at week three

Altitude above the ground	Resolution
1.6 m	0.87 mm
20 m	10.83 mm
37.5 m	20.31 mm

6.4.2.1 Vegetation Results for Highest Spatial Resolution Imagery (0.87 mm)

Most of the VIA successfully classified soil and vegetation except for MExR (Table 6-23). There was only a small amount of misclassification. Overall, the VIA were unsuccessful in distinguishing between sorghum and weeds.

6.4.2.2 Vegetation Index Results for Medium Spatial Resolution Imagery (10.83 mm)

VIA successfully classified soil and vegetation for week three (Appendix JJ). The results illustrate the difficulty in identifying weeds in sorghum. The sorghum and weeds were in the same class and this indicates that the spectral differences between sorghum and weeds are not detected by the method.

6.4.2.3 Vegetation Index Results for Lowest Spatial Resolution (20.31 mm)

VIA mostly successfully classified soil and vegetation at this resolution but some indices such as ExR, MTVI1, NRRCI, TVI and RVI misclassified vegetation and soil (Appendix KK). The lowest resolution produced the highest misclassification when using VIs. Most of the quadrats showed a “salt and pepper effect” at this resolution specifically for RVI and TVI indices.

An accuracy assessment was not conducted because the qualitative assessment indicated there was poor classification by all VI tested. A visual examination of the classified image showed that VIA methods using the indices tested were not applicable to weed detection in sorghum.

Table 6-23 VI analysis for 0.87 mm (continued)

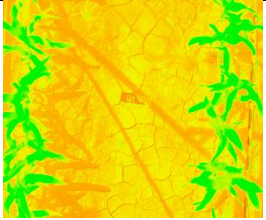
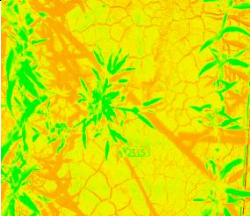
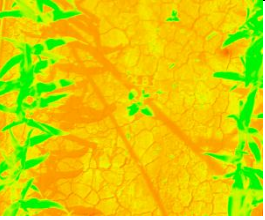
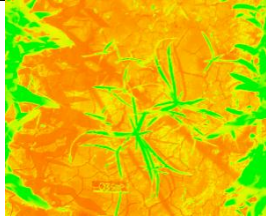
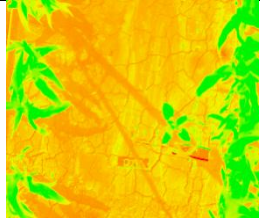
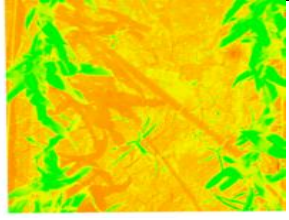
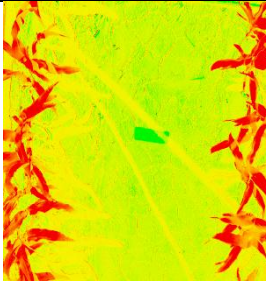
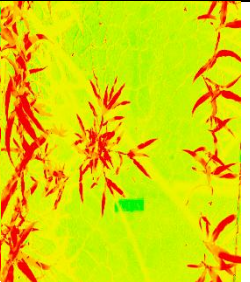

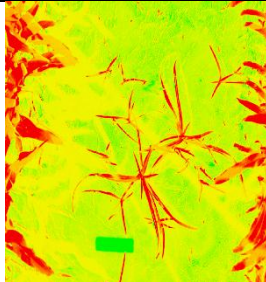
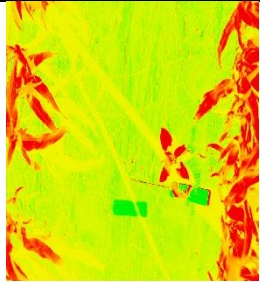
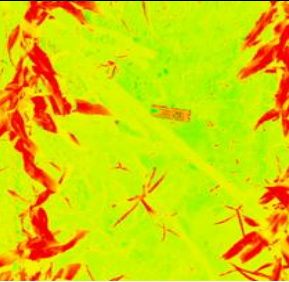
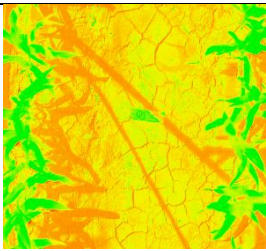
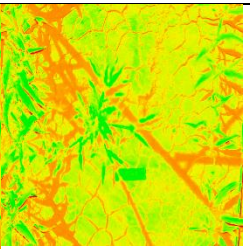
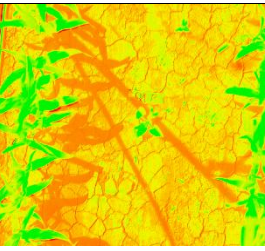
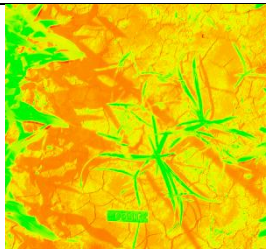
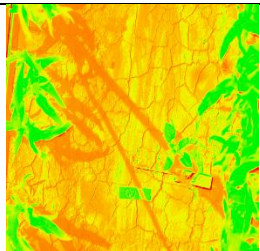
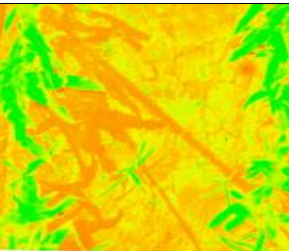
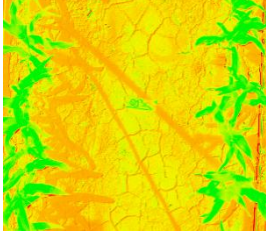
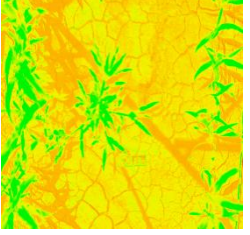
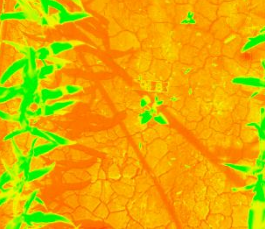
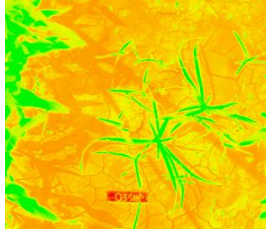
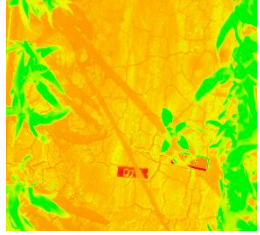
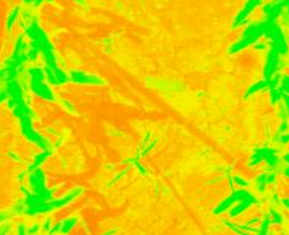
Vegetation Index	Sorghum Pre-emergence (SP)	Liverseed Grass	Bellvine	Sorghum non pre-emergence	Pigweed	Nutgrass
Different Vegetation Index (DVI)						
Excess Red (ExR)						
Modified Excess Red (MExR)						
Modified Triangular Vegetation Index 1 (MTVI1)						

Table 6-23 (continued) VI analysis for 0.87 mm

Vegetation Index	Sorghum Pre-emergence (SP)	Liverseed Grass	Bellvine	Sorghum non pre-emergence	Pigweed	Nutgrass
NIR, Red-edge(720) and Red Combine Index (NRRCI)						
Triangular Veg. Index(TVI)						
Red-edge Veg. Stress Index (RVSI)						
Red Vegetation Index (RVI)						

High Low

6.4.3 Mosaic Analysis Results

Mosaicing was done using Agisoft Photoscan at three different resolutions for imagery captured on week four after planting. The MCA 6 images did not produce high quality mosaic (Figure 6-30). However, the results suggest that this method is acceptable for this research because of the small size of the paddock and the flatness of the topography. According to Turner et al. (2016), the MCA 6 mosaiced imagery was unsuccessful using Agisoft in their study because of the problem in the sensor noise issue and the area was hilly which compounded image registration compared to the Gatton sorghum field which was very flat and allowed easier image to image registration. The CMOS sensors in the MCA 6 have a rolling shutter, which built up each image as a scan from top to bottom rather than a whole-frame snapshot and leads to geometric distortions in each image (Turner et al. 2014). However, Turner et al. (2016) solved the issue by automatically the image mosaic by using their own algorithm, Scale Invariant Feature Transform (SIFT). Figure 6-29 shows the mosaic image at 5.42 mm spatial resolution (10 m elevation image capture). In this very high resolution image, most weeds were correctly classified. This indicates result which is suitable for weed mapping.

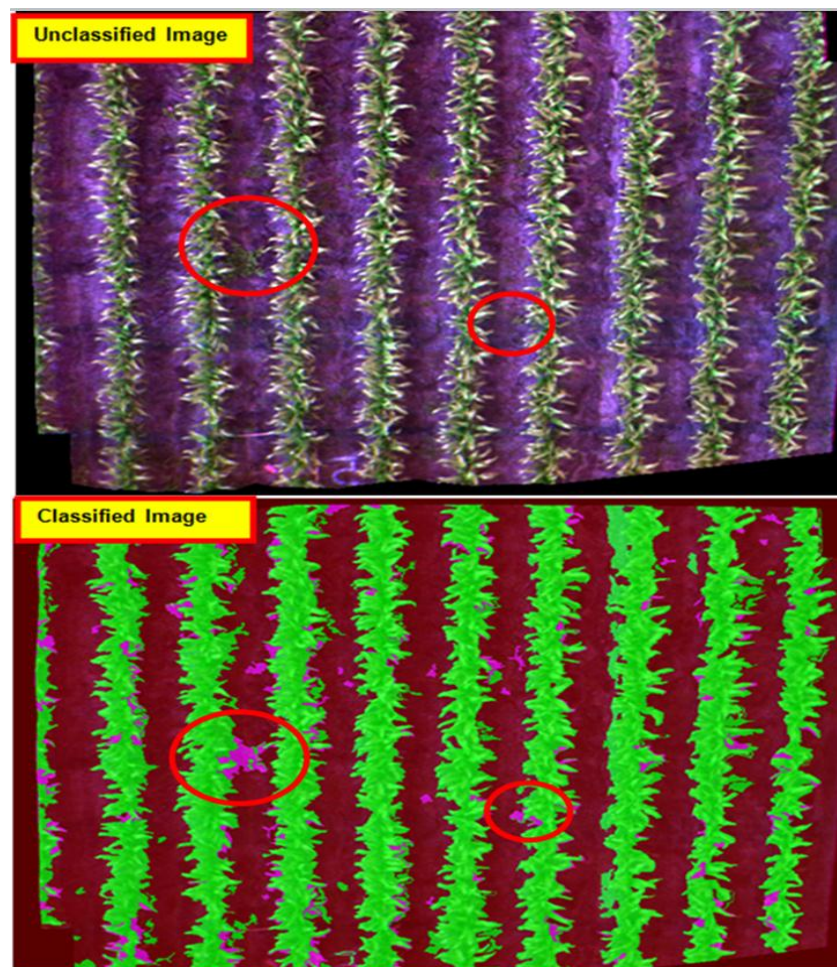


Figure 6-29 Mosaic image at 5.42 mm resolution

The analysis for 10.83 mm resolution (20 m elevation image capture) shows some of the weeds and sorghum were misclassified. The red circles show weeds patches that were classified as sorghum. The patches were of high density and near to the sorghum crop. However, some weeds in the map were correctly classified. This proves that OBIA can detect weeds at 10.83 mm spatial resolution depending on the density of the weeds.

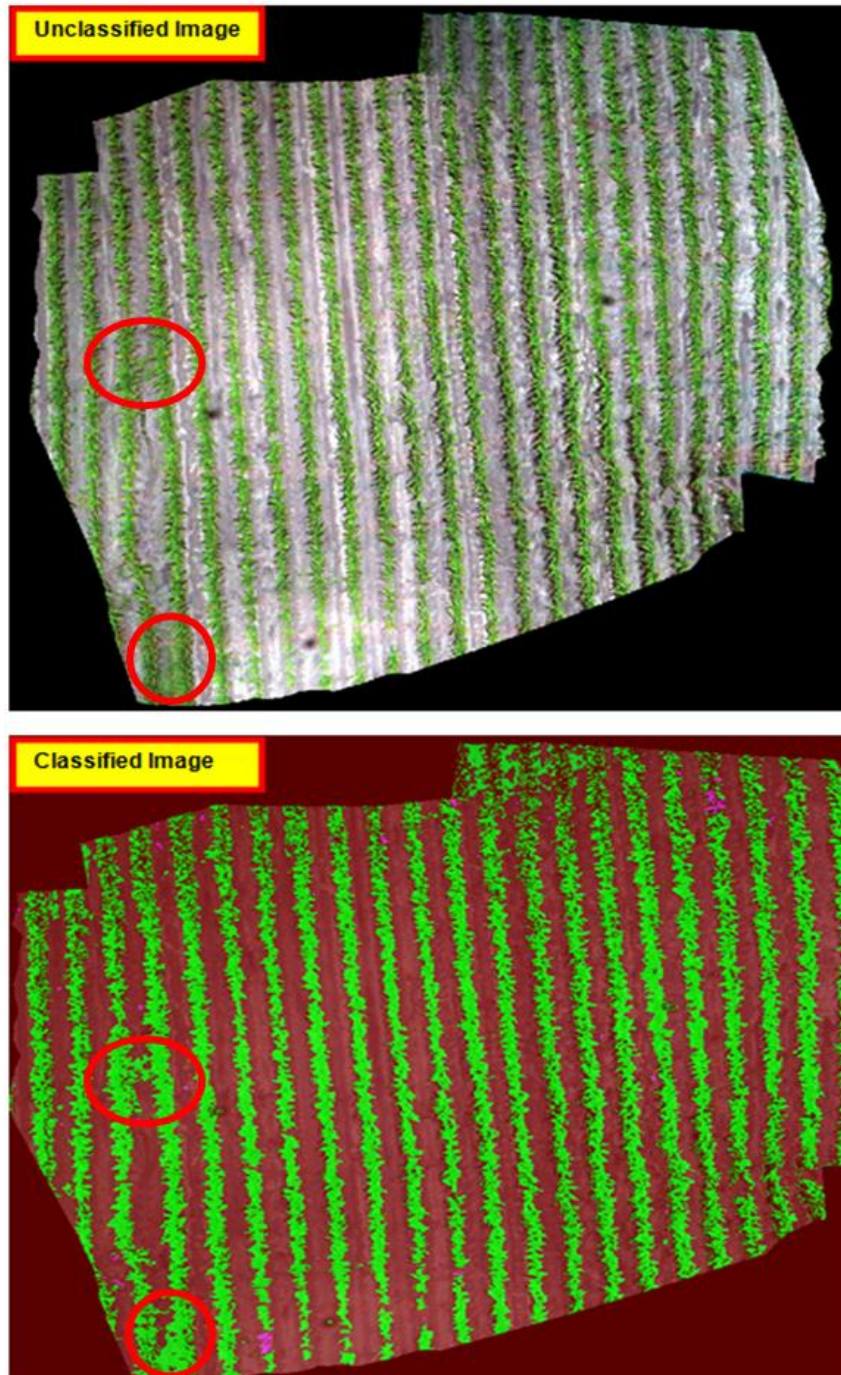


Figure 6-30 Mosaic image at 10.83 mm resolution

Figure 6-31 shows that the majority of weed patches can be detected using OBIA at 20.31 mm resolution imagery (37.5 m elevation image capture). In addition, some of smaller patches were also detected.

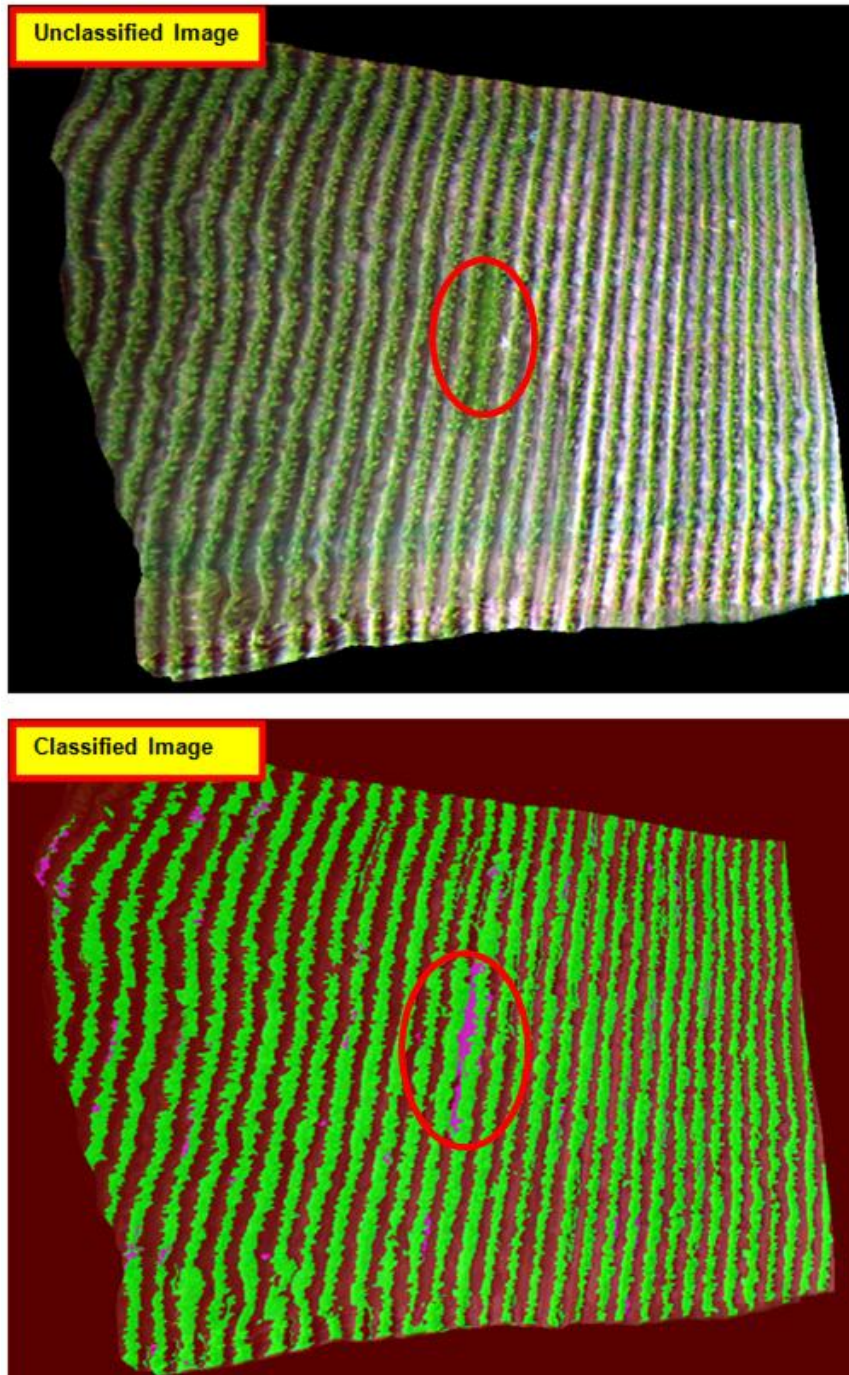


Figure 6-31 Mosaic image at 20.31 mm resolution

6.5 ACCURACY ASSESSMENT

6.5.1 OBIA Analysis Accuracy

6.5.1.1 Confusion Matrix Accuracy Analysis (Spatial Resolution: 0.87 mm)

OBIA accuracy analysis was done using the Confusion matrix technique. Each species was selected from the same quadrat for week three and four after planting (Figure 6-32). Only one quadrat was chosen for each species. The quadrat selected was the most accurately classified quadrat.

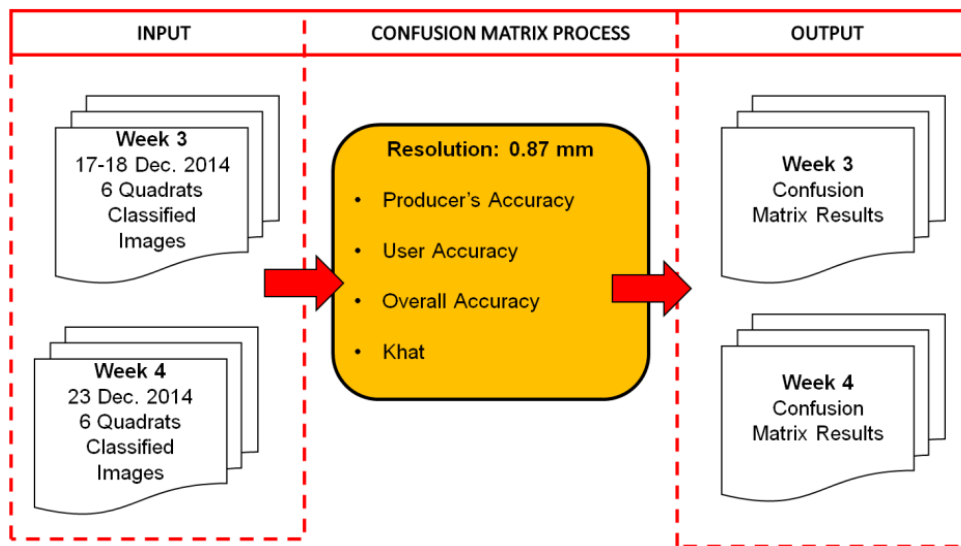


Figure 6-32 Confusion matrix analysis for 17 December 2014 quadrats

The overall Confusion Matrix for 0.87 mm resolution imagery (on week 3, 17th Dec. 2014) is summarized in Table 6-24. Liverseed grass and sorghum non pre-emergence had higher Producer's Accuracies than User Accuracies indicating that these species were overestimated while pigweed, nutgrass and bellvine had higher User Accuracies indicating that they were underestimated. Soil was over estimated (higher Producer's Accuracy) relative to liverseed grass, sorghum non pre-emergence, pigweed and nutgrass and underestimated relative to bellvine. Sorghum was underestimated (lower Producer's Accuracy) relative to liverseed grass, sorghum non pre-emergence and pigweed and was overestimated relative to bellvine. Overall and Khat accuracies were high for all species indicating accurate classification.

Table 6-24 Error Matrix for 0.87 mm resolution (Week three: 17th Dec. 2014)

Species	Confusion Matrix	Weed (%)	Soil (%)	Sorghum (%)
Liverseed grass (LS)	Producer's Accuracy	78	100	87
	User Accuracy	58	99	95
	Overall Accuracy	94		
	Khat	89		
Sorghum non pre-emergence (SNP)	Producer's Accuracy	100	100	37
	User Accuracy	53	92	100
	Overall Accuracy	80		
	Khat	68		
Sorghum Pre-emergence (SP)	Producer's Accuracy	0	100	100
	User Accuracy	0	100	100
	Overall Accuracy	100		
	Khat	100		
Pigweed (PG)	Producer's Accuracy	64	93	80
	User accuracy	78	86	89
	Overall Accuracy	87		
	Khat	74		
Nutgrass (NG)	Producer's Accuracy	95	100	98
	User Accuracy	100	97	98
	Overall Accuracy	98		
	Khat	97		
Bellvine (B)	Producer's Accuracy	78	98	97
	User Accuracy	88	100	90
	Overall Accuracy	96		
	Khat	93		

The overall Confusion Matrix for 0.87 mm resolution imagery (on week 3, 18th Dec. 2014) is summarised in Table 6-25. Liverseed grass, pigweed and nutgrass had higher User Accuracy than Producer's Accuracy indicating that they were underestimated, while sorghum non pre-emergence had higher Producer's Accuracy than User Accuracy indicating that the weeds were overestimated.

Soil had a higher Producer's and User accuracy for all the species. Similar to sorghum, all the sorghum pre-emergence had higher accuracy (> 80%) except for liverseed grass. It shows that liverseed grass had low User Accuracy compared to Producer's Accuracy and indicates overestimating in sorghum class. Overall and Khat accuracies were high (> 80%) for all species except for pigweed and liverseed grass.

Table 6-25 Error Matrix for 0.87 mm resolution (Week three: 18th Dec. 2014)

Species	Confusion Matrix	Weed (%)	Soil (SO) (%)	Sorghum (SG) (%)
Sorghum pre-emergence (SP)	Producer's Accuracy	0	100	100
	User Accuracy	0	100	100
	Overall Accuracy	100		
	Khat	100		
Liverseed grass (LS)	Producer's Accuracy	40	100	45
	User Accuracy	79	99	15
	Overall Accuracy	76		
	Khat	58		
Bellvine (B)	Producer's Accuracy	100	100	100
	User Accuracy	100	100	100
	Overall Accuracy	100		
	Khat	100		
Sorghum non pre-emergence (SNP)	Producer's Accuracy	100	100	97
	User Accuracy	97	100	100
	Overall Accuracy	99		
	Khat	99		
Pigweed (PG)	Producer's Accuracy	64	93	80
	User Accuracy	78	86	89
	Overall Accuracy	87		
	Khat	74		
Nutgrass (NG)	Producer's Accuracy	84	95	96
	User Accuracy	95	97	87
	Overall Accuracy	93		
	Khat	97		

Table 6-26 summarises the Confusion Matrix for all species at 0.87 mm resolution on week four. Liverseed grass, sorghum non pre-emergence and nutgrass had higher Producer's Accuracy than User Accuracy indicating that these species were overestimated while pigweed had a lower Producer's Accuracy indicating that pigweed was underestimated.

Soil had 100 % accuracy for all the species. Sorghum was overestimated relative to pigweed and was underestimated relative to liverseed grass, sorghum non pre-emergence and nutgrass.

Overall accuracies were high for sorghum pre-emergence, bellvine, sorghum non pre-emergence and nutgrass. The Khat accuracy is high for all species except for liverseed grass, sorghum non pre-emergence and nutgrass (Khat < 80%).

Table 6-26 Error Matrix for 0.87 mm resolution (Week four)

Species	Confusion Matrix	Weed (%)	Soil (SO) (%)	Sorghum (SG) (%)
Sorghum pre-emergence (SP)	Producer's Accuracy	0	100	100
	User Accuracy	0	100	100
	Overall Accuracy	100		
	Khat	100		
Liverseed grass (LS)	Producer's Accuracy	100	100	47
	User Accuracy	13	100	100
	Overall Accuracy	67		
	Khat	52		
Bellvine (B)	Producer's Accuracy	100	100	100
	User Accuracy	100	100	100
	Overall Accuracy	100		
	Khat	100		
Sorghum non pre-emergence (SNP)	Producer's Accuracy	94	100	69
	User Accuracy	47	100	97
	Overall Accuracy	84		
	Khat	75		
Pigweed (PG)	Producer's Accuracy	85	100	100
	User Accuracy	100	100	95
	Overall Accuracy	98		
	Khat	97		
Nutgrass (NG)	Producer's Accuracy	100	100	65
	User Accuracy	34	100	100
	Overall Accuracy	83		
	Khat	74		

Figure 6-33 summarises the accuracy results for 0.87 mm image classification. The sorghum pre-emergence plants were always accurately classified. Bellvine plants were the next most accurately classified followed by pigweed and sorghum non pre-emergence.

OVERALL ACCURACY

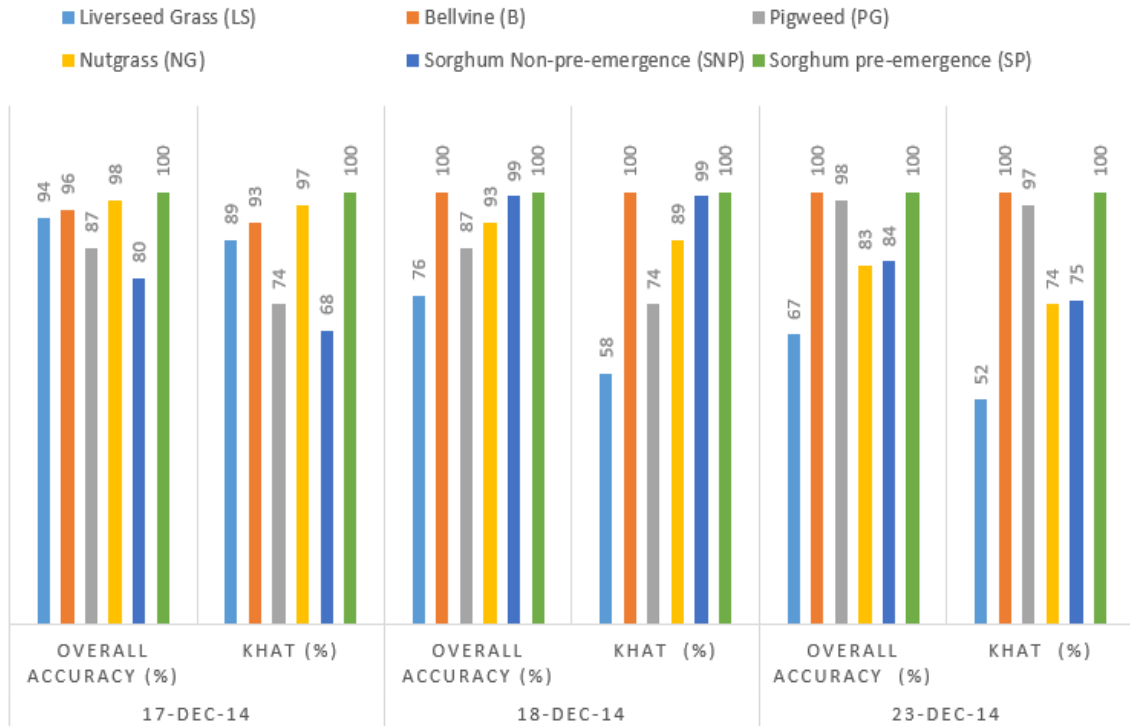


Figure 6-33 Summary of accuracies for Confusion Matrix analysis at 0.87 mm

Table 6-27 shows the Overall and Khat accuracies for 10.83 and 20.31 mm resolution image classification. At 10.83 mm resolution, all the accuracies were high (> 80%) except for nutgrass (Khat: 71%) on 15th Dec. 2014. The 20.31 mm resolution image resolution of nutgrass and sorghum non pre-emergence had a lower accuracy (<70%).

Overall accuracies (OA) had higher percentages for all the species except for nutgrass and sorghum non pre-emergence.

Table 6-27 Summary of Overall and Khat accuracies for 10.83 and 20.31 mm spatial resolution

Spatial Resolution	10.83 mm				20.31 mm			
	15.12.14 (%)		17.12.14 (%)		15.12.14 (%)		17.12.14 (%)	
Species	OA	Khat	OA	Khat	OA	Khat	OA	Khat
Liverseed Grass (LS)	100	100	94	89	88	80	94	89
Bellvine (B)	100	100	100	100	97	95	100	100
Pigweed (PG)	100	100	100	100	100	100	100	100
Nutgrass (NG)	81	71	90	82	73	61	98	97
Sorghum non pre-emergence (SNP)	100	100	95	92	81	69	95	92
Sorghum pre-emergence (SP)	100	100	100	100	100	100	100	100

6.5.1.2 Geometric Accuracy Analysis

The Geometric accuracy analysis was used to validate OBIA classification for sorghum, soil and weeds at 0.87 mm resolution (Figure 6-34). This assessment was only done for 0.87 mm resolution imagery because it was not feasible to digitise lower resolution imagery to create the required high accuracy Reference Map.

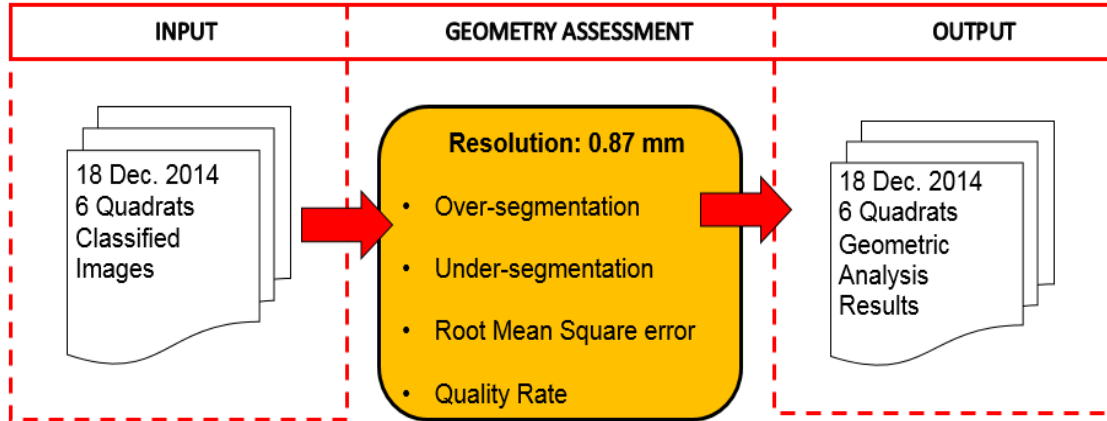


Figure 6-34 Geometric analysis accuracy assessment for 0.87 mm

The Area Fit Index, over-segmentation (Oseg), under-segmentation (Useg) and RMSE values showed promising results. The Geometric accuracy analysis was done on the same quadrat that was used in Confusion Matrix assessment. Table 6-28 shows the AFI results for each quadrat.

Table 6-28 Area Fit Index for the species

Class	Pigweed	Sorghum non pre-emergence	Liverseed grass	Sorghum Pre-emergence	Nutgrass	Bellvine
Sorghum	- 0.01	- 0.12	1.00	- 0.28	- 0.02	0.03
Weeds	0.00	- 2.29	- 2.60	0.00	0.22	0.29
Soil	0.09	0.08	0.08	0.12	0.00	- 0.02

The over-segmentation, under-segmentation, RMSE and Quality rate are shown in Table 6-29 for weeds. Sorghum pre-emergence shows 0.00 for all the matrices. Pigweed shows that most of the analyses were well matched because the values were close to 0.00 (Table 6-29). Most of the species had higher RMSE except for sorghum non pre-emergence and nutgrass. The Quality rate (Qr) shows that sorghum non pre-emergence, bellvine and nutgrass had higher values (Qr near to 1, accurate segmentation).

Table 6-29 Geometric assessment values for 0.87 mm resolution (Weeds)

Geometric: Weeds	Matrices			
Quadrats	Over-segmentation	Under-segmentation	RMSE	Quality Rate (Qr)
Pigweed	0.12	0.12	0.14	0.13
Sorghum non Pre-emergence	0.13	0.74	0.74	0.54
Liverseed grass	0.80	0.94	1.10	0.04
Sorghum Pre-emergence	0.00	0.00	0.00	0.00
Bellvine	0.37	0.12	0.29	0.63
Nutgrass	0.78	0.72	0.75	0.63

Table 6-30 shows the Geometric assessment for sorghum in each quadrat. Oseg, Useg and RMSE values indicate they were accurately segmented for all species except for nutgrass and liverseed grass (Table 6-30). Pigweed, non pre-emergence sorghum and liverseed grass were accurately segmented when they had a 0.00 for Useg.

Table 6-30 Geometric assessment values for 0.87 mm resolution (Sorghum)

Geometric: Sorghum	Matrices			
Quadrats	Over-segmentation	Under-segmentation	RMSE	Quality Rate (Qr)
Pigweed	0.10	0.00	0.07	1.41
Sorghum non pre-emergence	0.09	0.00	0.07	0.81
Liverseed grass	1.00	0.00	0.71	0.00
Sorghum Pre-emergence	0.05	0.26	0.26	0.95
Bellvine	0.38	0.35	0.44	0.66
Nutgrass	0.90	0.10	0.64	0.66

Table 6-31 shows the Geometric assessment for soil in the each quadrat. Overall, the results yielded an accurate match for all the quadrats except for LS. The Useg, Oseg and RMSE values for LS were close to 1 indicating that the segmentation is accurately segmented and of high accuracy respectively. The RMSE for all species were rightly segmented except for LS. According to Belgiu and Dragut (2014), the accuracy is considered high when the Useg value is near to 0.00.

Table 6-31 Geometric assessment values for 0.87 mm resolution (Soil)

Geometric: Soil	Matrices			
Quadrats	Over-segmentation	Under-segmentation	RMSE	Quality Rate (Qr)
Pigweed	0.05	-0.05	0.06	1.05
Sorghum non-pre-emergence	0.09	0.02	0.07	0.98
Liverseed grass	0.86	0.85	1.05	0.23
Sorghum Pre-emergence	0.13	0.01	0.09	0.87
Bellvine	0.12	0.13	0.16	0.92
Nutgrass	0.05	0.04	0.05	0.91

6.5.1.3 Mosaic Analysis Accuracy

Three different resolutions were validated using the Confusion Matrix technique (Table 6-32). At 5.42 mm resolution the accuracies for all the matrices were higher than the 10.83 and 20.31 mm resolution accuracy.

Weeds were underestimated at 10.83 and 20.31 mm resolution when the Producer's accuracies were lower than User accuracies. Soil and sorghum were overestimated (higher Producers accuracy) at 10.83 mm resolution and effectively equally estimated at 10.83 mm resolution. Overall and Khat accuracies were high for all resolution indicating accurate classification except for 20.31 mm (Khat <80%). However, the Khat statistic of 74% for 20.31 mm was still considered good (Lehmann et al. 2015).

Table 6-32 Confusion matrix for mosaic image resolution

Mosaic Resolution	Confusion matrix	Weed (%)	Soil (%)	Sorghum (%)
5.42 mm	Producer's Accuracy	81	100	90
	User Accuracy	81	100	90
	Overall Accuracy	92		
	Khat	97		
10.83 mm	Producer's Accuracy	68	100	94
	User Accuracy	87	98	89
	Overall Accuracy	93		
	Khat	88		
20.31 mm	Producer's Accuracy	56	98	77
	User Accuracy	61	95	77
	Overall Accuracy	84		
	Khat	74		

6.6 DISCUSSION

This chapter has applied the research results from previous chapters to image classification and weed mapping. The information was used to select specific band-pass filters to collect customised multispectral imagery unique to the challenge of detecting weeds in grain sorghum at Gatton, Queensland. The stage of growth of the plants at which the imagery was collected was also considered because previous investigators Lopez-Granados (2010) had reported different spectral characteristics at different stages of growth. It was also important because weeds need to be detected early enough to be controlled to minimise the amount of herbicide needed (Cepl and Kasal 2010) and minimise crop competition (Smith and Blackshaw 2003). Most of the results were depending on the shape and colour of the weeds and sorghum.

Multispectral images captured a series of spectral, spatial and temporal resolutions of the weeds and crop plants. OBIA and VIA procedures were evaluated for discriminating the weeds from the sorghum. The findings, as discussed in the following section, provide the basis for developing a commercial weed mapping program for sorghum.

6.6.1 Spectral Resolution

Selection of the spectral sensor to collect the multispectral imagery is very important in effectively detecting weeds in sorghum. The MCA 6 camera had six sensors each of which could be fitted with custom filters, to collect specific wavelengths of light. Filters for the significant wavelengths were chosen based on Linear Discriminant Analysis (LDA) of the reflectance profiles (Chapter 5). The bands were originally selected based on the weeds amaranth, liverseed grass, mallow weed and nutgrass (2013). However, for this part of the research the imagery was collected in 2014 when the weeds in the sorghum were liverseed grass, nutgrass, pigweed and bellvine.

The central wavelengths of the spectral bands (10 nm wide) collected by the multispectral imagery were 850, 720, 710, 680, 560 and 440 nm. The available six bands were expected to result in very accurate weed mapping. However, the results of image analysis showed that some of these bands were not suitable for the 2014 weed species. This occurred because the spectral bands were selected based on analysis of reflectance in 2013. Amaranth and mallow weed were only available in 2013 while, pigweed and liverseed grass were only available in 2014. Despite this, the spectral bands used in the research successfully detected weeds with high accuracy in many of the images. It was not possible to detect all the weeds in the 2014 crop. For example, liverseed grass (Appendix L), nutgrass (Appendix R), pigweed (Appendix T) and bellvine (U) were misclassified in some of the quadrats. Lopez-Granados (2010) reported that hyperspectral imagery might be useful to detect weeds in crop. Compared to our research, in which we are focusing on only six bands, hyperspectral imagery consists of much narrower bands about 100* bands (*depending on the sensor). It might be more practical to investigate a smaller number of bands (e.g. three) specifically selected for the current weed profile because this might be available in more affordable sensors and allow simpler processing.

6.6.2 Spatial Resolution

Different spatial resolutions were tested to determine which spatial resolution was most suitable for this type of weed mapping using OBIA (first method) and VIA (second method). At 0.87 mm resolution, most of the weeds were accurately identified at week three after planting using

OBIA (first method) (Table 6-25). At 10.83 mm resolution the classification accuracy remained high at > 80% for the Overall and Khat accuracies (except for nutgrass) (Table 6-27). At 20.31 mm resolution the accuracy was still high for most of the species (Overall and Khat accuracies > 80% except for nutgrass and sorghum non pre-emergence) (Table 6-27). Nutgrass and sorghum non pre-emergence were the most difficult weeds to discriminate from sorghum plants with Khat value of 61% and 69% respectively (Table 6-27). According to Lehmann et al. (2015), Kappa statistics in the range of 0.61-0.80 indicate good classification. They are considered comparable to 61- 80% Khat values.

While imagery at 0.87 mm (1.6 m) resolution produced the most accurate classification, it was not practical to fly a UAV with the MCA 6 camera below 10 m elevation (5.42 mm resolution). Mosaiced imagery at 5.42 mm resolution accurately classified weeds (92% and 97% for Overall and Khat accuracies) (Table 6-32). These findings are consistent with the findings of Mestas-Carrascosa et al. (2015), Kamal et al. (2015), and Laliberte et al. (2011) who found that the weed mapping requires very high resolution (large scale) imagery. Moreover, the crop row spacing in this research was 75 cm and the resolution should be higher than 75 cm. This is in agreement with Torres-Sanchez et al. (2014) who, stated that the at least four pixels were needed for the 15 cm crop rows to detect small objects in such images.

The same resolutions were tested using VIA (second method). The results from VIs were misclassified where the sorghum and weeds were in same class because of the “salt and pepper effects” for all the resolutions. This is consistent with (Aziz 2014), who found that a spatial resolution of 30 m was not effective because of the “salt and pepper effect” in the processed imagery when trying to detect the ages of mangroves plantation.

6.6.3 Stage of Growth

Imagery was initially collected each week for four weeks after planting. However, it became more practical to focus the collection and analysis on week three and week four imagery. The results showed that weeds and sorghum were most accurately classified at week three after planting. This is because the weeds were still small, were not very dense and remained separate from the sorghum plants. The weeds started to become intermixed with sorghum plants at week four and this resulted in decreased classification accuracy. This illustrates the importance of the time of data collection in terms of stage of growth of the target species when planning data collection for weed mapping. Weed detection early in their growth is consistent with weed control strategies designed to minimize competition with the sorghum plants (Pena et al. 2013). In later stages of growth, weeds were found to be more difficult to detect. This was also found by Lopez-Granados (2010).

Nutgrass was successfully classified at week three after planting. The size of the leaves was small and the plants were not very dense at this stage. By week four nutgrass leaves were overlapped by sorghum leaves and it was misclassified most of the time because of their similar shape. The colours of sorghum and weeds were similar and in this case the colour factors did not produce a significant impact in the identification process.

Liverseed grass showed the same pattern of results. At week three after planting it was more successfully classified than week four when the leaves were mixed with the sorghum leaves. Also, this poor classification at week four was due to the shape of the liverseed grass leaves being similar to sorghum leaves.

Broad leaf weeds (Pigweed and Bellvine) were more successfully classified at week three than the narrow leaf weeds. The shape of the weed's leaves affects their classification (Blaschke et al. 2014). Lopez-Granados (2010) found that mapping of grass weed seedlings in monocotyledonous crops and seedlings of broad-leaf weeds in dicotyledonous crops was more challenging in later growth stages. According to Thorp and Tian (2004), monocotyledonous crops have similar spectral reflectances at the early growth of stage. At the early stage of growth the size of weeds were small. The spectral reflectances of the weeds were affected by the colour of the soil due to recent weather conditions. Therefore, week three is the best time to collect the hyperspectral reflectance for image processing.

Background reflectance of the imagery also influences the classification between weeds and sorghum (Alsharrah et al. 2015). For example, soil background reflectance can be used by OBIA to identify the shape of weed leaves more accurately compared with a sorghum background. For this reason the background was extracted as a black shade (low digital number) in the image analysis. This is consistent with Steward and Tian (1999) who normalised RGB data into hue, saturation and intensity (HSI) image space to segment the plant images against background regions. The HSI transformation is a standard technique for numerically describing colour in the image domain, using spherical coordinates roughly analogous to the conventional perceptual attributes of hue, saturation and lightness (Gillespie et al. 1986). Their research was on images collected under artificial light in comparison to this research where the images were collected under field illumination conditions.

6.6.4 Image Processing

OBIA and VIA approaches were tested for classifying weeds in sorghum. Rule set construction in OBIA is flexible and can be modified to get optimal results. For example, a given rule set was found to produce different results at different stages of growth and different spatial resolutions. Kamal et al. (2015) found that rule sets needed to be modified to accommodate the

stage of plant growth and the image environment. In this research, the same basic rule set was used throughout, but the scale, shape and compactness settings were modified based on the spatial resolution of the imagery (Table 6-7). The second stage segmentation settings depended on how much segmentation was achieved by the first stage segmentation settings and how much more the image needed to be segmented.

Multiresolution segmentation has been used in this research and by many other researchers (Phinn et al. 2012; Pena et al. 2013; Aziz 2014; Roelfsema et al. 2014; Kamal et al. 2015). It generates objects by merging several pixels together based on homogeneity criteria (Lehmann et al. 2015). However, other algorithm techniques can be used to investigate the effectiveness of the segmentation (Alsharrah et al. 2015).

Since the classification was focussed on identifying weeds in sorghum, the soil class was only of minor interest. This is because the soil class was in the same group as “shadow objects”. For future work, the shadow objects might be able to be separated into a separate class to get more accurate results (Slaughter 2014). It also highlights the desirability of collecting imagery when there are fewest shadows (noon).

Image analysis could be enhanced by automatic processing in OBIA. According to Arroyo et al. (2010) GEOBIA automatic classification has the potential for processing large areas and might be useful for automatically processing multiple images. Pena et al. (2013) suggested an alternative of detecting crop rows as an initial step before identifying weeds in the crop. This was considered possible because the crop rows are at fixed locations and the weeds occurred randomly in the crop.

How objects are sampled is important to get unbiased and accurate results (Johansen et al. 2011). Since this research focused only on three main classes of objects, Khat statistics were considered acceptable. According to Foody (2002) kappa coefficients of agreement, are frequently derived to express classification accuracy and are more accurate compared to basic percentages.

Segmentation and overlap are well matched when the values are close to 0.00 (Levine and Nazif 1985; Lucieer and Stein 2002; Clinton et al. 2010) and when the Quality rate value is close to 1 (Winter 2000). Sorghum pre-emergence has a 0.00 value for segmentation and Overlap in all matrices. This indicates a perfect match and was expected since there were no weeds found in the sorghum pre-emergence quadrat compared with others quadrats.

VIA was explored for weed detection using formulae from the literature applied to the wavelengths of the custom bands in our images. The results cannot be directly compared with the comparable VI literature results because of the different band wavelengths. The results showed that no VIA that were tested were effective at detecting weeds in sorghum at 0.87, 10.83 and 20.31 mm spatial resolution. All the spatial resolution imagery showed that weeds cannot be detected using the

VIA. Quantitative accuracy assessment on the VIA results was not done because a qualitative assessment showed that these methods did not detect weeds separate from sorghum.

All six spectral bands were used in this analysis. It might be useful to choose fewer bands or combination of bands for future analysis. For example, Pena-Barragan et al. (2012a) also used six bands imagery in segmentation analysis for weed detection. However, they narrowed these down to calculate the NDVI bands to discriminate between vegetation and soil.

6.7 CONCLUSIONS

The spectral, physical and contextual characteristics of the weeds and sorghum affect the development and efficiency of the rule sets in the segmentation and classification procedures. Small modifications to the rule sets were needed to accurately identify weeds at different stages of growth. The accuracy of mapping increased with increased spatial resolution and optimal stage of growth.

This research has demonstrated the use of multispectral imagery at high spatial resolutions for weed detection in sorghum. The imagery that was most useful for mapping weeds was collected at the early stages of growth (week three after planting) and OBIA image analysis was the most successful analytic approach. Six different spectral bands (850, 720, 710, 680, 560 and 440 nm) were collected by the imagery. The results showed that weeds can be detected accurately in images at high spatial resolutions. Combinations of fewer bands could be tested in future experiments. There may also be a trade-off between the numbers of bands and the spatial resolution of the imagery.

Very high spatial resolution imagery (0.87 mm) was used as the basis to develop the analytic procedure to detect weeds in images of individual quadrats. It is not practical to fly UAVs at 1.6 m elevation commercially. The results from flying at 10 m (5.42 mm resolution), 20 m (10.83 mm resolution) and 37.5 m (20.31 mm resolution) show that weeds can be more accurately discriminated at 5.42 mm resolution.

There are implications for band alignment that have to be overcome when using a MCA 6 camera at these object distances. Using fewer bands at this object distance would make band alignment easier. However, this could be overcome by optimisation of sensor focal length and spatial resolution in a commercial application.

At week three after planting, the size of the weeds is neither too small nor too large and they are still individually identifiable compared to week four after planting. During week four after planting, the weeds are larger and not separately identifiable from the sorghum plants especially for liverseed grass and nutgrass. It appears that the similarity of the shape of their leaves to sorghum leaves makes it more difficult to detect and classify them correctly.

OBIA was more feasible and effective than VIs for detecting weeds in sorghum. The conceptual hierarchical model of multi-scale weed species detection was used successfully to simplify the OBIA rule sets for weed mapping. Weeds were detected accurately (92% for Overall Accuracy) in 5.42 mm (10 m elevation) resolution mosaiced imagery. On the other hand, OBIA was also able to detect weeds in sorghum at a spatial resolution of 20.31 mm (30 m elevation) with an Overall Accuracy of 84%. The same approach was used by Pena-Barragan et al. (2012a) who used 2 cm resolution imagery to detect weeds in maize. They obtained 90% accuracy for weed detection using a combination of NDVI and OBIA.

VIA differentiated soil and vegetation but did not distinguish weeds from sorghum at 0.87 mm spatial resolutions. An algorithm combining multiple VIs might be developed to classify weeds from sorghum based on the differences in their shape and spectral signatures.

The contribution of this research has been to confirm the importance of optimum spectral and spatial resolution and stage of growth for image capture for weed detection in sorghum. An OBIA image processing method successfully detected weeds in the sorghum crop. The findings are important for overcoming the difficulties in weed detection mapping in sorghum. The results provide guidelines that can be used to produce an accurate weed map. The results are limited to the analysis procedures used on the multispectral imagery collected of the weeds and sorghum at the Gatton field site in 2013 and 2014.

Chapter 7

CONCLUSION AND RECOMMENDATIONS

7.1 INTRODUCTION

This section summarizes the findings on weed detection in sorghum at different temporal, spatial and spectral resolutions using multispectral imagery. Spectral reflectances of the weeds were collected and analysed to identify the differences between weed and sorghum wavelengths (Chapter 4). The most significant six bands (850, 720, 710, 680, 560 and 440 nm) for identifying each species were determined using Linear Discriminant Analysis (LDA) (Chapter 5).

The six significant bands were used in a MCA 6 camera to collect multispectral imagery with an Unmanned Aerial Vehicle (UAV) at different elevations. Object Based Image Analysis (OBIA) and Vegetation Index Analysis (VIA) were used to discriminate weeds from the crop plants. OBIA successfully discriminated weeds in sorghum with a high accuracy (> 80%) while VIA did not discriminate between weeds and sorghum. This research provides procedures for discriminating weeds in sorghum and developing a sorghum crop weed map.

7.2 MAIN FINDINGS AND OUTCOMES

The research outcomes and main findings are organized and presented in this section according to the sequence of research objectives discussed in this introduction. The first research objective involved the investigation of the relationship between moisture content and the spectral reflectance of each species of weed analysed in the study. The second research objective analysed and identified the significant bands of the spectral reflectance of weed to be used in the image processing stage. The third research objective analysed the multispectral imagery derived from the selected significant bands identified in the second research objective for weed delineation and differentiating weeds from sorghum. The final research objective, which relied on the findings of the previous three research objectives, was focused on formulating guidelines for the effective production of weed map a based on spectral reflectance, multispectral imagery and image processing analysis.

7.2.1 Weed and crop spectral discrimination (Objective one)

The research explored the differences in hyperspectral reflectance data as a basis to identify the differences between weeds and sorghum (Chapter 4). The relationship of moisture content (MC) on reflectance was tested and found not to affect reflectance from weeds and sorghum in the wavelengths of interest in this research.

The reflectance data were binned and plotted for each species to visualise their spectral profile. The spectral differences between weeds and sorghum can be identified from the spectral profile between each species. The spectral profile changed with the stage of growth. It showed that the green, red-edge and NIR regions were the areas of most difference between the weeds and the weeds and sorghum.

The binned and First Derivative (FD) spectra were used to illustrate the differences. The FD data showed the differences in the spectral profiles clearer than the raw reflectance (binned) data. This allows the identification of the bands that are most likely to be significant for species discrimination.

7.2.2 Multispectral band selected for weed and crop discrimination (Objective two)

Weed detection is essential to control weeds at the early stages of growth to avoid competition between weeds and crop for nutrients, light and moisture. Stepwise Linear Discriminant Analysis (SLDA) and Linear Discriminant Analysis (LDA) were applied to reflectance profiles from eight species of weeds collected over three years (2012-2014). LDA identified the six most significant bands (850, 720, 710, 680, 560 and 440 nm) for discriminating weeds from sorghum. Specific bands were identified to discriminate amaranth, nutgrass, liverseed grass and mallow weed. The results also provide a better understanding of how the stages of growth (shape and size of the plants) affect their classification. Classification accuracy increased progressively from week one to week four. The results indicate that four weeks after planting is the best time to collect hyperspectral reflectance for discriminating weeds and sorghum. This may vary depending on the weed profile in the sorghum crop. However, for the image detection using MCA6 showed that week three was the best time to identify weeds and sorghum.

The significant bands can be used to select band pass filters to detect the weeds. Six filters were used for the MCA 6 camera based on the results of the LDA analysis (Chapter 5).

7.2.3 Image processing procedure for weed and crop separation (Objective three)

This research provides spectral and spatial resolution guidelines to detect weeds in sorghum. The MCA 6 camera collected images of quadrats (four replicates for each) at each stage of growth (weeks one to four after planting) at four spatial resolutions. Four weeds were identified from the multispectral imagery, namely nutgrass, bellvine, liverseed grass and pigweed. These species were most successfully identified at week three after planting. Weed detection at an early stage allows early control and prevents competitions with the crop (Cepl 2010).

The multispectral imagery was analysed using OBIA and VIA procedures. Imagery collected using band pass filters selected in section 7.2.2 was processed to classify weeds in sorghum. The OBIA method successfully detected weeds in the imagery with higher accuracy than the VIA method. OBIA segmentation was used to segment the imagery and to classify it into the specific feature objects. The classification accuracy shows that higher spatial resolution yielded a higher accuracy. The highest accuracy in this research was achieved by collecting 0.87 mm resolution imagery as explained in Chapter 3. This approach was time consuming and is not practical with present technology in a farm situation. Thus, by using a UAV (fitted with the MCA 6 camera) the imagery can be collected in a more efficient way. Accuracy testing showed that the 2 cm resolution imagery (30 m elevation) produced the best practical accuracy for the weed mapping (> 80%) for most of the species. At this distance the band images have to be manually aligned to be in focus. Tetracam (2015) recommend using the MCA 6 camera 100m or more from the object for all the lenses to be in automatic focus resulting in self-aligned band images

Eight VIs were investigated (Chapter 6) for detecting weeds in the sorghum. The results show that VIA is not suitable for this imagery due the lack of discrimination between weeds and sorghum.

7.2.4 Weed mapping in sorghum (Objective four).

Selecting the most appropriate spatial and spectral resolution in weed detection in sorghum is essential to produce a quality weed map. The results of this research provide a guideline on producing a weed map using multispectral imagery in sorghum.

OBIA image processing can be used to produce a weed map. The segmentation settings in the OBIA rule sets influence classification of the imagery.

OBIA classification of mosaiced imagery at three different spatial resolutions produced positive results. The results showed a small error in the mosaic imagery using Agisoft Photoscan software. The accuracy of classification of the mosaiced image was considered high for Overall and

Khat accuracies (> 70%). However, the accuracy could be improved by designing an more efficient experimental design for the mosaic map in future research. This study recommends a side-lap and forward-lap setting at 50% and 80% respectively to get a good mosaic (Whiteside, 2016). The control points for the mosaic map are also important. According to Turner et al. (2016), at least 10 control points are required for accurate mosaic mapping.

7.3 LIMITATIONS AND FUTURE RESEARCH

This research is limited to the selected images, image processing techniques and location of the field crop. Further research is necessary to extend the use of different types of images (e.g: hyperspectral) and image processing procedures. The possibility of utilising a selected smaller number of bands (eg. three bands) in the OBIA classification could also be investigated. To ensure the OBIA Rule Sets can be used in other applications, the conceptual hierarchical model might be investigated for sorghum at different locations and for other crops.

The main limitations of this research and recommendations for future research are:

- Adjusted rule sets

The hierarchy of the rule sets in OBIA depends on the objective of the mapping. The rule sets were used to segment and class the feature objects to produce a map. Thus, the same rule sets can be used for different datasets. However, in this research we found that to classify the weeds species accurately, modifications of the rule sets were necessary. Application of the rule sets could be improved by automatic processing. Due to limited time and expertise, this research only focused on manual techniques.

- Investigation of different datasets

The weed map was derived based on the multispectral imagery which contains six different spectral bands. The bands were chosen based on identification of the significant spectra for the weeds and sorghum. However, different data sets could be used to investigate the classification of weeds in sorghum. For example, the Agriculture Digital Camera (ADC) from Tetracam provides three bands in its images. This camera could be fitted with the three most significant bands for detecting weeds in sorghum and tested.

- Limited time and power supply to collect the imagery

The reflectance spectra and multispectral imagery collected depend on good experimental field conditions. It is necessary to consider i) weather and stage of growth of the plants, ii) weather and spectral reflectance and iii) weather and imagery (both static and UAV).

- Future research can integrate this analysis with Leaf Area Index (LAI) analysis and build a digital spectral library for the spectral collections.
- Further investigation of other image processing techniques may be useful for detecting weeds in sorghum. For example, a combination between OBIA and VIA might be useful to improve the accuracy of classification. In addition, fewer bands might be investigated to test the classification accuracy between weeds and sorghum (e.g. three bands).

7.4 CONTRIBUTION TO KNOWLEDGE

The methodology and procedures presented in this research provide a basis for weed mapping in sorghum using multispectral imagery. This research successfully found the significant spectral bands for detecting weeds and these can be fitted to any camera with variable filters or used for a custom made camera. These results provide a guideline for choosing appropriate band pass filters for the image collection and weed mapping in sorghum. It provides guidelines on selecting suitable spatial and temporal resolutions. Steps for use of object-based image analysis are also provided.

In summary, the contributions of this research are:

- Identifying the significant bands for detecting weeds in sorghum.
- Identifying the band pass filters for the MCA 6 camera for image collection for weed mapping in sorghum.
- Exploring the effects of moisture content of weeds on their reflectance spectra.
- Identifying optimal spatial and spectral resolutions for accurate weed mapping in sorghum.
- Discovering the most suitable stages of growth to detect weeds in sorghum.
- Demonstrating the effectiveness of a conceptual hierarchical model for OBIA.
- Developing object-based rule sets for weed mapping.
- Showing different cost effective ways for error assessment by using the fishnet function in ArcGIS.

References

- Aasen, H., Burkart, A., Bolten, A. and Bareth, G. (2015). Generating 3d Hyperspectral Information with Lightweight UAV Snapshot Cameras for Vegetation Monitoring: From Camera Calibration to Quality Assurance. *ISPRS Journal of Photogrammetry and Remote Sensing*, 108:245-259.
- Adam, E. and Mutanga, O. (2009). Spectral Discrimination of Papyrus Vegetation (*Cyperus Papyrus L.*) in Swamp Wetlands Using Field Spectrometry. *Journal of Photogrammetry and Remote Sensing*, 64(6):612-620.
- Agrawal, K.N., Singh, K., Bora, G.C. and Lin, D. (2012). Weed Recognition Using Image-Processing Technique Based on Leaf Parameters . *Journal of Agricultural Science and Technology*, 2:899-908.
- Agisoft PhotoScan (2013). User Manual Professional Edition, Version 1.0.0. Retrieved 15.10.2015, 2015, http://downloads.agisoft.ru/pdf/photoscan-pro_1_0_0_en.pdf
- Aitkenhead, M., Dalgetty, I., Mullins, C., McDonald, A. and Strachan, N. (2003). Weed and Crop Discrimination Using Image Analysis and Artificial Intelligence Methods. *Computers and Electronics in Agriculture*, 39(3):157-171.
- Almeida, T. and Filho, D.S. (2004). Principal Component Analysis Applied to Feature-Oriented Band Ratios of Hyperspectral Data: A Tool for Vegetation Studies. *International Journal of Remote Sensing*, 25(22):5005-5023.
- Amelinckx, S. (2010). Spatial and Spectral Separability of Grasslands in the inner Turku Archipelago using Landsat Thematic Mapper Satellite Imagery, Master, Department of Geography, University of Turku, Finland.
- An, N., Goldsby, A.L., Price, K.P. and Bremer, D.J. (2015). Using Hyperspectral Radiometry to Predict the Green Leaf Area Index of Turfgrass. *International Journal of Remote Sensing*, 36(5):1470-1483.
- Andujar, D., Barroso, J., Fernández-Quintanilla, C. and Dorado, J. (2012). Spatial and Temporal Dynamics of *Sorghum Halepense* Patches in Maize Crops. *Weed Research*, 52(5):411-420.
- Andujar, D., Escolà, A., Dorado, J. and Fernández-Quintanilla, C. (2011). Weed Discrimination Using Ultrasonic Sensors. *Weed Research*, 51(6):543-547.
- Andujar, D., Ribeiro, A., Fernandez-Quintanilla, C. and Dorado, J. (2011). Accuracy and Feasibility of Optoelectronic Sensors for Weed Mapping in Wide Row Crops. *Sensors*, 11(3):2304-2318.
- Arafat, S.M., Aboelghar, M.A. and Ahmed, E.F. (2013). Crop Discrimination Using Field Hyper Spectral Remotely Sensed Data. *Advances in Remote Sensing*, 2(2):63-70.
- Armstrong, J.J.Q., Dirks, R.D. and Gibson, K.D. (2007). The Use of Early Season Multispectral Images for Weed Detection in Corn. *Weed Technology*, 21(4):857-862.
- Arroyo, L.A., Johansen, K. and Phinn, S., (eds) (2010). *Mapping Land Cover Types from Very High Spatial Resolution Imagery: Automatic Application of an Object Based Classification Scheme*, Proceedings of the GEOBIA 2010: Geographic Object-Based Image Analysis, Ghent, Belgium, 29 June - 2 July; 2010. International Society for Photogrammetry and Remote Sensing.
- ASDi. (2014, 2014). Handheld 2: Hand-Held VNIR Spectroradiometer. *FieldSpec* Retrieved 26.9.15, 2015, <http://www.asdi.com/products/fieldspec-spectroradiometres/handheld-2-portable-spectroradiometer>
- Australian Bureau Statistics. (2012, 24.05.2012). Agriculture Production. *Year Book Australia* Retrieved 28.09.2015, 2015, <http://www.abs.gov.au/ausstats/abs@.nsf/Lookup/by%20Subject/1301.0~2012~Main%20Features~Agricultural%20production~260>.

- Aziz, A.A. (2014). Integrating a Redd+ Project into the Management of a Production Mangrove Forest in Matang Forest Reserve, Malaysia, Ph.D, School of Geography, Planning and Environmental Management, The University of Queensland, Australia.
- Bakker, T., Wouters, H., van Asselt, K., Bontsema, J., Tang, L., Müller, J. and van Straten, G. (2008). A Vision Based Row Detection System for Sugar Beet. *Computers and Electronics in Agriculture*, 60(1):87-95.
- Banskota, A., Wynne, R.H. and Kayastha, N. (2011). Improving within-Genus Tree Species Discrimination Using the Discrete Wavelet Transform Applied to Airborne Hyperspectral Data. *International Journal of Remote Sensing*, 32(13):3551-3563.
- Batte, M.T. and Ehsani, M.R. (2006). The Economics of Precision Guidance with Auto-Boom Control for Farmer-Owned Agricultural Sprayers. *Computers and Electronics in Agriculture*, 53(1):28-44.
- Belasque Jr, J., Gasparoto, M. and Marcassa, L. (2008). Detection of Mechanical and Disease Stresses in Citrus Plants by Fluorescence Spectroscopy. *Applied Optics*, 47(11):1922-1926.
- Belgiu, M. and Dragut, L. (2014). Comparing Supervised and Unsupervised Multiresolution Segmentation Approaches for Extracting Buildings from Very High Resolution Imagery. *Journal of Photogrammetry and Remote Sensing*, 96:67-75.
- Berge, T.W., Goldberg, S., Kaspersen, K. and Netland, J. (2012). Towards Machine Vision Based Site-Specific Weed Management in Cereals. *Computers and Electronics in Agriculture*, 81:79-86.
- Berni, J., Zarco-Tejada, P., Suárez, L., González-Dugo, V. and Fereres, E. (2009a). Remote Sensing of Vegetation from UAV Platforms Using Lightweight Multispectral and Thermal Imaging Sensors. *International Architecture Photogrammetry Remote Sensing Spatial Information Science. Spatial Information. Sci*, 38:6.
- Berni, J., Zarco-Tejada, P.J., Suarez, L. and Fereres, E. (2009b). Thermal and Narrowband Multispectral Remote Sensing for Vegetation Monitoring from an Unmanned Aerial Vehicle. *Geoscience and Remote Sensing*, 47(3):722-738.
- Bill, R., Nash, E. and Grenzdörffer, G. (2012). Geoinformatic in Agriculture. In: Kresse, W. and Danko, D.M. (eds), *Springer Handbook of Geographic Information*. Springer, Dordrecht, Netherlands, 795-819.
- Biller, R.H. (1998). Reduced Input of Herbicides by Use of Optoelectronic Sensors. *Journal of Agricultural Engineering Research*, 71(4):357-362.
- Birch, C., Cooper, I., Gill, G., Adkins, S. and Gupta, M. (2011). Weed Management in Rainfed Agricultural Systems. In: Tow, P., Cooper, I., Partridge, I. and Birch, C. (eds), *Rainfed Farming Systems*. Springer, Dordrecht, Netherlands, 215-232.
- Blackburn, G.A. (2007). Hyperspectral Remote Sensing of Plant Pigments. *Journal of Experimental Botany*, 58(4):855-867.
- Blasco, J., Aleixos, N., Gómez, J. and Moltó, E. (2007). Citrus Sorting by Identification of the Most Common Defects Using Multispectral Computer Vision. *Journal of Food Engineering*, 83(3):384-393.
- Blaschke, T. (2010). Object Based Image Analysis for Remote Sensing. *ISPRS journal of photogrammetry and remote sensing*, 65(1):2-16.
- Borra-Serrano, I., Peña, J.M., Torres-Sánchez, J., Mesas-Carrascosa, F.J. and López-Granados, F. (2015). Spatial Quality Evaluation of Resampled Unmanned Aerial Vehicle-Imagery for Weed Mapping. *Sensors*, 15(8):19688-19708.
- Borregaard, T., Nielsen, H., Nørgaard, L. and Have, H. (2000). Crop-Weed Discrimination by Line Imaging Spectroscopy. *Journal of Agricultural Engineering Research*, 75(4):389-400.
- Broge, N.H. and Leblanc, E. (2001). Comparing Prediction Power and Stability of Broadband and Hyperspectral Vegetation Indices for Estimation of Green Leaf Area Index and Canopy Chlorophyll Density. *Remote sensing of environment*, 76(2):156-172.

- Bueren, S., Burkart, A., Hueni, A., Rascher, U., Tuohy, M. and Yule, I. (2015). Deploying Four Optical Unmanned Aerial Vehicle-Based Sensors over Grassland: Challenges and Limitations. *Biogeosciences*, 12(1):163-175.
- Bullen, K. (2002). Grain Sorghum. *Crop Management Notes, Darling Downs and Moreton*:10-29.
- Calderon, R., Navas-Cortés, J.A., Lucena, C. and Zarco-Tejada, P.J. (2013). High-Resolution Airborne Hyperspectral and Thermal Imagery for Early Detection of *Verticillium* Wilt of Olive Using Fluorescence, Temperature and Narrow-Band Spectral Indices. *Remote Sensing of Environment*, 139:231-245.
- Calderón, R., Navas-Cortés, J.A. and Zarco-Tejada, P.J. (2015). Early Detection and Quantification of *Verticillium* Wilt in Olive Using Hyperspectral and Thermal Imagery over Large Areas. *Remote Sensing*, 7(5):5584-5610.
- Calha, I., Sousa, E. and González-Andújar, J. (2014). Infestation Maps and Spatial Stability of Main Weed Species in Maize Culture. *Planta Daninha*, 32(2):275-282.
- Carter, G.A. (1993). Responses of Leaf Spectral Reflectance to Plant Stress. *American Journal of Botany*:239-243.
- Carter, G.A. and Knapp, A.K. (2001). Leaf Optical Properties in Higher Plants: Linking Spectral Characteristics to Stress and Chlorophyll Concentration. *American Journal of Botany*, 88(4):677-684.
- Carvalho, S., Schlerf, M., van der Putten, W.H. and Skidmore, A.K. (2013). Hyperspectral Reflectance of Leaves and Flowers of an Outbreak Species Discriminates Season and Successional Stage of Vegetation. *International Journal of Applied Earth Observation and Geoinformation*, 24(0):32-41.
- Castillejo-Gonzalez, I.L., Peña-Barragán, J.M., Jurado-Expósito, M., Mesas-Carrascosa, F.J. and López-Granados, F. (2014). Evaluation of Pixel and Object-Based Approaches for Mapping Wild Oat (*Avena Sterilis*) Weed Patches in Wheat Fields Using Quickbird Imagery for Site-Specific Management. *European Journal of Agronomy*, 59(0):57-66.
- Castro-Esau, K.L., (ed.) (2006). *Hyperspectral Remote Sensing of Invasive Plants: Detecting Lianas in Panama*, Proceedings of the Fifteenth Australian Weeds Conference: Managing Weeds in a Changing Climate; 2006 Weed Management Society of South Australia Inc, Adelaide.
- Cepl, J. and Kasal, P. (2010). Weed Mapping: A Way to Reduce Herbicide Doses. *Potato Research*, 53(4):359-371.
- Chaerle, L., Leinonen, I., Jones, H.G. and Van Der Straeten, D. (2007). Monitoring and Screening Plant Populations with Combined Thermal and Chlorophyll Fluorescence Imaging. *Journal of Experimental Botany*, 58(4):773-784.
- Chaerle, L. and Van Der Straeten, D. (2000). Imaging Techniques and the Early Detection of Plant Stress. *Trends in Plant Science*, 5(11):495-501.
- Chang, J., Sharon, A.C., Clay, D.E. and Dalsted, K. (2004). Detecting Weed-Free and Weed-Infested Areas of a Soybean Field Using Spectral Data. *Weed Science*, 52(4):642-648.
- Chappelle, E.W., Wood, F.M., McMurtrey, J.E. and Newcomb, W.W. (1984). Laser-Induced Fluorescence of Green Plants. 1: A Technique for the Remote Detection of Plant Stress and Species Differentiation. *Applied Optics*, 23(1):134-138.
- Chen, G. and Hay, G.J. (2011). An Airborne Lidar Sampling Strategy to Model Forest Canopy Height from Quickbird Imagery and Geobias. *Remote Sensing of Environment*, 115(6):1532-1542.
- Chene, Y., Rousseau, D., Lucidarme, P., Bertheloot, J., Caffier, V., Morel, P., Belin, É. and Chapeau-Blondeau, F. (2012). On the Use of Depth Camera for 3-D Phenotyping of Entire Plants. *Computers and Electronics in Agriculture*, 82:122-127.
- Christensen, S., Sjøgaard, H.T., Kudsk, P., Nørremark, M., Lund, I., Nadimi, E.S. and Jørgensen, R. (2009). Site-Specific Weed Control Technologies. *Weed Research*, 49(3):233-241.

- Christensen, S.D., Ransom, C.V., Edvarchuk, K.A. and Rasmussen, V.P. (2011). Efficiency and Accuracy of Wildland Weed Mapping Methods. *Invasive Plant Science and Management*, 4(4):458-466.
- Clark, M.L., Roberts, D.A. and Clark, D.B. (2005). Hyperspectral Discrimination of Tropical Rain Forest Tree Species at Leaf to Crown Scales. *Remote Sensing of Environment*, 96(3-4):375-398.
- Clark, C.J., McGlone, V.A. and Jordan, R.B. (2003). Detection of Brownheart in 'Braeburn' Apple by Transmission NIR Spectroscopy. *Postharvest Biology and Technology*, 28(1):87-96.
- Clevers, J.G.P.W. (1999). The Use of Imaging Spectrometry for Agricultural Applications. *Journal of Photogrammetry and Remote Sensing*, 54(5-6):299-304.
- Clinton, N., Holt, A., Scarborough, J., Yan, L. and Gong, P. (2010). Accuracy Assessment Measures for Object-Based Image Segmentation Goodness. *Photogrammetric Engineering and Remote Sensing*, 76(3):289-299.
- Cohen, J. (1960). A Coefficient of Agreement for Nominal Scales. *Educational and Psychological Measurement*, 20(1):37-46.
- Congalton, R.G. (1991). A Review of Assessing the Accuracy of Classifications of Remotely Sensed Data. *Remote Sensing of Environment*, 37(1):35-46.
- Congalton, R.G. (1991). A Review of Assessing the Accuracy of Classifications of Remotely Sensed Data. *Remote Sensing of Environment*, 37(1):35-46.
- Corbane, C., Raclot, D., Jacob, F., Albergel, J. and Andrieux, P. (2008). Remote Sensing of Soil Surface Characteristics from a Multiscale Classification Approach. *Catena*, 75(3):308-318.
- Costa, J.M., Grant, O.M. and Chaves, M.M. (2013). Thermography to Explore Plant-Environment Interactions. *Journal of Experimental Botany*, 64(13):3937-3949.
- Crespi, M., Fratarcangeli, F., Giannone, F. and Pieralice, F. (2011). A New Rigorous Model for High-Resolution Satellite Imagery Orientation: Application to Quickbird. *International Journal of Remote Sensing*, 33(8):2321-2354.
- Dale, L.M., Thewis, A., Boudry, C., Rotar, I., Păcurar, F.S., Abbas, O., Dardenne, P., Baeten, V., Pfister, J. and Fernández Pierna, J.A. (2013). Discrimination of Grassland Species and Their Classification in Botanical Families by Laboratory Scale NIR Hyperspectral Imaging: Preliminary Results. *Talanta Journal*, 116:149-154.
- Daughtry, C. and Walthall, C. (1998). Spectral Discrimination of *Cannabis Sativa* L. Leaves and Canopies. *Remote Sensing of Environment*, 64(2):192-201.
- De Baerdemaeker, J. (2014). Future Adoption of Automation in Weed Control, *Automation: The Future of Weed Control in Cropping Systems*. Springer, 221-234.
- De Castro, A.-I., Jurado-Expósito, M., Gómez-Casero, M.-T. and López-Granados, F. (2012). Applying Neural Networks to Hyperspectral and Multispectral Field Data for Discrimination of Cruciferous Weeds in Winter Crops, *The Scientific World Journal*, (Serial online), 2012(Available from URL: <http://hindawi.com/journals/tswj/2012/630390/abs>).
- De Castro, A., Ehsani, R., Ploetz, R., Crane, J. and Abdulridha, J. (2015). Optimum Spectral and Geometric Parameters for Early Detection of Laurel Wilt Disease in Avocado. *Remote Sensing of Environment*, 171:33-44.
- Definiens Imaging (2004). *eCognition User Guide 4*. Trimble Geospatial Imaging, Munich, Germany.
- Delalieux, S., Van Aardt, J., Keulemans, W., Schrevels, E. and Coppin, P. (2007). Detection of Biotic Stress (*Venturia Inaequalis*) in Apple Trees Using Hyperspectral Data: Non-Parametric Statistical Approaches and Physiological Implications. *European Journal of Agronomy*, 27(1):130-143.
- Delegido, J., Verrelst, J., Meza, C.M., Rivera, J.P., Alonso, L. and Moreno, J. (2013). A Red-Edge Spectral Index for Remote Sensing Estimation of Green LAI over Agroecosystems. *European Journal of Agronomy*, 46(0):42-52.
- Delwiche, S. and Graybosch, R.A. (2002). Identification of Waxy Wheat by near-Infrared Reflectance Spectroscopy. *Journal of Cereal Science*, 35(1):29-38.

- Deng, W., Chen, L., Meng, Z., Wu, G. and Zhang, R. (2010). Review of Non-Chemical Weed Management for Green Agriculture. *International Journal of Agricultural and Biological Engineering*, 3(4):52-60.
- Department of Agriculture and Fisheries. (2012). Overview of the Sorghum Industry. Retrieved 28.8.2015, 2015, <https://www.daf.qld.gov.au/plants/field-crops-and-pastures/broadacre-field-crops/sorghum/overview>
- Donoghue, D.N., Watt, P.J., Cox, N.J. and Wilson, J. (2007). Remote Sensing of Species Mixtures in Conifer Plantations Using LiDAR Height and Intensity Data. *Remote Sensing of Environment*, 110(4):509-522.
- Eddy, P., Smith, A., Hill, B., Peddle, D., Coburn, C. and Blackshaw, R. (2008). Hybrid Segmentation-Artificial Neural Network Classification of High Resolution Hyperspectral Imagery for Site-Specific Herbicide Management in Agriculture. *Photogrammetric Engineering and Remote Sensing*, 74(10):1249-1257.
- Eddy, P.R., Smith, A.M., Hill, B.D., Peddle, D.R., Coburn, C.A. and Blackshaw, R.E. (2013). Weed and Crop Discrimination Using Hyperspectral Image Data and Reduced Bandsets. *Canadian Journal of Remote Sensing*, 39(6):481-490.
- Eisenbeiss, H. and Sauerbier, M. (2011). Investigation of UAV Systems and Flight Modes for Photogrammetric Applications. *The Photogrammetric Record*, 26(136):400-421.
- Elowitz, R.M. (2015). What Is Imaging Spectroscopy (Hyperspectral Imaging)?, (Serial online). Available from URL: <http://www.markelowitz.com/Hyperspectral.html>.
- Elvidge, C.D. and Chen, Z. (1995). Comparison of Broad-Band and Narrow-Band Red and near-Infrared Vegetation Indices. *Remote Sensing of Environment*, 54(1):38-48.
- ESRI. (2015). Geoinformatic Dictionary. *Support*. Retrieved 4.2.2016, 2016, <http://support.esri.com/en/knowledgebase/GISDictionary/term/band%20ratio>
- Eure, P.M., Culpepper, A.S., Merchant, R.M., Roberts, P.M. and Collins, G.C. (2015). Weed Control, Crop Response, and Profitability When Intercropping Cantaloupe and Cotton. *Weed Technology*, 29(2):217-225.
- Evain, S., Flexas, J. and Moya, I. (2004). A New Instrument for Passive Remote Sensing: 2. Measurement of Leaf and Canopy Reflectance Changes at 531 nm and Their Relationship with Photosynthesis and Chlorophyll Fluorescence. *Remote Sensing of Environment*, 91(2):175-185.
- Evans, F.H. and Diggle, A.J., (eds) (2008). *A Spatio-Temporal Modelling Framework for Assessing the Impact of Weed Management Technologies on the Spread of Herbicide Resistance*, Proceedings of the Proceedings of the 16th Australian Weeds Conference, ed. by Van Klinken RD, Osten VA, Panetta FD and Scanlan JC. Queensland Weeds Society, Brisbane, Qld, Australia; 2008.
- Everitt, J.H., Yang, C., Summy, K., Glomski, L.M. and Owens, C. (2011). Evaluation of Hyperspectral Reflectance Data for Discriminating Six Aquatic Weeds. *Journal of Aquatic Plant Management*, 49:94-100.
- Favier, J.F., Ross, D.W., Tshenko, R., Kennedy, D.D., Muir, A.Y. and Fleming, J., (eds) (1999). *Discrimination of Weeds in Brassica Crops Using Optical Spectral Reflectance and Leaf Texture Analysis*, Proceedings of the Photonics East (ISAM, VVDC, IEMB); 1999. International Society for Optics and Photonics.
- Fernandes, M.R., Aguiar, F.C., Silva, J.M.N., Ferreira, M.T. and Pereira, J.M.C. (2014). Optimal Attributes for the Object Based Detection of Giant Reed in Riparian Habitats: A Comparative Study between Airborne High Spatial Resolution and Worldview-2 Imagery. *International Journal of Applied Earth Observation and Geoinformation*, 32:79-91.
- Fisher, R.A. (1936). The Use of Multiple Measurements in Taxonomic Problems. *Annals of Eugenics*, 7(2):179-188.
- Flexas, J., Briantais, J.-M., Cerovic, Z., Medrano, H. and Moya, I. (2000). Steady-State and Maximum Chlorophyll Fluorescence Responses to Water Stress in Grapevine Leaves: A New Remote Sensing System. *Remote Sensing of Environment*, 73(3):283-297.

- Foody, G.M. (2002). Status of Land Cover Classification Accuracy Assessment. *Remote Sensing of Environment*, 80(1):185-201.
- Fukatsu, T., Watanabe, T., Hu, H., Yoichi, H. and Hirafuji, M. (2012). Field Monitoring Support System for the Occurrence of *Leptocorisa Chinensis* Dallas (Hemiptera: Alydidae) Using Synthetic Attractants, Field Servers, and Image Analysis. *Computers and Electronics in Agriculture*, 80:8-16.
- Fyfe, S.K. (2003). Spatial and Temporal Variation in Spectral Reflectance: Are Seagrass Species Spectrally Distinct? *Limnology and Oceanography*, 48(1):464-479.
- Gamon, J., Field, C., Bilger, W., Björkman, O., Fredeen, A. and Peñuelas, J. (1990). Remote Sensing of the Xanthophyll Cycle and Chlorophyll Fluorescence in Sunflower Leaves and Canopies. *Oecologia*, 85(1):1-7.
- Garcia-Ruiz, F.J., Wulfsohn, D. and Rasmussen, J. (2015). Sugar Beet (*Beta Vulgaris* L.) and Thistle (*Cirsium Arvensis* L.) Discrimination Based on Field Spectral Data. *Biosystems Engineering*, 139:1-15.
- Gay, A., Stewart, T., Angel, R., Easey, M., Eves, A., Thomas, N., Pearce, D. and Kemp, A., (eds) (2009). *Developing Unmanned Aerial Vehicles for Local and Flexible Environmental and Agricultural Monitoring. New Dimensions in Earth Observation*; 2009.
- Gholizadeh, A., Borůvka, L., Saberioon, M. and Vašát, R. (2013). Visible, and Mid-Infrared Spectroscopy Applications for Soil Assessment with Emphasis on Soil Organic Matter Content and Quality: State-of-the-Art and Key Issues. *Applied Spectroscopy*, 67(12):1349-1362.
- Gillespie, A.R., Kahle, A.B. and Walker, R.E. (1986). Color Enhancement of Highly Correlated Images. I. Decorrelation and Hsi Contrast Stretches. *Remote Sensing of Environment*, 20(3):209-235.
- Gillieson, D.S., Lawson, T.J. and Searle, L.E. (2006). *Applications of High Resolution Remote Sensing in Rainforest Ecology and Management*. Cooperative Research Centre for Tropical Rainforest Ecology and Management, Cairns, Qld.
- Glenn, N.F., Mundt, J.T., Weber, K.T., Prather, T.S., Lass, L.W. and Pettingill, J. (2005). Hyperspectral Data Processing for Repeat Detection of Small Infestations of Leafy Spurge. *Remote Sensing of Environment*, 95(3):399-412.
- Goel, P.K., Prasher, S.O., Landry, J.A., Patel, R.M., Bonnell, R.B., Viau, A.A. and Miller, J.R. (2003). Potential of Airborne Hyperspectral Remote Sensing to Detect Nitrogen Deficiency and Weed Infestation in Corn. *Computers and Electronics in Agriculture*, 38(2):99-124.
- Goktogan, A., Sukkarieh, S., Bryson, M., Randle, J., Lupton, T. and Hung, C. (2010). A Rotary-Wing Unmanned Air Vehicle for Aquatic Weed Surveillance and Management. *Journal of Intelligent and Robotic Systems*, 57(1-4):467-484.
- Golzarian, M.R. and Frick, R.A. (2011). Classification of Images of Wheat, Ryegrass and Brome Grass Species at Early Growth Stages Using Principal Component Analysis. *Plant Methods*, 7(1):28.
- Gomez-Candon, D., De Castro, A. and López-Granados, F. (2014). Assessing the Accuracy of Mosaics from Unmanned Aerial Vehicle (UAV) Imagery for Precision Agriculture Purposes in Wheat. *Precision Agriculture*, 15(1):44-56.
- Gowen, A., O'Donnell, C., Cullen, P., Downey, G. and Frias, J. (2007). Hyperspectral Imaging—An Emerging Process Analytical Tool for Food Quality and Safety Control. *Trends in Food Science and Technology*, 18(12):590-598.
- Gray, C.J., Shaw, D.R. and Bruce, L.M. (2009). Utility of Hyperspectral Reflectance for Differentiating Soybean (*Glycine Max*) and Six Weed Species. *Weed Technology*, 23(1):108-119.
- Gumz, M.S.P. (2007). Development of Remote Sensing Based Site Specific Weed Management for Midwest Mint Production, Doctor of Philosophy Purdue University.
- Gutjahr, C. and Gerhards, R. (2010). Decision Rules for Site-Specific Weed Management, *Precision Crop Protection-the Challenge and Use of Heterogeneity*. Springer, 223-239.

- Haff, R.P., Slaughter, D.C. and Jackson, E.S. (2011). X-Ray Based Stem Detection in an Automatic Tomato Weeding System. *Applied Engineering in Agriculture*, 27(5):803-810.
- Haboudane, D., Miller, J.R., Pattey, E., Zarco-Tejada, P.J. and Strachan, I.B. (2004). Hyperspectral Vegetation Indices and Novel Algorithms for Predicting Green Lai of Crop Canopies: Modeling and Validation in the Context of Precision Agriculture. *Remote sensing of environment*, 90(3):337-352.
- Harker, K., O'Donovan, J., Blackshaw, R., Hall, L., Willenborg, C., Kutcher, H., Gan, Y., Lafond, G., May, W. and Grant, C. (2013). Effect of Agronomic Inputs and Crop Rotation on Biodiesel Quality and Fatty Acid Profiles of Direct-Seeded Canola. *Canadian Journal of Plant Science*, 93:1-12.
- Hay, G. and Castilla, G. (2008). Geographic Object-Based Image Analysis (Geobia): a New Name for a New Discipline. In: Blaschke, T., Lang, S. and Hay, G.J. (eds), *Object-Based Image Analysis: Spatial Concepts for Knowledge-Driven Remote Sensing Applications*. Springer, Berlin, 75-89.
- Heap, I. The International Survey of Herbicide Resistant Weeds. Online. Internet. Thursday, June 23, 2016. Available www.weedscience.org
- Herwitz, S.R., Johnson, L.F., Arvesen, J., Higgins, R., Leung, J. and Dunagan, S. (2002). *Proceedings of the American Institute of Aeronautics and Astronautics UAV Conference*.
- Hestir, E.L., Khanna, S., Andrew, M.E., Santos, M.J., Viers, J.H., Greenberg, J.A., Rajapakse, S.S. and Ustin, S.L. (2008). Identification of Invasive Vegetation Using Hyperspectral Remote Sensing in the California Delta Ecosystem. *Remote Sensing of Environment*, 112(11):4034-4047.
- Hoang, V.D. and Binh, H.T.T. (2015). Effect of Maize-Soybean Intercropping and Hand Weeding on Weed Control. *Journal of Science*, 13(3):354-363.
- Hochberg, E.J., Atkinson, M.J. and Andréfouët, S. (2003). Spectral Reflectance of Coral Reef Bottom-Types Worldwide and Implications for Coral Reef Remote Sensing. *Remote Sensing of Environment*, 85(2):159-173.
- Holden, H. and LeDrew, E. (1998). Spectral Discrimination of Healthy and Non-Healthy Corals Based on Cluster Analysis, Principal Components Analysis, and Derivative Spectroscopy. *Remote Sensing of Environment*, 65(2):217-224.
- Hummel, J. and Stoller, E. (2002). On-the-Go Weed Sensing and Herbicide Application for the Northern Cornbelt. *Society for Engineering in Agriculture, Biological and Food Processing*.
- Hutto, K.C., Shaw, D.R., Byrd, J.D., Jr. and King, R.L. (2006). Differentiation of Turfgrass and Common Weed Species Using Hyperspectral Radiometry. *Weed Science*, 54(2):335-339.
- Im, J. and Jensen, J.R. (2008). Hyperspectral Remote Sensing of Vegetation. *Geography Compass*, 2(6):1943-1961.
- Jensen, H., Jacobsen, L.-B., Pedersen, S. and Tavella, E. (2012). Socioeconomic Impact of Widespread Adoption of Precision Farming and Controlled Traffic Systems in Denmark. *Precision Agriculture*, 13(6):661-677.
- Jensen, J.R. (2005). *Introductory Digital Image Processing : A Remote Sensing Perspective*, 3rd edn. Prentice Hall, Upper Saddle River, N.J.
- Jensen, J.R. (2007). *Remote Sensing of the Environment: An Earth Resource Perspective*, 2nd edn. Pearson Prentice Hall, Upper Saddle River.
- Jensen, J.R. (2016). *Introductory Digital Image Processing: A Remote Sensing Perspective*, 4th edn.
- Jensen, T., Apan, A., Young, F. and Zeller, L. (2007). Detecting the Attributes of a Wheat Crop Using Digital Imagery Acquired from a Low-Altitude Platform. *Computers and Electronics in Agriculture*, 59(1-2):66-77.
- Jin, J. and Tang, L. (2009). Corn Plant Sensing Using Real-Time Stereo Vision. *Journal of Field Robotics*, 26(6-7):591-608.
- Johansen, K., Phinn, S. and Witte, C. (2010). Mapping of Riparian Zone Attributes Using Discrete Return LiDAR, Quickbird and Spot-5 Imagery: Assessing Accuracy and Costs. *Remote Sensing of Environment*, 114(11):2679-2691.

- Johansen, K., Tiede, D., Blaschke, T., Arroyo, L.A. and Phinn, S. (2011). Automatic Geographic Object Based Mapping of Streambed and Riparian Zone Extent from LiDAR Data in a Temperate Rural Urban Environment, Australia. *Remote Sensing*, 3(6):1139-1156.
- Jones, G., Gée, C. and Truchetet, F. (2009a). Modelling Agronomic Images for Weed Detection and Comparison of Crop/Weed Discrimination Algorithm Performance. *Precision Agriculture*, 10(1):1-15.
- Jones, H.G., Serraj, R., Loveys, B.R., Xiong, L., Wheaton, A. and Price, A.H. (2009b). Thermal Infrared Imaging of Crop Canopies for the Remote Diagnosis and Quantification of Plant Responses to Water Stress in the Field. *Functional Plant Biology*, 36(11):978-989.
- Jordan, C.F. (1969). Derivation of Leaf-Area Index from Quality of Light on the Forest Floor. *Ecology*, 50(4):663-666.
- Kamal, M., Phinn, S. and Johansen, K. (2015). Object-Based Approach for Multi-Scale Mangrove Composition Mapping Using Multi-Resolution Image Datasets. *Remote Sensing*, 7(4):4753-4783.
- Knipling, E.B. (1970). Physical and Physiological Basis for the Reflectance of Visible and NIR Radiation from Vegetation. *Remote Sensing of Environment*, 1(3):155-159.
- Kandhro, M.N., Tunio, S., Rajpar, I. and Chachar, Q. (2014). Allelopathic Impact of Sorghum and Sunflower Intercropping on Weed Management and Yield Enhancement in Cotton. *Journal of Agriculture*, 30(3):311-318.
- Kefyalew, G., Mosali, J., Raun, W.R., Freeman, K.W. and et al. (2005). Identification of Optical Spectral Signatures for Detecting Cheat and Ryegrass in Winter Wheat. *Crop Science*, 45(2):477-485.
- Khorramnia, K., Shariff, A., Rahim, A.A. and Mansor, S. (2014). Toward Malaysian Sustainable Agriculture in 21st Century, *IOP Conference Series: Earth and Environmental Science*, (Serial online), 18(1). Available from URL: http://iopscience.iop.org/1755-1315/18/1/012142/pdf/1755-1315_18_1_012142.pdf.
- Kiani, S. and Jafari, A. (2012). Crop Detection and Positioning in the Field Using Discriminant Analysis and Neural Networks Based on Shape Features. *Journal of Agricultural Science and Technology*, 14(4):755-765.
- Kipp, S., Mistele, B., Baresel, P. and Schmidhalter, U. (2014). High-Throughput Phenotyping Early Plant Vigour of Winter Wheat. *European Journal of Agronomy*, 52:271-278.
- Kleynen, O., Leemans, V. and Destain, M.-F. (2005). Development of a Multi-Spectral Vision System for the Detection of Defects on Apples. *Journal of Food Engineering*, 69(1):41-49.
- Klodt, M., Herzog, K., Töpfer, R. and Cremers, D. (2015). Field Phenotyping of Grapevine Growth Using Dense Stereo Reconstruction. *Bioinformatics*, 16(1):143.
- Knipling, E.B. (1970). Physical and Physiological Basis for the Reflectance of Visible and NIR Radiation from Vegetation. *Remote Sensing of Environment*, 1(3):155-159.
- Kodagoda, S. and Zhang, Z. (2010). Multiple Sensor-Based Weed Segmentation. *Proceedings of the Institution of Mechanical Engineers, Part I: Journal of Systems and Control Engineering*, 224(7):799-810.
- Koenig, K., Höfle, B., Hämmerle, M., Jarmer, T., Siegmann, B. and Lilienthal, H. (2015). Comparative Classification Analysis of Post-Harvest Growth Detection from Terrestrial LiDAR Point Clouds in Precision Agriculture. *Journal of Photogrammetry and Remote Sensing*, 104:112-125.
- Koger, C.H., Shaw, D.R., Reddy, K.N. and Bruce, L.M. (2004). Detection of Pitted Morning glory (*Ipomoea Lacunosa*) by Hyperspectral Remote Sensing. I. Effects of Tillage and Cover Crop Residue. *Weed Science*, 52(2):222-229.
- Kumar, D.D., C.Vijaya and Janani, S.J. (2015). Autonomous Navigation of Mobile Robot for Automatic Weed Detection and Herbicide Spraying in Agriculture. *International Journal of Engineering Sciences and Research Technology*, 4(1):132-135.

- Kunisch, M. (2002). Precision Farming, a Tool for Weed Control. *Journal Plant Disease Protection*, 18:415-420.
- Laliberte, A.S., Goforth, M.A., Steele, C.M. and Rango, A. (2011). Multispectral Remote Sensing from Unmanned Aircraft: Image Processing Workflows and Applications for Rangeland Environments. *Remote Sensing*, 3(12):2529-2551.
- Laliberte, A.S., Herrick, J.E., Rango, A. and Winters, C. (2010). Acquisition, Orthorectification, and Object-Based Classification of Unmanned Aerial Vehicle (UAV) Imagery for Rangeland Monitoring. *Photogrammetric Engineering & Remote Sensing*, 76(6):661-672.
- Lamb, D.W. and Brown, R.B. (2001). Precision Agriculture: Remote-Sensing and Mapping of Weeds in Crops. *Journal of Agricultural Engineering Research*, 78(2):117-125.
- Lan, Y., Zhang, H., Lacey, R., Hoffman, W.C. and Wu, W. (2009). Development of an Integration Sensor and Instrumentation System for Measuring Crop Conditions. *Agricultural Engineering International Journal*.
- Lee, W.S., Alchanatis, V., Yang, C., Hirafuji, M., Moshou, D. and Li, C. (2010). Sensing Technologies for Precision Specialty Crop Production. *Computers and Electronics in Agriculture*, 74(1):2-33.
- Lehmann, J.R.K., Nieberding, F., Prinz, T. and Knoth, C. (2015). Analysis of Unmanned Aerial System-Based Cir Images in Forestry—a New Perspective to Monitor Pest Infestation Levels. *Forests*, 6(3):594-612.
- Leinonen, I. and Jones, H.G. (2004). Combining Thermal and Visible Imagery for Estimating Canopy Temperature and Identifying Plant Stress. *Journal of Experimental Botany*, 55(401):1423-1431.
- Lenk, S., Chaerle, L., Pfündel, E.E., Langsdorf, G., Hagenbeek, D., Lichtenthaler, H.K., Van Der Straeten, D. and Buschmann, C. (2007). Multispectral Fluorescence and Reflectance Imaging at the Leaf Level and Its Possible Applications. *Journal of Experimental Botany*, 58(4):807-814.
- Leon, J.X. and Woodroffe, C.D. (2013). Morphological Characterisation of Reef Types in Torres Strait and an Assessment of Their Carbonate Production. *Marine Geology*, 338:64-75.
- Levine, M.D. and Nazif, A.M. (1985). Dynamic Measurement of Computer Generated Image Segmentations. *Pattern Analysis and Machine Intelligence, IEEE Transactions on*(2):155-164.
- Li, L., Zhang, Q. and Huang, D. (2014). A Review of Imaging Techniques for Plant Phenotyping. *Sensors*, 14(11):20078-20111.
- Li, X. and He, Y. (2008). Discriminating Varieties of Tea Plant Based on VIS/NIR Spectral Characteristics and Using Artificial Neural Networks. *Biosystems Engineering*, 99(3):313-321.
- Li, X., Lee, W.S., Li, M., Ehsani, R., Mishra, A.R., Yang, C. and Mangan, R.L. (2012). Spectral Difference Analysis and Airborne Imaging Classification for Citrus Greening Infected Trees. *Computers and Electronics in Agriculture*, 83:32-46.
- Lillesand, T.M., Kiefer, R.W. and Chipman, J.W. (2004). *Remote Sensing and Image Interpretation*. John Wiley & Sons Ltd.
- Lisita, A., Sano, E.E. and Durieux, L. (2013). Identifying Potential Areas of Cannabis Sativa Plantations Using Object-Based Image Analysis of Spot-5 Satellite Data. *International journal of remote sensing*, 34(15):5409-5428.
- Liu, B., Fang, J.Y., Liu, X. and Zhang, L.F. (2010). Research on Crop-Weed Discrimination Using a Field Imaging Spectrometer. *Guang Pu Xue Yu Guang Pu Fen Xi*, 30(7):1830-1833.
- Liu, H., Saunders, C. and Lee, S. (2013). Development of a Proximal Machine Vision System for Off-Season Weed Mapping in Broadacre No-Tillage Fallows. *Journal of Computer Science*, 9(12):1803.
- Lizarazo, I. (2013). Meaningful Image Objects for Object-Oriented Image Analysis. *Remote Sensing Letters*, 4(5):419-426.

- Longchamps, L., Panneton, B., Samson, G., Leroux, G. and Thériault, R. (2010). Discrimination of Corn, Grasses and Dicot Weeds by Their UV-Induced Fluorescence Spectral Signature. *Precision Agriculture*, 11(2):181-197.
- Lopez-Granados, F. (2010). Weed Detection for Site-Specific Weed Management: Mapping and Real-Time Approaches. *Weed Research*, 51(1):1-11.
- Lopez-Granados, F., Torres-Sánchez, J., Serrano-Pérez, A., de Castro, A., Mesas-Carrascosa, F.J. and Peña, J.-M. (2015). Early Season Weed Mapping in Sunflower Using UAV Technology: Variability of Herbicide Treatment Maps against Weed Thresholds. *Precision Agriculture*:1-17.
- Louis L., Bernard P., Guy S., Gilles D. L., Roger T. (2010), Discrimination of corn, grasses and dicot weeds by their UV-induced fluorescence spectral signature, *Precision Agriculture Journal*, (11): 181–197
- Lu, H., Zheng, H., Hu, Y., Lou, H. and Kong, X. (2011). Bruise Detection on Red Bayberry (*Myrica Rubra Sieb. And Zucc.*) Using Fractal Analysis and Support Vector Machine. *Journal of Food Engineering*, 104(1):149-153.
- Lucieer, A., Malenovský, Z., Veness, T. and Wallace, L. (2014). Hyperuas—Imaging Spectroscopy from a Multirotor Unmanned Aircraft System. *Journal of Field Robotics*, 31(4):571-590.
- Lucieer, A. and Stein, A. (2002). Existential Uncertainty of Spatial Objects Segmented from Satellite Sensor Imagery. *IEEE Transactions on Geoscience and Remote Sensing*, 40(11):2518-2521.
- M.J. Farabee (2007). Photosynthesis, (Serial online). Available from URL: <http://www2.estrellamountain.edu/faculty/farabee/biobk/biobookps.html>.
- Mancini, F., Dubbini, M., Gattelli, M., Stecchi, F., Fabbri, S. and Gabbianelli, G. (2013). Using Unmanned Aerial Vehicles (UAV) for High-Resolution Reconstruction of Topography: The Structure from Motion Approach on Coastal Environments. *Remote Sensing Journal*, 5(12):6880-6898.
- Manevski, K., Manakos, I., Petropoulos, G.P. and Kalaitzidis, C. (2011). Discrimination of Common Mediterranean Plant Species Using Field Spectroradiometry. *International Journal of Applied Earth Observation and Geoinformation*, 13(6):922-933.
- Martin, M.P., Barreto, L. and Fernandez-Quintanilla, C. (2011). Discrimination of Sterile Oat (*Avena Sterilis*) in Winter Barley (*Hordeum Vulgare*) Using Quickbird Satellite Images. *Crop Protection*, 30(10):1363-1369.
- Marais Sicre, C., Baup, F. and Fieuzal, R. (2014). Determination of the Crop Row Orientations from Formosat-2 Multi-Temporal and Panchromatic Images. *ISPRS Journal of Photogrammetry and Remote Sensing*, 94(0):127-142.
- Mathews, A.J. (2014). Assessing Grapevine Canopy Health in the Texas Hill Country with Remote Sensing and Gis Techniques, Texas State University.
- Merotto Jr, A., Bredemeier, C., Vidal, R., Goulart, I., Bortoli, E. and Anderson, N. (2012). Reflectance Indices as a Diagnostic Tool for Weed Control Performed by Multipurpose Equipment in Precision Agriculture. *Planta Daninha Journal*, 30(2):437-447.
- Merton, R. and Huntington, J., (eds) (1999). *Early Simulation Results of the Aries-1 Satellite Sensor for Multi-Temporal Vegetation Research Derived from Aviris*, Proceedings of the Proceedings of the Eighth Annual JPL Airborne Earth Science Workshop; 1999. NASA, JPL Pasadena, CA.
- Mesas-Carrascosa, F.-J., Torres-Sánchez, J., Clavero-Rumbao, I., García-Ferrer, A., Peña, J.-M., Borra-Serrano, I. and López-Granados, F. (2015). Assessing Optimal Flight Parameters for Generating Accurate Multispectral Orthomosaics by UAV to Support Site-Specific Crop Management. *Remote Sensing*, 7(10):12793-12814.
- Meyer, G.E., Hindman, T.W. and Laksmi, K., (eds) (1999). *Machine Vision Detection Parameters for Plant Species Identification*, Proceedings of the Photonics East (ISAM, VVDC, IEMB); 1999. International Society for Optics and Photonics.

- Mission Planner. (2013). Mission Planner. Retrieved 15 October 2014, 2014, <http://ardupilot.com/downloads/?did=82>
- Mississippi State (2014). What Are the Growth Stages for Grain Sorghum?, *Sorghum Production in Mississippi*, (Serial online). Available from URL: <http://msucare.com/crops/sorghum.html>
- Monaco, T.J., C.Weller, S. and M.Ashton, F. (2001). *Weed Science: Principles and Practices*, 4th edn. Wiley, New York.
- Moshou, D., Bravo, C., Oberti, R., West, J., Bodria, L., McCartney, A. and Ramon, H. (2005). Plant Disease Detection Based on Data Fusion of Hyper-Spectral and Multi-Spectral Fluorescence Imaging Using Kohonen Maps. *Real-Time Imaging*, 11(2):75-83.
- Moshou, D., Kateris, D., Pantazi, X. and Gravalos, I. (2013). Crop and Weed Species Recognition Based on Hyperspectral Sensing and Active Learning, *Precision Agriculture '13*. Springer, 555-561.
- Müller-Linow, M., Rascher, U., Janssen, B. and Steier, A., (eds) (2015). *3-D Field Phenotyping of Crops Using Laser Scanning and Photogrammetric Approaches*, Proceedings of the Workshop on laser scanning applications; 2015.
- Müllerová, J., Pergl, J. and Pyšek, P. (2013). Remote Sensing as a Tool for Monitoring Plant Invasions: Testing the Effects of Data Resolution and Image Classification Approach on the Detection of a Model Plant Species *Heracleum Mantegazzianum* (Giant Hogweed). *International Journal of Applied Earth Observation and Geoinformation*, 25(0):55-65.
- Mutanga, O. and Skidmore, A.K. (2004). Hyperspectral Band Depth Analysis for a Better Estimation of Grass Biomass (*Cenchrus Ciliaris*) Measured under Controlled Laboratory Conditions. *International Journal of Applied Earth Observation and Geoinformation*, 5(2):87-96.
- Naidu, R.A., Perry, E.M., Pierce, F.J. and Mekuria, T. (2009). The Potential of Spectral Reflectance Technique for the Detection of Grapevine Leafroll-Associated Virus-3 in Two Red-Berried Wine Grape Cultivars. *Computers and Electronics in Agriculture*, 66(1):38-45.
- Nebiker, S., Annen, A., Scherrer, M. and Oesch, D. (2008). A Light-Weight Multispectral Sensor for Micro UAV—Opportunities for Very High Resolution Airborne Remote Sensing. *The International Archives of the Photogrammetry, Remote Sensing and Spatial Information Sciences*, 37:1193-2000.
- Nicolai, B.M., Beullens, K., Bobelyn, E., Peirs, A., Saeys, W., Theron, K.I. and Lammertyn, J. (2007). Nondestructive Measurement of Fruit and Vegetable Quality by Means of NIR Spectroscopy: A Review. *Postharvest Biology and Technology*, 46(2):99-118.
- Nieuwenhuizen, A.T., Hofstee, J.W., van de Zande, J.C., Meuleman, J. and van Henten, E.J. (2010). Classification of Sugar Beet and Volunteer Potato Reflection Spectra with a Neural Network and Statistical Discriminant Analysis to Select Discriminative Wavelengths. *Computers and Electronics in Agriculture*, 73(2):146-153.
- Noble, S.D. and Brown, R.B., (eds) (2009). *Plant Species Discrimination Using Spectral/Spatial Descriptive Statistics*, Proceedings of the Proceedings of the 1st International Workshop on Computer Image Analysis in Agriculture held in Potsdam, Germany; 2009.
- Noonan, M. and Chafer, C. (2007). A Method for Mapping the Distribution of Willow at a Catchment Scale Using Bi-Seasonal Spot 5 Imagery. *Weed Research*, 47(2):173-181.
- Oerke, E.-C. (2006). Crop Losses to Pests. *Journal of Agricultural Science*, 144(1):31.
- Okamoto, H., Suzuki, Y. and Noguchi, N. (2014). Field Applications of Automated Weed Control: Asia. In: Young, S.L. and Pierce, F.J. (eds), *Automation: The Future of Weed Control in Cropping Systems*. Springer, Dordrecht, Netherlands, 189-200.
- Ortiz-Monasterio, J.I. and Lobell, D.B. (2007). Remote Sensing Assessment of Regional Yield Losses Due to Sub-Optimal Planting Dates and Fallow Period Weed Management. *Field Crops Research*, 101(1):80-87.
- Ortiz, B. and Shaw, J., N., (2011). Basics of Crop Sensing. Retrieved 29.9.2015, 2015, <http://www.aces.edu/pubs/docs/A/ANR-1398/index2.tmpl>

- Parsons, D.J., Benjamin, L.R., Clarke, J., Ginsburg, D., Mayes, A., Milne, A.E. and Wilkinson, D.J. (2009). Weed Manager-a Model-Based Decision Support System for Weed Management in Arable Crops. *Computers and Electronics in Agriculture*, 65(2):155-167.
- Peltzer, S.C., Hashem, A., Osten, V.A., Gupta, M.L., Diggle, A.J., Riethmuller, G.P., Douglas, A., Moore, J.M. and Koetz, E.A. (2009). Weed Management in Wide-Row Cropping Systems: A Review of Current Practices and Risks for Australian Farming Systems. *Crop and Pasture Science*, 60(5):395-406.
- Pena-Barragan, J.M., M. Kelly, A. I. de-Castro and F. Lopez-Granados, (eds) (2012a). *Object-Based Approach for Crop Row Characterization in UAV Images for Site-Specific Weed Management*, Proceedings of the Proceedings of the 4th GEOBIA, Rio de Janeiro, Brazil, 7-9 May; 2012
- Pena-Barragan, J.M., López-Granados, F., Jurado-Expósito, M. and García-Torres, L. (2010). Sunflower Yield Related to Multi-Temporal Aerial Photography, Land Elevation and Weed Infestation. *Precision agriculture*, 11(5):568-585.
- Pena-Barragan, J.M., Lopez-Granados, F., Jurado-Exposito, M. and Garcia-Torres, L. (2007). Mapping *Ridolfia Segetum* Patches in Sunflower Crop Using Remote Sensing. *Weed Research*, 47(2):164-172.
- Pena, J.M., Torres-Sánchez, J., Castro, A.I.d., Kelly, M. and López-Granados, F. (2013). Weed Mapping in Early-Season Maize Fields Using Object-Based Analysis of Unmanned Aerial Vehicle (UAV) Images. *PLOS ONE*, 8(10):1-11.
- Pena, J.M., Torres-Sánchez, J., Serrano-Pérez, A., de Castro, A.I. and López-Granados, F. (2015). Quantifying Efficacy and Limits of Unmanned Aerial Vehicle (UAV) Technology for Weed Seedling Detection as Affected by Sensor Resolution. *Sensors*, 15(3):5609-5626.
- Penuelas, J., Filella, I., Biel, C., Serrano, L. and Savé, R. (1993). The Reflectance at the 950–970 nm Region as an Indicator of Plant Water Status. *International Journal of Remote Sensing*, 14(10):1887-1905.
- Perez-Ortiz, M., Peña, J.M., Gutiérrez, P.A., Torres-Sánchez, J., Hervás-Martínez, C. and López-Granados, F. (2015). A Semi-Supervised System for Weed Mapping in Sunflower Crops Using Unmanned Aerial Vehicles and a Crop Row Detection Method. *Applied Software Computing*.
- Phinn, S.R., Roelfsema, C.M. and Mumby, P.J. (2012). Multi-Scale, Object-Based Image Analysis for Mapping Geomorphic and Ecological Zones on Coral Reefs. *International Journal of Remote Sensing*, 33(12):3768-3797.
- PhotoScan, A. (2013). Agisoft Photoscan User Manual. in 1.0.0, V. (ed.).
- Powers, R.P., Hay, G.J. and Chen, G. (2012). How Wetland Type and Area Differ through Scale: A Geobia Case Study in Alberta's Boreal Plains. *Remote Sensing of Environment*, 117(0):135-145.
- Prasad, S.T., John, G.L. and Alfredo, H. (2011). Advances in Hyperspectral Remote Sensing of Vegetation and Agricultural Croplands, *Hyperspectral Remote Sensing of Vegetation*, 3-36.
- Price, J.C. (1987). Calibration of Satellite Radiometers and the Comparison of Vegetation Indices. *Remote Sensing of Environment*, 21(1):15-27.
- Price, J.C. (1992). Variability of High-Resolution Crop Reflectance Spectra. *International Journal of Remote Sensing*, 13(14):2593-2610.
- Primicerio, J., Di Gennaro, S., Fiorillo, E., Genesio, L., Lugato, E., Matese, A. and Vaccari, F. (2012). A Flexible Unmanned Aerial Vehicle for Precision Agriculture. *Precision Agriculture*, 13(4):517-523.
- Psomas, A., Zimmermann, N.E., Kneubühler, M., Kellenberger, T. and Itten, K., (eds) (2005). *Seasonal Variability in Spectral Reflectance for Discriminating Grasslands Along a Dry-Mesic Gradient in Switzerland*, Proceedings of the Proceedings of the 4th European Association of Remote Sensing Laboratories Workshop on Imaging Spectroscopy; 2005.
- Purves et al (2014). Life: The Science of Biology, (Serial online). Available from URL: http://www.sinauer.com/life-the-science-of-biology-769.html#table_of_contents.

- Qin, J., Burks, T.F., Ritenour, M.A. and Bonn, W.G. (2009). Detection of Citrus Canker Using Hyperspectral Reflectance Imaging with Spectral Information Divergence. *Journal of Food Engineering*, 93(2):183-191.
- Rabatel, G., Ougache, F., Gorretta, N. and Ecartot, M. (2011). Hyperspectral Imagery to Discriminate Weeds in Wheat, *Proceedings of the First International Workshop on Robotics and Associated High Technologies and Equipment for Agriculture (RHEA-2011), Montpellier, France*, (Serial online). Available from URL: <http://hal.archives-ouvertes.fr/docs/00/77/79/68/PDF/mo2011-pub00036815.pdf>.
- Reeves, T.G., (ed.) (2008). *Global Changes: Impacts on Weeds in Cropping Systems*, Proceedings of the Proceedings of the 16th Australian Weeds Conference, Cairns Convention Centre, North Queensland, Australia, 18-22 May, 2008.; 2008. Queensland Weed Society.
- Rey, C., Martín, M., Lobo, A., Luna, I., Diago, M., Millan, B. and Tardáguila, J. (2013). Multispectral Imagery Acquired from a UAV to Assess the Spatial Variability of a Tempranillo Vineyard, *Precision Agriculture '13*. Springer, 617-624.
- Richards, J.A. (2013). *Remote Sensing Digital Image Analysis : An Introduction*, 5th ed. edn. Springer, Berlin ; London
- Roelfsema, C.M., Lyons, M., Kovacs, E.M., Maxwell, P., Saunders, M.I., Samper-Villarreal, J. and Phinn, S.R. (2014). Multi-Temporal Mapping of Seagrass Cover, Species and Biomass: A Semi-Automated Object Based Image Analysis Approach. *Remote Sensing of Environment*, 150(0):172-187.
- Saberioon, M., Amin, M., Aimrun, W., Anuar, A. and Gholizadeh, A. (2013). Multi-Spectral Images Tetracam Agriculture Digital Camera to Estimate Nitrogen and Grain Yield of Rice at Different Growth Stages. *The Philippine Agricultural Scientist*, 96(1).
- Saberioon, M.M., Amin, M.S.M., Anuar, A.R., Gholizadeh, A., Wayayok, A. and Khairunniza-Bejo, S. (2014). Assessment of Rice Leaf Chlorophyll Content Using Visible Bands at Different Growth Stages at Both the Leaf and Canopy Scale. *International Journal of Applied Earth Observation and Geoinformation*, 32(0):35-45.
- Sahoo, R.N., Ray S.S. and Manjhunath, K.R. (2015). Hypeerspectral Remote Sensing of Agriculture. *Current Sci.*, 108(5):848-859.
- Sankaran, S., Khot, L.R., Espinoza, C.Z., Jarolmasjed, S., Sathuvalli, V.R., Vandemark, G.J., Miklas, P.N., Carter, A.H., Pumphrey, M.O., Knowles, N.R. and Pavek, M.J. (2015). Low-Altitude, High-Resolution Aerial Imaging Systems for Row and Field Crop Phenotyping: A Review. *European Journal of Agronomy*, 70:112-123.
- Santi, A., Bona, S., Lamego, F., Basso, C., Eitelwein, M., Cherubin, M., Kasparý, T., Ruchel, Q. and Gallon, M. (2014). Phytosociological Variability of Weeds in Soybean Field. *Planta Daninha*, 32(1):39-49.
- Schepers, J.S., Blackmer, T.M., Wilhelm, W.W. and Resende, M. (1996). Transmittance and Reflectance Measurements of Corn Leaves from Plants with Different Nitrogen and Water Supply. *Journal of Plant Physiology*, 148(5):523-529.
- Schliep, M., Cavigliasso, G., Quinnell, R.G., Stranger, R. and Larkum, A.W.D. (2013). Formyl Group Modification of Chlorophyll A: A Major Evolutionary Mechanism in Oxygenic Photosynthesis. *Plant, Cell & Environment*, 36(3):521-527.
- Schmidt, K.S. and Skidmore, A.K. (2004). Smoothing Vegetation Spectra with Wavelets. *International Journal of Remote Sensing*, 25(6):1167-1184.
- Schuster, I., Nordmeyer, H. and Rath, T. (2007). Comparison of Vision-Based and Manual Weed Mapping in Sugar Beet. *Biosystems Engineering*, 98(1):17-25.
- Seiffert, U., Bollenbeck, F., Mock, H.-P. and Matros, A., (eds) (2010). *Clustering of Crop Phenotypes by Means of Hyperspectral Signatures Using Artificial Neural Networks*, Proceedings of the Hyperspectral Image and Signal Processing: Evolution in Remote Sensing (WHISPERS), 2010 2nd Workshop on; 2010.

- Shafri, H.Z.M., Anuar, M.I., Seman, I.A. and Noor, N.M. (2011). Spectral Discrimination of Healthy and Ganoderma-Infected Oil Palms from Hyperspectral Data. *International Journal of Remote Sensing*, 32(22):7111-7129.
- Shaw, D., Malthus, T. and Kupiec, J. (1998). High-Spectral Resolution Data for Monitoring Scots Pine (*Pinus Sylvestris L.*) Regeneration. *International Journal of Remote Sensing*, 19(13):2601-2608.
- Shilpakala, V. (2014). Pest Surveillance, Remote Sensing and Gis-Role in IPM. Retrieved 29.09.2015, 2015, <http://www.slideshare.net/srikalamusku/remote-sensing-and-gis-role-in-IPM>
- Shim, D.H., Han, J.S. and Yeo, H.-T. (2009). A Development of Unmanned Helicopters for Industrial Applications. In: Valavanis, K.P., Oh, P. and Pieggl, L.A. (eds), *Unmanned Aircraft Systems*. Springer, Dordrecht, Netherlands, 407-421.
- Slaughter, A.L. (2014). The Utility of Multispectral Imagery from an Unmanned Aircraft System for Detering the Spatial Distribution of Eragrostis Lehmanniana (Lehmann Lovegrass) in Rangelands, New Mexico State University.
- Siddiqi, M.H., Lee, S.-W. and Khan, A.M. (2014). Weed Image Classification Using Wavelet Transform, Stepwise Linear Discriminant Analysis, and Support Vector Machines for an Automatic Spray Control System. *Journal of Information Science and Engineering*, 30(4):1227-1244.
- Smith, A.M. and Blackshaw, R.E. (2003). Weed: Crop Discrimination Using Remote Sensing: A Detached Leaf Experiment. *Weed Technology*, 17(4):811-820.
- Smith, K. and Scott, B. (2010). 7-Weed Control in Grain Sorghum.
- Smit, J., Sithole, G. and Strever, A. (2010). Vine Signal Extraction: An Application of Remote Sensing in Precision Viticulture.
- Smith, A.M. and Blackshaw, R.E. (2003). Weed: Crop Discrimination Using Remote Sensing: a Detached Leaf Experiment. *Weed Technology*, 17(4):811-820.
- Steward, B. and Tian, L. (1999). Machine-Vision Weed Density Estimation for Real-Time, Outdoor Lighting Conditions. *Transactions of the ASAE*, 42(6):1897.
- Sui, R., Thomasson, J.A., Hanks, J. and Wooten, J. (2008). Ground-Based Sensing System for Weed Mapping in Cotton. *Computers and Electronics in Agriculture*, 60(1):31-38.
- Surface Optics Corporation. (2015). Precision Agriculture and Hyperspectral Sensors: Monitoring against Drought, Disease, and Nutrient Stress. Retrieved 02.10.2015, 2015, <https://surfaceoptics.com/applications/precision-agriculture-hyperspectral-sensors/>
- Svensgaard, J., Roitsch, T. and Christensen, S. (2014). Development of a Mobile Multispectral Imaging Platform for Precise Field Phenotyping. *Agronomy*, 4(3):322-336.
- Swain, K.C., Jayasuriya, H. and Salokhe, V. (2007). Low-Altitude Remote Sensing with Unmanned Radio-Controlled Helicopter Platforms: A Potential Substitution to Satellite-Based Systems for Precision Agriculture Adoption under Farming Conditions in Developing Countries. *Agriculture Engineering International*, 9(12).
- Syngenta (2015a). Dualgold Herbicides (960 G/L S-Metolachlor, (Serial online). Available from URL:<http://www3.syngenta.com/country/ke/en/products/selectiveherbicides/Pages/dualgold960ec.aspx>.
- Syngenta (2015b). Flowable Gesaprin 600 Sc Liquid Herbicides (600 G/L Altrazine), (Serial online). Available from URL: <http://www3.syngenta.com/country/au/SiteCollectionDocuments/Labels/GESAPRIM%20600%20SC%20-%20website%20bl%20-%2053892-0610.pdf>.
- Tang, L., Tian, L.F. and Steward, B.L. (2000). Color Image Segmentation with Genetic Algorithm for in-Field Weed Sensing. *Transactions of the American Society of Association Executives*, 43(4):1019.
- Tetracam. (2015). Micro-MCA 6. Retrieved 22.09.2015, 2015, http://www.tetracam.com/Products-Micro_MCA.htm

- Thenkabail, P.S. (2015). *Remotely Sensed Data Characterization, Classification, and Accuracies*. CRC Press.
- Thenkabail, P.S., Enclona, E.A., Ashton, M.S. and Van Der Meer, B. (2004). Accuracy Assessments of Hyperspectral Waveband Performance for Vegetation Analysis Applications. *Remote Sensing of Environment*, 91(3–4):354-376.
- Thenkabail, P.S., Smith, R.B. and De Pauw, E. (2000). Hyperspectral Vegetation Indices and Their Relationships with Agricultural Crop Characteristics. *Remote Sensing of Environment*, 71(2):158-182.
- Thenkabail, P.S., Smith, R.B. and De Pauw, E. (2002). Evaluation of Narrowband and Broadband Vegetation Indices for Determining Optimal Hyperspectral Wavebands for Agricultural Crop Characterization. *Photogrammetric Engineering and Remote Sensing*, 68(6):607-621.
- Tormos, T., Kosuth, P., Durrieu, S., Dupuy, S., Villeneuve, B. and Wasson, J. (2012). Object-Based Image Analysis for Operational Fine-Scale Regional Mapping of Land Cover within River Corridors from Multispectral Imagery and Thematic Data. *International journal of remote sensing*, 33(14):4603-4633.
- Torres-Sanchez, J., López-Granados, F., De Castro, A.I. and Peña-Barragán, J.M. (2013a). Configuration and Specifications of an Unmanned Aerial Vehicle (UAV) for Early Site Specific Weed Management, *PloS ONE*, (Serial online), 8(3). Available from URL: <http://www.ncbi.nlm.nih.gov/pmc/articles/PMC3590160/pdf/pone.0058210.pdf>.
- Torres-Sánchez, J., López-Granados, F. and Peña, J. (2015). An Automatic Object-Based Method for Optimal Thresholding in UAV Images: Application for Vegetation Detection in Herbaceous Crops. *Computers and electronics in Agriculture*, 114:43-52.
- Torres-Sanchez, J., Peña, J., de Castro, A. and López-Granados, F. (2014). Multi-Temporal Mapping of the Vegetation Fraction in Early-Season Wheat Fields Using Images from UAV. *Computers and Electronics in Agriculture*, 103:104-113.
- Torres-Sospedra, J. and Nebot, P. (2014). Two-Stage Procedure Based on Smoothed Ensembles of Neural Networks Applied to Weed Detection in Orange Groves. *Biosystems Engineering*, 123(0):40-55.
- Tumbo, S., Salyani, M., Whitney, J., Wheaton, T. and Miller, W. (2002). Investigation of Laser and Ultrasonic Ranging Sensors for Measurements of Citrus Canopy Volume. *Applied Engineering in Agriculture*, 18(3):367-372.
- Turner, D., Arko, L., Zbyněk, M., Diana, H., and Sharon, R. (2016). *Co-Registration of Visible, Multispectral and Thermal Imagery Collected over Antarctic Moss Beds*, Proceedings of the UAS4RS Conference 2016 University of Queensland.
- Turner, D., Lucieer, A. and Watson, C. (2012). An Automated Technique for Generating Georectified Mosaics from Ultra-High Resolution Unmanned Aerial Vehicle (UAV) Imagery, Based on Structure from Motion (Sfm) Point Clouds. *Remote Sensing*, 4(5):1392-1410.
- Underwood, E., Mulitsch, M., Greenberg, J., Whiting, M., Ustin, S. and Kefauver, S. (2006). Mapping Invasive Aquatic Vegetation in the Sacramento-San Joaquin Delta Using Hyperspectral Imagery. *Environmental Monitoring and Assessment*, 121(1-3):47-64.
- University of Texas. (2015). Classification Accuracy Assessment. *Lecture 9*. Retrieved 02.03.2016, 2016, <http://www.utsa.edu/lrsg/teaching/ees5083/19-classaccuracy.pdf>
- University of Hawaii. (2009). Remote Sensing of Invasive Species in Makaha Valley. Retrieved 29.09.2015, 2015, http://www.ctahr.hawaii.edu/miuralab/projects/makaha/intro_RS.html
- University of Illinois. (2012). Sorghum Growth Stage Development. Retrieved 30.08.2015, 2015, <http://weedsoft.unl.edu/documents/growthstagesmodule/sorghum/sorg.htm#>
- United State Department of Agriculture (USDA). (2016). Australia Sorghum Production by year. <http://www.indexmundi.com/agriculture/?country=au&commodity=sorghum&graph=production> (Assessed April 12, 2016).

- Vaiphasa, C., Ongsomwang, S., Vaiphasa, T. and Skidmore, A.K. (2005). Tropical Mangrove Species Discrimination Using Hyperspectral Data: A Laboratory Study. *Estuarine, Coastal and Shelf Science*, 65(1–2):371-379.
- Van der Wal, T., Abma, B., Viguria, A., Prévinaire, E., Zarco-Tejada, P., Serruys, P., van Valkengoed, E. and van der Voet, P. (2013). Fieldcopter: Unmanned Aerial Systems for Crop Monitoring Services, *Precision Agriculture '13*. Springer, 169-175.
- Vanderlip, R. (1993). *How a Sorghum Plant Develops*. Kansas State University, U.S.A, Kansas State University, U.S.A.
- Visser, F. and Wallis, C. (2010). Object-Based Analysis and Multispectral Low-Altitude Remote Sensing for Low-Cost Mapping of Chalk Stream Macrophytes. *The International Archives of the Photogrammetry, Remote Sensing and Spatial Information Sciences*, 37(I-4/C7).
- Voss, K., Franke, J., Mewes, T., Menz, G. and Kühbauch, W. (2010). Remote Sensing for Precision Crop Protection – a Matter of Scale. In: Oerke, E.-C., Gerhards, R., Menz, G. and Sikora, R.A. (eds), *Precision Crop Protection: The Challenge and Use of Heterogeneity*. Springer, Dordrecht, Netherlands, 101-118.
- Vrindts, E., De Baerdemaeker, J. and Ramon, H. (2002). Weed Detection Using Canopy Reflection. *Precision Agriculture*, 3(1):63-80.
- Wallace, L., Lucieer, A., Watson, C. and Turner, D. (2012). Development of a UAV-LiDAR System with Application to Forest Inventory. *Remote Sensing*, 4(6):1519-1543.
- Weidner, U. (2008). Contribution to the Assessment of Segmentation Quality for Remote Sensing Applications. *International Archives of Photogrammetry, Remote Sensing and Spatial Information Sciences*, 37(B7):479-484.
- Whiteside, T. and Bartolo, R., (eds) (2016). *Monitoring the Vegetation Success of a Rehabilitated Mine Site Using Multispectral UAV Imagery*, Proceedings of the UAS4RS Conference; 2016 University of Queensland.
- Whiteside, T., Maier, S. and Boggs, G. (2012). Site-Specific Area-Based Validation of Classified Objects. *Proceedings of the 4th GEOgraphic-Object-Based Image Analysis, Rio de Janeiro, Brazil*:153-157.
- Widderick. (2009, 17.09.2009). Common Sowthistle and Flaxleaf Fleabane. Understanding the Weeds Lifecycles for Management Strategies That Work. Retrieved 25.08.2015, 2015, <https://www.grdc.com.au/Research-and-Development/GRDC-Update-Papers/2009/09/COMMON-SOWTHISTLE-AND-FLAXLEAF-FLEABANE-UNDERSTANDING-THE-WEEDS-LIFECYCLES-FOR-MANAGEMENT-STRATEGIES-THAT-WORK>
- Wilson, J.H., Zhang, C. and Kovacs, J.M. (2014). Separating Crop Species in Northeastern Ontario Using Hyperspectral Data. *Remote Sensing*, 6(2):925-945.
- Winter, S. (2000). Location Similarity of Regions. *ISPRS Journal of Photogrammetry and Remote Sensing*, 55(3):189-200.
- Wollenhaupt, N. and Wolkowski, R. (1994). Grid Soil Sampling. *Better Crops*, 78(4):6-9.
- Wood, P. (2000). *Weeds: The Ute Guide : Northern Grain Belt Edition*. Farming Systems Institute, Toowoomba, Queensland.
- Xiang, H. and Tian, L. (2011). Method for Automatic Georeferencing Aerial Remote Sensing (Rs) Images from an Unmanned Aerial Vehicle (UAV) Platform. *Biosystems Engineering*, 108(2):104-113.
- Xing, J., Bravo, C., Moshou, D., Ramon, H. and De Baerdemaeker, J. (2006). Bruise Detection on 'Golden Delicious' Apples by Vis/NIR Spectroscopy. *Computers and Electronics in Agriculture*, 52(1):11-20.
- Yan, L., Gou, Z. and Duan, Y. (2009). A Uav Remote Sensing System: Design and Tests. In: Li, D., Shan, J. and Gong, J. (eds), *Geospatial Technology for Earth Observation*. Springer, New York, 27-44.

- Yang, C. and Everitt, J. (2010a). Comparison of Hyperspectral Imagery with Aerial Photography and Multispectral Imagery for Mapping Broom Snakeweed. *International Journal of Remote Sensing*, 31(20):5423-5438.
- Yang, C. and Everitt, J.H. (2010b). Mapping Three Invasive Weeds Using Airborne Hyperspectral Imagery. *Ecological Informatics*, 5(5):429-439.
- Yang, C.H., Everitt, J.H. and Goolsby, J.A. (2011). Mapping Giant Reed (*Arundo Donax*) Infestations Along the Texas-Mexico Portion of the Rio Grande with Aerial Photography. *Invasive Plant Science and Management*, 4(4):402-410.
- Ye, X.J., Sakai, K., Asada, S.I. and Sasao, A. (2007). Use of Airborne Multispectral Imagery to Discriminate and Map Weed Infestations in a Citrus Orchard. *Weed Biology and Management*, 7(1):23-30.
- Zaman, A., M., Vergara, O., Araus, J., Tarekegne, A., Magorokosho, C., Zarco-Tejada, P., Hornero, A., Albà, A.H., Das, B. and Craufurd, P. (2015). Unmanned Aerial Platform-Based Multi-Spectral Imaging for Field Phenotyping of Maize. *Plant Methods*, 11(1):35.
- Zhang, N., Ning, W., John, K. and Floyd D., (1998). *Potential Use of Plant Spectral Characteristics in Weed Detection*, Proceedings of the American Society of Association Executives; 12 - 16 July 1998 Florida.
- Zimdahl, R.L. (2013). *Fundamentals of Weed Science*. Academic Press.
- Zwiggelaar, R. (1998). A Review of Spectral Properties of Plants and Their Potential Use for Crop/Weed Discrimination in Row-Crops. *Crop Protection*, 17(3):189-206.

Appendices.

Appendix A

R Code

```
# setwd("E:/Hardisk 500 Gb/3rd EXP 2014/Spectral Reading/1. 11 Dec 2014 9 30 am Full
Rage")
# setwd("E:/Hardisk 500 Gb/3rd EXP 2014/Spectral Reading/2. 14 Dec 14 Spectral data dan
MCA Data")
setwd("E:/Hardisk 500 Gb/3rd EXP 2014/Spectral Reading/3. 21 Dec 14 Spectral Data")
# Select the appropriate working directory above using comment symbol.
masterlist=read.csv("FileID.csv")
# We assume that the individual data files are in a subfolder called ASCII in the current working
folder masterlist$FileName = paste0("ASCII/",masterlist$SpectrumID,".asd.txt")
library(reshape)
# Ensure that the variable names in the FileID file are correct. They MUST be correctly named -
including case
# as SpectrumID, Week, Crop, Plant and Rep. Order is not important, but naming is.

# Create a dummy data frame to act as a base that we append data to
# The variables here - other than the first 2 - must correspond to the first row of FileID
V1 <- c(5000)
V2 <- c(0.00000001)
Week <- c("WK0")
Crop <- c("XX")
Plant <- c(0)
Rep <- c("R0")
allspec<-data.frame(V1, V2, Week, Crop, Plant, Rep)

# Now loop through the contents of our master list
for (i in 1:length(masterlist$FileName)) {
  tmp1<-read.delim(file=masterlist$FileName[i],skip=36,header=F)
  # add in the extra identifying information
  tmp1$Week = masterlist$Week[i]
  tmp1$Crop = masterlist$Crop[i]
  tmp1$Plant = masterlist$Plant[i]
  tmp1$Rep = masterlist$Rep[i]
  # now we need to append the data frame we have just built to our base
  allspec <- rbind(allspec,tmp1)
}
```

```
# A bit of tidying up at the end
allspec=rename(allspec, c(V1="Wavelength", V2="Reflectance"))
rm(V1, V2, Week, Crop, Plant, Rep, tmp1)
# The following writes the combined data out as a csv in the current working directory
write.csv(allspec,"temp.csv",row.names=FALSE)
```

**Appendix B. Three-band combinations of seven
available band-pass filters (2013)**

3-band combinations	Bands (nm)		
Combination 1	660	680	710
Combination 2	660	680	720
Combination 3	660	680	730
Combination 4	660	680	750
Combination 5	660	680	830
Combination 6	660	710	720
Combination 7	660	710	730
Combination 8	660	710	750
Combination 9	660	710	830
Combination 10	660	720	730
Combination 11	660	720	750
Combination 12	660	720	830
Combination 13	660	730	750
Combination 14	660	730	830
Combination 15	660	750	830
Combination 16	680	710	720
Combination 17	680	710	730
Combination 18	680	710	750
Combination 19	680	710	830
Combination 20	680	720	730
Combination 21	680	720	750
Combination 22	680	720	830
Combination 23	680	730	750
Combination 24	680	730	830
Combination 25	680	750	830
Combination 26	710	720	730
Combination 27	710	720	750
Combination 28	710	720	830
Combination 29	710	730	750
Combination 30	710	730	830
Combination 31	710	750	830
Combination 32	720	730	750
Combination 33	720	730	830
Combination 34	720	750	830
Combination 35	730	750	830

**Appendix C. Six-band combinations of eight available
band-pass filters (2013)**

6-band combinations	Bands (nm)					
Combination 1	440	560	680	710	720	730
Combination 2	440	560	680	710	720	750
Combination 3	440	560	680	710	720	850
Combination 4	440	560	680	710	730	750
Combination 5	440	560	680	710	730	850
Combination 6	440	560	680	710	750	850
Combination 7	440	560	680	720	730	750
Combination 8	440	560	680	720	730	850
Combination 9	440	560	680	720	750	850
Combination 10	440	560	680	730	750	850
Combination 11	440	560	710	720	730	750
Combination 12	440	560	710	720	730	850
Combination 13	440	560	710	720	750	850
Combination 14	440	560	710	730	750	850
Combination 15	440	560	720	730	750	850
Combination 16	440	680	710	720	730	750
Combination 17	440	680	710	720	730	850
Combination 18	440	710	720	730	750	850
Combination 19	440	680	710	730	750	850
Combination 20	440	680	720	730	750	850
Combination 21	440	710	720	730	750	850
Combination 22	560	680	710	720	730	750
Combination 23	560	680	710	720	730	850
Combination 24	560	680	710	720	750	850
Combination 25	560	680	710	720	750	850
Combination 26	560	680	720	730	750	850
Combination 27	560	710	720	730	750	850
Combination 28	680	710	720	730	750	850

Appendix D. The combination of five bands based on six most accurate for Validation 2014 data

Combination bands	Bands (nm)				
Combination 1	720	440	560	680	710
Combination 2	720	440	560	680	850
Combination 3	720	440	680	710	850
Combination 4	720	560	680	710	850
Combination 5	440	560	680	710	850

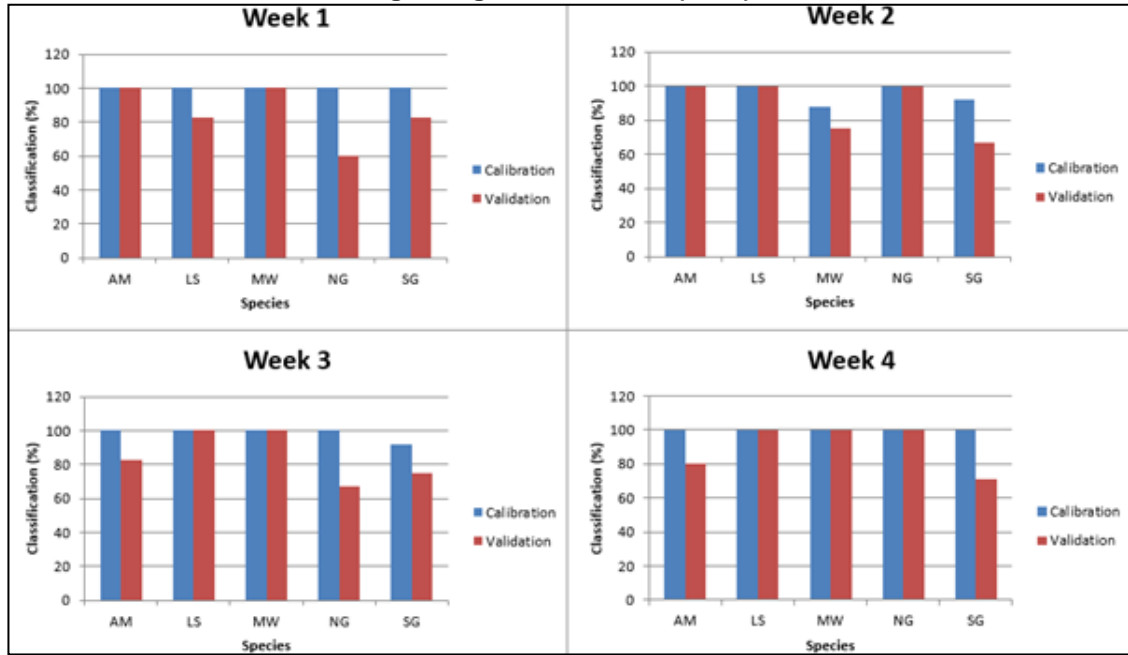
Appendix E The combination of four bands based on six most accurate for Validation data 2014

Combination bands	Bands (nm)			
Combination 1	720	440	560	680
Combination 2	720	440	560	710
Combination 3	720	440	560	850
Combination 4	720	440	680	710
Combination 5	720	440	680	850
Combination 6	720	440	710	850
Combination 7	720	560	680	710
Combination 8	720	560	680	850
Combination 9	720	560	710	850
Combination 10	720	680	710	850
Combination 11	440	560	680	710
Combination 12	440	560	680	850
Combination 13	560	680	710	850

Appendix F The combination of three bands of the six most accurate for Validation data 2014

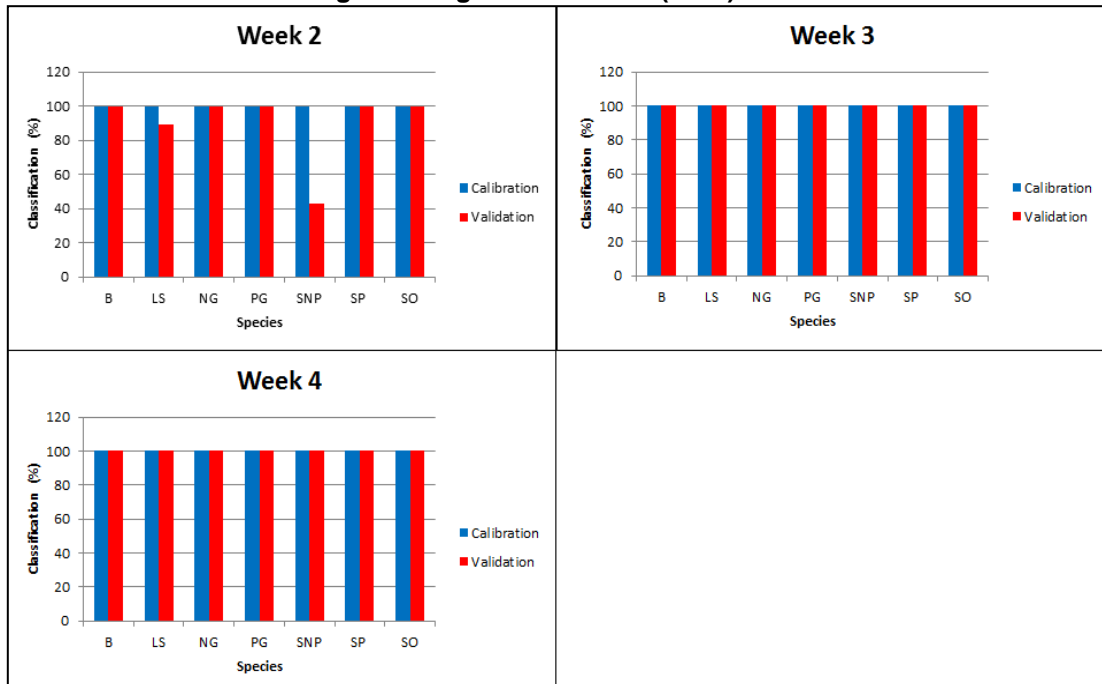
Combination bands	Bands (nm)		
Combination 1	720	440	560
Combination 2	720	440	680
Combination 3	720	440	710
Combination 4	720	440	850
Combination 5	720	560	680
Combination 6	720	560	710
Combination 7	720	560	850
Combination 8	720	680	710
Combination 9	720	680	850
Combination 10	720	710	850
Combination 11	440	560	680
Combination 12	440	560	710
Combination 13	440	560	850
Combination 14	560	680	710
Combination 15	560	680	850
Combination 16	680	710	850

Appendix G. Calibration and validation analysis for weeks one – four using 20 significant bands (2013)



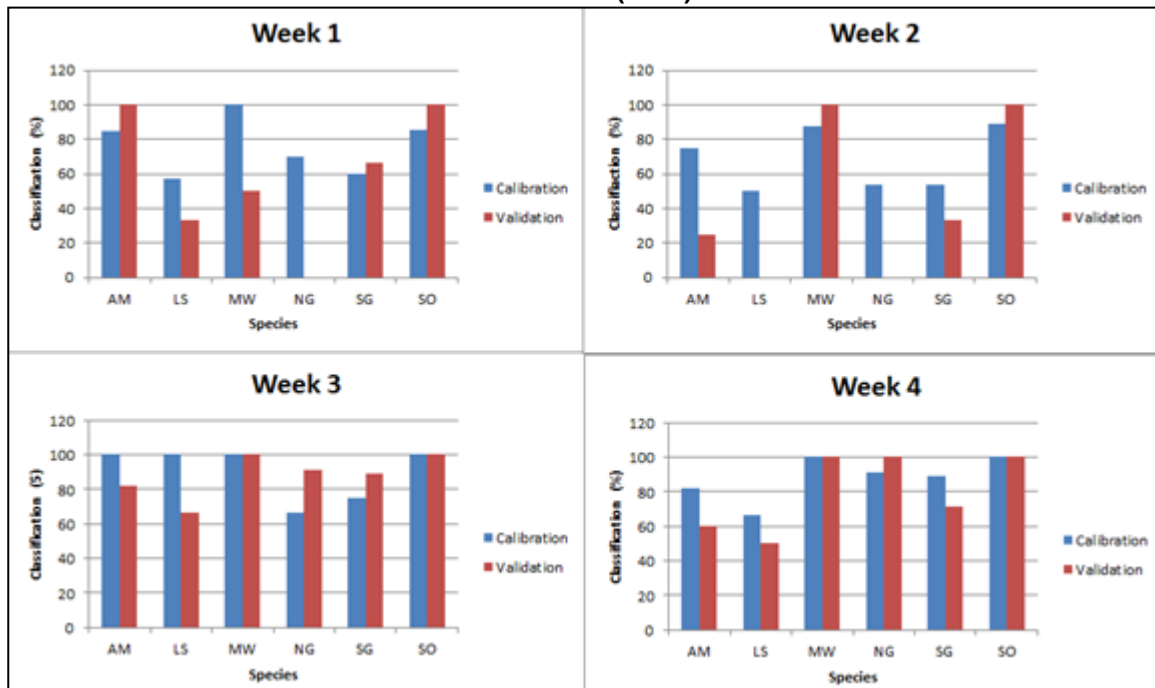
AM = Amaranth, LS = Liverseed Grass, MW = Mallow Weed, NG = Nutgrass and SG = Sorghum

Appendix H. Calibration and validation analysis for week two – four using all 20 significant bands (2014)



B = Bellvine, LS = Liverseed Grass, NG = Nutgrass, PG = Pigweed, SNP = Sorghum non Pre-emergence, SP = Sorghum Pre-emergence and SO = Soil


Appendix I. Calibration and validation analysis for weeks one – four using eight available bands (2013)



AM = Amaranth, LS = Liverseed Grass, MW = Mallow Weed, NG = Nutgrass and SG = Sorghum and SO = Soil


**Appendix J Classification results for all 6-band combinations based
on the bands in Appendix C**

Combination Number	6 bands combination (nm)	AM (%)	LS (%)	MW (%)	NG (%)	Mean (%)
1	440, 560, 680, 710, 720, 730	43	100	100	100	86
2	440, 560, 680, 710, 720, 750	43	100	100	100	86
3	440, 560, 680, 710, 720, 850	71	100	100	100	93
4	440, 560, 680, 710, 730, 750	43	100	100	100	86
5	440, 560, 680, 710, 730, 850	29	100	100	100	82
6	440, 560, 680, 710, 750, 850	43	100	100	75	80
7	440, 560, 680, 720, 730, 750	43	100	100	100	86
8	440, 560, 680, 720, 730, 850	43	100	100	100	86
9	440, 560, 680, 720, 750, 850	43	100	100	100	86
10	440, 560, 680, 730, 750, 850	43	100	100	100	86
11	440, 560, 710, 720, 730, 750	43	100	100	100	86
12	440, 560, 710, 720, 730, 850	43	100	100	100	86
13	440, 560, 710, 720, 750, 850	43	100	100	100	86
14	440, 560, 710, 730, 750, 850	57	100	100	100	89
15	440, 560, 720, 730, 750, 850	57	100	100	100	89
16	440, 680, 710, 720, 730, 750	71	100	50	100	80
17	440, 680, 710, 720, 730, 850	57	100	75	100	83
18	440, 710, 720, 730, 750, 850	57	67	50	100	69
19	440, 680, 710, 730, 750, 850	57	100	50	100	77
20	440, 680, 720, 730, 750, 850	57	100	50	75	71
21	440, 710, 720, 730, 750, 850	57	67	50	100	69
22	560, 680, 710, 720, 730, 750	57	100	100	100	89
23	560, 680, 710, 720, 730, 850	57	100	100	100	89
24	560, 680, 710, 720, 750, 850	43	100	100	100	86
25	560, 680, 710, 720, 750, 850	43	100	100	100	86
26	560, 680, 720, 730, 750, 850	29	100	75	50	64
27	560, 710, 720, 730, 750, 850	57	100	100	100	89
28	680, 710, 720, 730, 750, 850	71	67	50	100	72

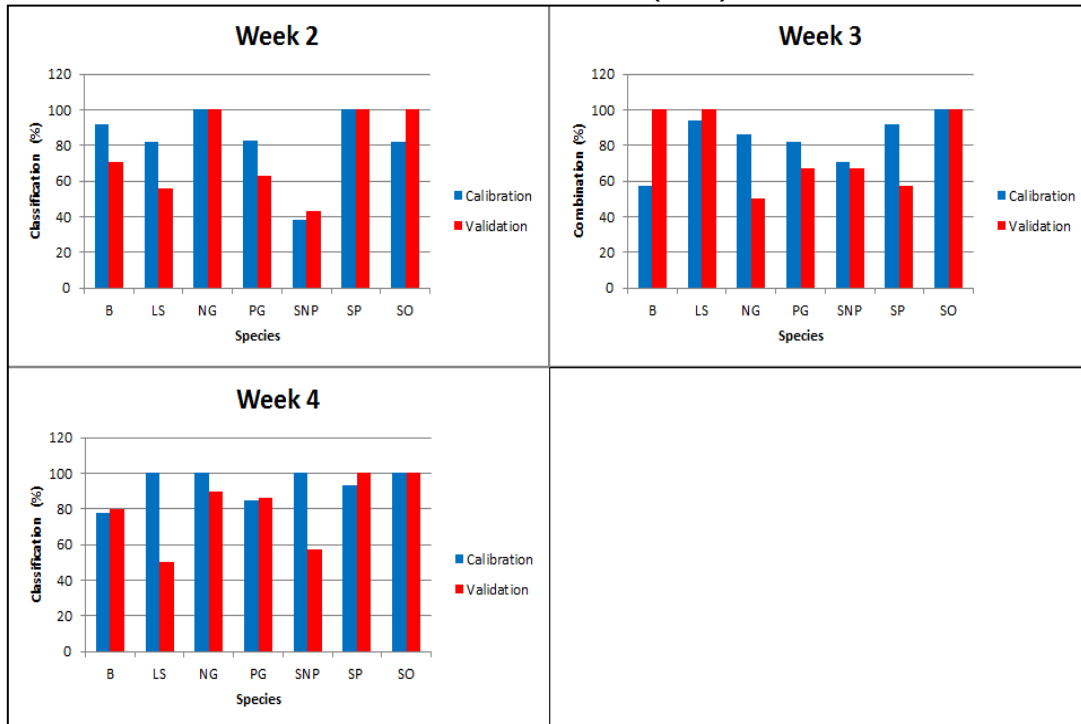
 = The high accuracy, AM = Amaranth, Liverseed Grass = LS, Mallow Weed = MW, NG = Nut Grass

Appendix K. Classification results for all 3-band combinations based on the bands in Appendix B

Combination Number	3 bands combination (nm)	AM (%)	LS (%)	MW (%)	NG (%)	Mean (%)
1	660, 680, 710	80	50	100	100	83
2	660, 680, 720	80	50	75	100	76
3	660, 680, 730	60	33	50	100	61
4	660, 680, 750	80	33	50	100	66
5	660, 680, 850	80	17	50	100	62
6	660, 710, 720	0	50	100	100	63
7	660, 710, 730	20	50	75	100	61
8	660, 710, 750	0	50	75	100	56
9	660, 710, 850	33	0	100	20	38
10	660, 720, 730	20	50	75	100	61
11	660, 720, 750	0	50	75	100	56
12	660, 720, 850	0	50	50	100	50
13	660, 730, 750	0	50	25	100	44
14	660, 730, 830	0	33	50	100	46
15	660, 750, 830	0	33	25	75	33
16	680, 710, 720	60	50	100	100	78
17	680, 710, 730	60	50	100	100	78
18	680, 710, 750	60	50	100	50	65
19	680, 710, 830	20	50	100	100	68
20	680, 720, 730	40	67	100	50	64
21	680, 720, 750	60	50	100	50	65
22	680, 720, 830	0	67	100	75	61
23	680, 730, 750	60	67	100	50	69
24	680, 730, 830	60	67	100	50	69
25	680, 750, 830	60	17	100	50	57
26	710, 720, 730	20	33	100	100	63
27	710, 720, 750	0	50	100	100	63
28	710, 720, 850	0	33	100	50	46
29	710, 730, 750	0	50	100	75	56
30	710, 730, 830	0	33	100	75	52
31	710, 750, 830	20	33	100	50	51
32	720, 730, 750	20	50	100	50	55
33	720, 730, 830	0	33	100	75	52
34	720, 750, 830	0	33	100	65	50
35	730, 750, 830	0	33	100	50	46

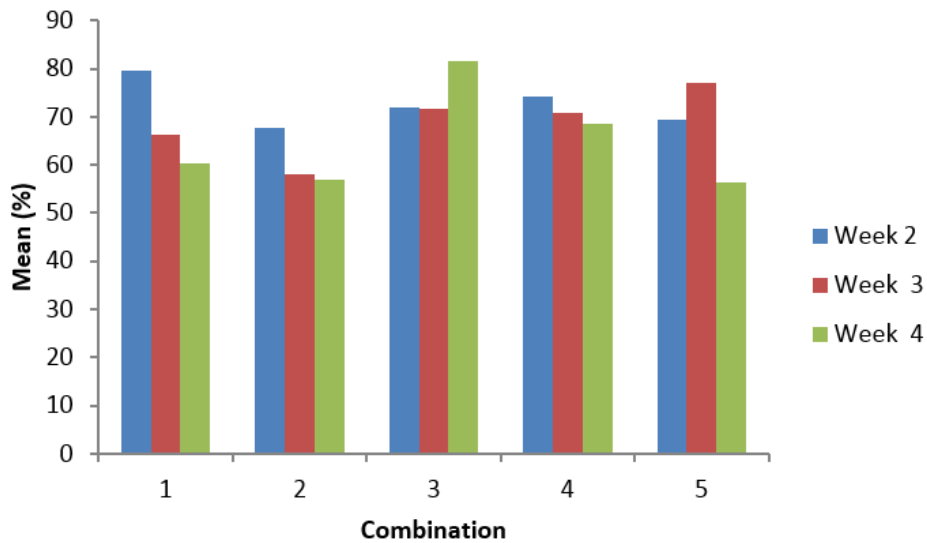
 = The high accuracy, AM = Amaranth, Liverseed Grass = LS, Mallow Weed = MW, NG = Nutgrass

Appendix L. Calibration and validation analysis for weeks two – four using 6-band combinations (2014)



B = Bellvine, LS = Liverseed Grass, NG = Nutgrass , PG = Pigweed, SNP = Sorghum non pre-emergence, SP = Sorghum Pre-emergence

Appendix M Classification accuracy of 5-band combinations (2014)

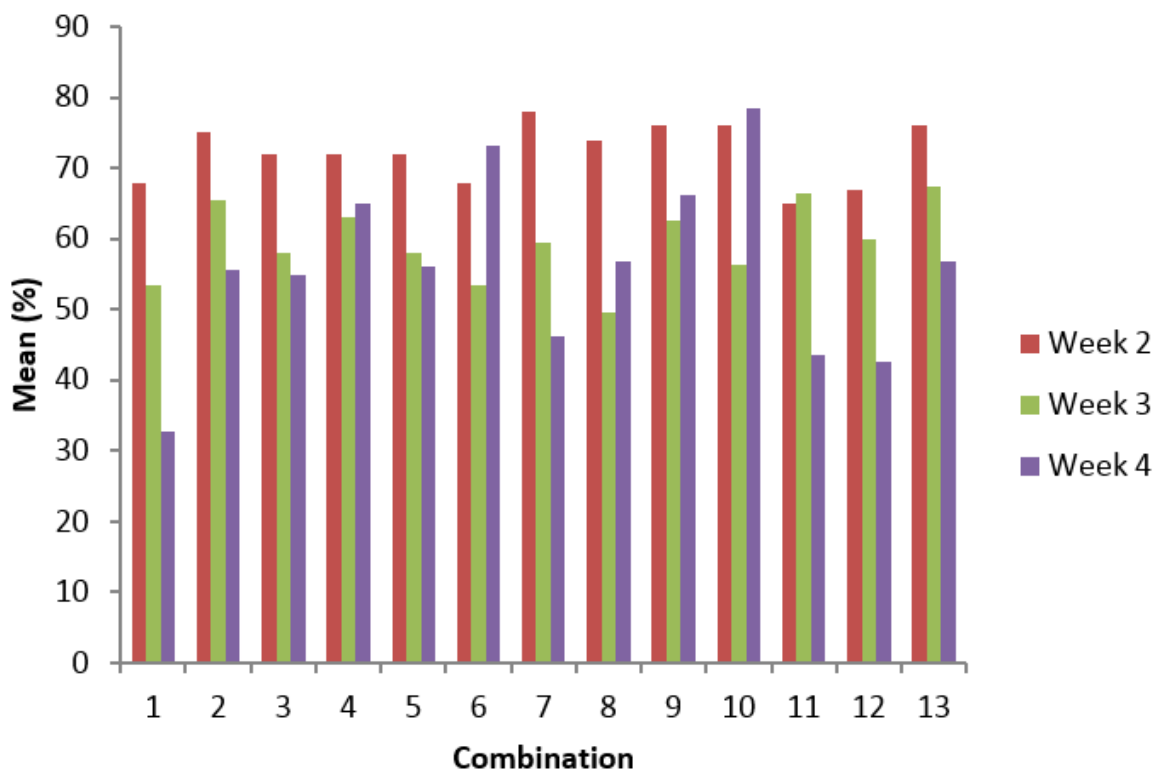


Appendix N. Classification results (%) for all 4-band combinations for 2014

Combinations Number	Combination	B	LS	NG	PG	SNP	SP	Mean
WEEK 2								
1	720, 440, 560, 680 nm	43	56	86	50	43	100	68
2	720, 440, 560, 710 nm	71	78	71	63	43	100	75
3	720, 440, 560, 850 nm	43	67	100	50	43	100	72
4	720, 440, 680, 710 nm	71	56	100	50	29	100	72
5	720, 440, 680, 850 nm	71	56	100	50	29	100	72
6	720, 440, 710, 850 nm	71	67	57	38	43	100	68
7	720, 560, 680, 710 nm	86	56	100	50	57	100	78
8	720, 560, 680, 850 nm	71	67	100	38	43	100	74
9	720, 560, 710, 850 nm	86	78	86	38	43	100	76
10	720, 680, 710, 850 nm	86	56	86	50	57	100	76
11	440, 560, 680, 710 nm	43	56	100	63	29	67	65
12	440, 560, 680, 850 nm	57	44	86	38	43	100	67
13	560, 680, 710, 850 nm	86	67	100	38	43	100	76
WEEK 3								
1	720, 440, 560, 680 nm	83	75	17	56	33	57	53
2	720, 440, 560, 710 nm	100	75	50	78	33	57	66
3	720, 440, 560, 850 nm	100	75	50	33	33	57	58
4	720, 440, 680, 710 nm	83	75	50	67	33	71	63
5	720, 440, 680, 850 nm	83	75	67	33	33	57	58
6	720, 440, 710, 850 nm	83	75	50	22	33	57	53
7	720, 560, 680, 710 nm	67	75	50	89	33	43	60
8	720, 560, 680, 850 nm	50	75	50	33	33	57	50
9	720, 560, 710, 850 nm	83	75	50	44	67	57	63
10	720, 680, 710, 850 nm	67	75	50	56	33	57	56
11	440, 560, 680, 710 nm	83	75	50	100	33	57	66
12	440, 560, 680, 850 nm	83	75	67	11	67	57	60
13	560, 680, 710, 850 nm	50	75	67	56	100	57	68
WEEK 4								
1	720, 440, 560, 680 nm	40	17	50	43	14	33	33
2	720, 440, 560, 710 nm	70	17	80	71	29	67	56
3	720, 440, 560, 850 nm	70	17	60	86	14	83	55
4	720, 440, 680, 710 nm	100	33	60	71	43	83	65
5	720, 440, 680, 850 nm	70	50	50	86	14	67	56
6	720, 440, 710, 850 nm	80	67	80	86	43	83	73
7	720, 560, 680, 710 nm	70	17	70	57	14	50	46
8	720, 560, 680, 850 nm	60	33	80	71	14	83	57
9	720, 560, 710, 850 nm	70	50	80	71	43	83	66
10	720, 680, 710, 850 nm	80	83	80	71	57	100	79
11	440, 560, 680, 710 nm	40	17	30	71	71	33	44
12	440, 560, 680, 850 nm	50	50	30	14	29	83	43
13	560, 680, 710, 850 nm	40	33	70	86	29	83	57

= High accuracy (> 80%), B = Bellvine, LS = Liverseed Grass, NG = Nutgrass, PG = Pigweed, SNP = Sorghum non pre-emergence, and SP = Sorghum Pre-emergence

Appendix O. Classification accuracy of 4-band combinations (2014)

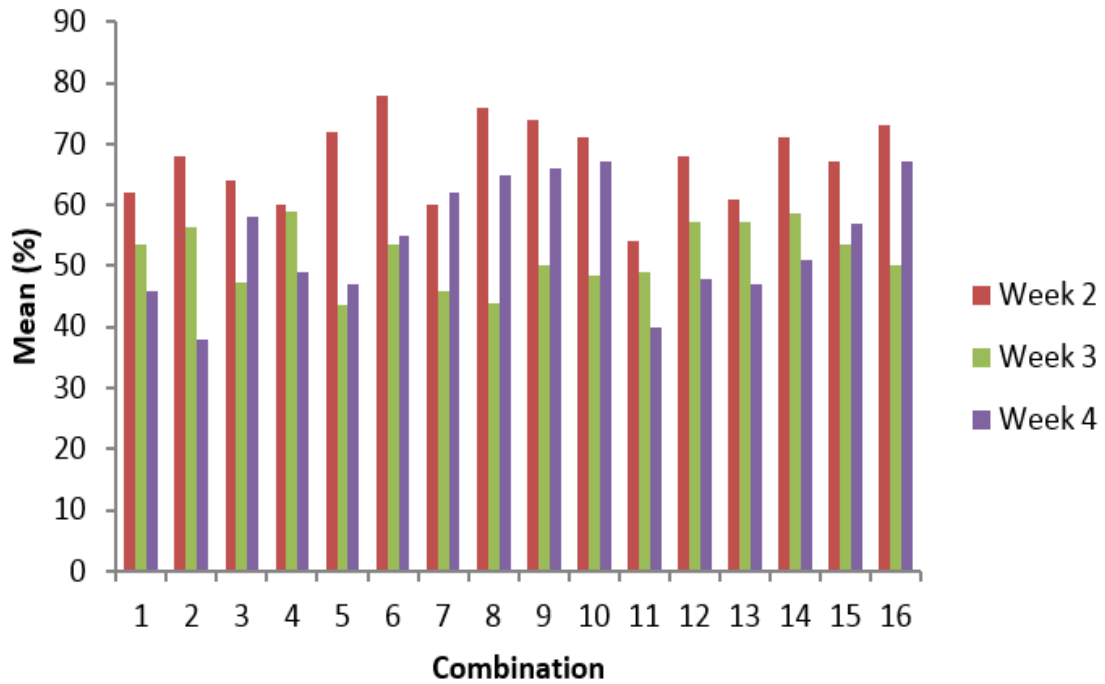


Appendix P. Classification results (%) for all 3-band combinations for 2014

Number	Bands	B	LS	NG	PG	SNP	SP	Mean
WEEK 2								
1	720, 440, 560 nm	85	45	69	58	15	65	62
2	720, 440, 680 nm	43	56	100	50	29	100	68
3	720, 440, 710 nm	43	67	57	38	43	100	64
4	720, 440, 850 nm	71	56	14	50	29	100	60
5	720, 560, 680 nm	57	56	100	50	43	100	72
6	720, 560, 710 nm	86	67	100	38	57	100	78
7	720, 560, 850 nm	71	67	86	50	14	33	60
8	720, 680, 710 nm	71	67	86	50	57	100	76
9	720, 680, 850 nm	86	67	100	38	29	100	74
10	720, 710, 850 nm	86	56	71	38	43	100	71
11	440, 560, 680 nm	29	22	57	25	43	100	54
12	440, 560, 710 nm	43	56	71	63	43	100	68
13	440, 560, 850 nm	71	56	57	50	29	67	61
14	560, 680, 710 nm	71	67	100	50	43	67	71
15	560, 680, 850 nm	57	44	86	38	43	100	67
16	680, 710, 850 nm	86	56	100	38	29	100	73
WEEK 3								
1	720, 440, 560 nm	100	75	00	56	33	57	54
2	720, 440, 680 nm	83	75	33	44	33	71	57
3	720, 440, 710 nm	67	75	33	33	33	43	47
4	720, 440, 850 nm	100	75	67	22	33	57	59
5	720, 560, 680 nm	50	75	17	44	33	43	44
6	720, 560, 710 nm	67	75	50	67	33	29	54
7	720, 560, 850 nm	33	75	33	44	33	57	46
8	720, 680, 710 nm	67	75	33	56	33	0	44
9	720, 680, 850 nm	67	75	50	33	33	43	50
10	720, 710, 850 nm	67	75	50	22	33	43	48
11	440, 560, 680 nm	67	75	17	11	67	57	49
12	440, 560, 710 nm	83	75	17	78	33	57	57
13	440, 560, 850 nm	83	75	50	11	67	57	57
14	560, 680, 710 nm	50	75	50	67	67	42	59
15	560, 680, 850 nm	67	75	67	22	33	57	54
16	680, 710, 850 nm	50	75	67	33	33	43	50
WEEK 4								
1	720, 440, 560 nm	30	33	40	43	29	50	46
2	720, 440, 680 nm	50	17	20	29	14	33	38
3	720, 440, 710 nm	100	17	50	57	29	50	58
4	720, 440, 850 nm	40	17	20	71	14	83	49
5	720, 560, 680 nm	40	17	80	43	14	33	47
6	720, 560, 710 nm	70	17	80	57	14	50	55
7	720, 560, 850 nm	70	17	80	71	14	83	62
8	720, 680, 710 nm	100	33	70	57	14	83	65
9	720, 680, 850 nm	50	50	80	86	14	83	66
10	720, 710, 850 nm	70	67	80	71	14	67	67
11	440, 560, 680 nm	30	17	30	0	71	33	40
12	440, 560, 710 nm	10	17	20	71	71	50	48
13	440, 560, 850 nm	40	17	20	29	43	83	47
14	560, 680, 710 nm	40	17	80	71	14	33	51
15	560, 680, 850 nm	50	50	70	14	29	83	57
16	680, 710, 850 nm	50	50	70	86	29	83	67

= High accuracy (> 80%), B = Bellvine, LS = Liverseed Grass, NG = Nutgrass, PG = Pigweed, SNP = Sorghum non pre-emergence, and SP = Sorghum Pre-emergence

Appendix Q. Classification accuracy of 3-band combinations (2014)

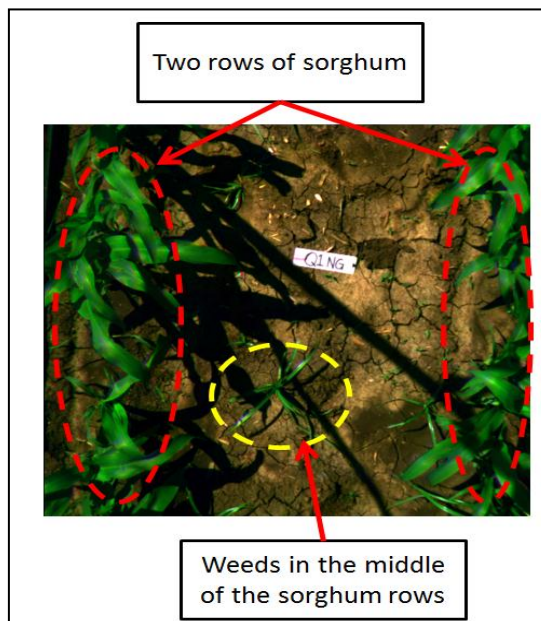


Notes:

The image below illustrates the location of sorghum and weeds from the MCA 6 imagery (before the OBIA classification) to help reader to understand the Appendices R to II.


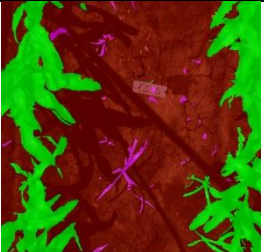
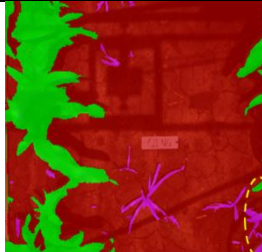
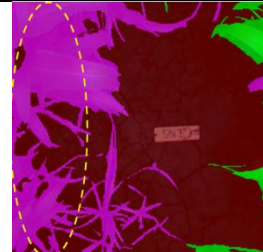

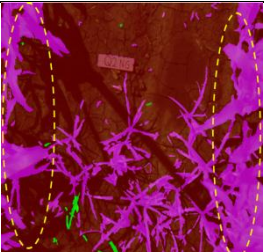
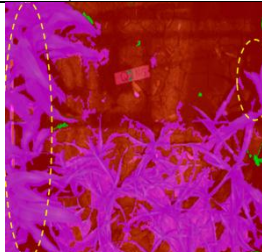
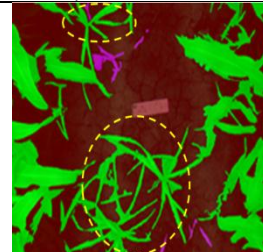

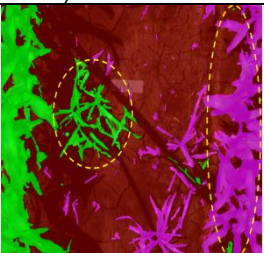
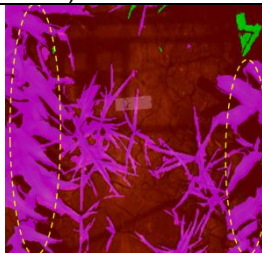
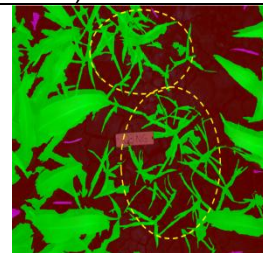


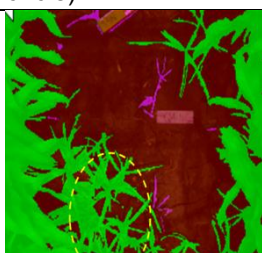
Resolution: 0.87 mm.

Size quadrat: 1 x 1 m.




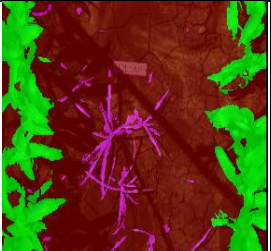
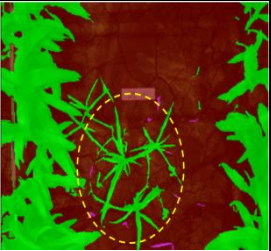
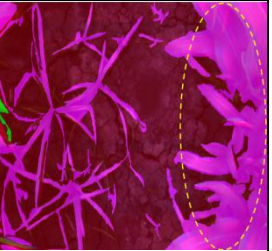
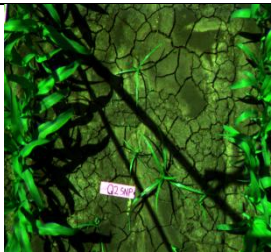
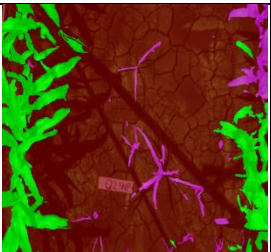
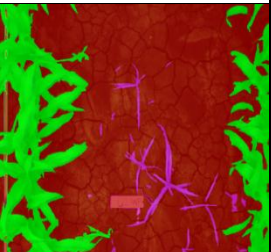

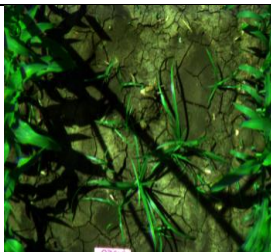
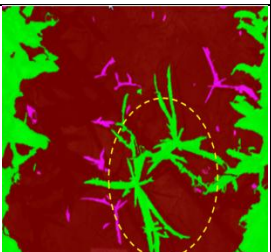
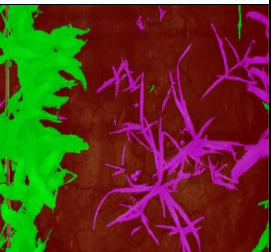
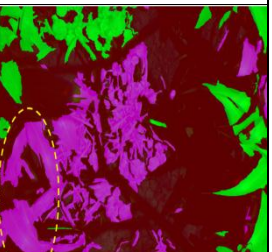

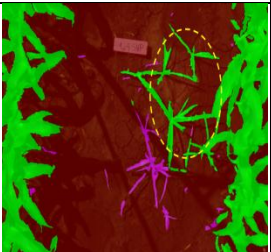
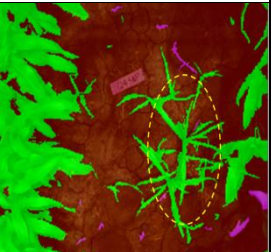
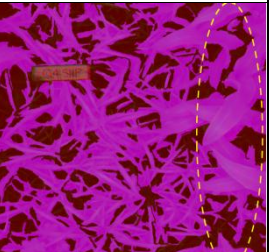
Appendix R. Nutgrass quadrats at two stages of growth for 0.87 resolution

Appendix R shows nutgrass quadrats at two stages of growth for 0.87 resolution. The first column is MCA 6 imagery of weeds and sorghum crop in 1 m x 1 m square and the second, third and fourth columns are classified images using OBIA.

Image (1.6 m)	Week 3		Week 4
	17 December 2014	18 December 2014	23 December 2014
 <p>Q1NG</p>	 <p>Correctly classified</p>	 <p>The misclassification of sorghum (In the circle)</p>	 <p>The misclassification of sorghum (In the circle)</p>
 <p>Q2NG</p>	 <p>The misclassification of sorghum (In the circle)</p>	 <p>The misclassification of sorghum (In the circle)</p>	 <p>The misclassification of weeds (In the circle)</p>
 <p>Q3NG</p>	 <p>The misclassification of sorghum and weeds (In the circle)</p>	 <p>The misclassification of sorghum (In the circle)</p>	 <p>The misclassification of weeds (In the circle)</p>
 <p>Q4NG</p>	 <p>The misclassification of weeds (In the circle)</p>	 <p>The misclassification of weeds (In the circle)</p>	<p>Not available</p>


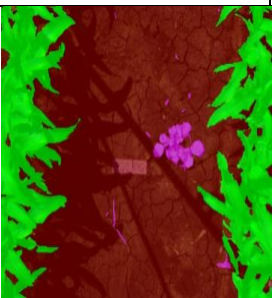
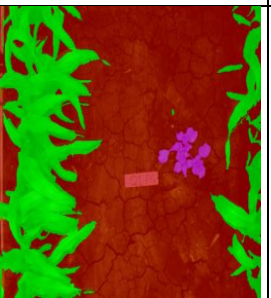
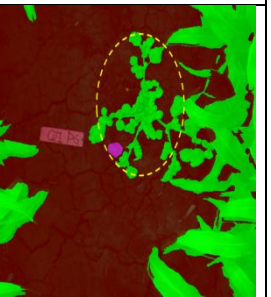

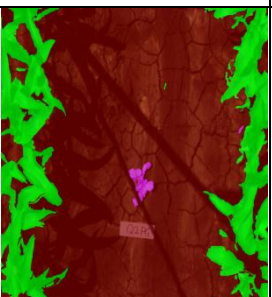

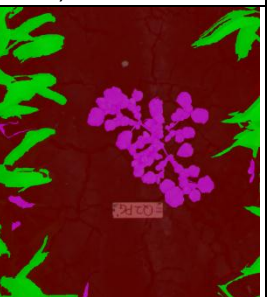

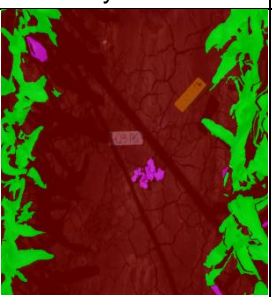

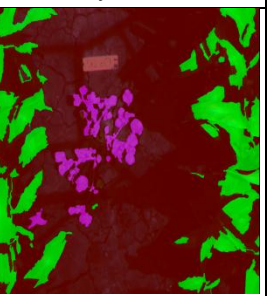

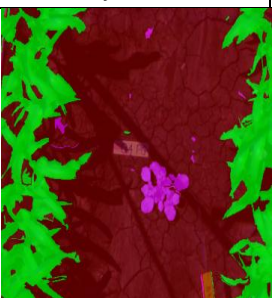


Appendix S. Sorghum non pre-emergence quadrats at two stages of growth for 0.87 resolution

Appendix S shows sorghum non pre-emergence quadrats at two stages of growth for 0.87 resolution. The first column is MCA 6 imagery of weeds and sorghum crop in 1 m x 1 m square and the second, third and fourth columns are classified images using OBIA.

Image (1.6 m)	Week 3		Week 4
	17 December 2014	18 December 2014	23 December 2014
 Q1SNP	 Correctly classified	 The misclassification of weeds (In the circle)	 The misclassification of sorghum (In the circle)
 Q2SNP	 Correctly classified	 Correctly classified	 The misclassification of weeds (In the circle)
 Q3SNP	 The misclassification of weeds (In the circle)	 Correctly classified	 The misclassification of sorghum (In the circle)
 Q4SNP	 The misclassification of weeds (In the circle)	 The misclassification of weeds (In the circle)	 The misclassification of sorghum (In the circle)

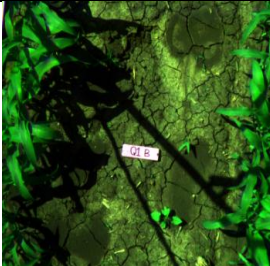
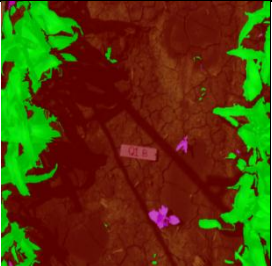
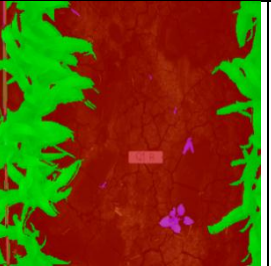
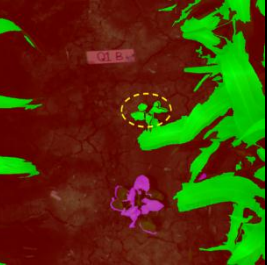
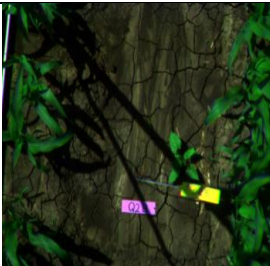
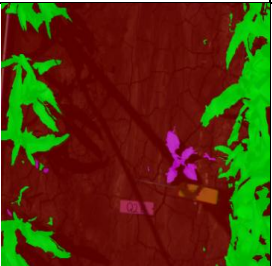

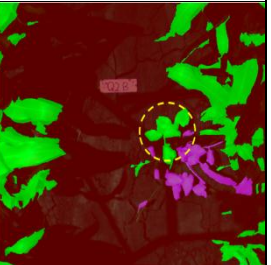
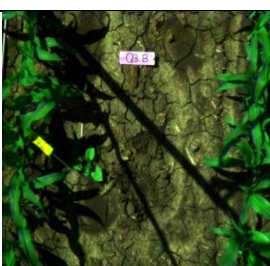
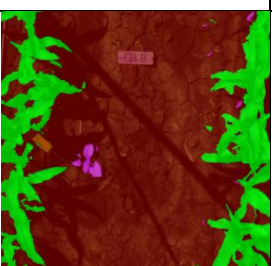
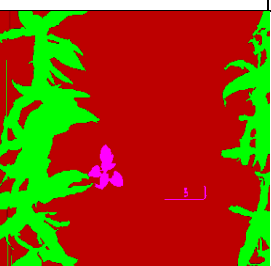
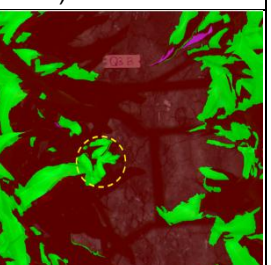

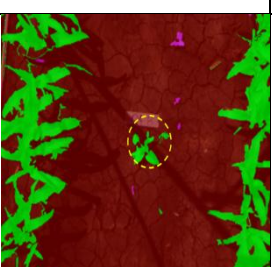
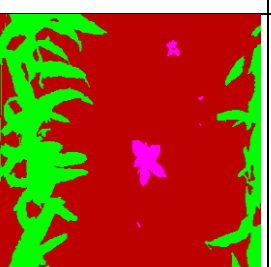

Appendix T. Pigweed quadrats at two stages of growth for 0.87 resolution

Appendix T shows pigweed quadrats at two stages of growth for 0.87 resolution. The first column is MCA 6 imagery of weeds and sorghum crop in 1 m x 1 m square and the second, third and fourth columns are classified images using OBIA.

Image (1.6 m)	Week 3		Week 4
	17 December 2014	18 December 2014	23 December 2014
 Q1PG	 Correctly classified	 Correctly classified	 The misclassification of weeds (In the circle)
 Q2PG	 Correctly classified	 Correctly classified	 Correctly classified
 Q3PG	 Correctly classified	 Correctly classified	 Correctly classified
 Q4PG	 Correctly classified	 Correctly classified	 The misclassification of weeds (In the circle)

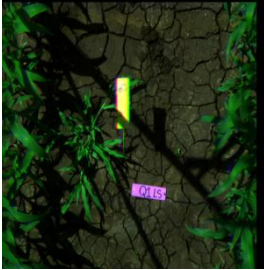
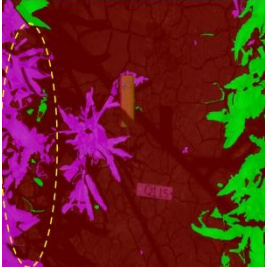
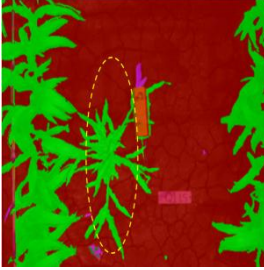

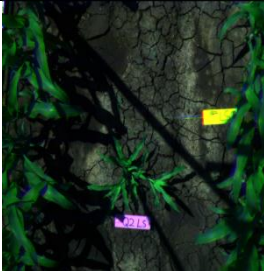
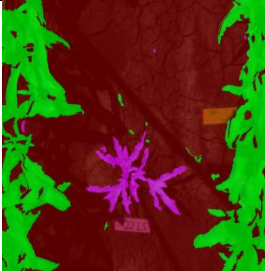

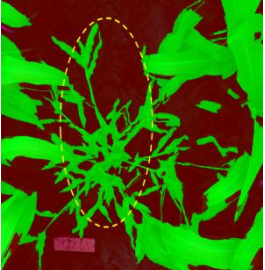
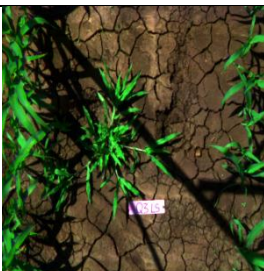
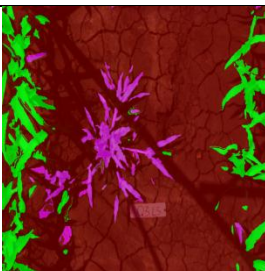
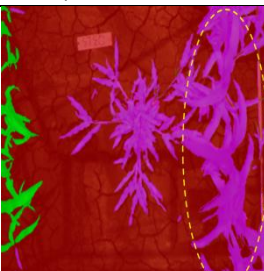
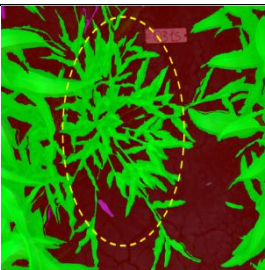
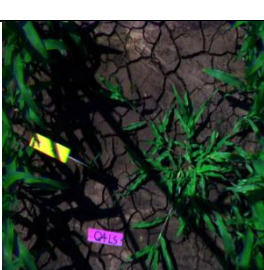
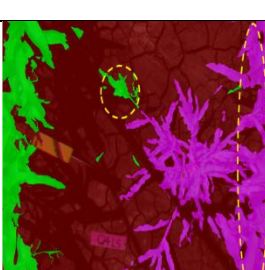


Appendix U. Bellvine quadrats at two stages of growth for 0.87 resolution

Appendix U shows bellvine quadrats at two stages of growth for 0.87 resolution. The first column is MCA 6 imagery of weeds and sorghum crop in 1 m x 1 m square and the second, third and fourth columns are classified images using OBIA.

Image (1.6 m)	Week 3		Week 4
	17 December 2014	18 December 2014	23 December 2014
 <p>Q1B</p>	 <p>Correctly classified</p>	 <p>Correctly classified</p>	 <p>The misclassification of weeds (In the circle)</p>
 <p>Q2B</p>	 <p>Correctly classified</p>	 <p>Correctly classified</p>	 <p>The misclassification of weeds (In the circle)</p>
 <p>Q3B</p>	 <p>Correctly classified</p>	 <p>Correctly classified</p>	 <p>The misclassification of weeds (In the circle)</p>
 <p>Q4B</p>	 <p>The misclassification of weeds (In the circle)</p>	 <p>Correctly classified</p>	 <p>Correctly classified</p>



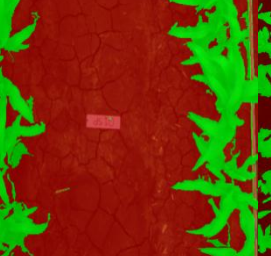
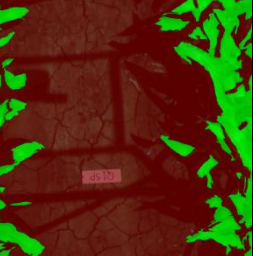



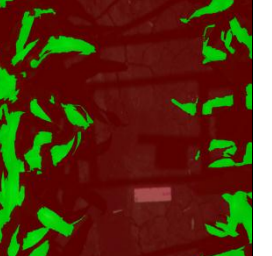

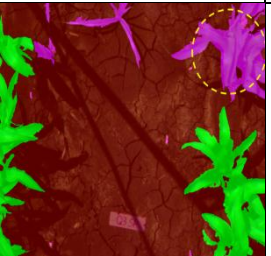
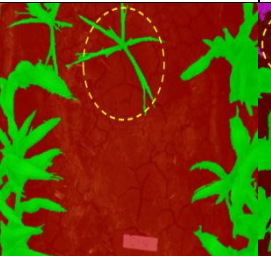
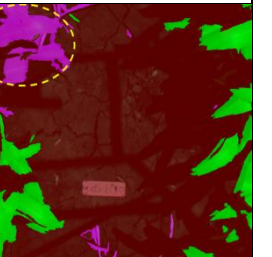



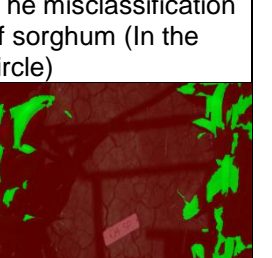
Appendix V. Liverseed grass quadrats at two stages of growth for 0.87 resolution

Appendix V shows liverseed grass quadrats at two stages of growth for 0.87 resolution. The first column is MCA 6 imagery of weeds and sorghum crop in 1 m x 1 m square and the second, third and fourth columns are classified images using OBIA.

Image (1.6 m)	Week 3		Week 4
	17 December 2014	18 December 2014	23 December 2014
 <p>Q1LS</p>	 <p>The misclassification of sorghum (In the circle)</p>	 <p>The misclassification of weeds (In the circle)</p>	 <p>The misclassification of weeds (In the circle)</p>
 <p>Q2LS</p>	 <p>Correctly classified</p>	 <p>The misclassification of sorghum (In the circle)</p>	 <p>The misclassification of weeds (In the circle)</p>
 <p>Q3LS</p>	 <p>Correctly classified</p>	 <p>The misclassification of sorghum (In the circle)</p>	 <p>The misclassification of weeds (In the circle)</p>
 <p>Q4LS</p>	 <p>The misclassification of weeds and sorghum (In the circle)</p>	 <p>The misclassification of weeds and sorghum (In the circle)</p>	 <p>The misclassification of weeds (In the circle)</p>

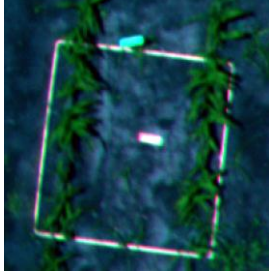
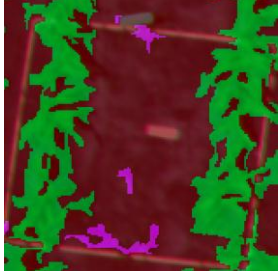
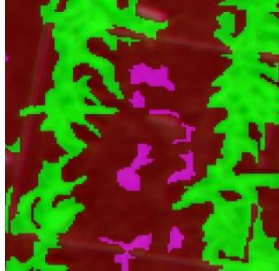
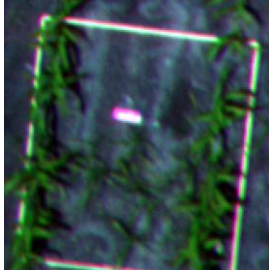
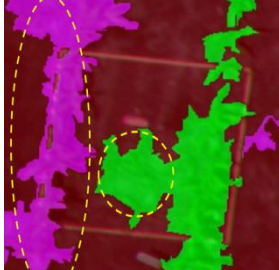
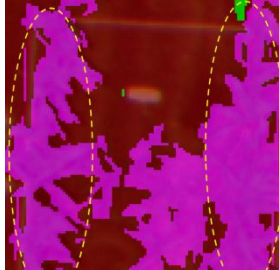
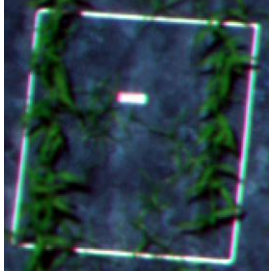
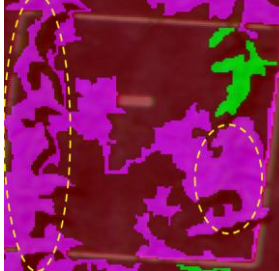
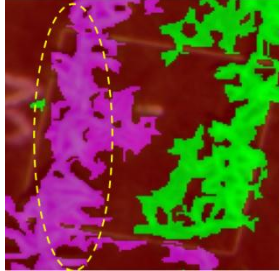
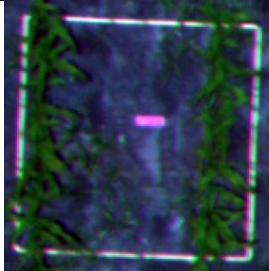
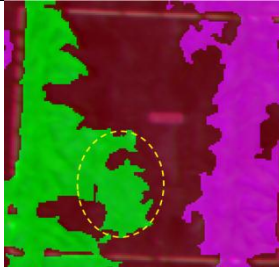
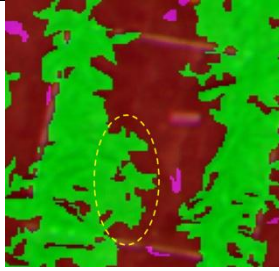
Appendix W. Sorghum pre-emergence quadrats at two stages of growth for 0.87 resolution

Appendix W shows Sorghum pre-emergence quadrats at two stages of growth for 0.87 resolution. The first column is MCA 6 imagery of weeds and sorghum crop in 1 m x 1 m square and the second, third and fourth columns are classified images using OBIA.

Image (1.6 m)	Week 3		Week 4
	17 December 2014	18 December 2014	23 December 2014
 <p>Q1SP</p>	 <p>Correctly classified</p>	 <p>Correctly classified</p>	 <p>Correctly classified</p>
 <p>Q2SP</p>	 <p>Correctly classified</p>	 <p>Correctly classified</p>	 <p>Correctly classified</p>
 <p>Q3SP</p>	 <p>The misclassification of sorghum (In the circle)</p>	 <p>The misclassification of weeds (In the circle)</p>	 <p>The misclassification of sorghum (In the circle)</p>
 <p>Q4SP</p>	 <p>Correctly classified</p>	 <p>Correctly classified</p>	 <p>Correctly classified</p>

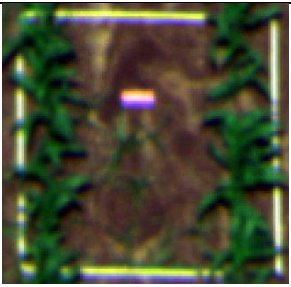
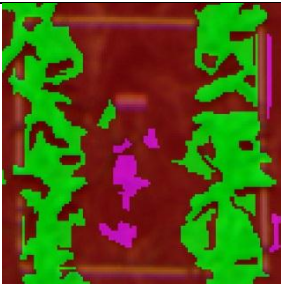
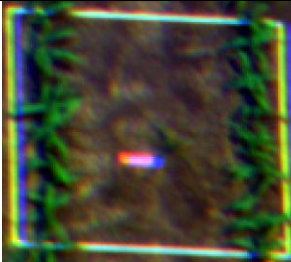
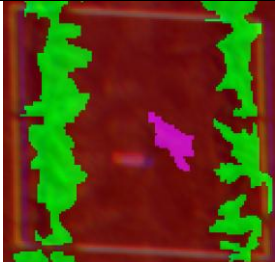
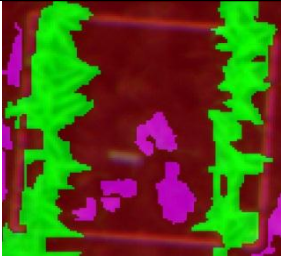
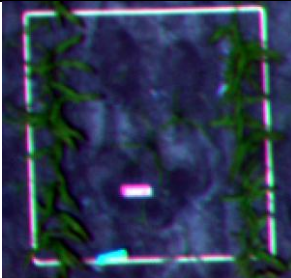
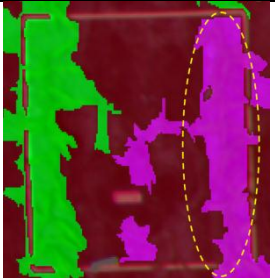
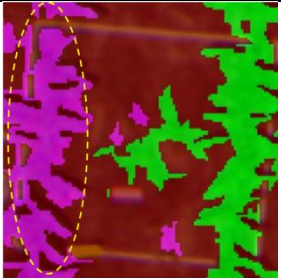
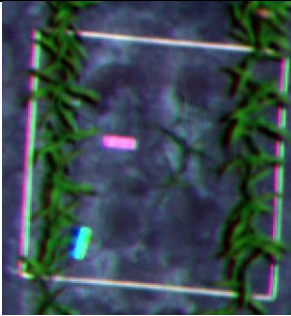
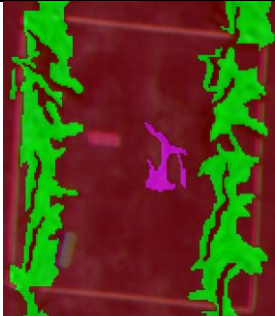
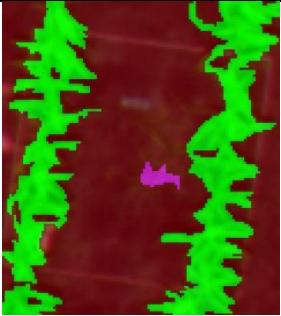
Appendix X. Nutgrass quadrats at week three for 10.83mm resolution

Appendix X shows nutgrass quadrats at two stages of growth for 10.83 mm resolution. The first column is MCA 6 imagery of weeds and sorghum crop in 1 m x 1 m square and the second and third columns are classified images using OBIA

Image (20 m)	Week 3	
	15 December 2014	17 December 2014
 <p>Q1NG</p>	 <p>Correctly classified</p>	 <p>Correctly classified</p>
 <p>Q2NG</p>	 <p>The misclassification of weeds and sorghum (In the circle)</p>	 <p>The misclassification of sorghum (In the circle)</p>
 <p>Q3NG</p>	 <p>The misclassification of sorghum (In the circle)</p>	 <p>The misclassification of sorghum (In the circle)</p>
 <p>Q4NG</p>	 <p>The misclassification of weeds (In the circle)</p>	 <p>The misclassification of weeds (In the circle)</p>

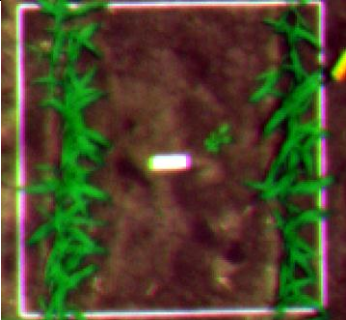
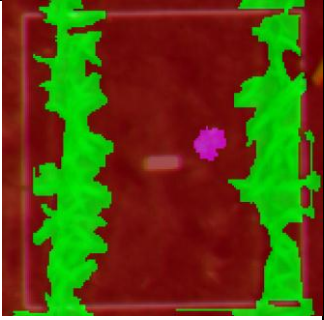
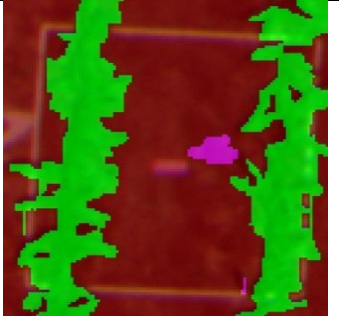
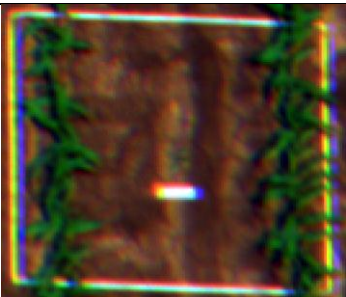
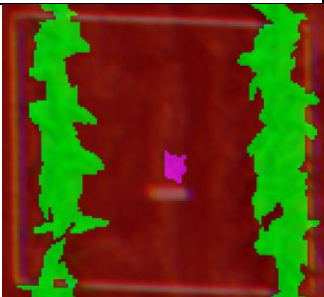
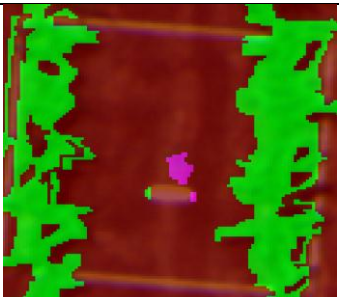
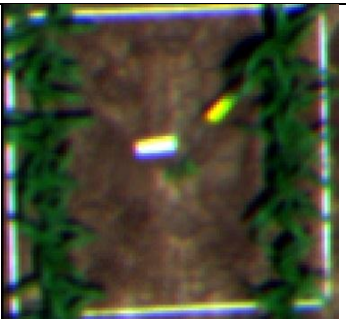
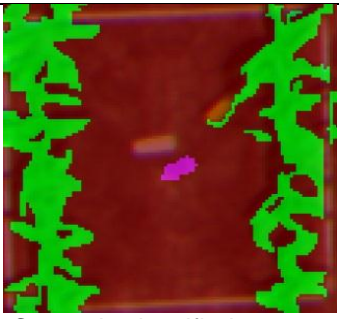
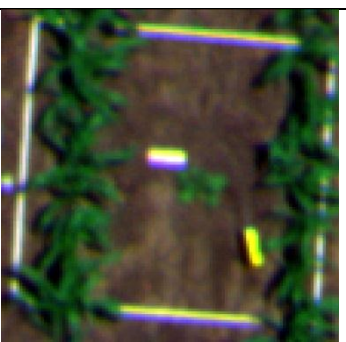
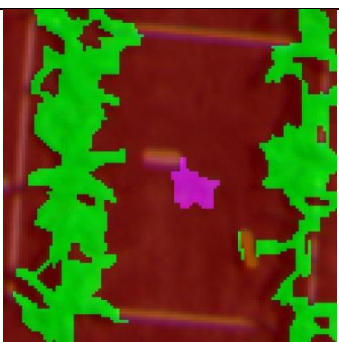
Appendix Y. Sorghum non pre-emergence quadrats at week three for 10.83mm resolution

Appendix Y shows sorghum non pre-emergence nutgrass quadrats at two stages of growth for 10.83 mm resolution. The first column is MCA 6 imagery of weeds and sorghum crop in 1 m x 1 m square and the second and third columns are classified images using OBIA

Image (20 m)	Week 3	
	15 December 2014	17 December 2014
 <p>Q1SNP</p>	<p>Not available</p>	 <p>Correctly classified</p>
 <p>Q2SNP</p>	 <p>Correctly classified</p>	 <p>Correctly classified</p>
 <p>Q3SNP</p>	 <p>The misclassification of sorghum (In the circle)</p>	 <p>The misclassification of sorghum (In the circle)</p>
 <p>Q4SNP</p>	 <p>Correctly classified</p>	 <p>Correctly classified</p>

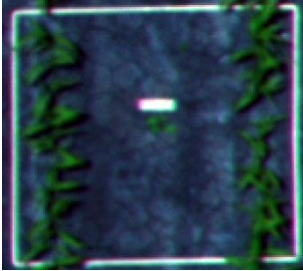
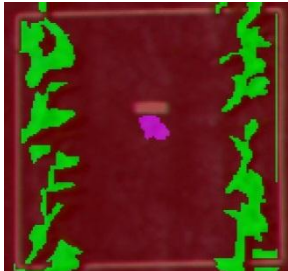
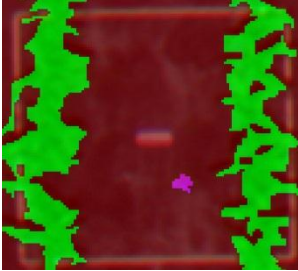
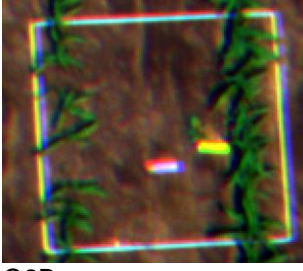
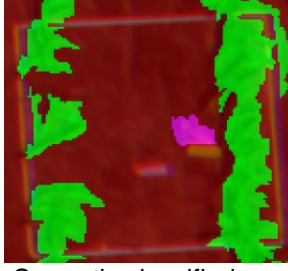
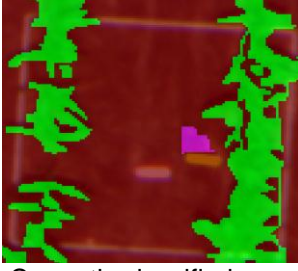
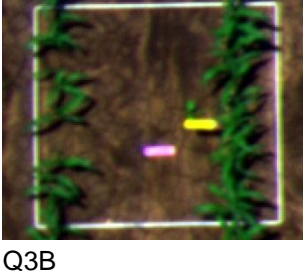
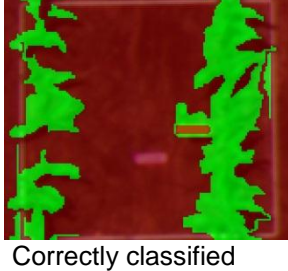
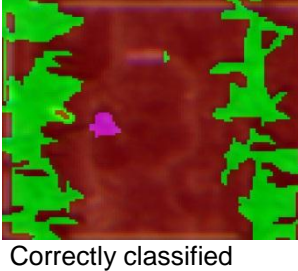
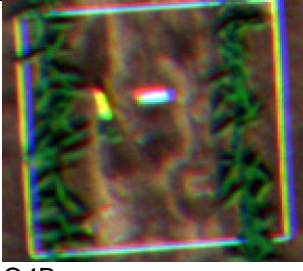
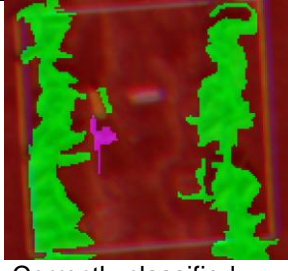

Appendix Z. Pigweed quadrats at week three for 10.83mm resolution

Appendix Z shows pigweed quadrats at two stages of growth for 10.83 mm resolution. The first column is MCA 6 imagery of weeds and sorghum crop in 1 m x 1 m square and the second and third columns are classified images using OBIA

Image (20 m)	Week 3	
	15 December 2014	17 December 2014
 <p>Q1PG</p>	 <p>Correctly classified</p>	 <p>Correctly classified</p>
 <p>Q2PG</p>	 <p>Correctly classified</p>	 <p>Correctly classified</p>
 <p>Q3PG</p>	<p>Not available</p>	 <p>Correctly classified</p>
 <p>Q4PG</p>	<p>Not available</p>	 <p>Correctly classified</p>

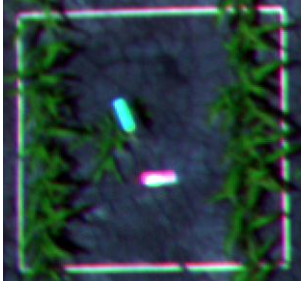
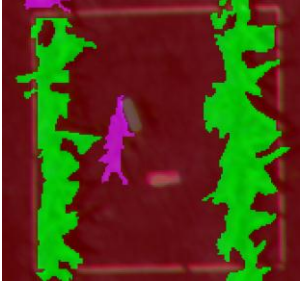
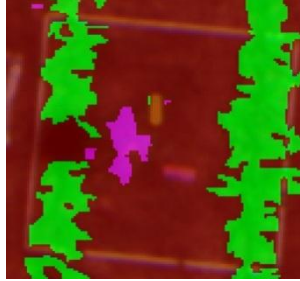
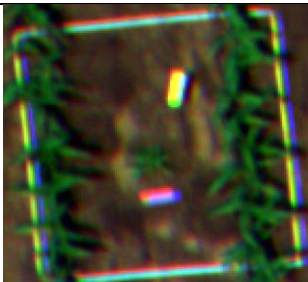
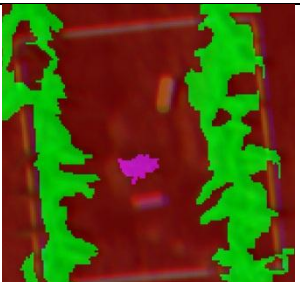
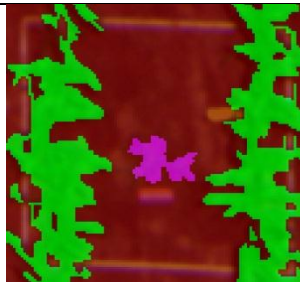
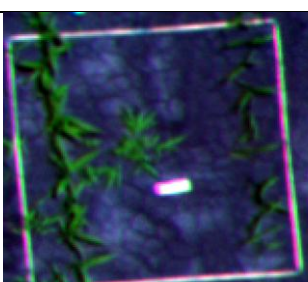

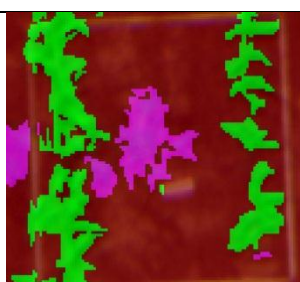
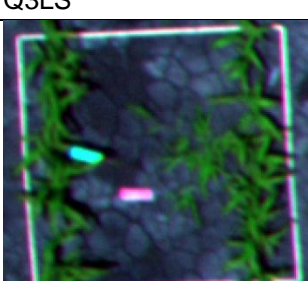
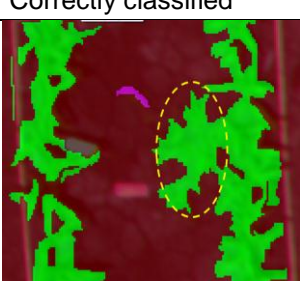
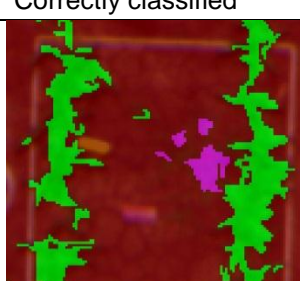
Appendix AA. Bellvine quadrats at week three for 10.83 mm resolution

Appendix AA shows bellvine quadrats at two stages of growth for 10.83 mm resolution. The first column is MCA 6 imagery of weeds and sorghum crop in 1 m x 1 m square and the second and third columns are classified images using OBIA

Image (20 m)	Week 3	
	15 December 2014	17 December 2014
 <p>Q1B</p>	 <p>Correctly classified</p>	 <p>Correctly classified</p>
 <p>Q2B</p>	 <p>Correctly classified</p>	 <p>Correctly classified</p>
 <p>Q3B</p>	 <p>Correctly classified</p>	 <p>Correctly classified</p>
 <p>Q4B</p>	 <p>Correctly classified</p>	 <p>Correctly classified</p>

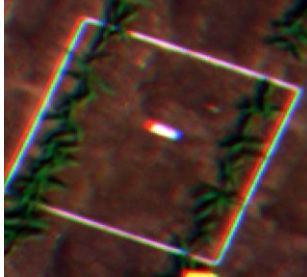
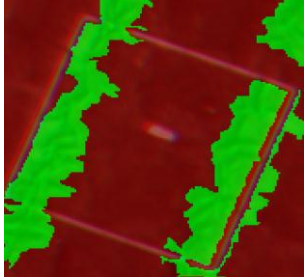
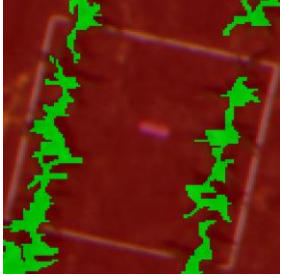
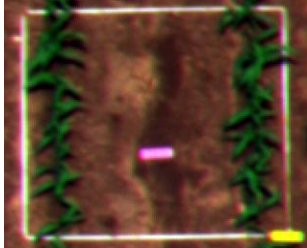
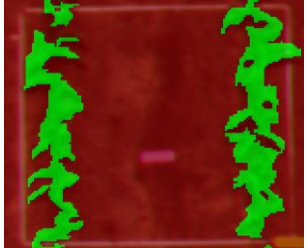
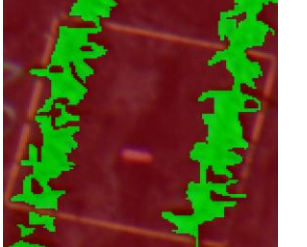
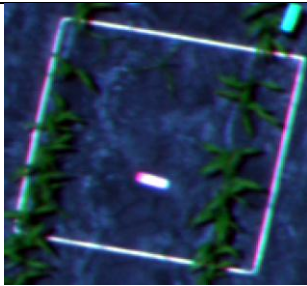
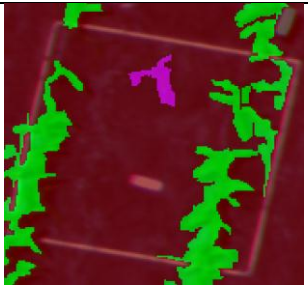
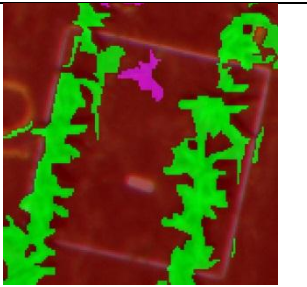
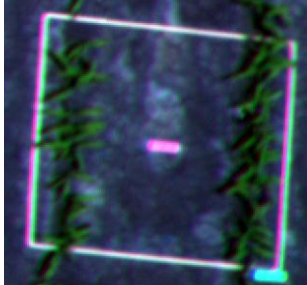
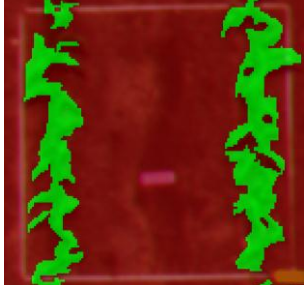
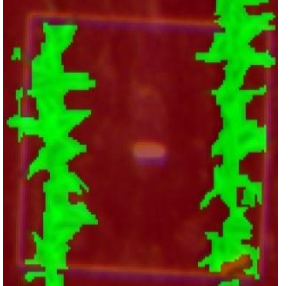
Appendix BB. Liverseed grass quadrats at week three for 10.83mm resolution

Appendix BB shows liverseed grass quadrats at two stages of growth for 10.83 mm resolution. The first column is MCA 6 imagery of weeds and sorghum crop in 1 m x 1 m square and the second and third columns are classified images using OBIA

Image (20 m)	Week 3	
	15 December 2014	17 December 2014
 <p>Q1LS</p>	 <p>Correctly classified</p>	 <p>Correctly classified</p>
 <p>Q2LS</p>	 <p>Correctly classified</p>	 <p>Correctly classified</p>
 <p>Q3LS</p>	 <p>Correctly classified</p>	 <p>Correctly classified</p>
 <p>Q4LS</p>	 <p>The misclassification of weeds (In the circle)</p>	 <p>Correctly classified</p>


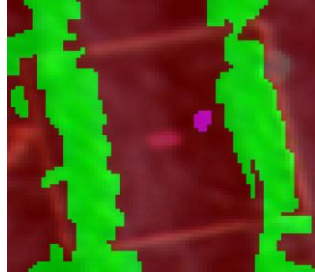
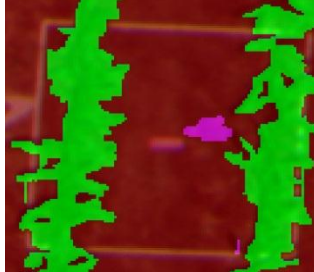

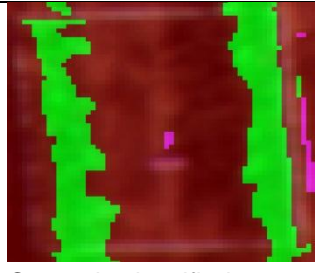
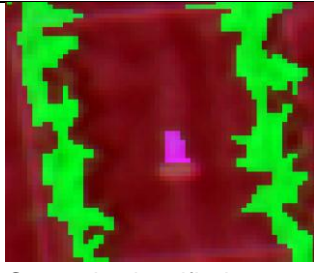

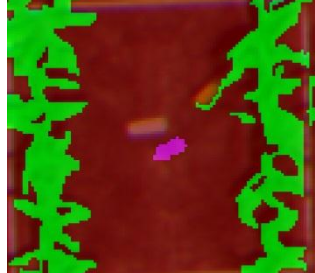
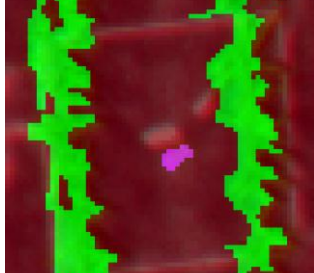
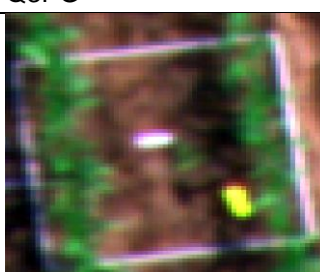

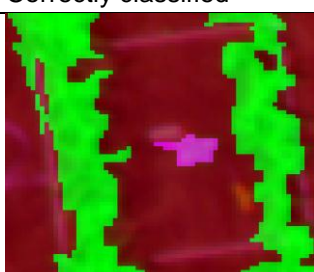
Appendix CC. Sorghum pre-emergence quadrats at week 3 for 10.83 mm resolution

Appendix CC shows sorghum pre-emergence quadrats at two stages of growth for 10.83 mm resolution. The first column is MCA 6 imagery of weeds and sorghum crop in 1 m x 1 m square and the second and third columns are classified images using OBIA

RAW (20 m)	Week 3	
	15 December 2014	17 December 2014
 Q1SP	 Correctly classified	 Correctly classified
 Q2SP	 Correctly classified	 Correctly classified
 Q3SP	 Correctly classified	 Correctly classified
 Q4SP	 Correctly classified	 Correctly classified

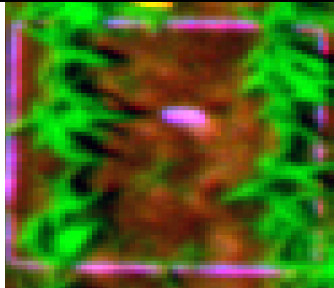
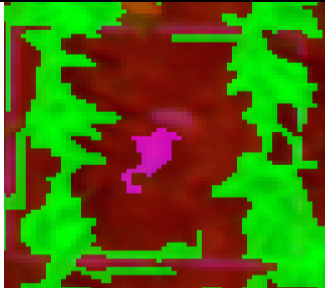
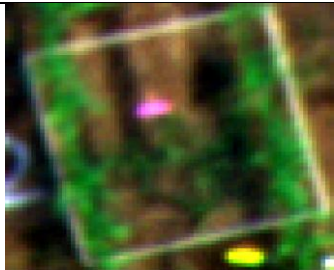
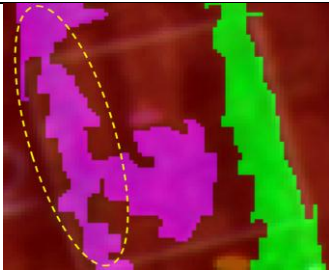
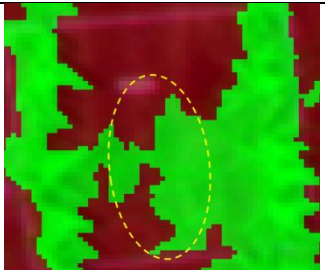
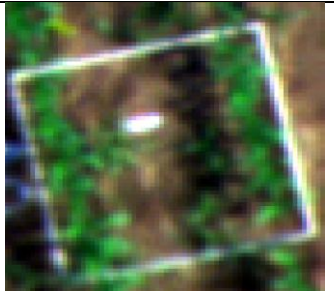
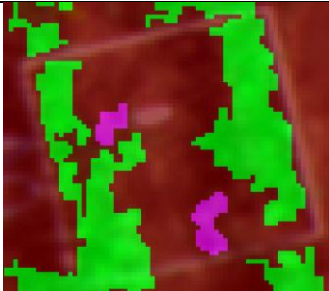
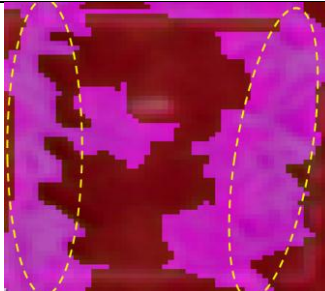

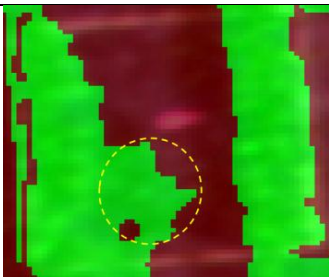
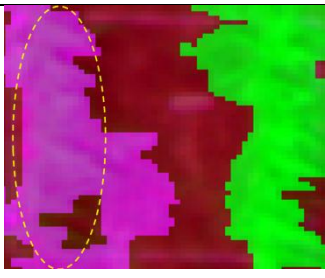
Appendix DD. Pigweed quadrats at week three for 20.31 resolution

Appendix DD shows pigweed quadrats at week three for 20.31 mm resolution. The first column is MCA 6 imagery of weeds and sorghum crop in 1 m x 1 m square and the second and third columns are classified images using OBIA

Image (37.5 m)	Week 3	
	15 December 2014	17 December 2014
 <p>Q1PG</p>	 <p>Correctly classified</p>	 <p>Correctly classified</p>
 <p>Q2PG</p>	 <p>Correctly classified</p>	 <p>Correctly classified</p>
 <p>Q3PG</p>	 <p>Correctly classified</p>	 <p>Correctly classified</p>
 <p>Q4PG</p>	 <p>Correctly classified</p>	 <p>Correctly classified</p>

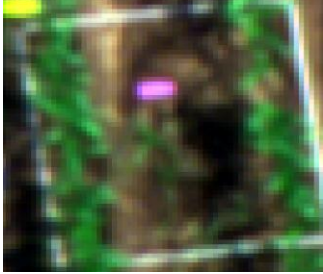

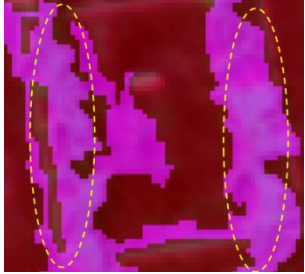

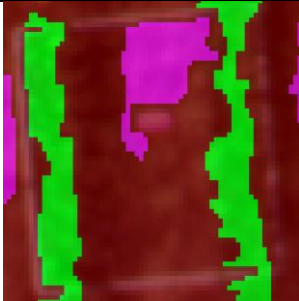
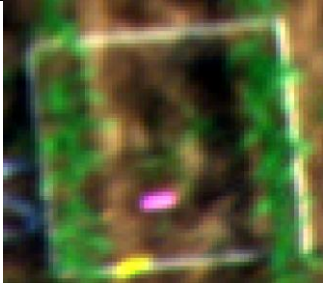
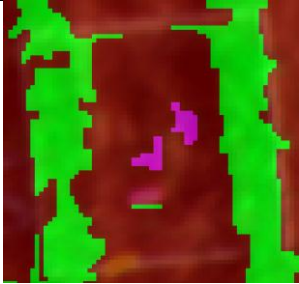
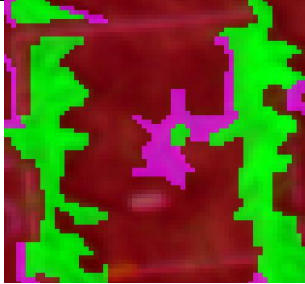
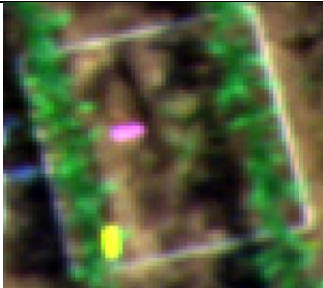
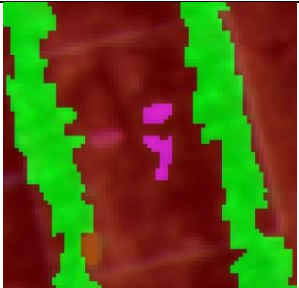
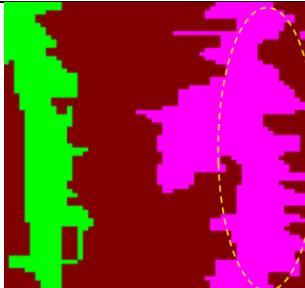
Appendix EE. Nutgrass quadrats at week three for 20.31 resolution

Appendix EE shows nutgrass quadrats at week three for 20.31 mm resolution. The first column is MCA 6 imagery of weeds and sorghum crop in 1 m x 1 m square and the second and third columns are classified images using OBIA

Image (37.5 m)	Week 3	
	15 December 2014	17 December 2014
 Q1NG	Not available	 Correctly classified
 Q2NG	 The misclassification of sorghum (In the circle)	 The misclassification of weeds (In the circle)
 Q3NG	 Correctly classified	 The misclassification of sorghum (In the circle)
 Q4NG	 The misclassification of weeds (In the circle)	 The misclassification of sorghum (In the circle)

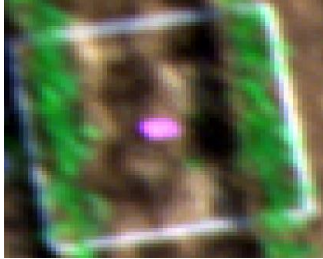
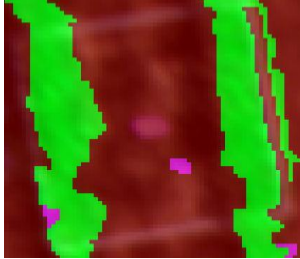
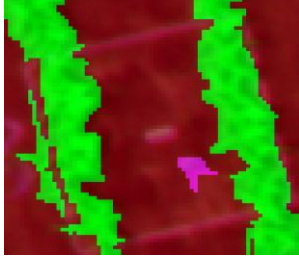
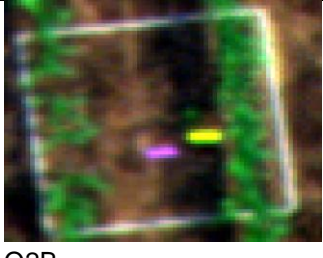
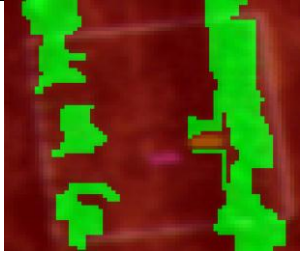
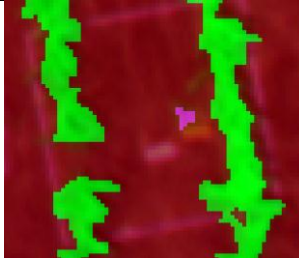
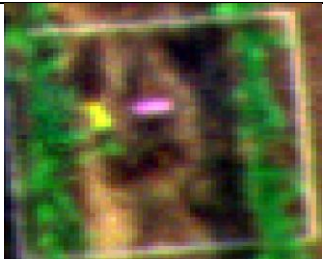
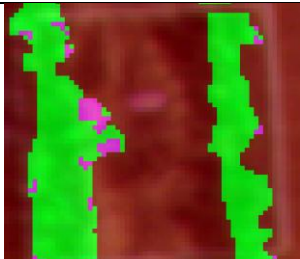
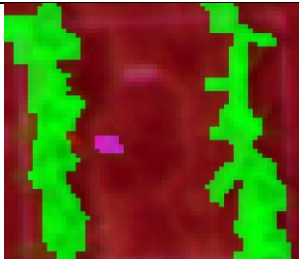

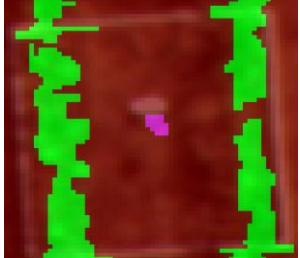

Appendix FF. Sorghum non pre-emergence quadrats at week three for 20.31 mm resolution

Appendix FF shows sorghum non pre-emergence quadrats at week three for 20.31 mm resolution. The First column is MCA 6 imagery of weeds and sorghum crop in 1 m x 1 m square and the second and third columns are classified images using OBIA.

Image (37.5 m)	Week 3	
	15 December 2014	17 December 2014
 Q1SNP	 The misclassification of weeds (In the circle)	 The misclassification of sorghum (In the circle)
 Q2SNP	 Correctly classified	Not available
 Q3SNP	 Correctly classified	 Correctly classified
 Q4SNP	 Correctly classified	 The misclassification of sorghum (In the circle)

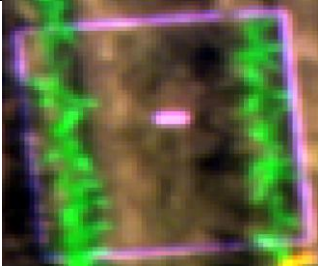
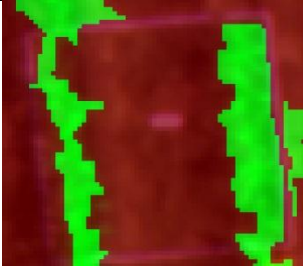
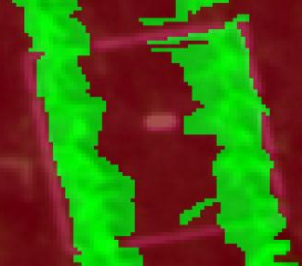
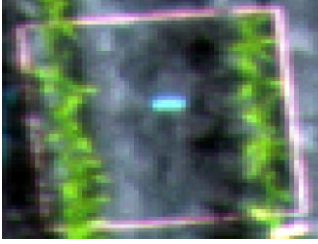
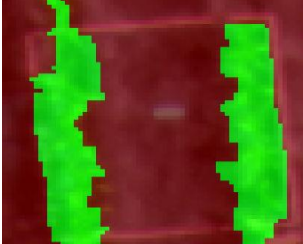
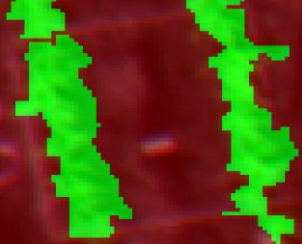
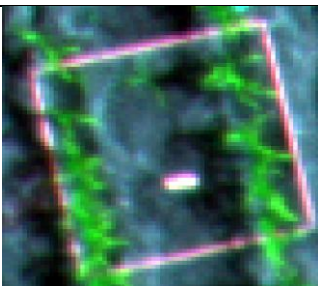
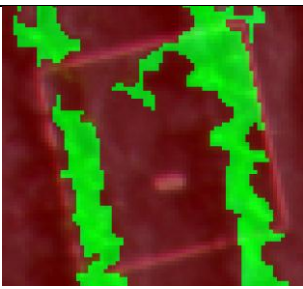
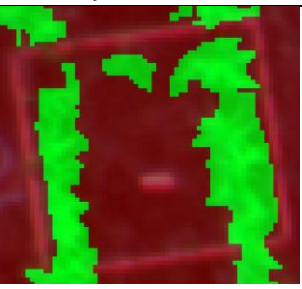
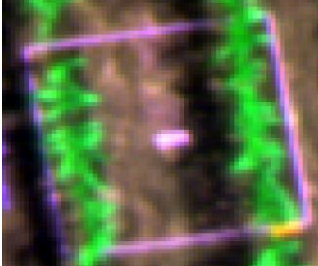
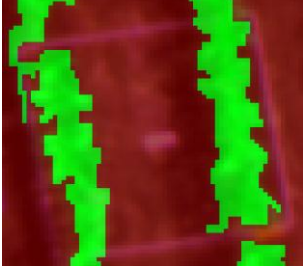
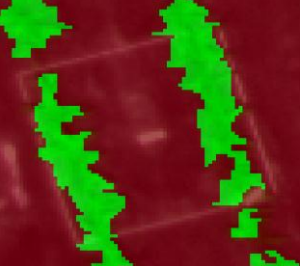
Appendix GG. Bellvine quadrats at week 3 for 20.31 mm resolution

Appendix GG shows bellvine quadrats at week three for 20.31 mm resolution. The first column is MCA 6 imagery of weeds and sorghum crop in 1 m x 1 m square and the second and third columns are classified images using OBIA.

Image (37.5 m)	Week 3	
	15 December 2014	17 December 2014
 <p>Q1B</p>	 <p>Correctly classified</p>	 <p>Correctly classified</p>
 <p>Q2B</p>	 <p>Correctly classified</p>	 <p>Correctly classified</p>
 <p>Q3B</p>	 <p>Correctly classified</p>	 <p>Correctly classified</p>
 <p>Q4B</p>	 <p>Correctly classified</p>	 <p>Correctly classified</p>

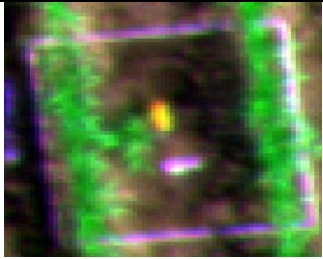
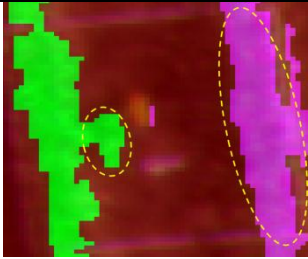
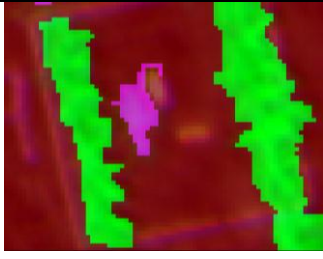
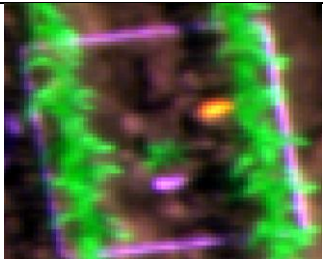
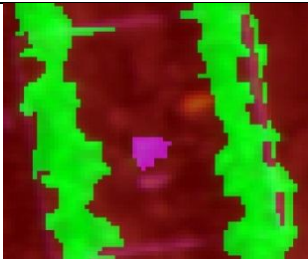
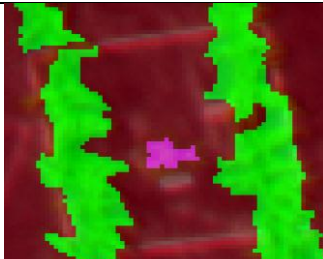
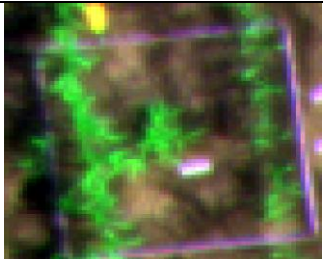
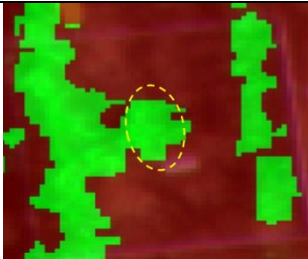
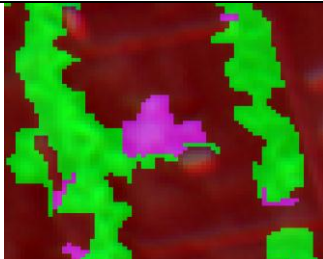
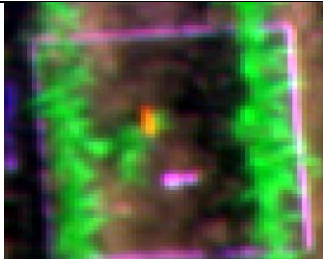
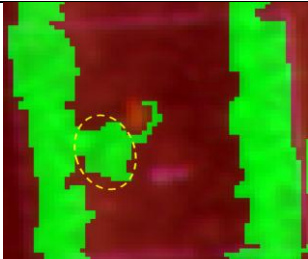
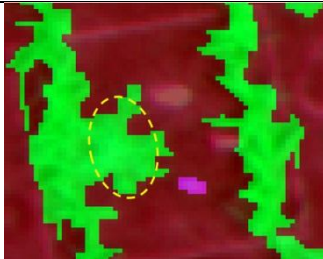
Appendix HH. Sorghum pre-emergence quadrats at week three for 20.31 mm resolution

Appendix HH shows sorghum pre-emergence quadrats at week three for 20.31 mm resolution. The first column is MCA 6 imagery of weeds and sorghum crop in 1 m x 1 m square and the second and third columns are classified images using OBIA.

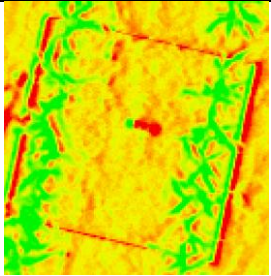
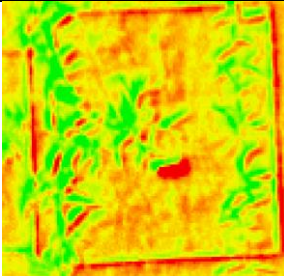
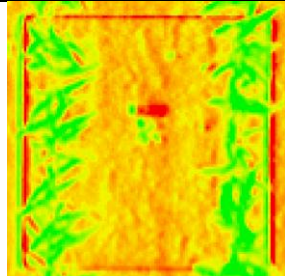
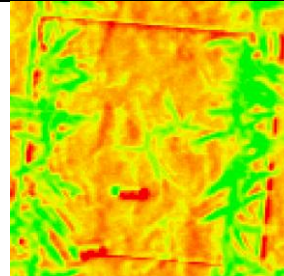
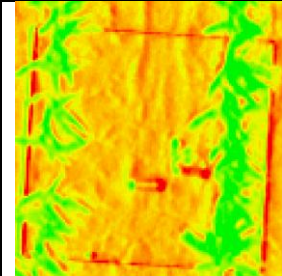
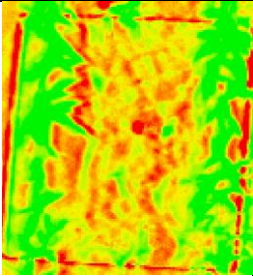
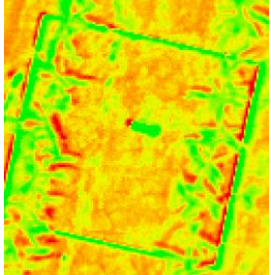
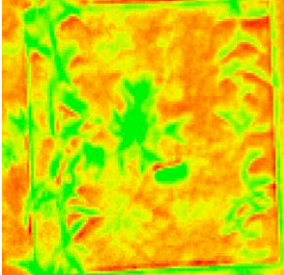
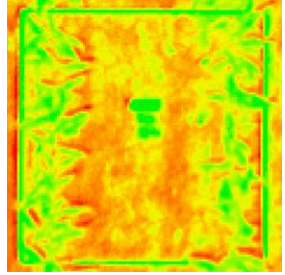
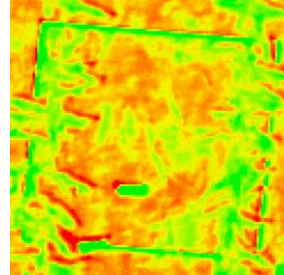
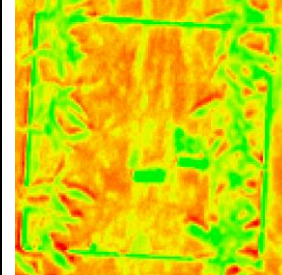
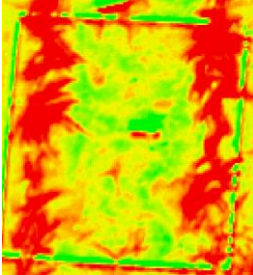
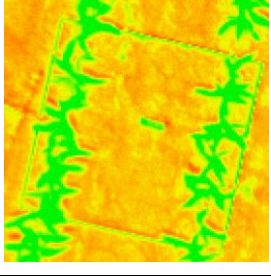
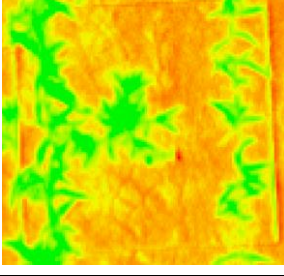
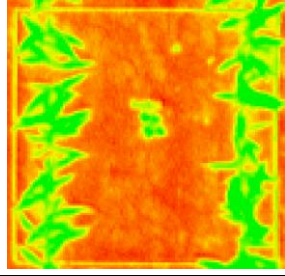
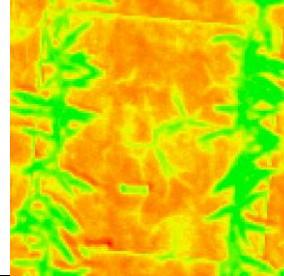
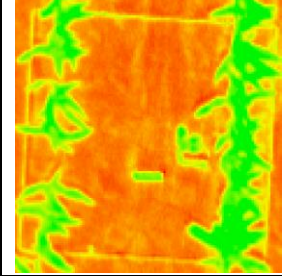
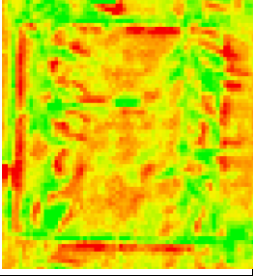
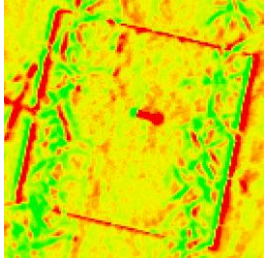
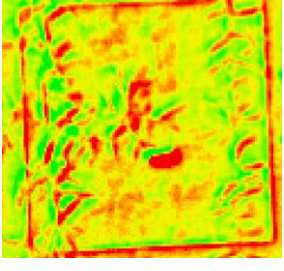
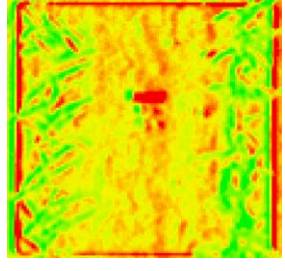
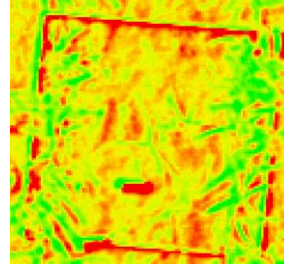
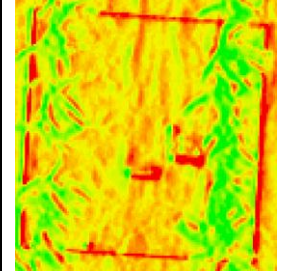
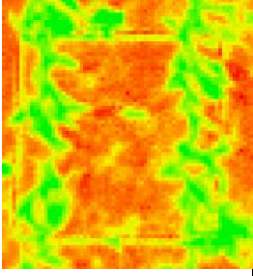
Image (37.5 m)	Week 3	
	15 December 2014	17 December 2014
 Q1SP	 Correctly classified	 Correctly classified
 Q2SP	 Correctly classified	 Correctly classified
 Q3SP	 Correctly classified	 Correctly classified
 Q4SP	 Correctly classified	 Correctly classified

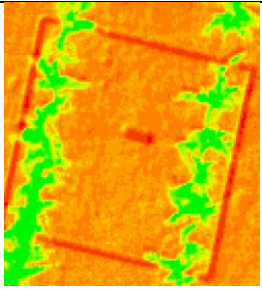
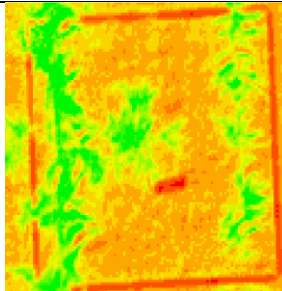
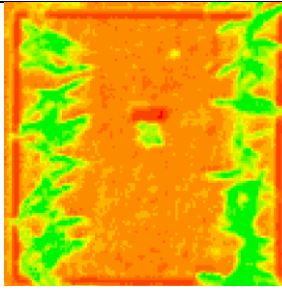
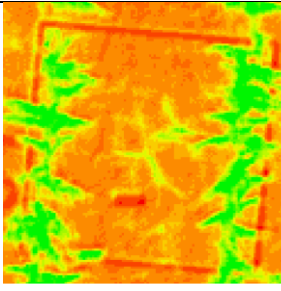
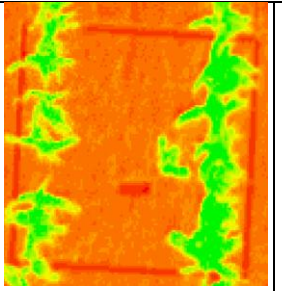
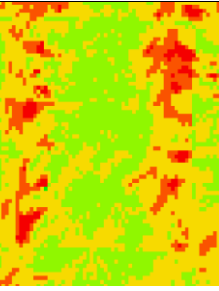
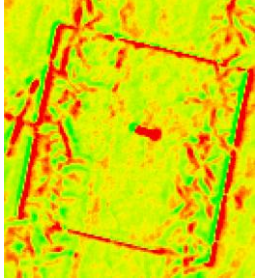
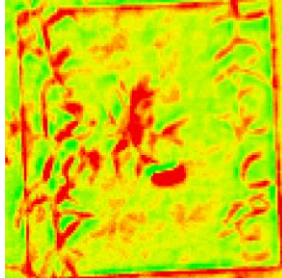
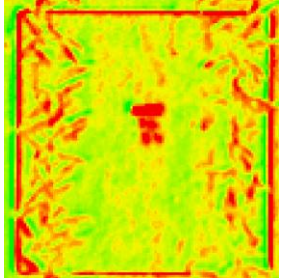
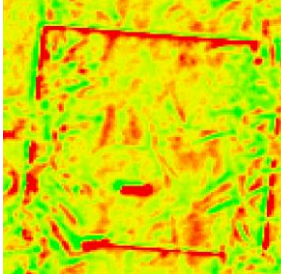
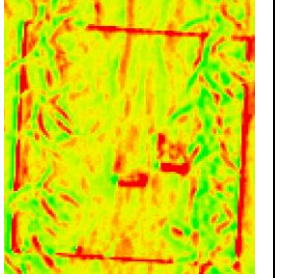
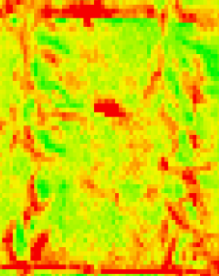
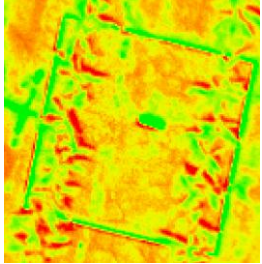
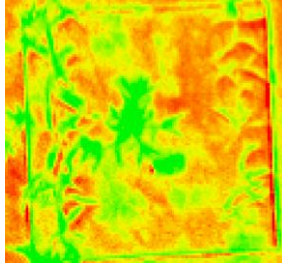
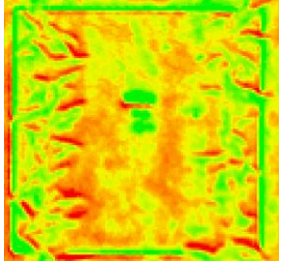
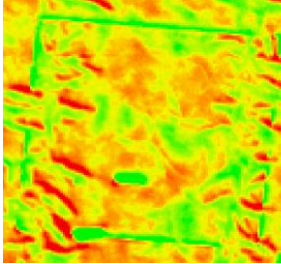
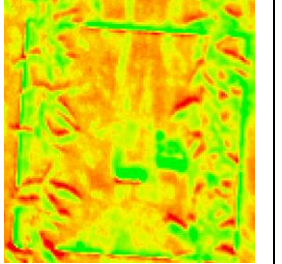
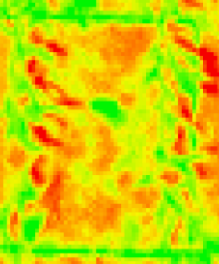
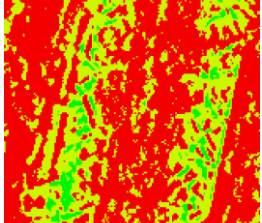
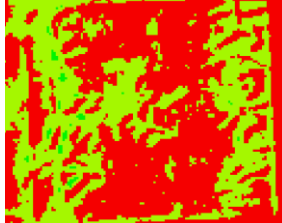
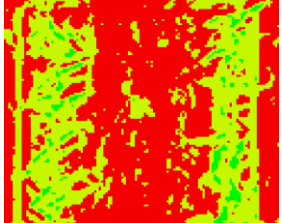
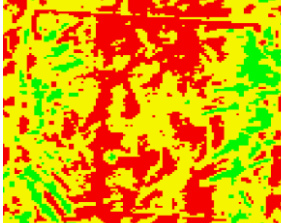
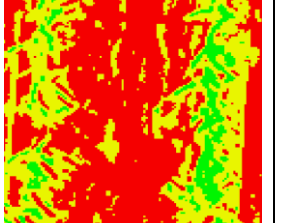
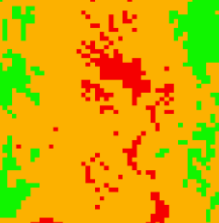
Appendix II. Liverseed grass quadrats at week three for 20.31 mm resolution

Appendix II shows liverseed grass quadrats at week three for 20.31 mm resolution. The first column is MCA 6 imagery of weeds and sorghum crop in 1 m x 1 m square and the second and third columns are classified images using OBIA

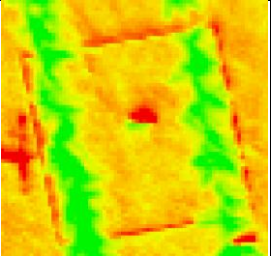
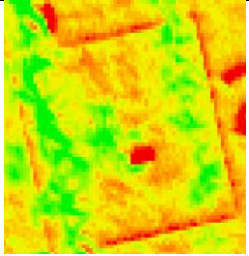
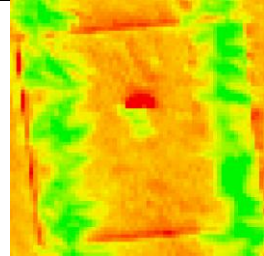
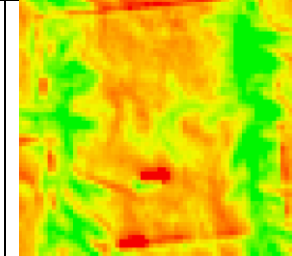
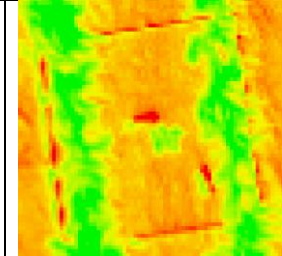
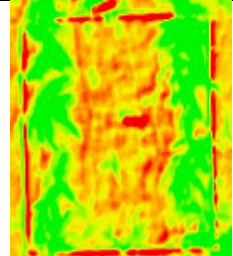
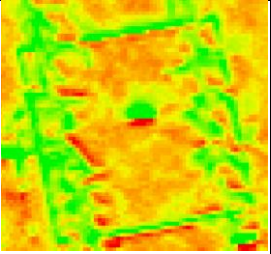
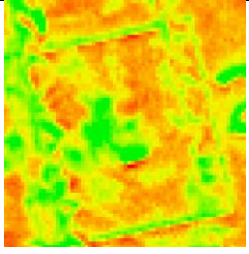
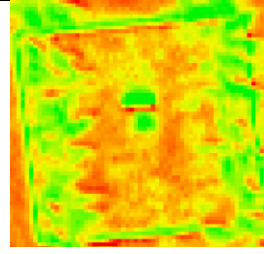
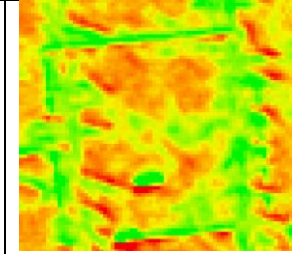
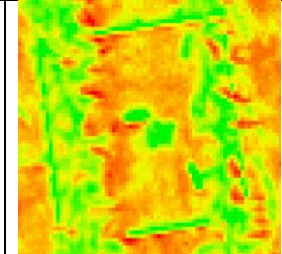
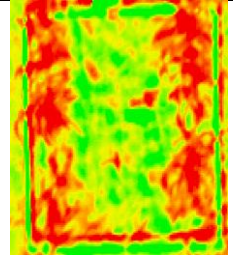
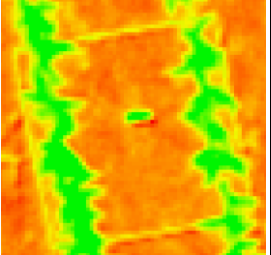
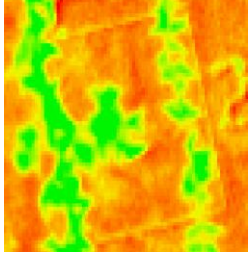
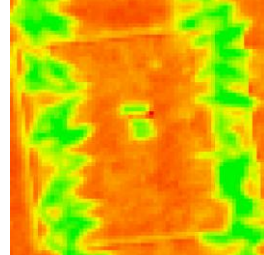
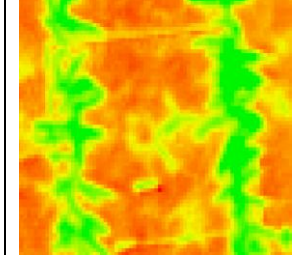
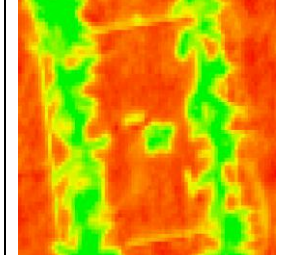
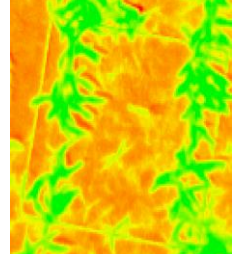
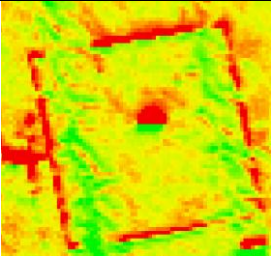
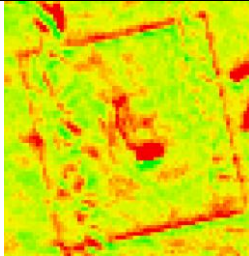
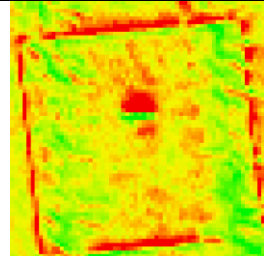
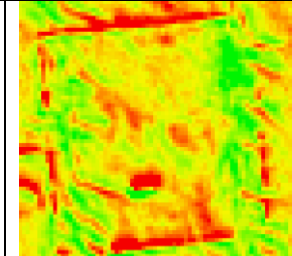
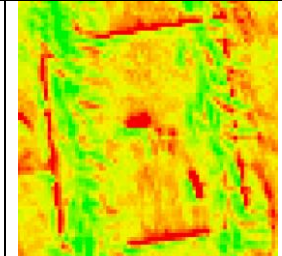
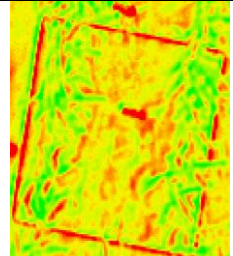
Image (37.5 m)	Week 3	
	15 December 2014	17 December 2014
 <p>Q1LS</p>	 <p>The misclassification of weeds and sorghum (In the circle)</p>	 <p>Correctly classified</p>
 <p>Q2LS</p>	 <p>Correctly classified</p>	 <p>Correctly classified</p>
 <p>Q3LS</p>	 <p>The misclassification of weeds (In the circle)</p>	 <p>Correctly classified</p>
 <p>Q4LS</p>	 <p>The misclassification of weeds (In the circle)</p>	 <p>The misclassification of weeds (In the circle)</p>

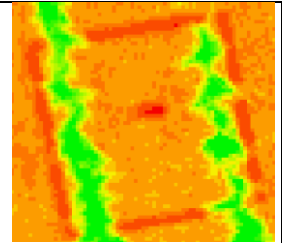
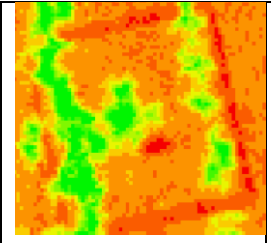
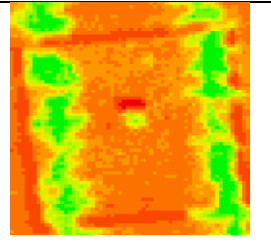
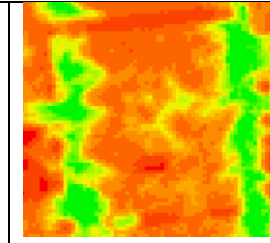
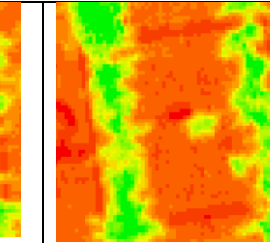
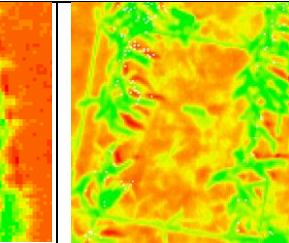
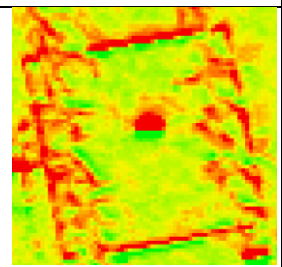
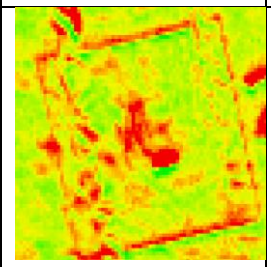
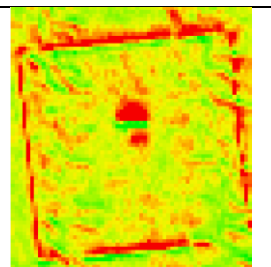
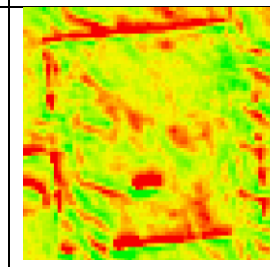
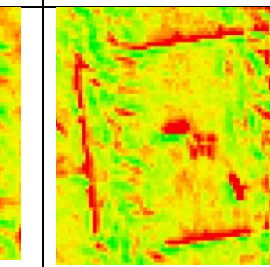
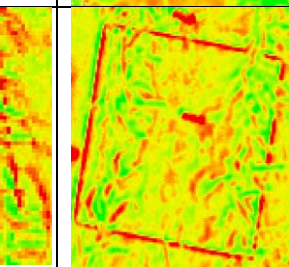
Appendix JJ. VI Analysis for 10.83 mm

Vegetation Index	Sorghum Pre-emergence	Liverseed Grass	Bellvine	Sorghum non pre-emergence	Pigweed	Nutgrass
Different Vegetation Index (DVI)						
Excess Red (ExR)						
Modified Excess Red (MExR)						
Modified Triangular Vegetation Index 1 (MTVI1)						

<p>NIR, Red-edge(720) and Red Combine Index (NRRCI)</p>						
<p>Triangular Veg. Index(TVI)</p>						
<p>Red-edge Veg. Stress Index (RVSI)</p>						
<p>Red Vegetation Index (RVI)</p>						

Appendix KK. VI Analysis 20.31 mm

Vegetation Index	Sorghum Pre-emergence	Liverseed Grass	Bellvine	Sorghum non pre-emergence	Pigweed	Nutgrass
Different Vegetation Index (DVI)						
Excess Red (ExR)						
Modified Excess Red (MExR)						
Modified Triangular Vegetation Index 1 (MTVI1)						

<p>NIR, Red-edge and Red Combine Index (NRRCI)</p>						
<p>Triangular Veg. Index(TVI)</p>						
<p>Red Vegetation Index (RVI)</p>	